Toughening of epoxy carbon fibre composites using dissolvable phenoxy fibres.

Wong, Doris Wai-Yin

Toughening of epoxy carbon fibre composites using dissolvable phenoxy fibres

By
Doris Wai-Yin Wong

A thesis submitted for the degree of Doctor of Philosophy in the Faculty of Engineering at the University of London

School of Engineering and Material Science
Queen Mary University of London
2013

Declaration

I hereby declare that this thesis, which I now submit for assessment leading to the award of Doctor of Philosophy is entirely my own work. Where other sources of information have been used, they have been acknowledged.

Signature: 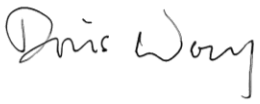

Date: 5 June 2012

Acknowledgement

I would like to thank the School of Engineering and Material Science for financial support during my study. The academic, technical and support staff and fellow students at the department have always been friendly and helpful, and I have made some great friends along the way.

I would like to thank Professor Paul Hogg, Professor Ton Pejis and Professor Terry McGrail for guidance and advice, and made this study possible.

I would also like to thank my family, especially my parents and husband for their continual understanding and support, for believing in me, and for allowing me the freedom to be myself and do my own things. Special mention to my baby girls, who cheer me up every day, and whose presence has made me more focused in whatever I do.

Abstract

The aim of this study is to investigate a novel toughening approach for liquid mouldable carbon fibre/epoxy composites. The toughening mechanism is based on the use of thermoplastics for the toughening of epoxy resins in which polymer blends are formed, leading to phase separated morphologies which allows for various toughening mechanisms to take place. Instead of standard melt or solution blending, the thermoplastic in this study is introduced as solid phenoxy fibres, which are combined with dry carbon fabric preforms. These phenoxy fibres remain solid during resin infusion and dissolve when the laminates are heated and phase separation takes place before curing completed. The main benefits of this approach are that the viscosity of matrix resin remains low, which makes liquid moulding of these laminates possible. Localised and selective toughening of particular regions within a structure can also be achieved. Process time and cost can also be reduced by eliminating the polymer blending process.

It was found that modification with phenoxy improved composite Mode-I interlaminar toughness significantly, with an increase of up to 10-folds for bifunctional epoxy composite and 100% for tetrafunctional epoxy composite, while tensile properties were not adversely affected. It was found that it is possible to combine the dissolvable phenoxy fibres with an undissolved aramid interleaf to improve toughness and damage properties. However, the phenoxy-epoxy systems had lowered environmental stability and degraded after hot-wet and solvent conditioning.

TABLE OF CONTENTS

List of publications

1. Doris W.Y. Wong, Lin Lin, P. Terry McGrail, Ton Peijs and Paul J. Hogg, *Improved fracture toughness of carbon fibre/epoxy composite laminates using dissolvable thermoplastic fibres*, Composites Part A: Applied Science and Manufacturing, Volume 41, Issue 6, June 2010, Pages 759-767

2. Fawad Inam, Doris W. Y. Wong, Manabu Kuwata and Ton Peijs, *Multiscale Hybrid Micro-Nanocomposites Based on Carbon Nanotubes and Carbon Fibers*, Journal of Nanomaterials, 2010, ISSN 16874110

3. *Improved fracture toughness of carbon fibre/tetra-functional epoxy composite laminates using dissolvable thermoplastic fibres* (in preparation)

4. *Effects of environmental conditioning on carbon fibre/epoxy composite laminates modified with dissolvable phenoxy fibres* (in preparation)

LIST OF FIGURES

LIST OF TABLES

Chapter 1

Introduction

Carbon fibre/epoxy matrix composites have many benefits such as high specific strength and stiffness, good thermal and chemical stability and have been used in many applications. However, epoxy matrix composites are brittle and prone to impact damage which includes failure modes such as transverse cracking, delaminations, fibre/matrix debonding and fibre fracture, all limiting their uses for many structural applications. Many works have been devoted on improving the fracture toughness of carbon fibre/epoxy composites and over the years several main approaches have been reported.

Attempts have been made to toughen the epoxy matrix by introducing a ductile second phase. The first and most studied method was reactive liquid rubber toughening [1-4] in which liquid rubber was mixed with uncured epoxy. The rubber then phase separate into discrete domains during the curing of epoxy, and various toughening mechanisms can then be generated. The downside of rubber toughening is that the thermal stability and modulus of the matrix is often sacrificed and that little toughening is achieved for a highly crosslinked epoxy. Thermoplastic toughening is similar to liquid rubber toughening in that phase separated morphologies are created upon curing. It is thought that with thermoplastic

toughening, thermal stability and modulus of epoxy matrices can be maintained. The most widely studied systems over the years have been polysulfone (PSF) [5-10] and polyetherimide (PEI) [11-13], while other polymers such as polyphenylene ether (PPE) [14, 15], poly(ethylene terephthalate) (PET) [16], phenoxy [17] and polycarbonate (PC) [18] have also been studied. Liquid rubber and thermoplastic toughening are normally achieved by melt blending at high temperatures or solvent blending before fibre impregnation. Processing at high temperatures can lead to degradation of the polymers and an increase in manufacturing cost, while any remaining solvent in the cured resin can have negative effects on its properties. Particulate toughening is also employed, including the use of inorganic silicates and oxides [19], rubber particles [20] and core-shell rubber particles [21]. More recently a wide range of nanoparticles, including inorganic silicates and oxides [22-24] and carbon nanotubes [22, 25-27] have also been studied.

Some toughening techniques specifically concentrate on damage prone areas in laminated composites such as interlaminar regions in which an interlayer or interleaf is placed between the reinforcing plies. There are different types of interleaves, including thermosetting adhesive films [28], non-woven fibre mats [29, 30], chopped fibre mats [31, 32] and thermoplastic particles [33] or films [34]. The fabric structure also plays an important part in preventing delamination in composites, and stitching, 3D fabrics, and Z-pinning have all been studied [35-37]. Composites made with hybrid reinforcement using high strain thermoplastic fibres such as polyethylene [38, 39], polypropylene, aramid and nylon have also been studied [30, 40, 41].

In the current study we explore a novel toughening concept based on using dissolvable thermoplastic fibres as localised toughening agent for carbon fibre/epoxy composites. The concept is basically a combination of existing toughening concepts based on the inclusion of thermoplastic as fibres, interleaving and as a dispersed phase in an epoxy matrix. The current study uses phenoxy fibres, which are

incorporated in solid form into a carbon fibre preform as a chopped fibre interleaf. Composite laminates are made by a vacuum infusion process, where the phenoxy fibres are expected to remain in solid form during infusion but then dissolve and subsequently phase separate when the resin is heated during curing.

The use of dissolvable thermoplastic fibres as toughener for composite is compatible with liquid composite moulding (LCM) processes as the viscosity of resin remains unchanged during infusion, and it is also compatible with other toughening concepts such as 3D, stitched or Z-pinned fabrics and non-woven interleaf mats. Common rubber and thermoplastic toughening additives cannot be utilised due to the dramatically increased viscosity of these resin systems. Similarly, the addition of even a small amount of nanoparticles can significantly increase the viscosity of the resin and it can also lead to heterogeneous particle dispersion throughout the preform due to filtering effects by the reinforcing fabric during liquid resin infusion [15, 16].

Chapter 2 is a literature review on toughening of epoxy fibre composites, in which the different toughening mechanisms and approaches to toughening are covered. Chapter 3 reports the mechanical and physical properties of the neat epoxy/phenoxy resin blends. Chapter 4 investigates the effect of adding dissolvable phenoxy fibres into the interlaminar region of carbon fibre/epoxy composites. Chapter 5 studied the combined effect of using dissolvable phenoxy fibres together with an aramid non-woven veil in the interlaminar region of a carbon fibre epoxy composites. Chapter 6 investigated the environmental stability of the dissolvable phenoxy fibre modified carbon fibre/epoxy composite, after hot-wet and solvent environmental conditioning. Chapter 7 reports on the addition of carbon nanotubes (CNT) to a carbon fibre/epoxy composite and involves a combination of micro (carbon fibre) and nano (CNT) toughening. Chapter 8 concludes the various findings in this study and outlines further research in this field which includes the combination of dissolvable phenoxy fibres and CNTs, in which the CNTs is

embedded in the phenoxy fibre to achieve selective localised toughening and/or sensing.

CHAPTER 2

LITERATURE REVIEW

2.1 Toughness of composites

Toughness is the resistance of a material against fracture and crack propagation. Toughness is quantified in terms of the energy absorbed per unit crack extension and any process which absorbs energy at the crack tip can give rise to an increase in toughness. The fracture mechanism and testing methods involved in this project are based on linear elastic fracture mechanics (LEFM). LEFM has a theoretical basis in that all energy dissipation is associated with the fracture process and the deformation which occurs is linear elastic. The theory is applied to brittle failures of polymers, impact tests, fatigue, and delamination of composites. When using LEFM in polymers certain assumptions are made, namely: (1) the material is linearly elastic; (2) the flaws within the material are sharp and (3) plane strain conditions apply in the crack front region.

A parameter called the *stress intensity factor* (*K*) is used to determine the fracture toughness of most materials. *K* is directly proportional to all crack tip stresses and is dependent on applied load and geometry. As a load is applied to a specimen, the crack will propagate until the critical stress intensity factor K_c is reached. K_c is temperature and rate dependent and the dependence is specific for any

material, but it is relatively independent of specimen geometry. K_c is a measure of material toughness and is related to G_c, the critical energy release rate.

For plane stress $$G_c = \frac{K_c^{\,2}}{E} \tag{2.1}$$

For plane strain $$G_c = \frac{K_c^{\,2}}{E}(1-\upsilon^2) \tag{2.2}$$

where E = *Young's modulus,*

υ = *Poisson's ratio*

The stress intensity factor is usually given a subscript to denote the mode of loading, i.e. K_I, K_{II}, or K_{III} for Mode-I, II and III, respectively. In a mixed-mode situation, the individual contributions to a given stress component are additive.

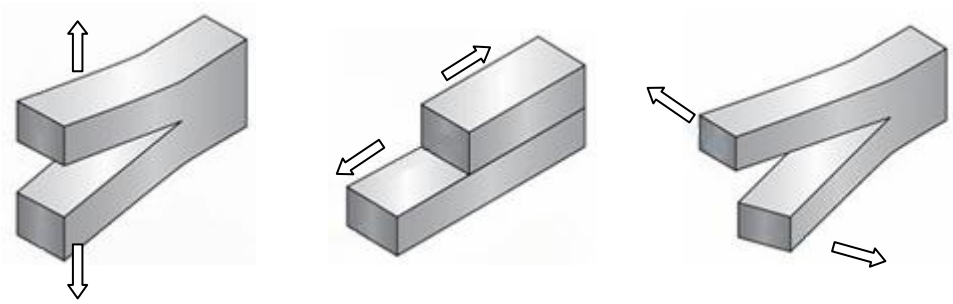

(a) Mode-I (b) Mode-II (c) Mode-III

Figure 2.1 Fracture modes of materials (a) opening mode, (b) sliding mode and (c) shearing mode.

In a composite laminate, a delamination acts as a crack-like discontinuity between the plies, which propagates during loading, and the study of delamination is therefore based on LEFM fracture mechanics. Interlaminar fracture toughness of laminates is normally expressed in terms of G_c. G_c is the measure of the fracture toughness of a material and as such it is a material property just like the Young's

modulus, yield stress, etc.. G_c is usually given in units of kJ/m^2 and smaller G_c values indicate lower toughness. Interlaminar fracture toughness can be measured in each of the modes shown in Figure 2.1 or in a combination of these modes. It is common to display the fracture toughness measured at various crack lengths as a resistance curve (R-curve).

Contrary to other mechanical and physical properties, the toughness of composites seldom follows a volume-average rule (or rule of mixture) and toughness is often greater than the sum of the toughness of all composite components. While the inherent toughness of each component is essential to the combined composite toughness, the toughening mechanisms of each component could be unique and their interactions would generate unpredictable behaviour using the volume-average rule.

There are many possible toughening mechanisms operating in composites and it can be difficult to determine the dominant mechanism. However, it is the combined effect of the different mechanisms that governs the overall toughness of a composite. Energy is dissipated during fracture, therefore by introducing different fracture modes in a composite and maximising the fracture energy related to each of these failure modes, toughness can be improved. Failure in composites occurs at both microscopic and macroscopic levels. On the microscopic level, the failure modes operate within the crack tip, or damage zone, and can appear in the form of fibre pull-out, matrix micro-cracking, fibre-matrix interfacial failure and fibre fracture. On the macroscopic level, the major failure modes include delamination, matrix cracking along the fibre direction in the individual plies, and failure of individual plies. The types and extent to which these failure mechanisms operate in any given system depends on the intrinsic materials parameters such as laminate configuration, material system, environmental conditions as well as loading conditions.

Figure 2.2 shows a schematic diagram of the various failure modes in a composite laminate. The descriptions of the different regions are:

1. Characteristic failure of brittle fibres

2. Fibre pull-out
3. Fibre/matrix debonding
4. Matrix micro-cracking
5. Ductile failure of fibre
6. Fibre fracture at a flaw and the associated plastic strain distribution in the matrix
7. Plastic strain distribution due to yielding at the tip of the main crack
8. Plastic shear strain distribution under the influence of shear stress
9. Longitudinal matrix or interfacial crack caused by tensile stress distribution
10. The dotted line highlights a possible zone of interlaminar shear failure between the longitudinal lamina shown and an adjacent off-axis lamina

In the following sections, some of these failure mechanisms are discussed in more detail.

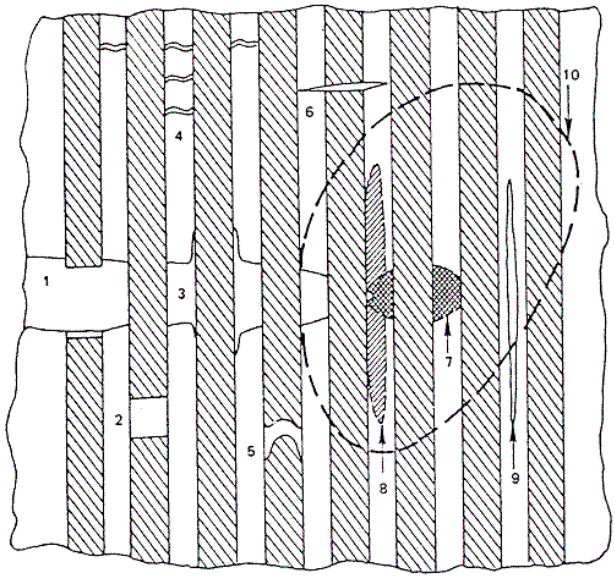

Figure 2.2 Schematic representation of possible failure mode in fibre reinforced composite [42].

2.2 Toughening mechanisms in composites

2.2.1 Crack perturbation

Crack pinning theory was proposed by Lange and Radford [43] to explain modification by particulate fillers. Lange showed that by inclusion of an inorganic particulate filler, the fracture energy of an epoxy matrix could be increased. The crack pinning mechanism based on the impeding characteristics of the particles proposes that a propagating crack front, when encountering an inhomogeneity, becomes temporarily pinned at that point. As the load increases, the degree of bowing between pinning points increases and this results in both a new fracture surface and an increase in the length of the crack front. Crack bowing reduces the stress intensity, *K*, on the matrix while producing an increase in *K* on the reinforcing phase. As the extent of the bowing increases so does *K* rises until fracture occurs and the crack advances. Lange proposed that when the bowed crack front attains a radius of *dp/2*, where *dp* is the inter-particle distance, it breaks away from the pinning positions and creates characteristic tails. It is seen that the fracture energy of the particulate composite will increase as the particle spacing decreases. It was found that the degree of toughening depended on both the volume fraction and the particle size of the filler. This mechanism mainly operates with inorganic fillers that resist fracture during failure of the epoxy matrix resin: it is generally considered to be less important in ductile matrix materials. A schematic diagram of the crack pinning mechanism is shown in Figure 2.3.

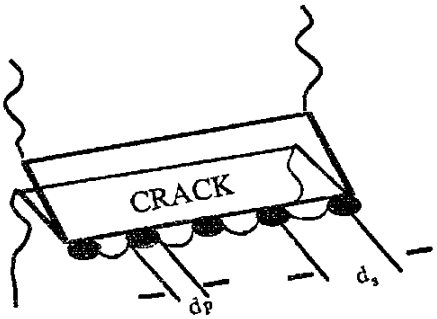

Figure 2.3 Schematic diagram of the crack pinning mechanisms [44].

Crack deflection (Figure 2.4) is similar to cracking bowing in that the reinforcing phase perturbs the crack front. Deflection results in a non-planar crack which requires an increase in the applied stress to maintain sufficient stress intensity for crack propagation. The effectiveness of the crack bowing and deflection mechanisms depends on the morphology of the reinforcing phase. The greatest improvement in toughness is obtained for a high aspect ratio filler and high reinforcement content. The interaction of the crack with the residual stress fields due to differences in the thermal expansion coefficients or elastic moduli between the matrix and the reinforcement can also cause deflection.

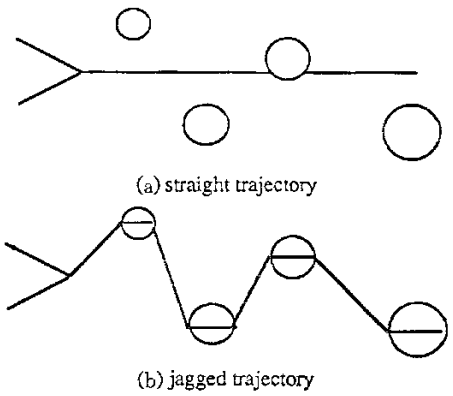

Figure 2.4 Schematic diagram of the crack deflection mechanism [44].

2.2.2 Matrix deformation

Plastic deformation in the matrix of polymer composites can be significant for a tough matrix. Shear deformation that occurs during failure is a considerable energy dissipation process. Shear flow in composites blunts sharp cracks, hence redistributing the local stress field. Davies *et al* [45] have shown that the fracture toughness corresponding to crack initiation is higher in specimens with a greater ability to undergo plastic flow. Apart from an improvement in fracture toughness, Hirschbuehler *et al*. [46] showed that matrices with high strains to failure offered

excellent compression after impact properties, when used in long fibre reinforced composites. The extent of matrix deformation during composite failure may differ from that of bulk unreinforced resin due to constraint effects. The matrix is unable to deform freely because it is surrounded by stiff and strong fibres. Triaxial stress states can build up and matrix plastic flow be inhibited.

2.2.3. Particle bridging (rigid particles)

In this toughening mechanism, it is proposed [44] that a rigid or ductile particle plays two roles:

(1) It acts as a bridging particle that applies compressive traction in the crack wake.

(2) The ductile particle deforms plastically in the material surrounding the crack tip, which provides additional crack shielding.

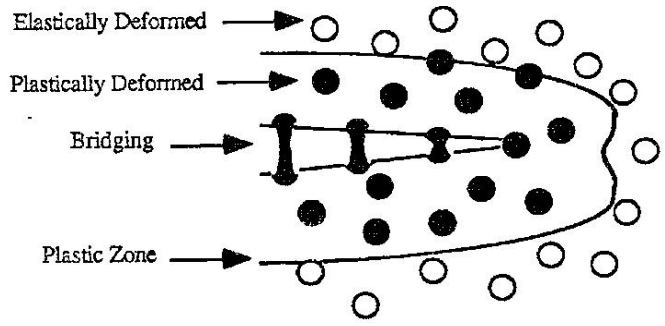

Figure 2.5 Schematic diagram of the particle bridging mechanisms [44].

It was pointed out that the effect of shielding contribution of particles is negligible, and particle bridging provides most of the improvement in toughness. In contrast to the crack pinning mechanism, the particle bridging mechanism (Figure 2.5) favours large particles and emphasizes the energy-to-rupture needed of the ductile phase.

2.2.4 Rubber tearing (particle deformation)

This theory is based on the early theories of the toughening mechanisms of toughened thermoplastics and the idea that particles stretch across the crack opening behind the crack tip thus hindering the advance of the crack. The energy absorbed in fracture being the sum of the energy required to fracture the matrix and that needed to break the rubber particles. A number of microscopic investigations have proved its validity in the case of rubber modified epoxies by providing evidence of stretched rubber particles spanning loaded cracks [47]. From such observations, Kunz-Douglass and Ashby [48] proposed that the toughness enhancement provided by rubber particle inclusion was dependent primarily on the degree of elastic energy stored in the rubber particles during loading of the two phase system. The mechanism put forward by Kunz and Beaumont [49] emphasises the role of deformation and fracture of the rubber particles, Stretching and tearing of rubber particles embedded in the epoxy matrix results in high energy absorption during failure. Rubber tearing was shown to be the main contributor to the failure energy of high molecular weight nitrile rubber modified epoxies [50]. However, the rubber tearing theory does not explain the existence of the stress whitening frequently observed in rubber modified epoxies. It also does not account for yielding and plastic flow contribution to the toughness. Therefore rubber tearing is generally not seen as the principle toughening mechanisms [51].

2.2.5 Cavitation – localized shear yielding

This toughening mechanism theory, proposed by Kinloch *et al* [52] and Pearson and Yee [53], is regarded as the most consistent in terms of experimental data generated in for rubber modified epoxy matrix composites. Kinloch suggested that the rubber tearing mechanism only makes a secondary contribution to toughening, as it does not represent the major toughening. The correlation between toughness and the extent of plastic deformation found on fracture surfaces has led to a mechanism based on yielding and plastic shear flow of the matrix as the primary

source of energy absorption in rubber modified epoxies. Enhanced plastic deformation in the matrix has been found to accompany the inclusion of rubber particles and the stress distribution existing around rubber particles located in the vicinity of a stressed crack tip becomes important. Initially the development of a tri-axial stress dilates the matrix and along with this, these tri-axial stresses inherently present in the rubber particles (due to differential thermal contraction effects during curing) provide the necessary conditions for cavitation of rubber particles. Rather than crazing of the epoxy matrix, it is the cavitation process which is considered responsible for the stress whitening effects usually observed in rubber modified epoxies. The increasing stress concentrations around rubber particles during loading would promote shear yield deformation zones in the matrix. Since the particles would also act as sites of yield terminations, yielding would remain localised in the vicinity of the crack tip. It is assumed that both cavitation and shear yielding would occur during the early stages of load application. Once initiated, rubber particle cavitation would further enhance shear yielding in the matrix. As a result crack tip blunting would increase extensively leading to the development of a plastic zone at the crack tip. Thus, toughness would be enhanced as has been observed. Bascom *et al* [54] attributed the toughness of a liquid carboxyl-terminated butadiene acrylonitrile (CTBN) rubber modified epoxy resin to an increase in the plastic zone size. At the same time Pearson and Yee attributed an order of magnitude increase in toughness to the cavitation of rubber particles followed by shear yielding of the epoxy matrix [53]. The absence of cavitations in solid rubber modified epoxies results from the high molecular weight of solid rubber which imparts it with greater tensile strength to the rubber, which can eliminate premature cavitation [50]. It is postulated that a low molecular weight CTBN rubber with low tensile strength is readily cavitated at the early stages of loading and it is interesting to note that the fracture toughness of these rubber-modified epoxies is dependent on loading rate [55]. The process of cavitation during fracture diminishes the importance of the rubber tearing mechanism because the failed rubber particles require little or no

tearing energy [56, 57].

2.2.6 Microcracking

Microcracks may be produced by differences in coefficients of thermal expansion in the components and/or ply stiffness variations in cross-ply layup during the application of applied stress. The microcracks increase the toughness by interacting with a propagating macro-crack, causing deflection and blunting of this crack. However, this mechanism occurs at the expense of composite strength, since the microcracks act as flaws. The presence of microcracks also makes a composite material susceptible to environmental damage.

For matrices toughened with rubber and rigid particles, microcracks due to these particles cause tensile yielding thus a large tensile deformation. Voids result when the microcracks open and these voids permit large strains. Evans *et al*. [58] developed a model to predict the toughness in materials where rigid glass spheres were not well bonded to the matrix. Debonding or microcracking effectively lowers the modulus in the frontal process zone around the crack tip, and thus effectively reduces the stress intensity at the tip.

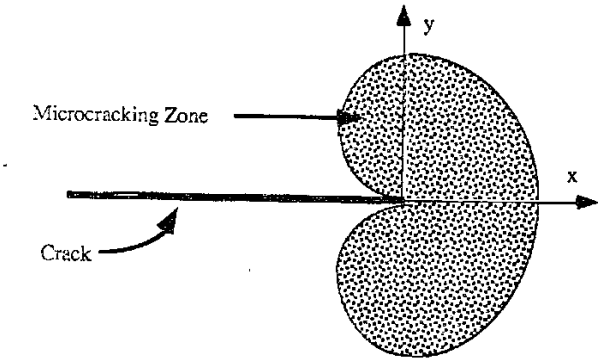

Figure 2.6 Schematic diagram of the microcracking mechanisms [44].

2.2.7 Fibre fracture

Fibres are the main load bearing constituents of a fibre reinforced composite, therefore fibre fracture can have a severe effect upon both the stiffness and strength of a composite. The fracture of even a very small number of fibres may be sufficient to initiate failure. Fibre fracture is considered the most detrimental to composite under tensile loading. The fracture energy associated with fibre fracture is commonly greater than that relating to matrix-dominated mechanisms. It has been shown in a carbon fibre/epoxy composite that transverse fibre fracture is the main energy absorbing mechanism in thin composites under impact [59].

2.2.8 Fibre/matrix debonding

When the stress in the fibre-matrix interface exceeds the local strength, debonding occurs and a crack forms, and extra energy is required due to the creation of new interfaces. Strong and thick fibres, low matrix shear strength and a strong interface, are needed to obtain high energies of debonding.

Beaumont [60] suggested that the energy for debonding in a continuous fibre reinforced composite is as follows:

$$W^d = \frac{\pi d^2 \sigma_f^2 l_d}{24 E_f} \tag{2.3}$$

where : d = fibre diameter

σ_f = tensile strength of the fibre

l_d = debonding length

E_f = modulus of the fibre

For a crack propagating normal to the direction of fibre alignment, debonding can occur if the crack is deflected on reaching the interface. Debonding can also be created under transverse or shear loading conditions.

2.2.9 Fibre pull-out

In a region of high stress concentration, such as a crack tip, fibres often fail and fracture. As the crack front continues to advance, these fibres are pulled out of the surrounding matrix. In overcoming the resultant frictional force, work is done and energy is dissipated. Depending on the interfacial roughness, contact pressure and sliding distance, this process can absorb large quantities of energy. It is potentially the most significant source work of fracture for most fibre composites.

Kelly and Tyson [61] assumed that the maximum fibre pull-out length is equivalent to half of the critical fibre length, l_c, and suggested that the work to pull out a fibre is:

$$W_p = \frac{\pi d \tau l_c^2}{24} \tag{2.4}$$

where l_c = critical stress transfer length

$$l_c = \frac{\sigma_f d}{2\tau} \tag{2.5}$$

σ_f = strength of fibre

d = fibre diameter

τ = interfacial shear strength

The critical length is derived from the theories for short fibre composites, whereby the fibre must be longer than the critical length in order to support the load transferred to the matrix. For fibre pull-out to occur, the end of the fibre to be pulled out must be shorter than the critical length, otherwise it would act as reinforcement and fibre failure would occur rather than fibre pull-out. When the fibre is shorter than the critical length, there are not enough shear forces to hold the fibre in the matrix, and the end will subsequently slip out. Drzal and Rich [62] studied the effect of matrix adhesion on composite fracture behaviour. Fracture of the composite

specimens in an opening mode with the crack perpendicular to the fibre axis showed a large degree of fibre pull-out in composite with low interfacial shear strength.

2.2.10 Fibre bridging

This happens when debonding has taken place, but the fibre is strong and has not fractured and the fibre will bridge the faces in the wake of a propagating crack. For the crack to continue to grow the faces must open. However, as the crack opens under the action of the applied stress, some of the stress will be transferred to the fibres, which will deform elastically. There is a corresponding reduction of stress intensity factor at the crack tip and hence crack propagation is hindered. This mechanism is most effective when strong fibres are used at a high volume fraction.

In Mode-I delamination testing, fibre bridging is observed between specimen halves when the delamination changes plane or if the interlaminar zone is poorly defined. Davies [63] pointed out that this phenomenon has been found more frequently in tough materials since their larger damage zones makes out-of-plane cracks more likely to occur. Schwartz and Hartness [64], however, indicated that the higher the toughness of the matrix, the less tendency there is for multiple crack formation and fibre bridging. They suggested that the fibre bridging phenomenon creates the additional fracture surface that is believed to give a high value of critical strain energy release rate, G_{1c}.

2.2.11 Delamination

Delamination is the debonding between adjacent lamellae. It occurs under a wide range of loadings such as in-plane quasi-static loading, tensile and compressive loading, and impact loading. Interlaminar shear stresses and normal stresses develop in laminated composite structures due to a mismatch in engineering properties between lamina within the laminate, and these stresses induce delamination initiation and propagation. Delamination is one the most important and frequently discussed

modes of failure in composite materials. Small areas of delamination are capable of reducing the compression strength of composite materials significantly [59, 65]. This form of interlaminar fracture reduces the stability of the load bearing fibres resulting in localised failure at low loads.

The fracture energy of delamination (Mode-I) can vary between 100 J/m^2 for epoxy composites to 3 kJ/m^2 for thermoplastic based composites [66]. Delamination is strongly dependent upon the ability of the matrix material to undergo shear flow. Delamination is rate dependent and fracture energy increases with strain rate [67]. Liu [68] has shown that under low velocity impact loading conditions, delamination is most severe at interfaces at which the difference in relative angle between the upper and lower plies is greatest, for example between ±45° plies.

Damage resistant designs to minimize the occurrence of delamination in composite structures typically focus on reducing the transverse normal interlaminar stresses in regions of stress concentrations. This is achieved, for example, by the proper selection of stacking sequences, the incorporation of wrapping plies in regions containing ply drops, avoiding curved sections with small radii, and the use of interleaves to reduce interlaminar stresses. Out-of-plane reinforcements, such as Z-pins and stitching, are also being considered for damage tolerant designs.

2.3 Approaches to epoxy matrix composite toughening

Epoxy resins are characterised by the presence of a three-membered ring containing two carbon atoms and an oxygen atom, which is variously called an epoxy group, an epoxide, an oxirane ring or an ethoxyline group. Epoxy resins are relatively low molecular weight prepolymers capable of being processed under a variety of conditions. They are either brittle, notch sensitive or both. There are many different types of epoxy resins available and the most extensively used resins are the diglycidyl ether of bisphenol A (DGEBA) and tetraglycidyl 4.4'-

diaminodiphenylmethane (TGDDM) [69]; the work presented in this thesis is based on these two epoxy resins.

The first liquid diepoxide reported was the reaction product of bisphenol-A with an access of epichlorohydrin in the presence of sodium hydroxide. The resin is commonly called diglycidyl ether of bisphenol A (DGEBA) and this is still the most important class of commercial epoxy resins. DGEBA is used extensively in industry due to its fluidity, processing ease, and good physical properties of the cured resin. The higher molecular weight homologs are represented by the following structure (Figure 2.7).

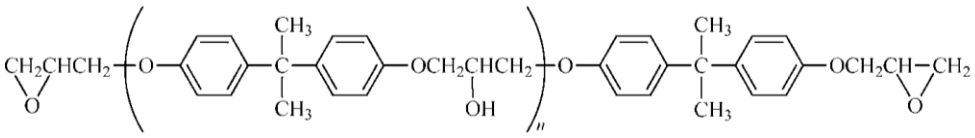

Figure 2.7 Structure of diglycidyl ether of bisphenol A (DGEBA).

TGDDM (Figure 2.8) is a tetrafunctional resin which provides higher cross-linking density than DGEBA, leading to improved thermal and chemical resistance compared to the cured DGEBA. It was one of the first systems to meet the performance requirements set by the aerospace industry. Because of its outstanding properties, this resin is often used as the primary resin in high temperature resistant formulations for military applications, despite its high cost. Among the attributes of the cured resin are excellent mechanical strength, high T_g, good chemical resistance, and radiation stability.

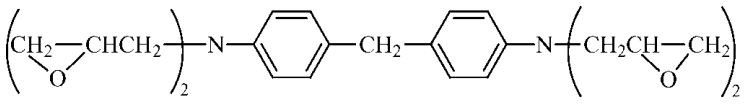

Figure 2.8 Structure of tetraglycidyl 4.4'-diaminodiphenylmethane (TGDDM).

2.3.1 Liquid rubber toughening

The incorporation of a rubbery phase into the matrix of a polymer is a common approach for toughening thermoplastics [2]. Therefore, as early as the 1970s, McGarry and co-workers [3] began to study the addition of certain liquid rubbers to thermosetting resins. In their studies, a relatively low molecular weight liquid rubber carboxyl terminated butadiene acrylonitrile (CTBN) was added to modify the DGEBA Epon 828. A significant improvement to the fracture toughness of the modified resins was observed. Since then, much research has been carried out on toughening epoxy resins by utilizing suitable liquid rubber copolymers of butadiene-acrylonitrile with various functional end-groups, including, amine (ATBN), hydroxyl (HTBN) epoxy (ETBN) and mercaptan (MTBN). However, the greatest benefit has been reported for CTBN (Table 2.1).

Table 2.1 Effect of functionality on the toughening ability of butadiene-acrylonitrile rubbers [70].

Rubber	Functionality	Fracture energy (kJ/m^2)
CTBN	carboxyl	2.8
PTBN	phenol	2.6-3.0
ETBN	epoxy	1.8-2.5
HTBN	hydroxyl	0.9-2.6
MTBN	mercaptan	0.2-0.4

The rubber domains are precipitated *in-situ* during cure, resulting in toughened epoxy materials. Numerous reports have been devoted to this area over the last two decades [4, 71]. Toughness enhancement of epoxy matrix with rubber demands a reaction (e.g. esterification) between the elastomer and the resin, which leads to an adequate bond between the rubber and epoxy phases. Attempts to apply HTBN for toughness improvement have encountered difficulties because the conditions required to promote the necessary hydroxyl-epoxy reaction generally lead

to self-polymerisation of the epoxy, the latter occurring at the expense of the former and, thus limiting the extent of rubber-epoxy reaction. A recent approach to this problem is to employ a co-reactant such as toluene diisocyanate (TDI), capable of reacting with both epoxide and hydroxyl functionalities resulting in the formation of both urethane [72] and oxazolidone links between the elastomeric and epoxide components. Silane coupling agents can also be used to improve the epoxy-rubber interface [73].

Toughened epoxy resins are prepared *in-situ* by quiescent bulk polymerisation of epoxy in the presence of dissolved rubber. Epoxy resin, curing agent and curing accelerator are mixed at room temperature in a specific ratio. The liquid rubber is added and carefully mixed until the mixture is homogeneous and clear. In order to control the rubber particle morphology and the final properties, the composition and concentration of rubber and hardener and curing temperature must be carefully controlled. During curing, the rubber phase separates directly into droplets without passing through a phase inversion step. Before the gel point, further nucleation and growth of the rubber phase may take place. Occlusions of epoxy resins are often formed during cure (Figure 2.9). Matrix-rubber particle adhesion develops because of the early chain extension reaction between the carboxyl groups in the rubber and the epoxy resin. The cured resin usually contains dissolved and solid rubber particles [74].

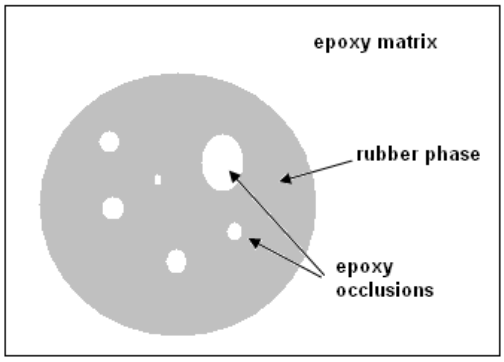

Figure 2.9 A schematic diagram showing phase separated rubber phase with epoxy occlusions.

The effect of rubber particle size on deformation mechanisms in epoxy system was studied by Sultan and McGarry [75], and it was found that there is a lower limit to the particle size below which only modest increases in fracture toughness are observed. They showed that 1 to 1.5μm particles were five times more effective than 0.1μm particles in increasing the fracture energy. Kinloch and Hunston [76] reported that a bimodal distribution of particle sizes of 0.1μm and 1.3μm resulted in higher values than unimodal distribution with a particle size of 1.2 μm. However, this enhancement of G_{1c} was found only over a range of temperature and rates, indicating that matrix effects also play an important role.

An increase in rubber volume fraction of the dispersed rubber phase generally promotes toughness of a multiphase thermoset. With a rubber volume fraction of 0.1 to 0.2 the fracture energy G_{1c} may be increased 10-20 fold. The main toughening mechanisms are localised shear in the form of shear bands running between rubber particles and internal cavitation or debonding of rubber particles with subsequent plastic growth of voids in the epoxy matrix [77]. A linear relationship exists in epoxy resin containing 8.7% CTBN, between the fracture surface energy and rubber phase volume fraction [1]. Kinloch and Hunston [76] showed that in the case of unimodal distribution of rubber particles at low test temperature, G_{1c} increases slowly with increasing volume fraction and then reaches a plateau. At high temperature the relationship is almost linear and the rate of increase of G_{1c} is far greater than that at low temperature.

Fracture toughness of rubber modified epoxy resin is strongly dependent on the crosslink density of the epoxy resin, the size of the rubber particles, and the cohesive strength of the particle. The addition of soft rubbery particles to an epoxy reduces its elastic modulus, yield strength, and thermal and creep resistance. In addition, rubber modification does not significantly improve fracture toughness in highly crosslinked systems [78]. This is not desirable as most advanced thermosetting resins used in aerospace applications are composed of highly

crosslinked network polymers, which are often very brittle.

Mechanical properties of rubber-modified epoxy resins depend on the extent of rubber phase separation and on the morphological features of the rubber phase. Dissolved rubber causes plastic deformation and necking at low strains, but does not result in impact toughening. The presence of rubber particles is a necessity but is not a sufficient condition for achieving high impact resistance. Optimum properties are obtained using materials comprising both dissolved and phase separated rubber [74]. Figure 2.10 illustrates the variation in notched Izod impact strength with an epoxy composition containing 15% CTBN; rubber particle size in these compositions varied up to 1 μm.

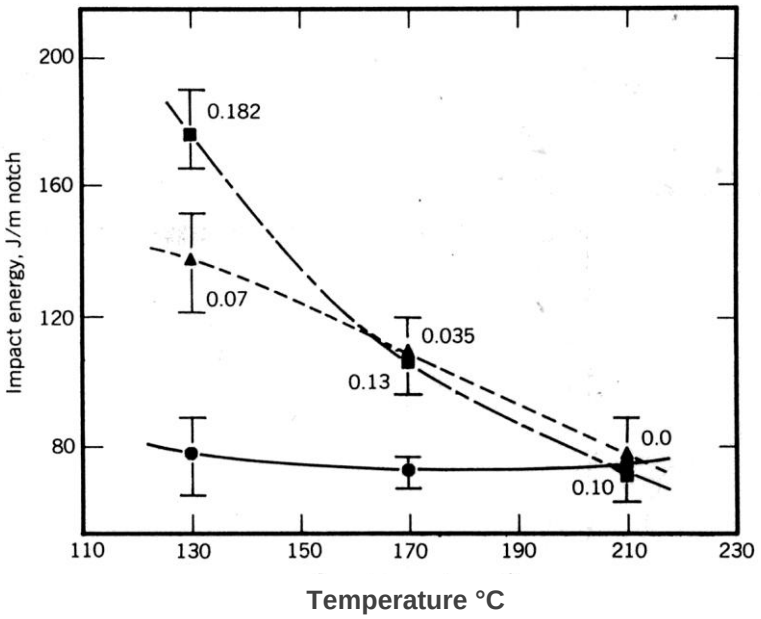

Figure 2.10 Notched Izod impact strength of toughened epoxy plotted against cure temperature: ■ 17% acrylonitrile (AN) in CTBN; ▲ 27% AN; ● no rubber. Numbers indicated volume fraction of phase separated rubber [74].

Rubber modified epoxy resins exhibit increased fracture toughness, but also show the deterioration of other important properties compared to the unmodified

resin. For example, Verchere *et al*. [79, 80] studied an ETBN modified epoxy and found that the fracture toughness K_{1c} and fracture energy G_{1c} increased slightly with an increasing volume fraction of the dispersed rubber phase, while the value of T_g decreased in a roughly linear way with the initial amount of rubber added to the formulation, which indicates dissolved rubber in the epoxy matrix. Hwang et al. [81] blended ATBN and ETBN into an epoxy matrix and found that the stress, fracture toughness and fracture energy were increased, while Young's modulus and yield strength decreased slightly when rubber was incorporated. It was found that the addition of CTBN can decrease the oxidation stability of epoxies, due to the high amount of unsaturated bonds in the CTBN backbone. This resulted in deterioration of the chemical and physical properties of the resin, especially at elevated temperature [82]. As an option, different kinds of liquid rubbers based on functionalised acrylic oligomers were chosen as toughening modifiers. These rubber modifiers do not contain unsaturated bonds in the backbone and can result in good resistance against oxidation processes [83, 84]. However the improved fracture toughness was accompanied by a decrease in the modulus and T_g of the modified epoxy resins.

Yan *et al.* [85] studied the toughening of a carbon fibre/DGEBA epoxy laminate modified with liquid rubber. It was found that 15 wt% of liquid rubber greatly improved the bulk resin toughness more than four-fold. However, the improvement of resin toughness was not translated to the laminate. The laminate toughness only improved two-fold with the addition of liquid rubber. The main toughening mechanism suggested was extensive plastic deformation near the crack tip due to the contribution of rubber domains to the matrix, such as lower yield strength and higher failure strain. In the laminates, the plastic deformation within the resin layer is limited by the neighbouring carbon fibre layers and the plastic zone ahead of crack tip is much smaller than in the bulk resin (Figure 2.11). High triaxiality is maintained at crack tip which suppressed plastic deformation and crack tip blunting.

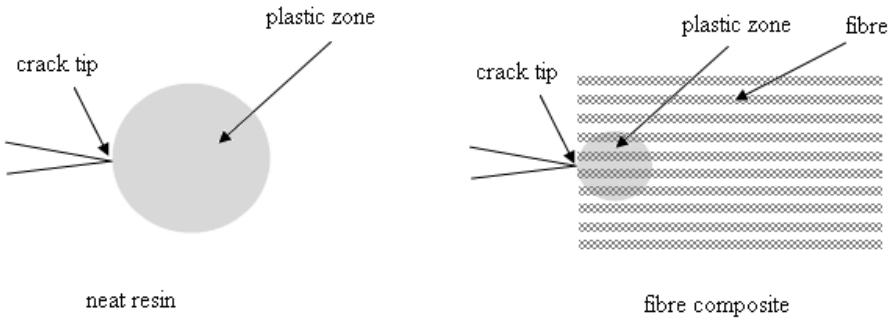

Figure 2.11 Plastic zone ahead of crack tip for neat resin and fibre composite

2.3.2 Thermoplastic toughening of epoxy resins

Liquid rubber-toughened epoxy resins have a major limitation: increased toughness can be achieved only by sacrificing both the high glass transition temperature and the modulus. Some industries, such as the aerospace industry, have growing demands for materials that display high thermal stability as well as toughness. As an alternative method, engineering thermoplastics have been used to improve the poor fracture properties of epoxy resins. These have been studied since the early 1980s, the main advantage of using thermoplastics in epoxy toughening is that there need not be a significant decrease in desirable properties as is the case with rubber toughening. As engineering thermoplastic modifiers are tough, ductile, chemically and thermally stable, and often have high T_g, they can toughen epoxy resins without negatively affecting their high temperature performance.

Min *et al*. [86] pointed out that, regardless of the type of modifiers, the properties of modified epoxy resins are determined by two major factors: (1) the basic properties of the resin as the bulk phase, and (2) the effect of the microstructure resulting from the presence of a second polymeric phase. These two factors are influenced concurrently by processing variables such as the matrix reactant ratios [87], the structure and reactivity of the curing agent, and the cure conditions [74, 88,

89]. The resultant microstructure is influenced by concentration [79], molecular weight [90], solubility parameter and the type of modifier.

Many thermoplastic-epoxy systems have been evaluated with regard to toughness. Not all attempts were successful (Table 2.2) [91], but successful attempts do share a similarity in that there is a two-phase morphology that consists of a ductile thermoplastic phase together with a brittle epoxy phase. However, the specific requirements of the toughening phase have not been identified. The influences of type of morphology, particle size, particle-matrix adhesion, and the mechanical attributes of the thermoplastic phase have not been clearly established. It appears that thermoplastic toughening of epoxy is not as well understood as rubber toughening. This is because a schematic study is difficult since different epoxy resins, curing agents, thermoplastics, and processing cycles were used in the various studies.

Table 2.2 Properties of various thermoplastic modified epoxy blends [91].

Thermoplastic modifier	T_g (°C)	Tensile modulus (MPa)	Yield stress (MPa)	Phase separation	Max ΔK_{Ic} (MPa $m^{1/2}$)
Polyetherimide (PEI)	220	2.8	105	no	0.0
Polyphenylene oxide (PPO)	205	2.6	78	yes	0.9
Polycarbonate (PC)	245	2.4	62	no	0.0
Polybutylene terepthalate (PBT)	50	2.3	55	no	0.0
Reactive polystyrene (RPS)	105	3.3	35	yes	-0.1
Polyetherimide dimethyl siloxane (PEI-PDMS)	-	0.5	‹30	yes	0.9
Polycarbonate dimethyl siloxane (PC-PDMS)	100, 120	0.3	-	yes	0.2
Polystyrene butadiene styrene (SBS)	81, 87	0.03	N/A	yes	N/A

A brief description of the main groups of thermoplastics that are added to epoxy resins given below and studies related to them are outlined. One thing to note though is that some of the polymers mentioned below are employed as thermoplastic matrices for composites.

2.3.2.1 Epoxy/phenoxy blends

Teng and Chang [92] looked at phase separation of phenoxy/DGEBA epoxy blends and found that the resulting morphology could be controlled by kinetic control of curing by altering the amount of accelerator added. It was also found that the viscosity at the initiation of phase separation was an important factor in determining the final morphology. It was pointed out that if the critical viscosity was reached, the phenoxy suffered complete freeze-in or lock-in within the epoxy matrix, making diffusion and coalescence difficult. The mechanical properties of the blends are shown in Table 2.3.

It was found that blends with higher concentrations achieved high fracture toughness as the dissolved phenoxy improved the intrinsic toughness of epoxy, but the modulus, stiffness and T_g were reduced. The key toughening mechanism suggested was particle induced shear yielding, which could contribute to crack tip blunting prior to crack initiation and localised energy dissipation during crack propagation [17]. Guo [93] studied the effect of curing agents on phenoxy/DGEBA epoxy blends. It was found that when any one of 4,4'-diaminodiphenylmethane (DDM), aliphatic anhydrides or hexahydrophthalic anhydride (HHPA) was used as curing agent, no phase separation occurred. However, phase separation (droplet structure) did occur when either 4.4'-diaminodiphenyl sulfone (DDS) or phthalic anhydride (PA) was used as curing agent, and the interface between the phenoxy phase and the epoxy matrix was stronger in the PA cured system than in the DDS cured system.

Table 2.3 Properties of phenoxy/epoxy blends cured with curing agent DDS and accelerator 1-cyanoethyl-2-ethyl-4-methylimidazole (CEMI). Phenoxy content was 10 phr [17].

Blend	Phase separation	Tensile strength (MPA)	Tensile modulus (GPa)	K_{Ic} (MPam$^{1/2}$)	G_{Ic} (J/m^2)	T_g (°C)	
						Phenoxy	Epoxy
Phenoxy	-	61	1.9			93	
Epoxy/DDS	-	73	3.0	0.75	158		194
Phenoxy/Epoxy/ DDS (0 wt% CEMI)	Yes	71	2.9	1.06	325	89	189
Phenoxy/Epoxy/ DDS (0.1 wt% CEMI)	Yes	71	2.8	1.08	350	92	190
Phenoxy/Epoxy/ DDS (0.15 wt% CEMI)	Incomplete	70	2.6	1.08	377	104	189
Phenoxy/Epoxy/ DDS (0.3 wt% CEMI)	No	68	2.5	1.11	414	-	184
Phenoxy/Epoxy/ DDS (0.5 wt% CEMI)	No	65	2.2	1.20	550	-	178

.

Table 2.4 Properties of phenoxy/epoxy blends cured with DDS with different phenoxy content [94].

Blend	Phase separation	Tensile strength (MPa)	Tensile modulus (GPa)	Tensile strain (%)	K_{Ic} (MPam$^{1/2}$)
Epoxy/DDS	-	33 ± 3	3 ± 0.1	1.9 ± 0.6	0.7
Phenoxy/Epoxy/DDS 10 wt% phenoxy	Droplet	41± 3	3 ± 0.1	2.8 ± 0.4	0.9 ± 0.2
Phenoxy/Epoxy/DDS 20 wt% phenoxy	Interconnected globules	74 ± 10	2.9 ± 0.1	6.7 ± 1.3	3.2 ± 0.9
Phenoxy/Epoxy/DDS 30 wt% phenoxy	Phase inverted	62 ± 5	2.8 ± 0.1	5.6 ± 0.7	2.3 ± 0.3
Phenoxy/Epoxy/DDS 40 wt% phenoxy	Phase inverted	47	2.5	3.4 ± 0.3	1.1 ± 0.1

Improvement in fracture toughness was also observed in another study with phenoxy/DEGDA blends cured with DDS (Table 2.4) [94], and various morphologies were observed depending on phenoxy loading. It was suggested that an interconnected globular morphology was beneficial for enhancing toughness by stretching and tearing of the phenoxy phase

In a study on an epoxy-PMMA-phenoxy system [95], it was observed that a particulate morphology was formed at low thermoplastic (TP) loading (<5 wt%), co-continuous morphology at moderate loading (10 wt%) and a phase inverted morphology at higher loading (15 wt%). A significant increase in fracture toughness (Table 2.5) was observed especially for the mixtures with some level of co-continuity. However, phase inversion led to poor strength and also fracture toughness, which suggested that a high TP loading would not be recommended.

Table 2.5 Mechanical properties of ternary epoxy mixture with phenoxy as the main thermoplastic [96].

PMMA (%)	Phenoxy (%)	Tensile modulus (MPa)	Flexural strength (MPa)	K_{Ic} (MPa $m^{1/2}$)	G_{Ic} (J/m^2)	T_{g1} (°C)	T_{g2} (°C)
0	0	2580 ± 20	120 ± 1	0.80 ± 0.1	230 ± 30	-	224
0	5	2680 ± 40	125 ± 2	1.00 ± 0.06	320 ± 40	95	222
2	5	2745 ± 80	132 ± 4	1.28 ± 0.10	525 ± 50	95	220
5	5	3010 ± 35	123 ± 8	1.45 ± 0.12	615 ± 100	105	216
0	10	2515 ± 70	115 ± 5	1.34 ± 0.34	650 ± 315	95	213
2	10	2720 ± 35	121 ± 2	1.51 ± 0.10	735 ± 90	95	213
5	10	2810 ± 55	130 ± 3	1.70 ± 0.13	905 ± 135	106	213
0	15	2790 ± 25	130 ± 2	1.03 ± 0.08	335 ± 50	95	210

Woo and Mao [18] introduced three commercially available amorphous thermoplastics (PEI, PC and phenoxy) in powder form (~ 10 μm) onto the surface of a unidirectional tape prepreg, based on carbon fibre with epoxy TGDDM and DDS

as hardener (Table 2.6), by spraying the thermoplastic powder to obtain an areal density varying from 0 to 40 g/m^2. The fibre volume fraction of the laminates was between 60 and 62 vol%. The addition of phenoxy to epoxy improved the G_{1c} and the degree of improvement was said to be similar to that of PEI modified composite [13], however, the areal densities of the PEI and phenoxy were different (17.5 gm^{-2} for PEI and 21.5 gm^{-2} for phenoxy) which might have had an effect on the values. The G_{IIc} values for the phenoxy system were found to be lower than for the PEI system, although no explanation was presented. Woo and Mao [18] also found that the morphology of the phenoxy modified system reflected phase inversion, in which the epoxy particles were surrounded by a continuous phenoxy-rich phase. The epoxy particles were around 3-5 μm in diameter. When etched with THF, the insoluble epoxy particles were not fully exposed and had rough surfaces and it was suggested there might have been chemical reaction at the epoxy/phenoxy interface.

Table 2.6 Comparison of fracture toughness of composites toughened with PEI, phenoxy and PC [13].

Polymer	Areal density (g/m^2)	G_{Ic} (J/m^2)	G_{IIc}(J/m^2)
None	0	165	290
PEI	17	420	910
Phenoxy	21.5	440	640
PC	9.5	108	-
PC	20	100	-

2.3.2.2 Epoxy/polyester blends

In one study [97], the tensile strength and impact strength of specimens of DGEBA epoxy resin containing levels of PET ranging from 0-24 wt% were measured. Enhancement in impact strength and tensile strength was found in all PET modified specimens. It was found that the impact strength increased with increasing

PET content up to 16 wt%, but beyond that, the enhancement in impact strength decreased. At the optimum PET content (16 wt%) a 138% increase in impact strength was observed. A similar trend was observed for the tensile strength, where the optimum PET content was 16 wt% which showed a 46%. There was no change in the T_g of the PET modified specimens. DGEBA has been found to be a good solvent for PET and has been studied as a reactive solvent for PET in order to reduce the viscosity of PET during processing [98, 99], while work has also been done on the studying the miscibility of epoxy-PET blends [100].

One of the first studies on PBT modified epoxy was carried out by Kim and Robertson [19]. It was found that PBT was an effective toughening agent compared to other polymers (Figure 2.12).

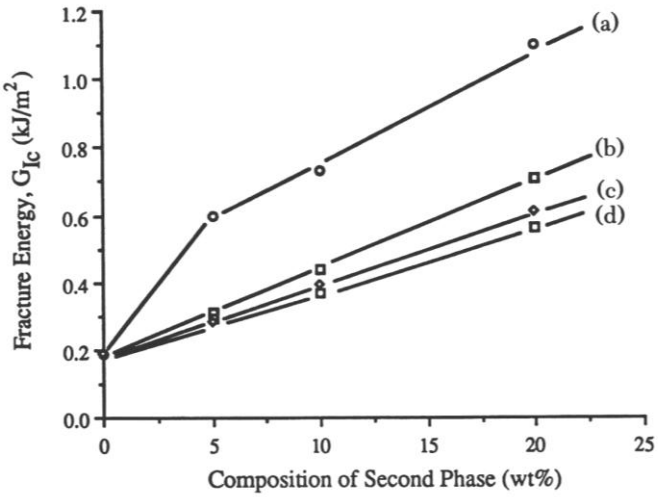

Figure 2.12 Initiation fracture energy for (a) PBT; (b) nylon 6; (c) CTBN; (d) PVDF [19].

Processing conditions were also found to affect the morphology and final properties significantly [19]. The recommended procedure was to mix the PBT particles with epoxy at an elevated temperature prior to adding the curing agent at room temperature, followed by curing of the epoxy resin. The T_g of the epoxy and

the melting temperature of the PBT were generally lowered. The Young's modulus and yield strength remained unchanged with the addition of PBT.

Oyanguren *et al.* [101] studied the phase separation behaviour of PBT in epoxy by constructing conversion temperature transformation (CTT) diagrams. It was found that by using different curing agents and curing temperature, different morphologies could be obtained. The PBT could be either kept in solution or phase separated. It was found that PBT crystallisation could be made to take place either initially or in the course of the cure. Different ways of segregating PBT from the matrix were therefore found to be possible. When crystallisation happened before gelation, a broad distribution of irregular shaped crystals was formed, and a narrow distribution of small spherical particles was produced by reaction induced phase separation. It was suggested [102] that the generation of a second phase rich in modifier is a necessary condition to introduce a toughening effect and that crack bridging by highly drawn thermoplastic particles is the main toughening mechanism. However, in contrast to the previous study by Kim and Robertson [19], the improvement in toughness was only modest for a PBT loading of up to 7.5 wt%. Similar results were presented in another study [103] in which the K_{Ic} value of the modified resin changes only slightly, although the values of K_{IIc} were found to have increased. The effect of the morphology and crystallinity of the PBT phase on modified epoxy were further studied by varying the blending temperature [104]. PBT spherulites with a well-developed crystallinity were found to be most effective for epoxy toughening. It was suggested the improvement in toughness was achieved *via* phase transformation, which has been known in zirconia containing ceramics. The claim is based on the fact that PBT undergoes a stress induced transformation with volume expansion like zirconia. However, no direct observation of the phase transformation could be made The fracture surfaces of the blend revealed other toughening mechanisms such as bifurcation, plastic deformation of the PBT phase, crack path alteration and crack bridging. Similar results and conclusions were presented when poly(tetramethyleneglycol) (PTMG) [105] was added to the epoxy-

PBT blend to create a ternary system. It was found that the addition of PBT-PTMG combination could increase the toughness more than either component used alone. It might be worth noting that in both studies, the samples made from mixing pre-made TP powder had higher fracture toughness that the ones made from dissolution-precipitation via melt blending. It was explained that more perfect crystals could be formed by using pre made powder, although no evidence was shown in the study whether the two processing routes had any effect on phase separation or the final morphology. The size of the TP phase was found to be dependent on the composition of the blends, but a relationship between phase size and fracture toughness could not be drawn.

Hydroxyl terminated polyester of different molecular weights (Figure 2.13) were added to DGEBA in order to produce different morphologies [106]. Low molecular weight polyester produced a single phase morphology (up to 20 wt% TP) while phase separation and phase inversion occurred for polyesters with higher molecular weight. Both dissolved and phase separated polyester proved to be capable of increasing toughness although the phase separated polyester particles improved toughness by a larger extent.

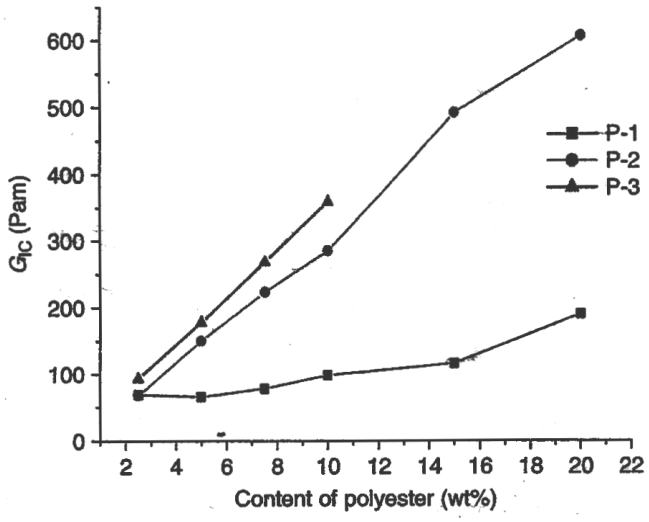

Polyester	M_n (g/mol)	M_w (g/mol)
P-1	6430	10400
P-2	8550	23500
P-3	24000	58100

Figure 2.13 Effect of polyester content on the G_{Ic} of different polyester/epoxy blends [106].

Tanoglu *et al.* [107] studied the effect of adding a polyester binder (~ 250 μm diameter) to a woven glass fabric/DGEBA-amine system. It was found that the G_{Ic} was lowered by 60% when 2.6 wt% of binder was added, and the T_g by 6 ºC, which is very significant. There was evidence that the dissolution of the polyester binder within the reacting matrix resin was limited by the standard cure cycle employed, however, there was no indication on how this might have affected the results. While it was clear that the polyester had a significant effect on the mechanical properties of the composite, the underlying mechanism was not presented.

More recently the use of hyper-branched polyesters (HBP) as modifiers has attracted much attention. HBP molecules are composed of three parts: a multifunctional core, several layers of monomer molecules and a multifunctional shell. This structure ensures that they have a very high level of functionality compared to linear additives enabling their interaction with a polymer matrix to be controlled through varying the terminal functionalities. The highly branched architecture minimises chain-chain entanglement and imparts high solubility and low melt viscosity to these polymers. HBPs have been shown to be suitable for modifying epoxy resins, since they can form a miscible blend with the epoxy followed by phase separation during cure. The viscosity of HBP-epoxy blends remains low, making liquid moulding possible.

HBPs were first studied by Boogh and co-workers [108]. It was reported that with the appropriate choice of end groups, an HBP loading of 5% increased the G_{IC} by 6-fold and K_{Ic} by 2.5 fold. Toughening was reported to be more effective than with other modifiers without affecting the Young's modulus, T_g or the processability of the resin system. The observed toughening mechanism was particle cavitation, in which the particle induced large areas of stress concentration leading to extensive shear deformation. The high toughening capacity of HBP was suggested to be induced by a concentration gradient within the phase separated particles. Singularity or rigidity at the interface between the particle and the matrix was therefore

eliminated, which led to improved load transfer between the particle and matrix. Other authors have also successfully toughened epoxy resins with HBP, and have mentioned a threshold value for the HBP loading beyond which no further improvement in toughness was observed. However, there is disagreement over the threshold value, since some researchers quote 20 wt% [109], while another study found the value could be as low as 7.5 wt% [110].

One of the first studies of HBP modified epoxy composites was done by Mezzenga [109], in which a dendritic HBP was added to epoxy. It was shown that the G_{Ic} value increased by 100% for a DGEBA matrix modified with 5 wt% of HBP, for both glass and carbon fibre composites. For TGDDM, which is highly crosslinked, a higher amount of HBP (15 wt%) was required to achieve a similar degree of toughening. It was suggested that the processing of a composite has a significant role in controlling phase separation and, therefore, affecting the final properties. The proposed composite toughening strategy using HBP is summarised in Figure 2.14. It was suggested that modifier filtration should be avoided and optimum toughening performance could be achieved with a particulate structure of HBP within the matrix. In order to obtain this the HBP used should be fully soluble in the uncured resin and should phase separate during curing. It was also mentioned that time-temperature-transformation diagrams (Figure 2.15) could be a useful tool in determining the optimal processing conditions. Impregnation should be performed above the phase separation temperature and before it occurs. In the study, different curing cycles were used to show the effect of processing conditions on internal stress, but their effect on toughness was not available. As well as increasing toughness, it was shown that HBP addition can reduce the build up of internal thermal stresses in a composite material.

However, the increase in toughness with HBP modified resin is not guaranteed as it was found to be dependent on the adhesion between the modified resin and fibre at the interface [110]. It was found that while HBP modified resin

increased the toughness of the composite, the improvement was less than what could be achieved with bulk resin and there was a larger scatter of G_{1c} values (Figure 2.16). It was suggested that when HBP (7.5 wt%) modified epoxy was used as a matrix for carbon fibre composite, the HBP consumes the amine groups near the fibres. A possible solution is to apply suitable surface treatment to the fibres (e.g. amine-silanes) or to have an excess amount of amine in the resin. It was found that by adding the extra amine, the G_{Ic} value of the composite increased by 130%. However, excess amine might have affected the curing of the epoxy and the T_g was decreased by 30ºC. The stiffness of the systems was also lowered by the inclusion of HBP.

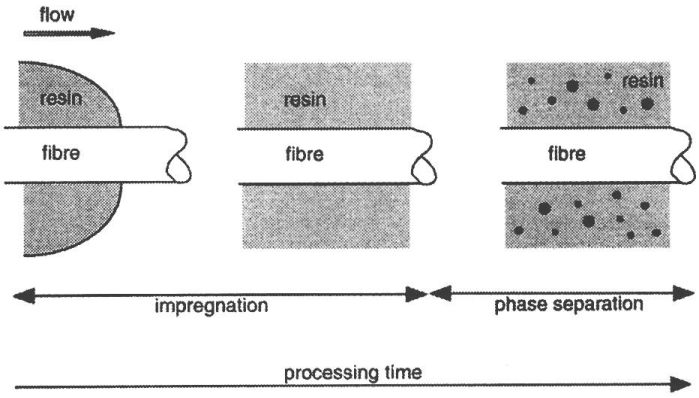

Figure 2.14 Proposed phase separation mechanism with regard to processing [109].

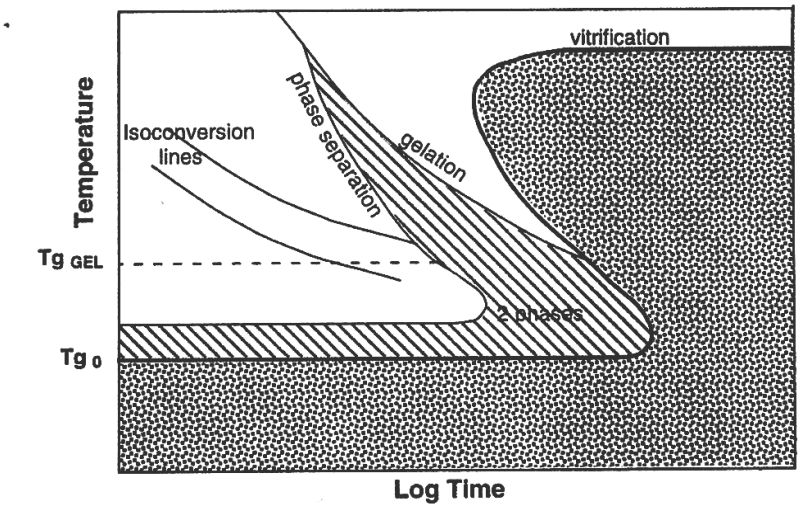

Figure 2.15 A typical TTT diagram for a HBP modified epoxy resin [109].

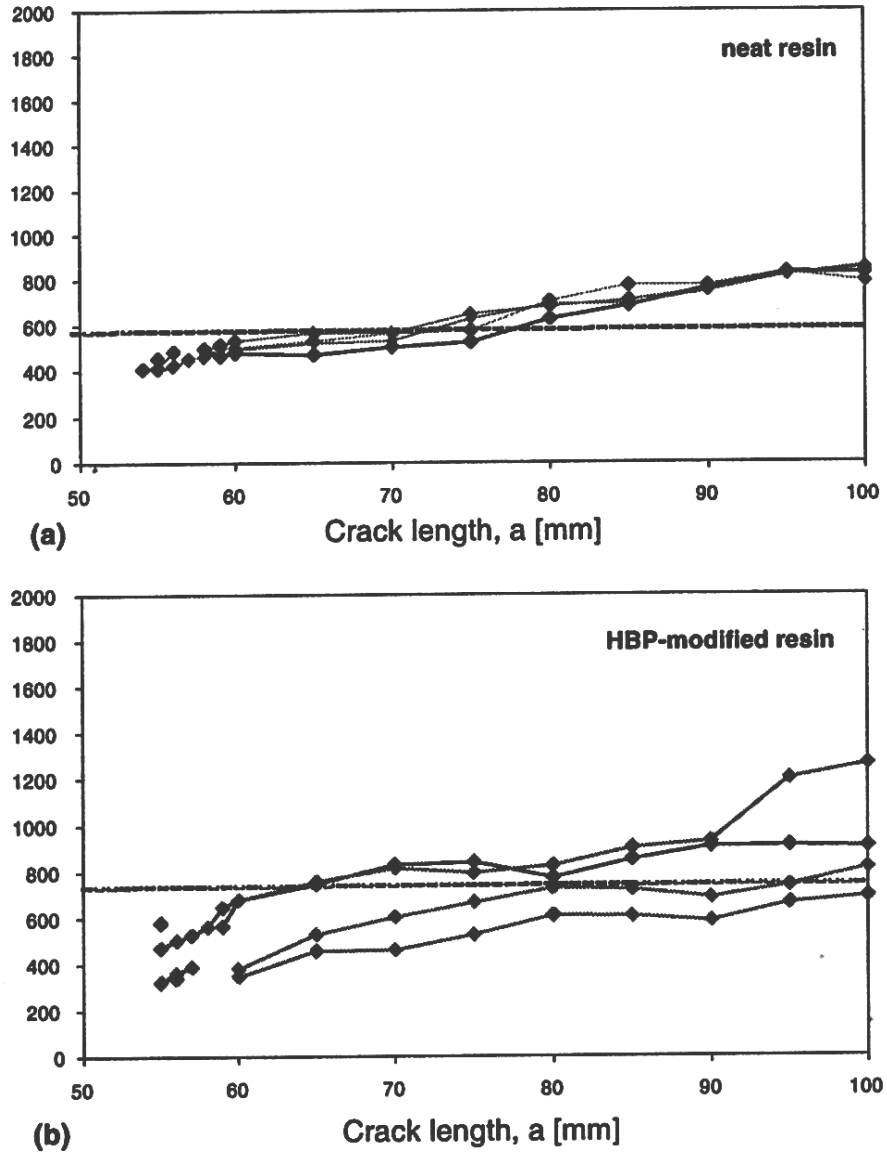

Figure 2.16 Fracture toughness, G_{Ic} , for unmodified (a) and HPB modified (b) laminates [110].

DeCarli and co-workers' work [111] on an epoxy-anhydride matrix modified with a commercially available aliphatic polyester HBP in a unidirectional carbon fibre prepreg system showed marked improvements in G_{Ic}. An increase of 224% in G_{Ic} was achieved when 10 wt% of HBP was added. The source of improvement was

suggested to be the large degree of interaction between HBP particles and epoxy matrix. The fracture toughness of the bulk resin was found to increase linearly with HBP content, but for composites, a maximum increase was found at 10 wt% HBP (Figure 2.17) [111]. It was suggested that the carbon fibre acts as a rigid filler and constrains plastic deformation at the crack tip. Decreases in modulus and other properties are shown in Table 2.9. There was no apparent phase separation when the sample was viewed under SEM. There was also no explanation given for the toughening mechanisms.

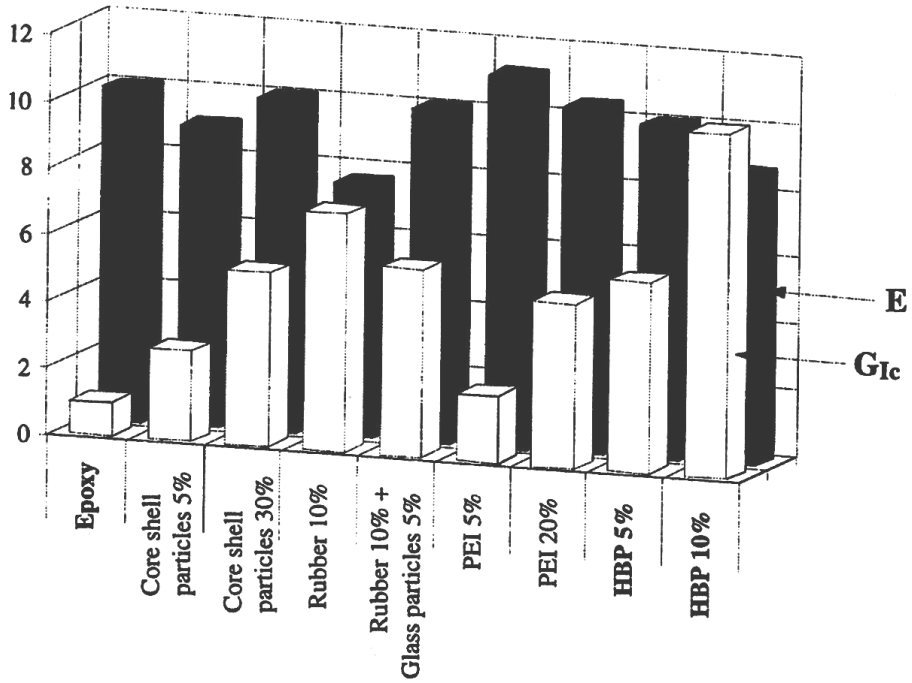

Figure 2.17 Comparison for various epoxy blends toughened with commercially available tougheners. Toughness, $G_{Ic,}$ and modulus E, are normalised to the unmodified epoxy resin [111].

Table 2.7 Mechanical properties for HBP modified systems [111].

Sample	Flexural modulus (GPa)	Flexural strength (MPa)	ILSS (MPa)	ILSS decrease at 121°C (%)
Neat resin	107.2 (2.8)	851.2 (98.7)	47.0 (1.2)	51.1
5 wt% HBP	108.7 (3.8)	819.7 (70.4)	45.8 (2.3)	58.5
10 wt% HBP	96.7 (1.6)	740.0 (65.2)	38.0 (2.3)	57.6
15 wt% HBP	96.9 (1.9)	733.9 (32.3)	36.7 (2.4)	59.2
20 wt% HBP	96.9 (3.4)	709.8 (61.9)	36.9 (3.8)	64.2

2.3.2.3 Epoxy/polyimide blends

Bucknall and Gilbert [112] used a commercial PEI to modify epoxy with considerable success (Figure 2.18). It was concluded that the toughening mechanism was particle bridging. Hourston *et al*. [113] added PEI to different epoxies having different functionalities and looked at the effect on tougheness. It was found that the mixtures of di- and tri-functional epoxies, which have the lowest crosslink density and highest ductility were more toughenable than those with a higher crosslink density. The blend expected to have the highest crosslink density (75/25 TGDDM/TGPAP) showed a slight decrease in fracture toughness (Figure 2.19). Su *et al*. [114] investigated the effect of PEI addition to epoxy and found that PEI increased the reaction rate during epoxy curing. It was suggested that this was due to the enhanced mobility of the network caused by the plasticization of the epoxy phase by the PEI. Another reason suggested was that the epoxy also plasticized the PEI rich phase, resulting in an epoxy network with a lowered crosslink density. Based on previous works on polysulfone (PSF) [9], a thin film of PEI was prepared and its dissolution and consequent phase separation were studied. It was observed that a range of morphologies were present due to the concentration gradient of the PEI.

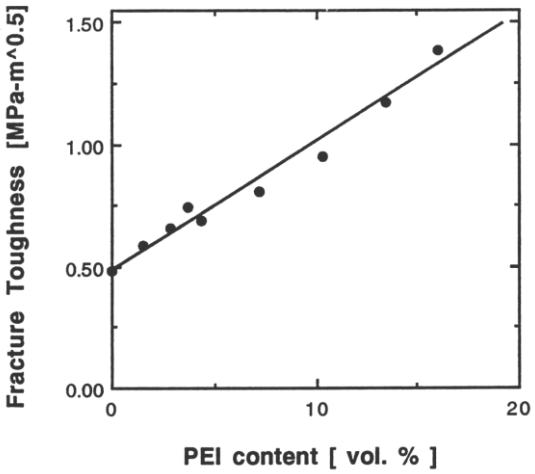

Figure 2.18 Fracture toughness of a tetrafunctional epoxy system modified with a commercially available PEI [112].

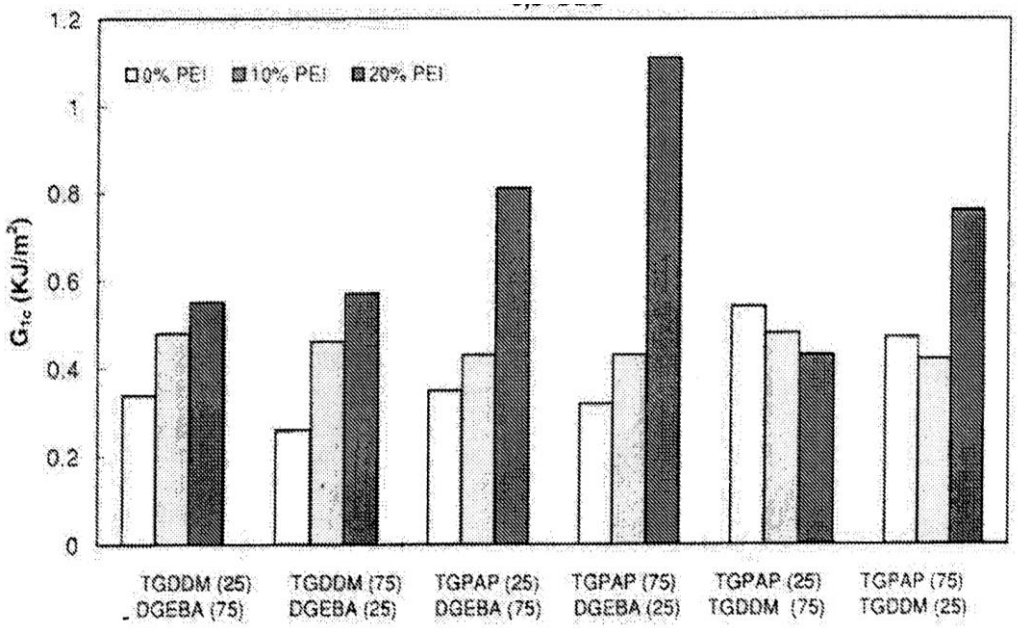

Figure 2.19 Fracture toughness of PEI modified epoxy of different functionalities [113].

A copolymer of PEI:PSF was used as a toughener by Giannitti *et al.* [115] with a TP loading of 10 wt% to 15 wt% in epoxy. It was found that by replacing a small amount of PEI with PSF, the morphology was changed drastically compared to

systems including only PEI. Replacing 25% of PEI by PSF changed from particulate to a co-continuous structure (at 10 wt% total TP). Maximum fracture toughness was associated with a co-continuous morphology. Ductile tearing of the TP phase, crack bridging and crack pinning were the suggested toughening mechanisms.

Woo and Mao [18] introduced three commercially available amorphous thermoplastics, PEI, PC and phenoxy in powder form (~ 10 μm) to a unidirectional tape prepreg based on carbon fibre and epoxy TGDDM with DDS as hardener (Table 2.6). The thermoplastic powder was sprayed on top of the prepreg and the areal density varied from 0 to 40 g/m^2. The fibre volume fraction of the laminates were between 60 to 62 vol% and the addition of phenoxy to epoxy improved the G_{1c} (Figure 2.20). For the PEI/epoxy blend, the PEI powder was initially melted and dissolved into the epoxy matrix before phase decomposition occurred as the crosslink density increased by the cure reactions. The morphology developed in the interlaminar region was a phase-in-phase domain type thought to result from spinodal decomposition, with discrete, spherical epoxy domains surrounded by PEI domains which, in turn are occluded by a much larger epoxy continuous phase domain.

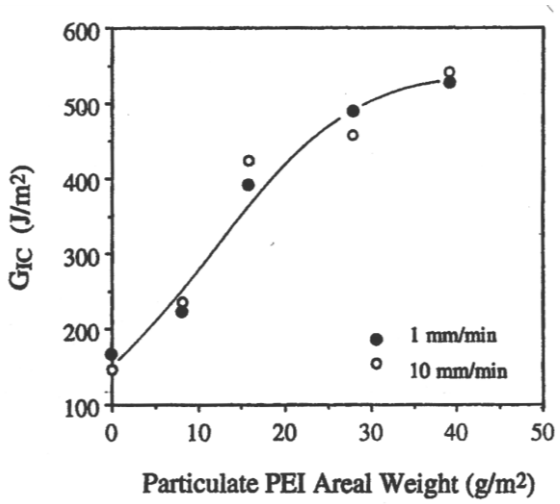

Figure 2.20 G_{Ic} as a function of PEI particulate areal weight. The two sets of data represent those tested under two crosshead speeds, 1 and 10 mm/min, respectively [18].

Turmel and Partridge [11] prepared PEI/DGEBA prepreg with unidirectional (UD) glass fibre. Heterogeneous phase separation between PEI-rich and epoxy-rich regions was observed in the vicinity of glass fibres. There was preferential wetting of glass fibres by the epoxy-rich phase. Discrete epoxy-rich layers could be found around the fibre in blends that had a co-continuous morphology, i.e. 15 to 20 wt% of PEI in the blends. While the toughness of the composites improved, the extent of improvement significantly lagged behind that for bulk resin (**Error! Reference source not found.**). The lack of property transfer from pure resin matrix to the composite was attributed to the premature interfacial failure either at the interface of the epoxy-rich phase with the fibre at low PEI content, or at the interface between the epoxy-rich phase and the PEI-rich phase at high PEI content. It should be noted that no heterogeneous phase separation was observed for carbon and aramid fibres. Preferential wetting of epoxy around carbon fibres was also observed in a system in which epoxy was used as a reactive solvent for a poly(phenylene ether) (PPE) matrix [14]. An epoxy-rich layer was formed around the fibre with the matrix mainly consisting of PPE. Instead of lowering the fracture toughness, as with the epoxy/PEI composite, the presence of the epoxy interface enhanced fracture toughness of this system here, as the adhesion between the epoxy-rich phase and CF is stronger than between the neat PPE and CF interface.

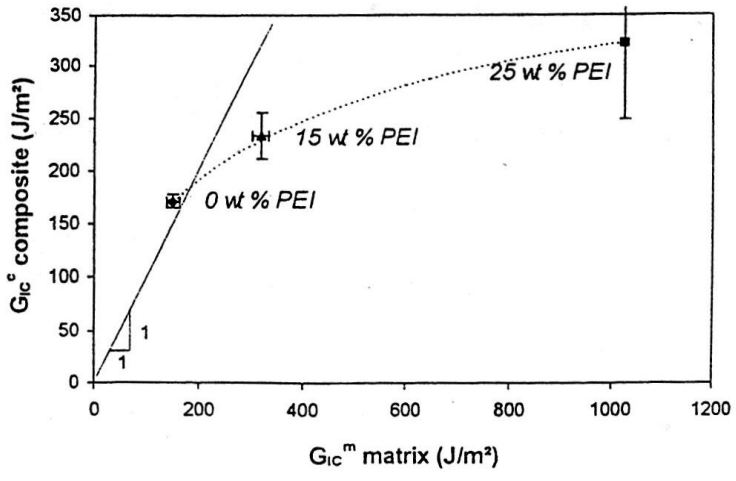

Figure 2.21 Variation of fracture toughness of composite and bulk resin of PEI modified epoxy [11].

Another study on PEI-epoxy by Bonnaud *et al.* [12] again concentrated on how the introduction of glass fibre into the resin affected the morphology and properties. Here, the PEI was melt blended with DGEBA and the composite pregreg was made by filament winding. The addition of PEI improved composite toughness and it was found that when up to 10 wt% commercial PEI was added to the epoxy, the blend became heterogeneous and a range of morphologies was observed. In the bulk matrix area, a phase-inverted morphology was obtained and in the area having a higher concentration of fibres, the morphology was formed by PEI rich nodules dispersed in an epoxy-rich continuous phase. Similar results were obtained for carbon fibres. It was suggested that the fibres acted as a barrier against PEI flow and that a physical effect was being observed. An amino-grafted PEI (PEI-NH_2) was also used with the aim to introduce chemical linkage between the PEI and epoxy, which could possibly result in a more uniform morphology. A homogeneous structure consisting of a regularly dispersed PEI-NH_2 rich phase (0.25 μm) was achieved and the improvement in toughness of such system was found to be higher than for a commercial PEI-modified system (G_{IIC} increased by 64% and 32% respectively with 10 wt% TP). It was mentioned that for PEI-NH_2 phase separation occurred around the gelation point, whereas for commercial PEI phase separation occurred before gelation. It was postulated that when phase separation occurs before gelation the separated PEI can migrate whereas, if phase separation occurs around gelation, the separated PEI will be locked in place. It was, therefore, concluded that the final morphology was dependent on both reaction rate and phase separation behaviour. However, if the final morphology relies on phase separation around the point of gelation, by selecting an appropriate curing cycle (with the use of a TTT diagram), commercial PEI modified epoxy matrix could potentially form a uniform morphology as well. In agreement with other studies, while the modified matrix improved the toughness of the composite, no direct relationship could be made between bulk resin and composites properties.

In a study where PEI film was used in composites prepared by resin transfer moulding (RTM) (Figure 2.22) [116]. The PEI film dissolved after resin injection thus keeping the viscosity of the epoxy resin low during injection. A matrix with a homogenous morphology was formed but phase separation was difficult to detect although there was evidence of a uniform distribution of small particles (~1 μm) when using 10 wt% PEI. With a PSF film [7], no distinct morphology was observed. It should be noted that for the PEI/epoxy system, no distinct morphology was observed even when the PEI film was dissolved in bulk epoxy without the presence of fibres, which is in contrast to a PSF/epoxy resin system by Min and Kim [9]. This was attributed to a fast diffusion rate with regard to the polymerisation kinetics and the subsequent phase separation. The study concentrated on the process of film dissolution and its effect on viscosity and mechanical properties was not presented. The study pointed out the need to study the relationship between processing time, temperature and film thickness in order to achieve complete film dissolution. The use of thin films allows for localised toughening as the films can be positioned wherever needed.

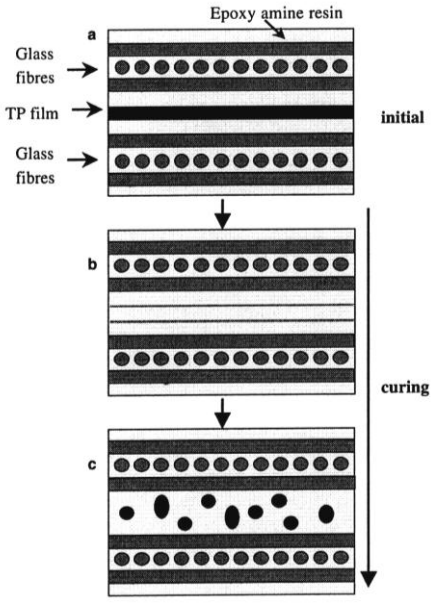

Figure 2.22 RTM processing based on in-situ generation of a thermoset/thermoplastic polymer blends: (a) insertion of a TP film between fibre plies, (b) dissolution of the TP film and polymerisation processes, (c) generation of a TP dispersed phase and final curing of the epoxy matrix [116].

2.3.2.4 Epoxy/polyether blends

Attempts have been made to use PC to epoxy as toughen epoxy by melt blending. Lu *et al*. added PC (6 to 12 wt%) to different epoxies [117] and found that PC increased the curing rate of epoxy, while there was also a chemical reaction between them. Not all the blends in their study phase separated and, while flexural modulus increased, the impact strength decreased for all the systems studied regardless of whether phase separation took place or not. Don *et al*. [118] looked at the effect of adding PC to epoxy in two ways, i.e. solution and melt blending. In samples prepared by solution blending, a separated crystalline phase was observed while no phase separation could be seen in samples made by melting blending. Similar to Lu's study, the tensile modulus was found to have increased. It was suggested that this could be caused by PC crystallites in the solution blended samples and by hydrogen bonding between PC and epoxy in both solution and melt blended samples. It was noted that no increase in fracture toughness was found in samples prepared by solution blending while an increase was found in the melt blended samples. It was suggested that the increase in toughness was due to the bonding of ductile PC chains onto the epoxy network through melt blending, which favoured plastic deformation.

Woo and Mao [18] introduced three commercially available amorphous thermoplastics, PEI, PC and phenoxy in powder form (~ 10 μm) to a unidirectional tape prepreg based on carbon fibre and epoxy TGDDM with DDS as hardener (Table 2.6). Amorphous PC is readily soluble in the TGDDM or DGEBA epoxy giving a homogeneous mixture. This then undergoes complex copolymerisation and exchange reactions and forms a homogeneous polymer/epoxy network after curing. It was originally thought that PC, which is tough and amorphous like PEI, would have a similar toughening effect to PEI or phenoxy polymer. However, it was found that PC did not improve fracture toughness and in some cases even decreased it. It was found that the initially amorphous PC was crystallized during powder processing and the

crystals would not melt at the curing temperature. The semi-crystalline PC powder was brittle and did not provide straining ability.

Similar to Woo and Mao's work, another work on PC modified epoxy [119] found that the addition of PC decreased the interlaminar shear strength (ILSS) of woven glass rovings composites. It was suggested here that the presence of PC lowers the bonding between the matrix and the glass (Figure 2.23).

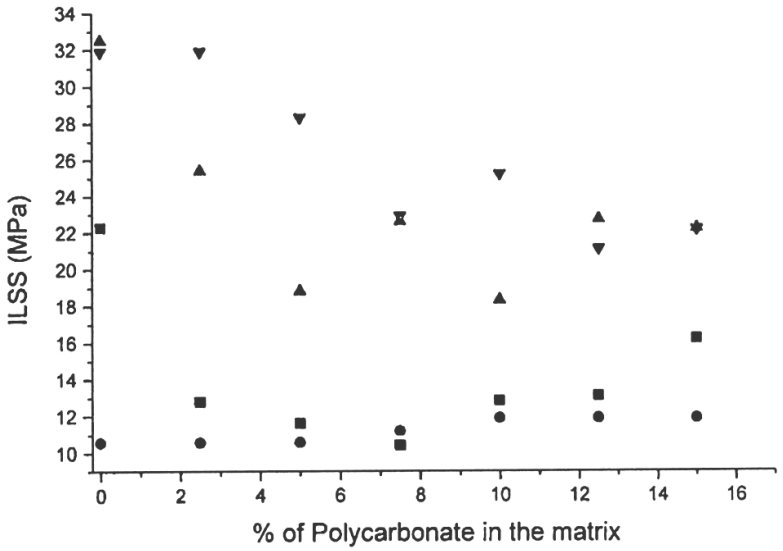

Figure 2.23 The variation of ILSS with wt% of PC in the matrix for different V_f of glass roving (■) 0.1 V_f, (▲) 0.2 V_f, (▼) V_f = 30% [119].

A study by Pearson and Yee on PPO modified epoxy found that toughness increased linearly with PPO content [120]. The tensile properties were independent of PPO content (Figure 2.24). The toughening mechanisms observed were crack bifurcation and microcracking, and evidence of particle bridging was also present. Pearson and Yee [53] also studied the phase separation process of adding PPO to epoxy and its consequence effect on fracture toughness. It was found that the use of a compatibiliser, which is commonly employed in polymer blending, could provide a better control of phase morphology and that a homogeneous structure across the specimen could be obtained.

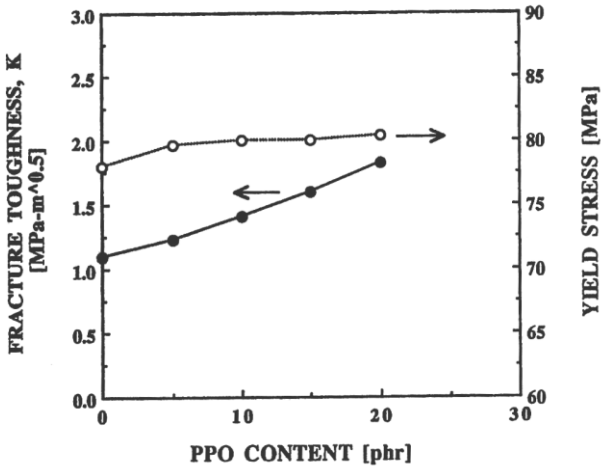

Figure 2.24 Fracture toughness and yield strength of PPO modified epoxy blends [53].

Often the immiscibility of semi-crystalline engineering thermoplastics with epoxy resin is a major concern for blending. Even solution blending can be difficult because of their excellent solvent resistant. A strategy for the improvement of the processability is to use functionalised polymers or polymers with bulky pendant groups. PEEK is insoluble in epoxy and blending is difficult even with the use of solvents. Therefore, instead of using commercially available semi-crystalline PEEK, amorphous PEEK was synthesised and studied. Phenolphthalein poly(ether ether ketone) (PEK-C) has been developed and found to be miscible with epoxy [121]. In a recent study, a functionally terminated PEEK with bulky pendant groups was used. PEEK with pendent methyl group (PEEKM) [122] was added to epoxy and its effect on fracture toughness and other mechanical properties is shown in Figure 2.25. The suggested toughening mechanisms were plastic deformation of the matrix, crack pinning, crack path deflection, crack bridging and particle tearing. At 15 wt% PEEKM, a co-continuous morphology was formed and this corresponded to a substantial increase in toughness. In another study on a PAEK, it was also found that a co-continuous structure favoured an increase in toughness [123].

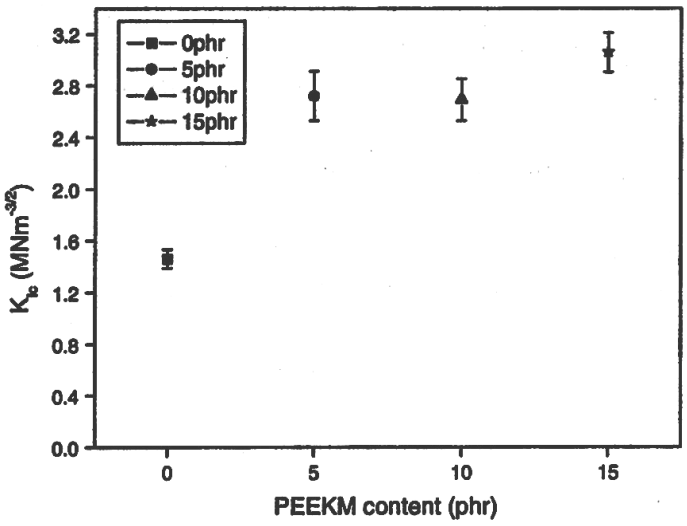

Figure 2.25 Fracture toughness (K_{Ic}) of PEEKM modified epoxy blends [122].

2.3.2.5 Epoxy/sulfur-containing polymer blends

Raghava [124] and Bucknall and Partridge [125] were the earliest researchers to study thermoplastics toughened epoxy resins. Their investigation involved mixing commercial grades of PES with epoxy resins. Phase separation (~0.5 μm) was observed but there was no significant improvement in fracture toughness and in some cases, the fracture toughness decreased. Raghava attributed this to poor adhesion between the phase separated components. It was stressed that adequate interfacial adhesion is necessary otherwise premature failure would occur at the particle-matrix interface, due to presence of high stress concentration at the boundary. Separation of a particle from the matrix will create a void or hole, and a brittle matrix will fail catastrophically without undergoing any significant plastic deformation either in the form of shear bands or crazes. In another study Raghava [126], used a higher molecular weight PES terminated with hydroxyl groups, but again failed to toughen the epoxy resin. Low elongations to failure for PES were cited as the reason for the lack of improvement. Fu and Sun [127] studied the use of PES and PSF to toughen

epoxies, similar to Raghava's study above, PES did not enhance toughness while PSF was found to be more effective, especially when added to a more ductile epoxy.

Various studies have also been carried out on the phase separation behaviour of PES and its copolymers in epoxy blends by studying the effect of various parameters including curing conditions, curing agents, and TP concentrations [128-130]. It was found that by altering the different parameters, different morphologies could be formed, although how this related to the mechanical properties was not discussed in great detail in these studies. MacKinnon *et al*. [131] studied the curing of a PES modified epoxy and found that the time to reach gelation and vitrification increased with increasing PES concentration. This was explained by postulating that the thermoplastic acts as a diluent, thus inhibiting the cure reaction. Similar results were obtained by Chen *et al*. who explained that the separated PES region restricted molecular diffusion thus restricting the chemical reaction between the curing agent and the epoxy. More recently, blends of polyethersulphone:polyetheretheresulphone (PES:PEES) copolymers with different end groups (CL, NH_2 and OH) with epoxy resins were studied (Table 2.8) [132]. It was found that the different end groups affect the morphology. All the blends showed phase separated morphologies. Those obtained from the chlorine and amine ended polymers showed a particulate morphology, but the blend obtained from the hydroxyl ended copolymer had a dominant phase inverted morphology with regions with a particulate morphology. However, the blends obtained with the amine ended copolymers showed higher toughness compared with the system modified with chlorine ended polymer, even when they had similar morphologies. It was noted the highest toughness improvement was achieves with a PES:PEES loading of 30 wt% [128].

The addition of a commercially available PSF was found to be beneficial for improving fracture toughness (Figure 2.26) [133]. It was found that control of morphology could be done by varying the processing temperature and that a co-continuous morphology gave the higher fracture toughness. When a low pre-curing

Table 2.8 Fracture toughness of PES:PEES modified epoxy with different end groups [132].

Modifier end group	M_n	G_{Ic} (kJ/m^2)	K_{Ic} (MPa m$^{1/2}$)
No modifier	-	0.23	0.92
Amine	5000	0.89	1.80
Amine	9000	1.15	2.07
Chlorine	10000	0.52	1.39
Hydroxyl	12000	1.33	2.2

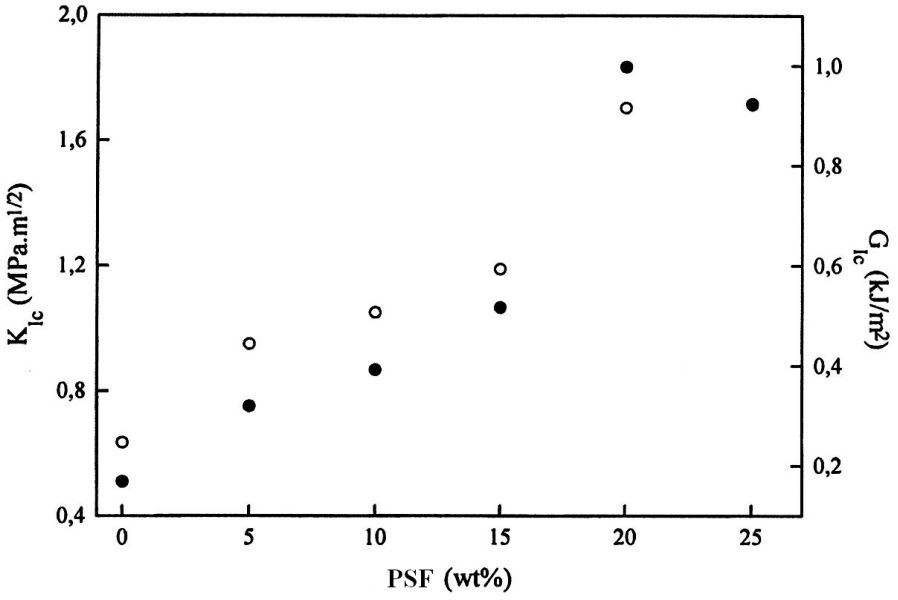

Figure 2.26 Fracture toughness of epoxy/PSF blends: (○) K_{Ic}; and (●) G_{Ic} [133].

temperature was used as phase separation was arrested, no phase separation was observed and this corresponded to a low fracture toughness (Figure 2.27). PSF addition was also found to delay on-set of curing due to both dilution effects and the increase in viscosity due to the presence of the TP. No evident interactions or chemical reactions were observed between the components of the mixture [133]. However, another study on PSF-epoxy blends [134] showed that the addition of PSF

had little effect on curing until the morphology became phase inverted (i.e. 20 wt% PSF). At a higher PSF concentration and lower cure temperature, the reaction was found to be more diffusion controlled and a decrease in conversion resulted from increasing the concentration of PSF. This was explained as being due to increased miscibility between the phases which occurred as a result of the phase inverted morphology.

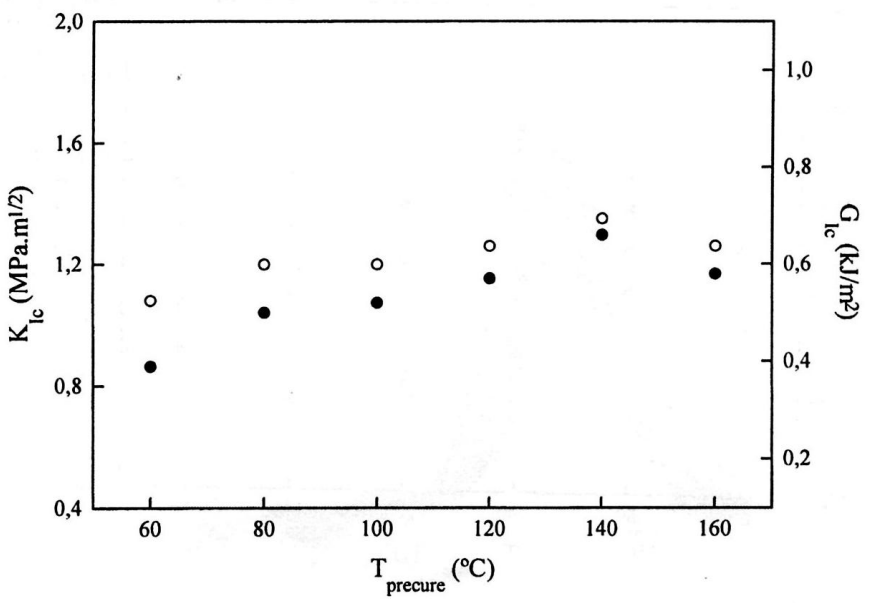

Figure 2.27 Fracture toughness of epoxy/PSF blends containing 15 wt% PSF and precured at different temperatures: (○) K_{Ic} and (●) G_{Ic} [133].

Mujika [8] studied a PSF modified epoxy and found that the addition of 10 wt% of PSF increased the G_{Ic} by 23% in a carbon fibre composite, for both DGEBA and TGDDM epoxy. The G_{Ic} values to improvements for the neat resins were higher than those for the corresponding composite. It was proposed that the carbon fibre prevented the development of a plastic zone at the crack tip and thus lowered toughness. It should be noted that PSF was significantly more effective at toughening

TGDDM than DGEBA bulk resin, suggesting PSF can be used to toughen a highly-cross-linked resin. However, no such effect was evident when carbon fibre was introduced, with both resin systems showing similar improvement.

Min and Kim [9] investigated the idea of a morphology spectrum by introducing PSF to epoxy resin in the form of a thin film. It was found that a range of morphologies was formed (Figure 2.28 and Table 2.9) due to the concentration gradient of PSF. For comparison, specimens were also prepared by blending the PSF with the epoxy to achieve uniform concentrations across specimens and the range of morphologies obtained is shown in Figure 2.29. The fracture toughness of the modified epoxy made by this thin film approach was found to be higher than those made by blending (Figure 2.30). The increase was thought to be due to plastic deformation of the continuous PSF rich phase.

Nam *et al*. [7] prepared a composite by inserting a PSF film between CF/epoxy prepreg. It was found that a co-continuous morphology was formed (~20 wt% PSF) which corresponded to an increase in fracture toughness (Figure 2.31). It was suggested that plastic deformation of the continuous PSF phase contributed to the improvement in toughness. However, in contrast to bulk resin studies, no morphology spectrum was observed in the composite and a uniform morphology was observed instead.

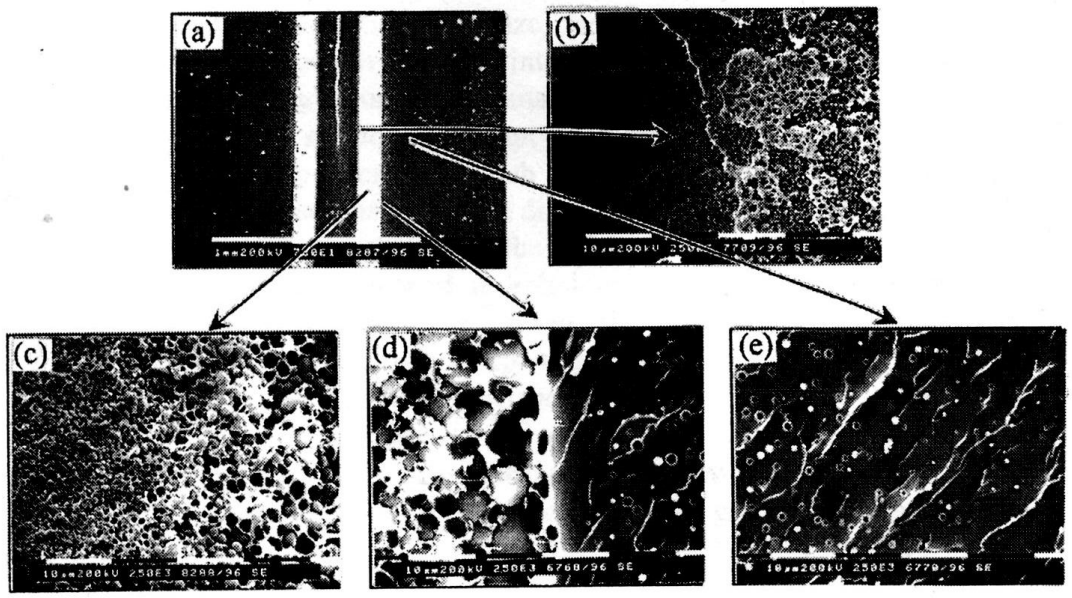

Figure 2.28 Morphology of epoxy resin modified with PSF film showing morphology spectrum across the specimen owning to a concentration gradient (overall PSF content of 8 wt%) : (a) low magnification with PSF film in the middle, (b) inverted sea-island morphology, (c) nodular structure, (d) boundary region and (e) sea-island morphology [9].

Table 2.9 The thickness of the different morphology layers observed in the morphology spectrum system [9].

PSf content (wt%)	4	6	8
Thickness of Morphology Layer	Nodular structure (240μm)	Homogeneous region (80μm)	Homogeneous region (180μm)
		Sea(PSf)-island(epoxy) (20μm)	Sea(PSf)-island(epoxy) (20μm)
		Nodular structure (240μm)	Nodular structure (240μm)
	Sea(epoxy)-island(PSf) (260μm)	Sea(epoxy)-island(PSf) (260μm)	Sea(epoxy)-island(PSf) (260μm)

(overall thickness of the sample = 3000μm)

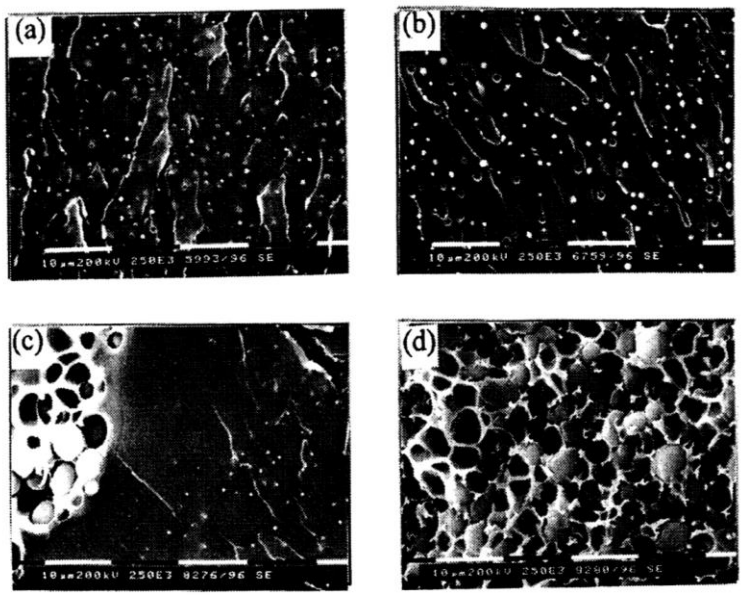

Figure 2.29 Morphology of epoxy resin modified with PSF by blending with uniform compositions: (a) 5 wt%, (b) 10 wt%, (c) 15 wt%, (d) 20 wt% [9].

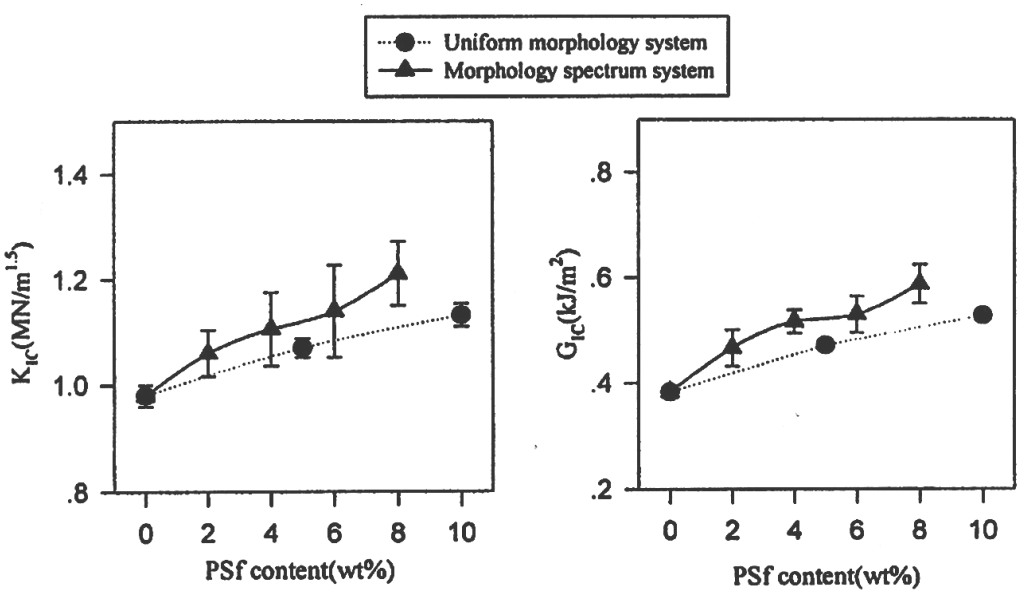

Figure 2.30 Fracture toughness of PSF modified epoxy with morphology spectrum compared with the counterpart with uniform morphology [9].

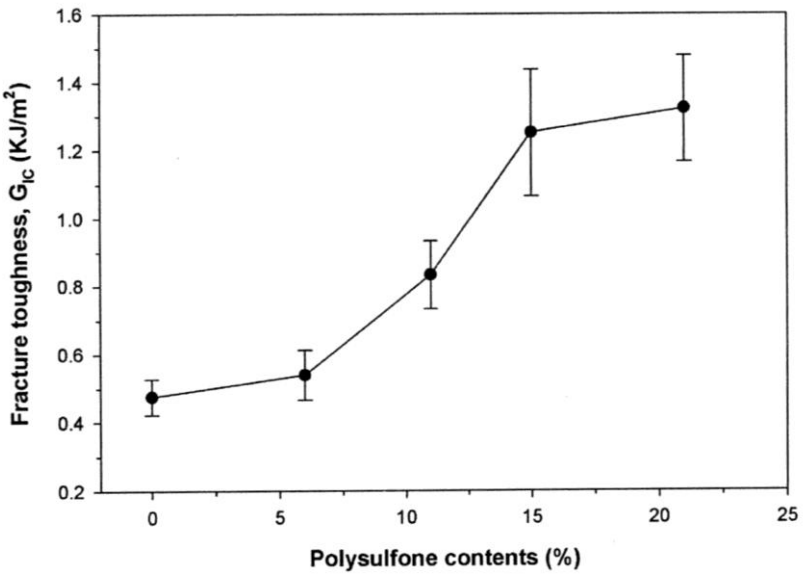

Figure 2.31 Fracture toughness of PSF film modified composite [7].

2.3.3 Preformed polymeric particle toughening

The incorporation of preformed particles into a resin or composite system has many advantages over the technique requiring phase separation. While toughness is increased through the phase separation approach, the amount and size of the phase domains has been found to be a complex function of the matrix composition and the cure cycle. This can bring limitations to certain applications because the final properties and thermal performance can be adversely affected. Some of the advantages using preformed particles as toughening agents are that they are relatively easy to form into different sizes and the volume fraction of the particles can be controlled and maximised.

Furthermore, preformed particles can be incorporated at higher quantities since there is no possibility of phase inversion as with materials utilising the phase separation mechanism. Unlike rubber toughening, there is no loss in

thermomechanical properties. With both rubber and thermoplastic toughening, solvents are required during processing. These solvents can impart voids in cured parts or can plasticise the cured material, which reduces the T_g. Preformed particle modifying systems do not require the use of solvents and, therefore, bypass such problems.

More recently, preformed particles such as thermoplastic powders or core shell rubber particles are increasingly being used as modifiers to improve the mechanical properties and thermal stabilities of thermosets and thermoplastics [135]. Riew *et al*. [136] prepared free-flowing, rigid, multilayer acrylic core-shell polymers with various particle sizes and used these to enhance the toughness of epoxy resins. The adhesive strength was improved by about four-fold and the G_{1c} increased by more than 100%.

Yan *et al*. [85] studied the toughening of a carbon fibre/DGEBA epoxy laminates modified with core-shell rubber particles. It was found that 15 wt% of core shell rubber greatly improved the bulk resin toughness by more than eighteen-fold. However, this improvement of resin toughness was not fully translated to the laminate. Laminate toughness only improved by 1.4 times with these core-shell rubbers. The high fracture toughness of the bulk resin was believed to be due to particle cavitation, which relieved the triaxiality in front of the crack-tip, followed by deformation due to the growth of voids and shear yielding of the matrix. For the laminates, it was found that although the plastic zone ahead of the crack tip could extend beyond two fibre layers, its size was much smaller than in the bulk resin. Consequently, dilation deformation and shear yielding was suppressed and high triaxiality was maintained at the crack-tip. Day *et al*. [21] modified a carbon fibre/epoxy laminate modified with core-shell particles that have a three-layer morphology in which the inner core is crosslinked poly(methyl methacrylate), the intermediate layer is crosslinked poly(butyl acrylate) rubber and the outer layer is a poly[(methyl methacrylate)-*co*-(ethyl acrylate)-*co*-(glycidyl methacrylate)]. The

presence of glycidyl groups in the outer layer facilitates chemical reaction with the matrix epoxy resin during curing. The functionalised particles had superior properties compared to non-functionalised particles and the CTBN liquid rubber modified counterpart. It was found that the tensile, compressive and impact properties, apart from Young's modulus, all showed improvements for the epoxy functionalised core-shell particle modified laminates.

2.3.4 Inorganic particulate toughening

Incorporation of particulate fillers such as silicates and alumina trihydrate can enhance the toughness of crosslinked epoxies. Particulates contribute to a greatly enhanced modulus which is a significant advantage over rubber modification where a reduction in modulus is observed. The degree of toughness improvement was found to depend upon the volume fraction as well as the particle size. It was found that toughness increased with increasing volume fraction of particles. Both G_{1c} and K_{1c} increased with an increase in silicate particle size. Figure 2.32 shows the effect of particle volume fraction on toughness while Figure 2.33 shows the effect of particles size.

Elongation at break, which is sometimes considered to be a measure of the ductility of a material, also decreased with increasing filler volume fraction. It is reported that added particles may decrease the impact resistance of epoxy [137, 138]. It was demonstrated that the fracture toughness of glass bead filled epoxies increased as the inherent matrix toughness increased [139], which could be attributed to the accompanying increases in micro shear banding and debonding/diffuse shear yielding. However, it was also shown that while fracture toughness is increased with particles size, the flexural, tensile and elongation at break values decreased [137, 140-142].

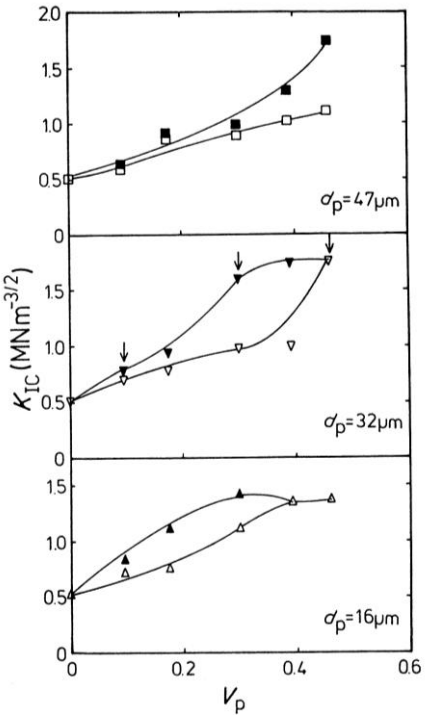

Figure 2.32 Variation of K_{Ic} with particulate volume fraction V_f and different particle size d_p. The closed markers are for initiation and the open ones for arrests [142].

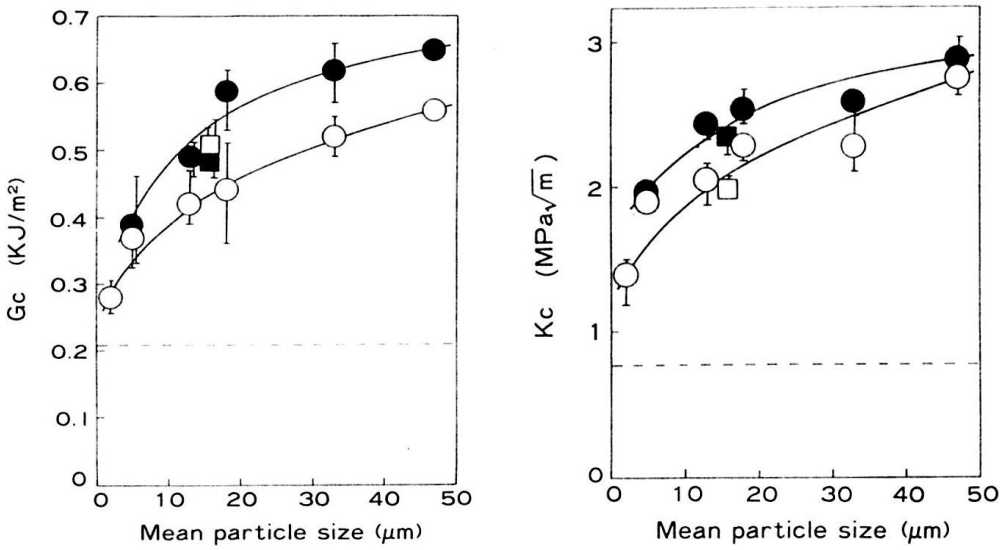

Figure 2.33 Effect of particle size on G_{Ic} and K_{Ic} by SENB of cured epoxy resins filled with original (□■) and classified (○●) angular-shaped silica particles at particle content of 55 wt% (□○) and 64 wt% (■●) [137].

The mechanism of particulate toughening is somewhat different from that of elastomeric modification. Lee and Yee [143] pointed out that the various micromechanical deformation mechanisms found in epoxies can be categorised into three possible major toughening mechanisms. They are: step formation, debonding of glass beads/diffuse matrix shearing and micro-shear banding.

Another approach of interest is to coat rigid particles with a thin layer of elastomer (about 1 to 4% of radius) to reduce the residual stresses concentrated at the interface during curing due to the very different thermal coefficients of the matrix and the filler. Other experimental studies conducted on glass beads [141, 144-146] confirm the value of such an approach. Figure 2.34 illustrates the effect of the glass bead coating on the resulting fracture toughness. The coating of glass bead with a thin layer of a crosslink elastomer greatly enhances the fracture properties and the coated particles display the largest plastic zone during fracture, leading to dissipation of energy by shear yielding. It is believed that introducing an inter-phase with controlled properties (thickness and modulus) lead to an improvement in impact and fracture properties without lowering the elastic properties. Such an effect could be possible by the modification of mechanisms for initiation and propagation of shear yielding in the epoxy matrix.

Although some modest improvements in toughness have been achieved with particulate reinforcement, these have not been of the same magnitude as elastomeric modification. Several studies have been conducted exploring the possibilities of combining both particulate and rubber particles modification of epoxies [147, 148]. Schröder *et al.* modified epoxy with glass beads and liquid rubber [149]. They found that modification with glass beads resulted in increased stiffness and toughness compared to the neat resin but reduced tensile strength. Compared to the glass bead–filled epoxy, additional modification with liquid rubber lead to a further increase in toughness and also to an increase in strength but did not alter stiffness and glass-transition temperature. This synergistic behaviour is explained by the fact that the

rubber separates preferably on the surface of the glass bead, forming a core–shell morphology during curing.

A substantial modulus increase accompanying toughness enhancement is a major advantage of particulate modification [141]. As well as modulus, the heat deflection temperature of the modified epoxy was also increased. Mould shrinkage is reduced in particulate filled polymers; this is primarily due the lower coefficient of thermal expansion of the filled polymers. Unfortunately, uniform mixing and good dispersion of these particles are rarely obtained because of the higher density of the inorganic filler particles compared to epoxy resins

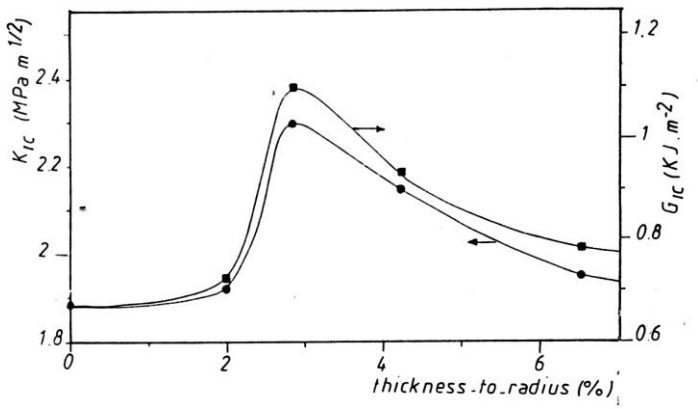

Figure 2.34 K_{Ic} and G_{Ic} vs elastomeric interlayer thickness for system based on 20% V_f of coated glass beads; silane treated glass (●), elastomer coated (■) [145].

2.3.5 Nano-reinforcement

The use of nano-sized organic and inorganic fillers in epoxy to improve the mechanical and physical properties has recently attracted a lot of attention. Owing to the near molecular size of their reinforcement, it is thought that polymer nanocomposites offer the possibility to develop new materials with unusual properties. The advantage of nano-scaled fillers over micro-scaled fillers is their enormous surface area, which acts as an interface for stress transfer. The main groups

of material studied include carbon nanotubes (CNT), nano-sized inorganic particles like silica, nanofibres and nanoclays. In the field of fibre reinforced composites, interlaminar fracture toughness is one area where the use of nanofillers could make a significant impact.

CNT were first reported by Iijima in 1991, and are built up of carbon atoms arranged in hexagons and pentagons, forming cylinders. CNT possess many unique properties such as high strength, modulus and, flexibility and good electrical conductivity. There are single-walled (SWCNT), double-walled (DWCNT) and multi-walled (MWCNT) CNT available. The potential of using CNTs as conductive fillers in polymers has been realised in numerous studies [150, 151]. However, the potential of CNTs in improving mechanical properties has been found to be more difficult to realise. While some studies have shown that the addition of CNTs to polymers, including epoxy resins [151, 152] can be advantageous, several major obstacles have to be overcome. The first is forming a homogenous and stable dispersion of the filler in the matrix. The second is the tuning of the interface between filler and matrix. Another complication is that the curing and, therefore, the resulting properties of epoxy resin are not only influenced by the processing history but also by the presence of the nanofillers [153, 154]. CNTs do not disperse readily in polymers because of the strong interaction between the individual CNT. They aggregate to form bundles or ropes that are very difficult to disrupt. Agglomeration of CNTs results in poor dispersion and reduces the aspect ratio of reinforcement. The weak interface is the result of the smooth and un-reactive surface of the CNTs. The stress transfer from the matrix to the CNTs occurs at the interface, thus a strong interface is crucial. Various dispersion methods have been studied, which include solvent or surfactant assisted dispersion, sonication, *in-situ* polymerisation, electric or magnetic field induced alignment of CNTs and calendaring. Surface modifications of CNTs include functionalization with amines, fluorine and alkanes; plasma functionalisation, treatment with strong acids, inorganic coating and polymer

wrapping. It has been found that functionalisation of CNTs can improve the dispersion and the interfacial bonding between CNT and resins [152, 155].

While many studies have concentrated on CNT modified epoxy resin, studies on three phase (epoxy, fibre and CNT) mirco-nano composites are somewhat limited, although there is a recent increase in interest. While the main area of improvement is thought to be in interlaminer toughness (Figure 2.35), there are some conflicting results.

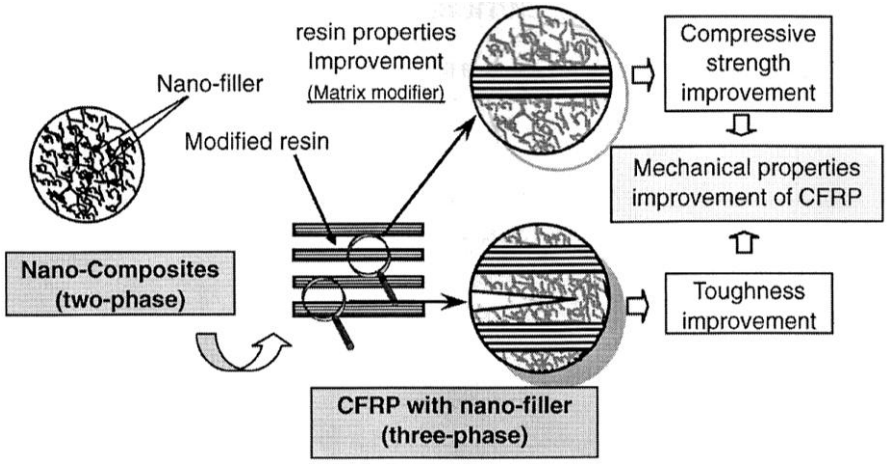

Figure 2.35 Scenario of mechanical properties improvement of CFRP by incorporation of nano-fillers [156].

In a study [157] where 1 wt% SWCNT was added to an epoxy matrix for a filament wound CFRP, no noticeable effect could be found. However, Veedu *et al*. [158] grew MWCNT on the surface of micro-fibre carbon fibre fabric, normal to the fibre direction, resulting in a 3D effect between plies under loading. It was suggested that the CNT "forests" resulted in the fastening of the adjacent ply, thus provided interlaminar strength and toughness under loading. Gojny *et al.* [25] reported the successful dispersion of CNT in epoxy by mini-calendaring, which resulted in a significant increase in fracture toughness. When such a technique was introduced to a glass fibre reinforced composite (GFRP) it was found that the interlaminar shear

strength (ILSS) increased by 19% with 0.3 wt% of amino-functionalised double wall CNT (DWCNT-NH_2) added to the epoxy matrix. (Figure 2.36). The GFRP was prepared by resin transfer moulding (RTM) and it was reported that the nano-sized dispersion of the filler was not filtered out by the glass fibre fabric.

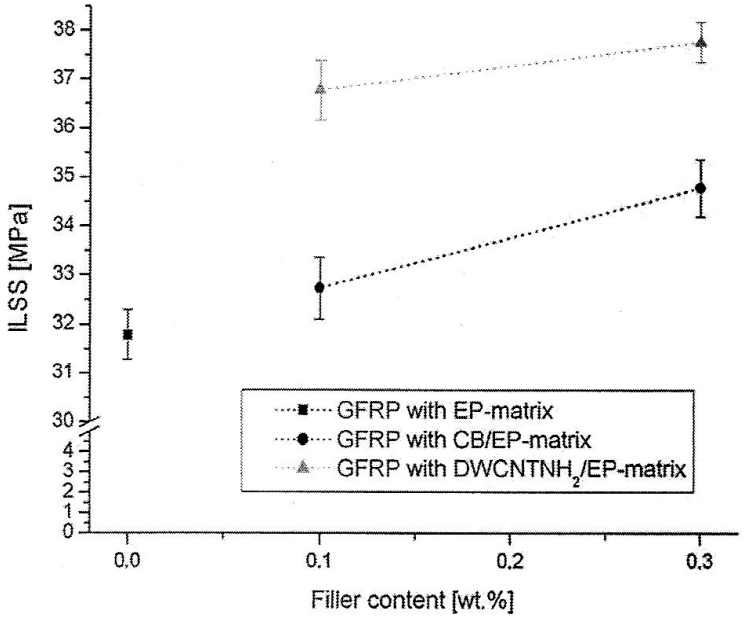

Figure 2.36 Interlaminar shear strength (ILSS) of nano-reinforced GFRPs [25].

Wichmann *et al*. [159] fabricated GFRP by a modified RTM method in which an electric charge was used to align the CNTs perpendicular to the fibre. It was found that the ILSS increased by 16% with a 0.3 wt% addition of CNT. The interlaminar toughness (G_{Ic} and G_{IIc}), however, was not affected in a comparable manner. The lack of improvement in mechanical properties was attributed to the poor interface between the CNT modified matrix and the glass fibre. In another study with a MWCNT modified glass fibre/epoxy laminate, ILSS and compressive strength were found to be improved [160]. Here, the CNTs did not penetrate deep into the glass fabric with most of the CNTs found in the matrix rich region and at the fibre/matrix interface. Porosity of the cured laminates increased due to increased viscosity at high

CNT loadings (3 and 5 wt%), accompanied by increased ply thickness. Doubts were cast by Chandrasekaran *et al*. [161] on the apparent improvement on ILSS in CNT modified laminates. They suggested that it was the preparation method of CNT modified laminates that affected the ILSS of the composites rather than the addition of CNTs itself. Yokozeki *et al* [156] reported the use of cup-stacked CNT (CSCNT) in a CFRP and observed a retardation of matrix and crack onset and accumulation of cracks was found. Godara *et al*. [162] prepared carbon fibre/epoxy composites modified with various types of CNT. Fracture toughness improved in the CNT modified composites (Figure 2.37) and it was suggested that fibre bridging took place. Tensile properties and ILSS, however, showed no conclusive effect with the addition of CNT. It was concluded that the addition of CNT to the fibre composites was complicated and the outcomes depended upon factors such as stability of dispersion, viscosity control and optimisation of surface modifications.

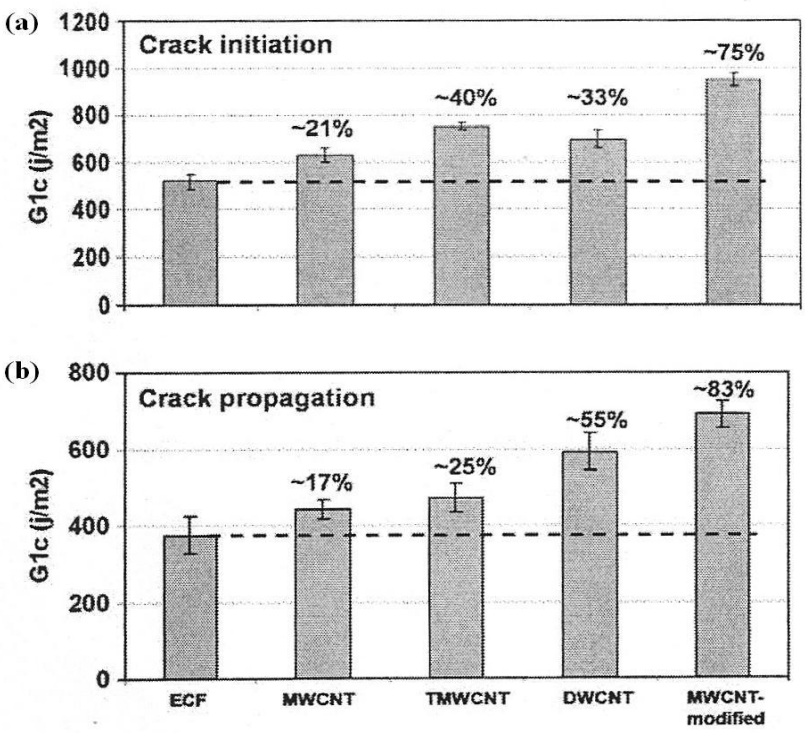

Figure 2.37 Effect of CNT content on fracture toughness of (a) crack initiation and (b) crack propagation between crack lengths 70-90 mm [162].

Out of the different nanofiller materials, carbon nano-fibres (CNF) are one of the most promising candidates. This promise is based on their high axial Young's modulus high aspect ratio, large surface area, and excellent thermal and electrical properties. Zhou *et al*. [163] investigated CNF modified bulk epoxy resin and epoxy carbon fibre composites. It was found that the tensile modulus, tensile strength (Figure 2.38) and fracture toughness (Figure 2.39) improved with the addition of CNF and that 2 wt% CNF was the preferred concentration. Fracture surface observations suggested crack deflection and fibre pull-out took place. For the carbon fibre laminates, tensile and flexural strengths were increased by 22.3% and 11% respectively with CNF modification, but no results on toughness were presented.

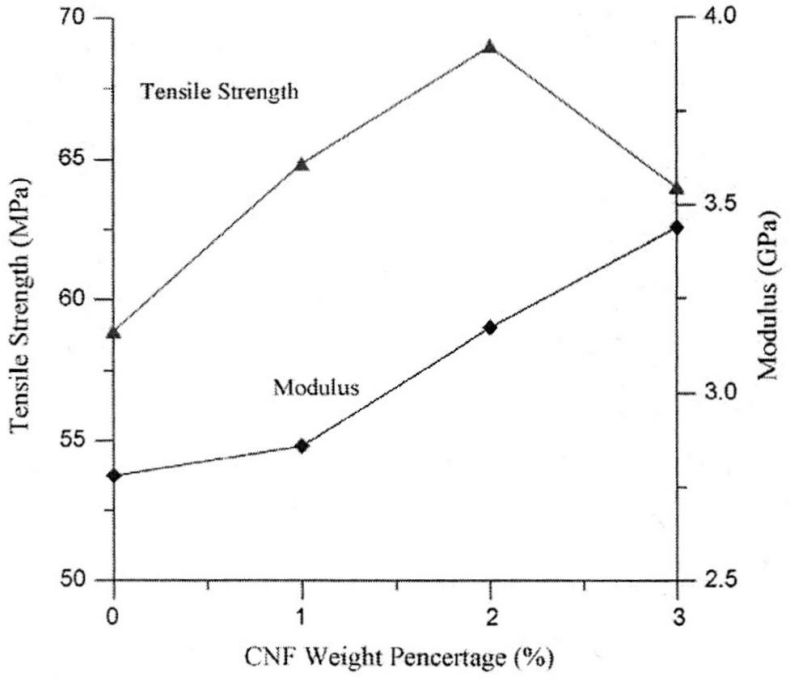

Figure 2.38 Effect of CNF content on tensile strength and modulus of epoxy [163].

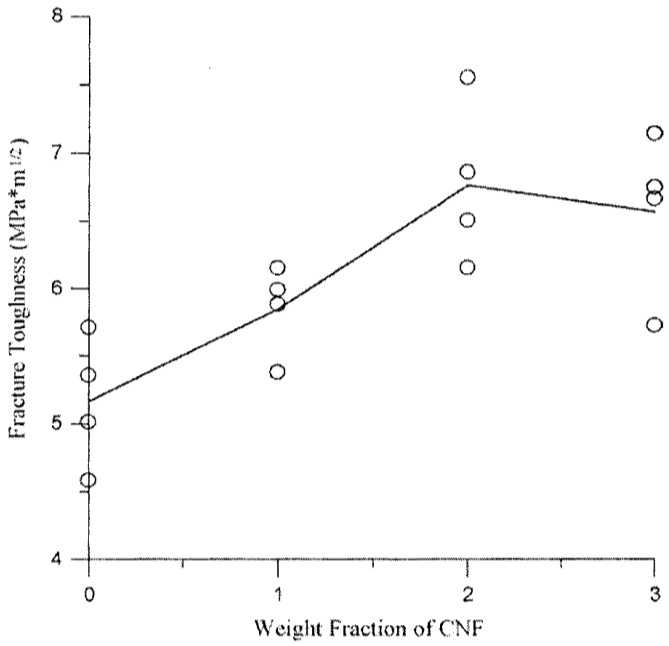

Figure 2.39 Effect of CNF content on fracture toughness [163].

Nanoclays have also been used to modify epoxy resins and epoxy composites. Siddiqui *et al*. [164] reported the mechanical and fracture properties of epoxy resin and carbon fibre/epoxy laminates modified with montmorillonite. The flexural modulus of epoxy resin was increased while flexural strength decreased with addition of nanoclay (Figure 2.39). Quasi-static fracture toughness improved while impact fracture toughness dropped sharply (Figure 2.41). For the CFRP laminates, the addition of nanoclay improved the flexural modulus and Mode-I delamination toughness. Suggested toughening mechanisms were crack bifurcation, fibre/matrix debonding and coalescence of micro-cracks. Nanoclays have neither good surface energy nor good interaction with polymer matrices, which makes modification necessary for good dispersion. This can be done by ion exchange [165]. Surface modification with silane was also found to enhance mechanical properties of nanoclay modified epoxy [166]. As well as enhancing mechanical properties,

nanoclays can also reduce flammability of epoxy resins due to the formation of a physical barrier of collapsed nanoclay particles [167].

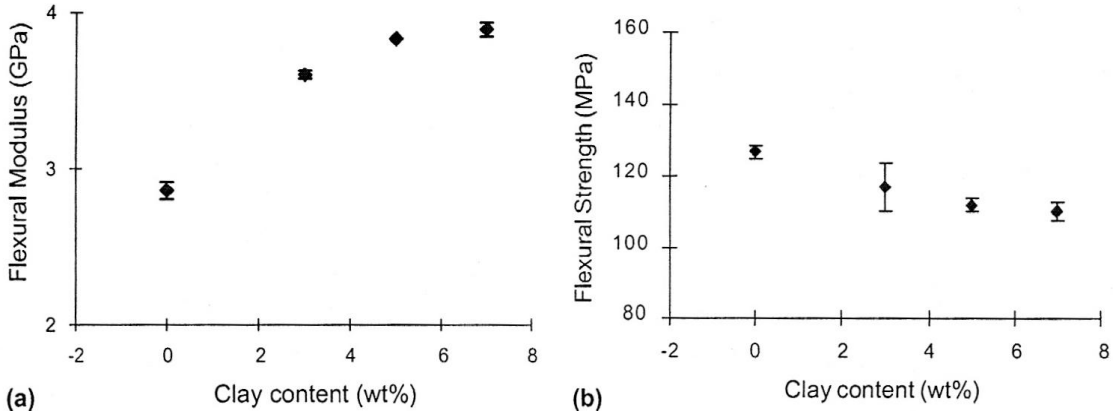

Figure 2. 40 Flexural properties of nanoclay epoxy nanocomposites as a function of clay content [164].

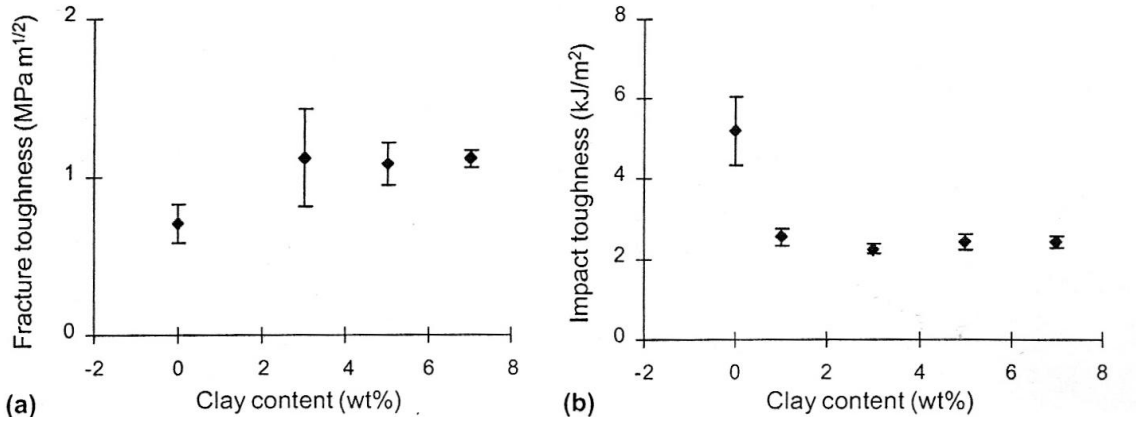

Figure 2.41 (a) Quasi-static and (b) Izod impact fracture of nanoclay epoxy nanocomposites as a function of clay content [164].

2.3.6 Interleaving

Interleaving is an interlaminar toughening technique which involves inserting a discrete, thin and tough polymer layer between plies in a laminate. When it was

first developed, a thin layer of resin was added to one side of standard prepreg tape which itself contains an improved, tough matrix [168]. Both thermoset and thermoplastic resins have been successfully employed as interleaf systems. The main criteria for this toughening mechanism to be successful, is that the interlayer used must have high shear strength and the interlayer must remain as a discrete layer after the laminate has been cured. A composite material is made tougher and more impact resistant by allowing for more expansion of the crack tip plastic zone between the plies, and by suppressing delamination at the interface.

It was found that the residual stress for compression-after-impact (CAI) tests were improved by 50 to 80% in laminates with thermosetting and thermoplastic resin interleaves [169]. Duarte *et al.* [170] presented the results of low-velocity impact and CAI tests conducted on interleaved and non-interleaved carbon/epoxy tape laminates. The results showed that the olefin film interleaves provided a strong interfacial bond, resulting in a reduction in projected damage area as seen in Figure 2.42(a). However, the compression strength of undamaged specimens decreased by using olefin interleaves (Figure 2.42 (b)). This was attributed to the lack of lateral support for fibres at the fibre/interleave interface, allowing fibre micro-buckling to occur at low loads. The problems with lack of lateral support under compression loading associated with the low modulus olefin interleaves was overcome by using a polyetherimide (PEI) interleave material. The results presented in Figure 2.42(c) show an increase in impact resistance, with damage initiation energy being increased to 2.7 J/mm. Due to its high shear modulus, the compressive strength of the undamaged specimen was comparable to the non-interleaved laminate. The CAI, however, was higher for the interleaved laminate than for the non-interleaved laminate, Figure 2.42(d).

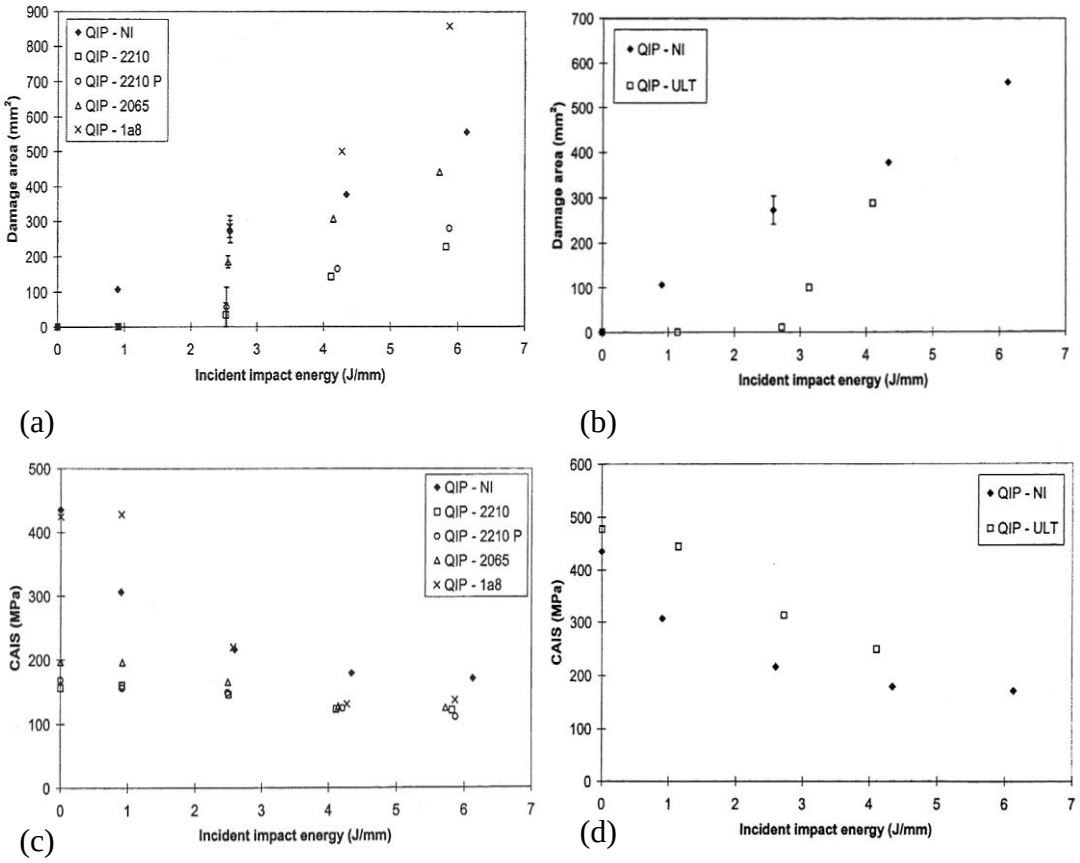

Key: NI – no interleaf; 2210 – polyolefin; 2210P – polyolefin; 2065 – polyolefin; 1a8 – copolyamide; ULT - polyetherimide

Figure 2.42 Effect of interleaving on impact resistance and damage tolerance of composite materials [170].

Mode-I and II delamination toughness was also found to be improved by interleafing with a resin interlayer. Ishai *et al*. [171] found that G_{Ic} improved up to six-fold and G_{IIc} up to four-fold in graphite/epoxy laminates. Ozdil and Carlsson [172] found that thermoplastic interleaves enhanced G_{Ic} (up to five-fold at 16μm interleaf thickness) to a much large extent than thermoset interleaves (Figure 2.43), due to a larger energy absorption capability in the fracture process. It was concluded that an optimum thickness and high toughness of the interleaf [173, 174], and good adhesion [172] between the interleaf and composite is necessary for toughness

improvement. Rechak and Sun [175] studied selective toughening interleaves and they found that the placement of interleaf is crucial to arrest matrix cracks and delamination. In a study which employed an ionomer as the interleaf [176], it was found that the ionomer mixed with the epoxy matrix formed an interphase. Failure occurred within this interphase and G_{Ic} was improved to a greater extent than specimens without interphase.

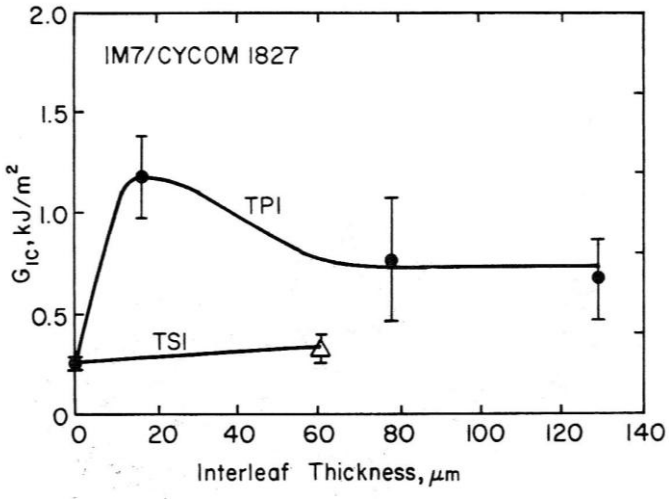

Figure 2.43 Mode-I interlaminar fracture toughness vs interleaf thickness for carbon fibre/epoxy laminates with thermoset and thermoplastic interleaves [172].

The first interleaving systems developed used resin interlayers as interleaves. Since then other forms of interleaves such as polymeric particles and non woven fibre mast have been studied. The use of nylon particles in interleaving resins was reported [177]. It was found that in a ductile epoxy system, the particles acted as a thickness control and in a brittle epoxy system, stress induced plastic deformation of the matrix and particle bridging were the suggested toughening mechanisms. In another study with thermoplastic particle interleaves [178], G_{IIc} was improved, the improvement was attributed to crack deflection, crack-tip shielding and deformation of the thermoplastic particles. Particle size and distribution were found to be

important parameters in toughening, in that a uniform particle size and distance distribution was preferred for high CAI [179].

The interleaving resin layers rely on crack limitation through plastic deformation of the interleaf that is inherently highly elastic. The advantage in creating plastic deformation is that it consumes large quantities of energy when compared to elastic failure. The advantage of this being that it increases the elastic storage capabilities and damage resistance energy of laminates during impact. The main disadvantage arising from these systems often includes reduced stiffness, lowered glass transition temperatures and poor tolerance to adverse environments. The use of short fibres as an interlaminar reinforcing material does not rely on the generation of plastic deformation. Short fibre methods rely on increasing the energy consumption using semi-elastic failure mechanisms of pull-out or fibre breakage [180]. The use of short fibres also creates a randomly orientated heterogeneous layer, which provides opportunities for a random and disturbed path. Sohn and Hu [181] reported a toughness improvements when short Kevlar fibres (5-7 mm) were added to the interlaminar region of the laminates. It was suggested that the short Kevlar fibres acted as a fibre bridging medium between continuous fibre layers. The fibre bridging effect was highly enhanced by the number of short fibre ends and the interfacial bond strength between short Kevlar fibres and the matrix material. In another study, Sohn *et al*. [32] interleaved laminates with Kelvar and Zylon fibres, a poly (ethylene-co-arylic acid) (PEEA) film and polyamide (PA) web (Table 2.10). It was reported that PEEA reduced the damage area after impact, but CAI was reduced. Zylon fibre, which are based on poly(p-phenylene-2,6-benzobisoxazole) (PBO) were found to have good interfacial bonding with epoxy and provided improvement in interlaminar fracture resistance. Yuan *et al*. improved the CAI of a carbon fibre/epoxy tube by incorporating a non-woven polyethylene terephthalate (PET) mat, which suppressed delamination.

Table 2.10 Carbon fibre/epoxy composite interleaved with various reinforcements and the resultant CAI strength [32].

Materials	Type	wt%	Areal density (g/m2)	CAI strength (MPa)
Plain	---	---	---	112
Kevlar (uniform)	15 mm	0.8	2.2	110
Kevlar (coarse)	15 mm	0.8	2.2	103
Kevlar	15 mm	0.4	1.1	133
Kevlar	5-7 mm	0.4	1.1	94
Zylon (high modulus)	6 mm	0.8	2.5	125
Zylon (medium modulus)	6mm	0.8	2.5	105
PEEA film	film	19	106	72
PA web	web	3.5	65	65

2.3.7 Modification of fibre architecture

Based on structural integrity and fibre linearity and continuity, fibre architecture can be classified into four categories: discrete, continuous, planar interlaced (2-D) and fully integrated (3-D) structures.

A discrete fibre system such as a whisker or fibre mats often has no material continuity. The structural integrity is derived mainly from inter-fibre interaction. The strength translation efficiency is quite low.

The second class of fibre structure is the continuous filament, or unidirectional (0°) system. This architecture has the highest level of property translation efficiency. The drawback of this fibre architecture is its intra- and interlaminar weakness owing to the lack of in-plane and out-of-plane interlacings.

The third class of fibre reinforcement is the 2-D planar interlaced and interloped system. Although the intralaminar failure problem associated with the continuous filament system is addressed with this fibre architecture, the interlaminar strength is limited by the matrix strength owing to the lack of through-thickness fibre reinforcement. Considering the geometry of 2-D fabric, crack propagation in 2-D fabric composites is more complex than that in unidirectional composites. The toughening effect and toughening mechanisms generated are dependent on the fabric pattern [182-185]. Curtis and Bishop [186] evaluated the impact performance of woven carbon fibre reinforced laminates with (0, 90), (±45) and mixed-woven (0, ±45) lay-ups, using incident energies of 1-9 J. The threshold energy for damage was similar for woven and non-woven laminates, but the extent of damage in the woven material was much less. The damage was principally in the form of delaminations between the layers, but at the point of impact, it was shown that there was tensile cracking towards the back surface and compressive buckling close to the front surface. The use of woven material restricted the extent of delamination, particularly the splitting along the fibre direction on the back surface. Various studies have been performed on the effect of fabric structures on toughness [187].

The fourth class of fibre reinforcement is the fully integrated system wherein the fibres are oriented in various in-plane and out-of-plane directions. The most attractive feature of the integrated structure is the additional reinforcement in the through-thickness direction which makes the composite virtually delamination-free. Another interesting aspect of many of the fully integrated structures such as 3-D woven, knits, braids and non-wovens is their ability to assume complex structural shapes. Various researchers have been investigating the effect of the 3-D fibre architecture on the impact damage resistance and/or damage tolerance of composites [188, 189]. Braided 3-D composites exhibit a much smaller degree of damage even though the damage threshold energy values were very similar [190]. In drop weight impact tests, the 3-D braided glass-epoxy composite required much higher levels of energy to initiate and propagate damage [191]. However, weaving, knitting and

braiding create large resin pockets throughout the structure thereby reducing the volume fraction of the in-plane fibres compared with analogous 2-D laminates. This results in a decrease in the in-plane properties [36].

2.3.8 Through-thickness reinforcement

An alternative approach that shows substantial improvement in the damage tolerance of composites structures is the introduction of through-thickness reinforcement into the laminate. A through-thickness reinforced composite is defined as a composite laminate with up to 5% volume of fibrous reinforcement oriented in a through thickness direction [192]. These materials may be considered a subset of 3-D composites, with the distinction that the material structure is a simple layered structure with only a few volume percent of reinforcement in through-thickness direction. The greatest problem with through-thickness techniques is manufacturing and tooling costs, as they are labour intensive and require specialised equipment.

Stitching involves continuous rovings, threads, yarns, or tows passing through the laminate plies with the use of industrial sewing/stitching technology. Though relatively cost effective, considerable fibre damage occurs through needle penetration. This can damage the load bearing plies, thus reducing the strength. In recent years, novel stitching techniques have been developed where the fibres are effectively spaced to reduce fibre breakage. Results from published reviews of stitched composites [192, 193] showed a significant improvement in the interlaminar-dominated responses such as compression after impact strength, fracture toughness, and interlaminar shear strength. The biggest improvement in properties was observed in Mode-I delamination tests. Stitching was also found to improve the Mode-II delamination resistance of CFRP but of a lower order than Mode-I. Dransfield *et al*. [36] found a fifteen-fold improvement in the Mode-I delamination toughness of stitched resin transfer moulded carbon/epoxy laminates. Delaminated surfaces of the stitched specimens were examined using scanning electron microscopy in order to determine the major energy absorbing mechanisms

responsible for the improvement. Evidence of thread breakage and subsequent pull-out was found. Thus, it was postulated that several processes were involved in increasing the toughness. Debonding of the thread/matrix interface allowed elastic stretching of the thread. This created fibre bridging of the crack by the stitch lines providing crack closure forces until thread failure and pullout occurred. They also found that the improvement is dependent on thread type, thread diameter, and stitch density. Jain *et al*. [194] reported that stitching generated an up to 4 times improvements in toughness. As before, these improvements were also found to be depended on thread type, stitch density and thread diameter.

Z-pinning is an alternative to stitching where small diameter reinforcing pins are inserted orthogonally to the plane of the composite plies during the manufacturing process, before the resin matrix is cured, effectively pinning the individual layers together (Figure 2.44). Z-pinning is suitable for localised reinforcement and is capable of enhancing delamination resistance by an order of magnitude (Figure 2.45) [195], accompanied by a loss of in-plane stiffness of 10%. It is shown that the main benefit of Z-pinning is to be expected from the high crack-stopping potential of selective placements of blocks of Z-pins in a composite structure.

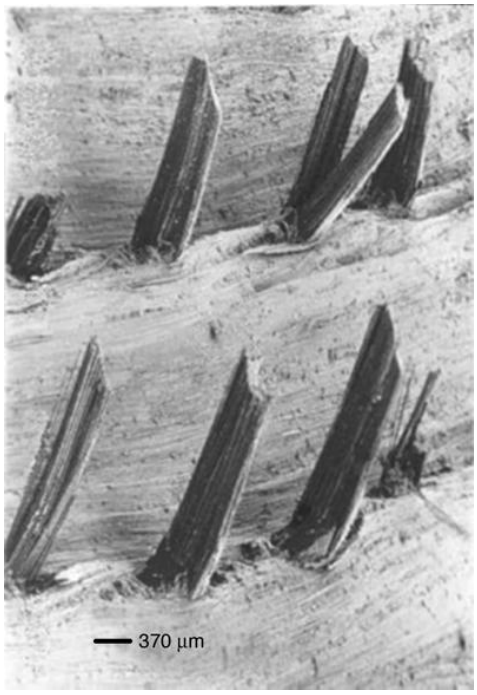

Figure 2.44 Reinforcing pins pulled out of a unidirectional (UD) laminate beam that had been broken open in Mode-I delamination fracture [195].

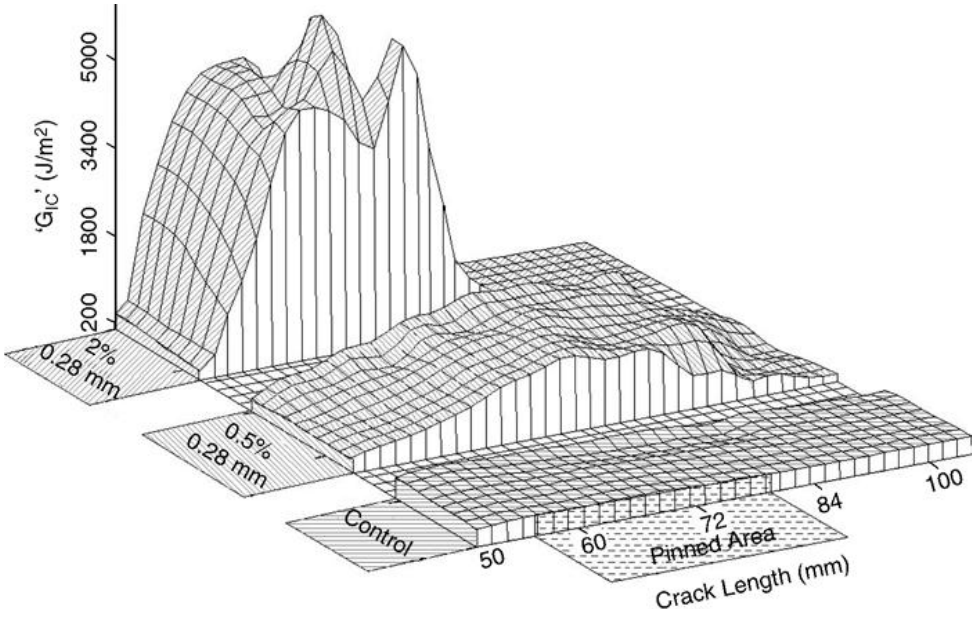

Figure 2.45 Mode-I loading case R-curves showing the effect of Z-pin areal density at a fixed Z-pin diameter (0.28 mm) in a uni-directional laminate IMS/924 [195].

2.3.9 Hybrid composites

Hybrid composites involve the reinforcement with two or more different types of fibre. The concept is an extension of the principle that materials of different properties can be combined to tailor desired properties. In carbon fibre/epoxy laminates, hybridisation can be achieved by replacing some of the structural carbon fibres with more ductile fibres. Various reports on the impact and improvement of carbon fibre composites *via* hybridisation with glass, aramid or other high failure strain fibres have been reported [196-198]. Parameters that affect the properties of hybridised laminates include volume fraction of each component fibre, lay-up sequence and orientation, properties of the fibres and resins and the interfaces between fibres and resins.

Peijs *et al.* studied hybrid composites based on polyethylene (PE) fibre/carbon fibre with epoxy matrix [199, 200]. It was found that the interfacial bonding could be altered by surface treatment of the PE fibre, and that a weak interface favoured improved impact properties [200]. The results were attributed to extensive debonding of PE fibres and longitudinal shear failures between PE and carbon fibres. It was shown that the addition of PE plies to the non-impact side of a laminate resulted in improved impact damage tolerance and resistance by altering the energy absorption mode via hybridisation [199]. It was thought that more energy was stored elastically in the PE fibres, leaving less energy available for damage in the structural carbon component of the hybrid. Additionally, it was suggested that delamination at the carbon fibre/PE fibre interface also absorbed energy, leading to reduced impact damage in the carbon fibre. The placement of the hybrid fibres was also found to be an important factor in optimising of the impact properties of hybrid composites [39].

Andonova *et al*. [201] presented a study based on a carbon fibre/epoxy laminate hybridised with PET fibres. It was shown that PET fibres that had been surface treated with amine groups showed superior thermal, fracture and impact

properties than its untreated counterparts. It was suggested that PET fibres could be used to improve impact resistance, however, little evidence was shown in the study itself. The hybridised laminates had lower fracture toughness than the control carbon fibre/epoxy laminate and a comparison of impact properties of control and hybridised laminates was not available.

Dutra *et al*. [196] prepared hybrid composites made of polypropylene fibres of moderate stiffness and carbon fibre in an epoxy matrix. It was found that the addition of PP fibre was beneficial in terms of impact strength and PP fibres functionalised with mercapto groups improved the impact resistance the most (Table 2.11), while at the same time they also increased the thermal stability. It was suggested that surface treated PP fibres had better adhesion with the matrix, which favoured stress transfer and improved impact performance. This finding is in contrast to the Peijs *et al.*'s study on high performance PE hybrid composites [200].

Table 2.11 Impact strength hybrid carbon fibre/PP/epoxy composites [196].

Composites	Epoxy resin (vol%)	Fibre (vol %)				Impact strength (J/m)
		Carbon fibre	PP fibre	PP fibre (mercapto treated)	Total	
Epoxy/carbon fibre	56	44	-	-	44	209 ± 32
Epoxy/PP fibre	55	-	45	-	45	259 ± 38
Epoxy/PP fibre (mercapto treated)	55	-	-	45	45	951 ± 148
Epoxy/carbon fibre/ PP fibre	60	15	25	-	40	246 ± 18
Epoxy/carbon fibre/ PP fibre (mercapto treated)	50	15	-	35	50	352 ± 78

2.4 Summary

A lot of work has been done on toughening epoxy resins and their composites over the past decades. The various systems and the toughening mechanisms have been reviewed in this chapter. It is found toughening is mainly achieved through matrix toughening (e.g. liquid rubber and thermoplastic toughening), and modification of fibre and composite architecture (e.g. interleaving and 3-D fabric).

The focus of the research presented in this thesis is based on using dissolvable phenoxy fibres to toughen carbon fibre epoxy composites, which is a combination of thermoplastic toughening and interleaving. The phenoxy fibres were placed between carbon fibre lamina during lay-up of composites, similar to interleaving using non-woven mat. The phenoxy fibres first dissolved in the matrix when the composites were heated during cure, forming epoxy/phenoxy blends. Phase separation followed as curing continued and completed. The phase separated morphology could generate some of the toughening mechanisms mentioned in this chapter such as crack pinning and crack deflection. This technique has the potential to provide localised toughening as the phenoxy fibres can be placed wherever is needed in the composite structure and leave other desirable properties such as high tensile strength and high fibre volume fraction of the composite largely unchanged. This one-step process also eliminates polymer blending prior to composite manufacturing.

CHAPTER 3

TOUGHENING OF NEAT EPOXY RESINS WITH PHENOXY

While the ultimate goal of this study is to improve the toughness of fibre reinforced epoxy composites, it is, however, important to understand the toughening in neat epoxy resin in the absence of reinforcing fibre. In this chapter the effectiveness on toughening of epoxy/phenoxy blends was studied. Two different types of epoxy resin, DGEBA and TGDDM and two phenoxy resins with different molecular weight were studied. DGEBA is difunctional and is the most widely used epoxy resin. It is found in a wide range of applications ranging from coatings and adhesives to fibre reinforced composites for the automotive industry. TGDDM is tetra-functional and can, therefore, be highly crosslinked. When it is fully cured it has a high modulus and high glass transition temperature and, consequently, is suitable for demanding applications such as aerospace-grade composites. Owing to the higher crosslink density, TGDDM is more brittle than DGEBA. The inherent toughness of the epoxy influences the degree of toughening that can be achieved in a composite. It has been found that rubbers are more effective at toughening a less crosslinked epoxy, while some thermoplastics are more effective at toughening a highly crosslinked epoxy [202-204].

The thermoplastic used in the current study is phenoxy resin, which is a high molecular weight linear thermoplastic made by reacting bisphenol A with the diglycidyl ether of bisphenol A making it chemically similar to DGEBA epoxy resin. Epoxy/phenoxy mixtures were found to be miscible on melt blending but, after curing, could be either miscible or immiscible, depending on the curing agent used [93] and cure kinetics [92]. Two different molecular weights of thermoplastic phenoxy were used to study the effect on toughening of epoxy, as it is generally acknowledged that a high molecular weight is beneficial in this respect [205, 206].

3.1 Experimental

3.1.1 Materials

Two epoxy resins with different chemical structures were used. One was Epon™ 828, a standard diglycidyl ether of the bisphenol A (DGEBA) type (Figure 2.7) supplied by Shell Chemicals. The other was Araldite™ MY721, a tetraglycidyl diamino diphenyl methane (TGDDM) type (Figure 2.8), supplied by Huntsman Advanced Materials. The curing agent was 4, 4'-diaminodiphenylsulfone (4'4-DDS) (Figure 3.1) supplied by Sigma Aldrich. A stoichiometric ratio of 0.75 DDS:epoxy resin was used throughout the study. This corresponds to a DDS: epoxy weight ratio of 24.5:100 for DGEBA and 46.6:100 for TGDDM.

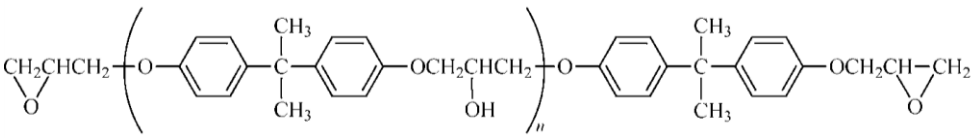

Figure 2.7 Structure of diglycidyl ether of bisphenol A (DGEBA).

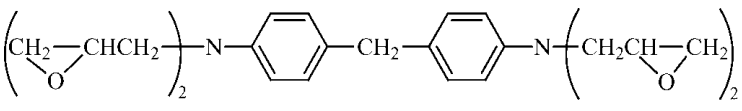

Figure 2.8 Structure of tetraglycidyl 4.4'-diaminodiphenylmethane (TGDDM).

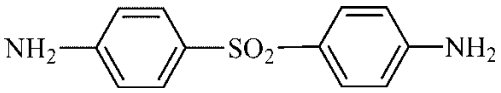

Figure 3.1 Chemical structure of DDS.

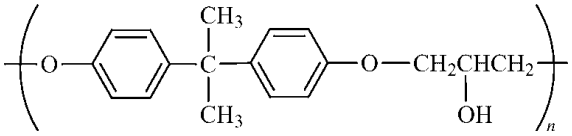

Figure 3. 2 Structure of phenoxy.

Phenoxy resins are thermoplastic polymers derived from bisphenol A and epichlorohydrin. They are chemically similar to DGEBA epoxy resins but have higher molecular weight (M_w). They lack terminal epoxides but have the same repeat unit as DGEBA epoxy resin and are classified as polyols or polyhydroxy ethers. Phenoxies are commercially offered as solids, solutions, and waterborne dispersions. The majority of phenoxy resins are used as thermoplastics per se, but some are used as additives in thermoset formulations where their high M_w provides improved flexibility and abrasion resistance. Smaller volumes of phenoxy resins are used as flexibilisers or rheology modifiers in composites and electrical laminate applications, and as composite resins. A new, emerging application is in fibre sizing, which utilizes waterborne phenoxies. They also have potential uses as compatiblizers for thermoplastic resins such as polyesters, nylons, and polycarbonates because of their high hydroxyl contents.

Two phenoxy resins of different molecular weights and in different forms were used in this study. One was low M_w (~900 Da), Epikote 1001, supplied by Shell Chemicals and available as granules. The other was high M_w (~37000 Da), Grilon® MS, available as a yarn of 500 dtex, supplied by EMS-Griltech. These yarns, with an individual filament diameter of 48 μm, were chopped to approximately 5 cm lengths to enable specimen manufacturing.

3.1.2 Specimen manufacturing

For neat, unmodified epoxy specimens, the resin was heated to 130ºC before adding the curing agent. The mixture was heated at this temperature and stirred until all curing agent was dissolved. This mixture was then poured into an open PTFE mould and degassed in a vacuum oven in two stages (medium and high vacuum), releasing the vacuum between stages. The epoxy resin was cured by heating to 180ºC at 3ºC/min followed by a dwell time of 2 hr at 180ºC, before cooling to room temperature at 3ºC/min. A dog-bone mould was used to prepare tensile specimen according to ASTM 638 Type V [207] requirements (Figure 3.3). Another rectangular mould was used to make fracture toughness and DMA specimen, which were cut to size (30 mm x 6 mm x 3 mm), after curing.

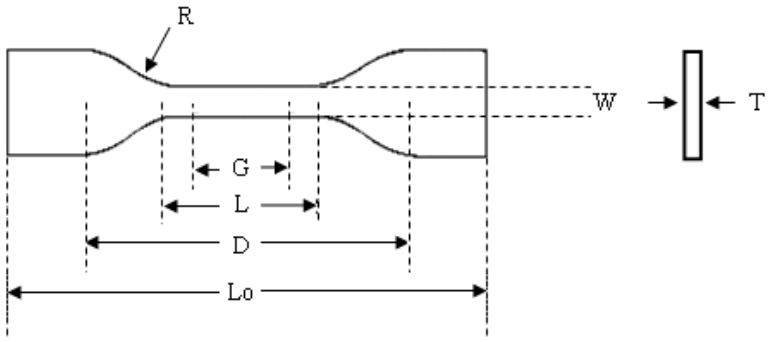

	Dimension (mm)
R – Radius of fillet	12.5
G - Gauge length	7.5
L -Length of narrow section	9.5
D – Distance between grip	25
Lo - Specimen length	65
W - Width of narrow section	3.2
T - Thickness	3

Figure 3.3 Specimen dimensions of neat resin tensile specimen.

The open mould had two parts, the top half contained cut-outs of the specimen shape required, and the lower half was a flat plate. The two halves were sealed with tacky tapes to prevent leaking. An open mould was selected due to the need for out-gassing. The mould was made of PTFE for ease of specimen removal, however, the use of mould release agent is still recommended. A two parts mould makes removing the cured epoxy specimens possible as the two halves can be separated and the specimens pushed out. However,, special care needed to be taken to prevent leaking. One of the major problems with the open mould was that the cured specimens were not flat and had raised edges as concave meniscus was formed. The cured specimens were grinded and polished with polishing wheels until the surface was flat and smooth.

For epoxy/phenoxy blend specimens, epoxy was again first heated to 130ºC before 5 wt% and 10 wt% of chopped (~ 50 mm) phenoxy fibre was added. The mixture was heated and stirred at this temperature until the fibre fully dissolved and the mixture became transparent. Curing agent was then added and the same mixing, degassing and curing procedure were carried out as described above.

3.1.3 Characterisations

3.1.3.1 Hot-stage microscopy

Hot-stage microscopy was used to observe dissolution of phenoxy fibre in epoxy resin, with and without curing agent, at different temperatures. A Linkam THMS 600 hot-stage with TP-90 controller was fitted to an Olympus BX60 optical microscope. Pure epoxy resin was first pre-heated to around 80ºC and a drop of resin was placed on a thin glass microscope slide before a few strands of phenoxy fibre, ~1 cm in length, were placed on top of the resin droplet. Another thin glass slide was then placed on top of the fibre in the epoxy resin. The specimen was subsequently

heated in the hot-stage to 80ºC and observed under the optical microscope, with the time needed to dissolve the fibre being noted. This procedure was repeated for 90ºC, 100ºC, 110ºC, 120ºC, and 130ºC. For epoxy with added curing agent, the curing agent was mixed with epoxy at 130ºC, and the mixture was then cooled to 80ºC before the phenoxy fibre was added and hot-stage microscopy carried out.

3.1.3.2 Tensile testing

Neat resin dog-bone Type V specimens were tested according to ASTM 638 [207] using an Instron universal testing machine at a test speed of 1 mm/min. An optical extensometer was used for strain measurement. Five specimens were tested for each type of specimens.

3.1.3.3 Fracture toughness

Fracture toughness tests on neat resin specimens were carried out according to ASTM D5045 (Figure 3.4) [208], using single notched 3-point bending specimen (30 mm x 6 mm x 3 mm). A notch, 2 mm deep, was machined in the middle of one side of the specimen before a fresh, sharp razor blade was slid repeatedly across the notch to create a total notch depth of 3 mm. The actual notch depth of each specimen was examined under an optical microscope after the test. 3-point bending tests were carried out using an Instron universal testing machine at a test speed of 1 mm/min and a span-to-thickness ratio of 4. Five specimens of each type were tested.

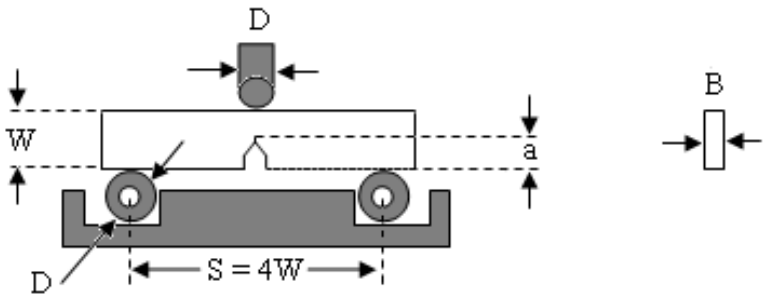

Figure 3.4 Specimen dimensions and set-up of fracture test.

3.1.3.4 Dynamic mechanical analysis (DMA)

Dynamic mechanical analysis (DMA) was carried out in a Q800, by TA Instruments, in 3-point bending mode and the specimens were simply supported. Sample size was (30 mm x 6 mm x 3 mm) and the span length was 20 mm. Specimens were heated from 30°C to 250°C at 3°C/min with amplitude of 25 µm at a frequency of 1 Hz. Values of storage modulus (*E'*), loss modulus (*E''*) and tan delta (*tan δ*) were recorded. Glass transition temperature, T_g, was taken at the *tan δ* peak. Three specimens of each type were tested.

3.1.3.5 Fractography

Mode I fracture surfaces of specimens were examined in a scanning electron microscope (SEM), Inspect F by FEI Company. Specimens were coated with gold and an electron beam of 20 kV was used. Fracture surfaces of neat resin specimens were obtained from fracture toughness tests with some of the specimens etched by immersing in tetrahydrofuran (THF) for a minute.

3.2 Results and Discussion

3.2.1 Phenoxy fibre dissolution

Hot-stage optical microscopy was used to observe the dissolution process of phenoxy fibre in epoxy resin at different temperatures. The main aim of the next chapter of this study was to introduce phenoxy fibres as a solid chopped fibre interleaf in a dry carbon fibre laminate preform which would then be infused with an epoxy resin under vacuum. The phenoxy fibres were expected to remain in solid form during infusion and first dissolve into the epoxy resin and then phase-separate during curing. It is, therefore, important to find out how phenoxy fibres would behave during the infusion process and then work out a suitable processing procedure so that the phenoxy fibres would not already dissolve during infusion but would dissolve completely during further heating.

Figure 3.5 shows the fibres in DGEBA resin before heating, with its outline clearly visible. As the heating continued, the fibres got thinner and after some time the fibres were no longer visible. Figure 3.6 plots the time required for the fibres to completely dissolve in DGEBA at different temperatures. It was found that the dissolution time increased when the curing agent was added to the epoxy, especially at lower temperatures. Another study [93] indicates that the type of curing agent used could affect the dissolution process of the phenoxy fibres.

Figure 3.7 shows the phenoxy fibres in TGDDM resin. The outline of the fibres could be seen at the beginning and became more blurred with time when heated until the fibres appeared to have merged into the epoxy. Figure 3.8 shows that the dissolution time decreased with the addition of curing agent, which is in contrast to the DGEBA system, and shows that it is not the curing agent *per se* but the combination of resin and curing agent that affects the dissolution process.

In both resins with curing agents, the fibres took more than 1 hr to dissolve at 80ºC, which means that the fibres should remain fully intact during the resin infusion process (both the fibre preform layup and the resins would be heated to 80ºC prior to infusion). Based on these results, a dwell time of 1 hr at 125ºC was selected for the fibre dissolution stage during composite preparation, which would allow the phenoxy fibre to fully dissolve in the epoxy resin before curing.

It should be noted that the maximum observation time for fibre dissolution was 60 minutes, therefore at certain temperatures while the results shown suggest a dissolution time of 60 minutes, the actual dissolution time was longer. It was decided from experience that 60 minutes would be ample for composites resin infusion to complete with the current set up. The fibres were observed at 1 minute increments and the dissolution time was defined as the time when outlines of the fibres could no longer be seen.

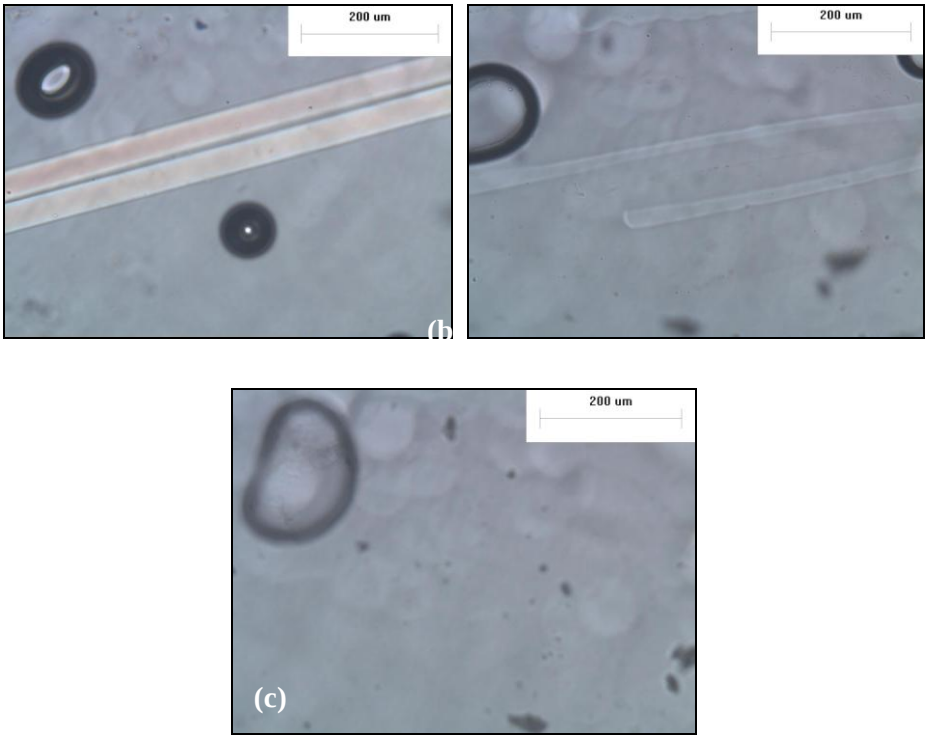

Figure 3.5 Hot-stage microscopy of phenoxy fibre in DGEBA epoxy + curing agent at 110ºC for (a) < 1 min, (b) 10 min and (c) 27 min.

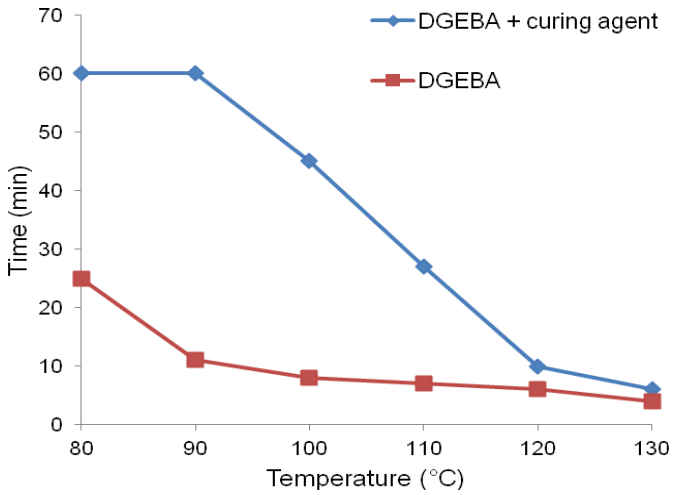

Figure 3.6 Phenoxy fibre dissolution in DGEBA epoxy.

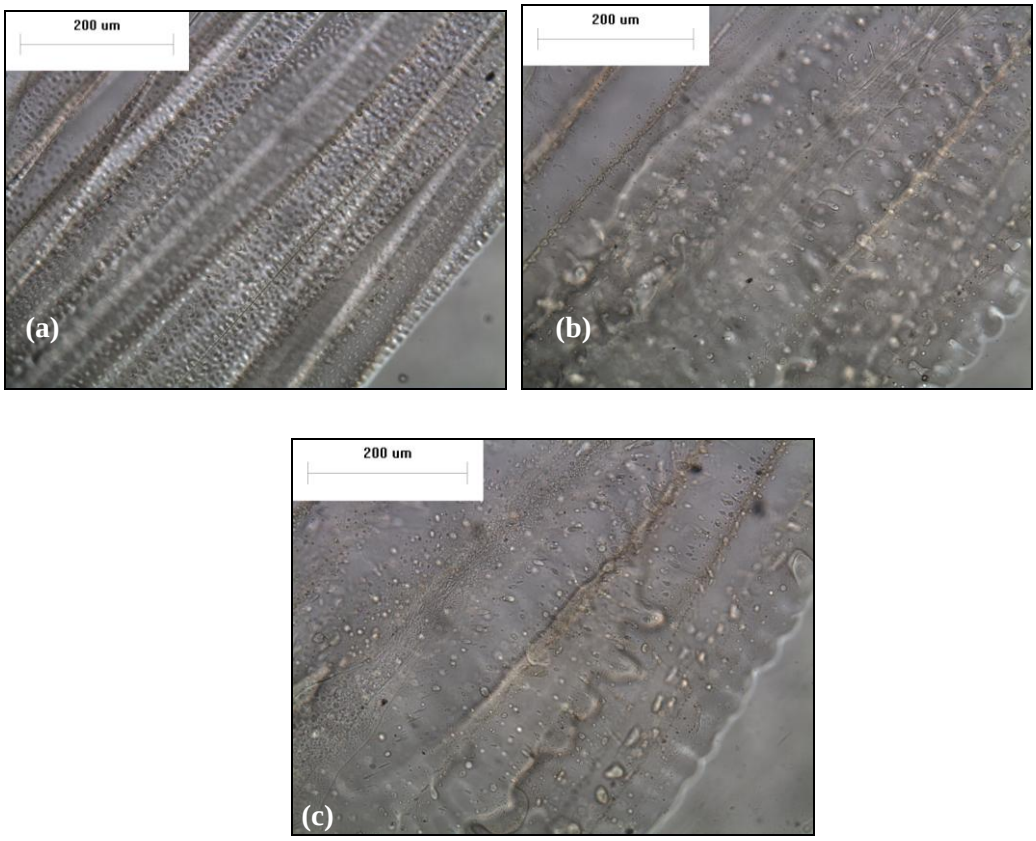

Figure 3.7 Hot-stage microscopy of phenoxy fibre in TGDDM epoxy + curing agent at 110°C for (a) < 1 min, (b) 10 min and (c) 20 min.

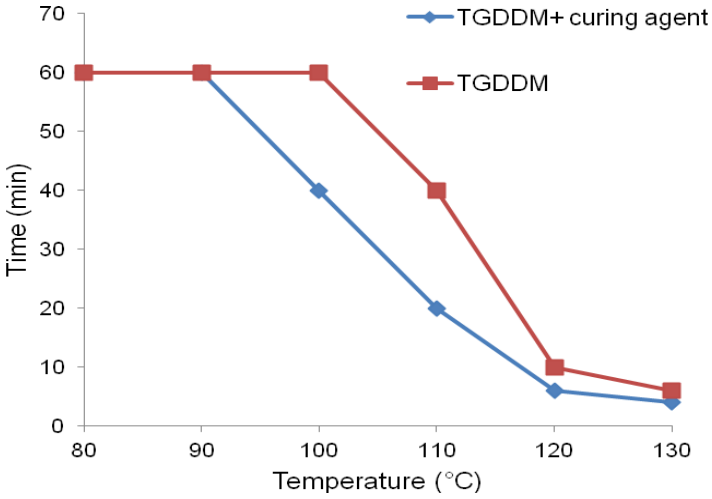

Figure 3.8 Phenoxy fibre dissolution in TGDDM epoxy.

3.2.2 Mechanical properties

Figure 3.9 shows the tensile properties of neat resin specimens made from DGEBA/low M_w phenoxy blends. Tensile modulus, strength and strain all decreased with the addition of low M_w phenoxy, especially at 5 wt% loading. Fracture toughness (Figure 3.10) of the blends was either not significantly improved (5 wt% phenoxy) or decreased (10 wt%) with the low M_w phenoxy. This suggests that low M_w phenoxy is not effective in toughening DGEBA epoxy while having a negative effect on the tensile properties. The performance of the 5 wt% blend was found to be worse than the 10 wt% blend in terms of both tensile properties and toughness.

For DGEBA/high M_w phenoxy blends, Figure 3.10 shows tensile properties did not change significantly when 5 wt% phenoxy was added, but that tensile modulus, strength and strain all increased when 10 wt% of phenoxy was added. However, In terms of fracture toughness, both epoxy/phenoxy blends showed improved K_{1c} and G_{Ic} values (Figure 3.11), with the 10 wt% phenoxy specimen showing the most significant increase in toughness at more than 20%. These results

are interesting as they show that the addition of high M_w phenoxy can result in an improvement in toughness with no adverse effects on tensile properties.

Table 3.1 compares these results with available data from other DGEBA/phenoxy blends (high M_w), it was found that the toughness improvement achieved in this study is less than most of the other blends. The curing of thermoset/thermoplastics blends is complicated and the different materials and processing parameters employed all contributed to the differences in the properties of the cured specimens. In the study by Siddhamalli and Kyu [94], toughness peaked at 20 wt% phenoxy, whereas Schauer *et al.* [96] found the 10 wt% phenoxy blend showed the most improvement.

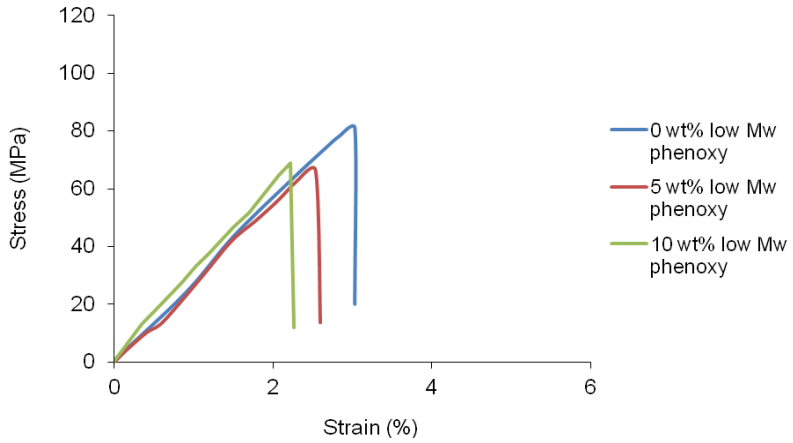

Resin	Low M_w phenoxy (wt%)	Modulus (GPa)			Strength (MPa)			Strain (%)		
		Ave	Max	Min	Ave	Max	Min	Ave	Max	Min
DGEBA	0	3.26	3.44	3.11	82.33	95.68	63.25	3.21	3.92	2.54
DGEBA	5	3.00	3.45	2.77	59.86	74.70	48.13	2.44	3.47	1.67
DGEBA	10	3.18	3.81	2.85	70.30	85.05	54.57	2.85	4.35	2.26

Figure 3.9 Tensile properties of DGEBA/low M_w phenoxy neat resin blends.

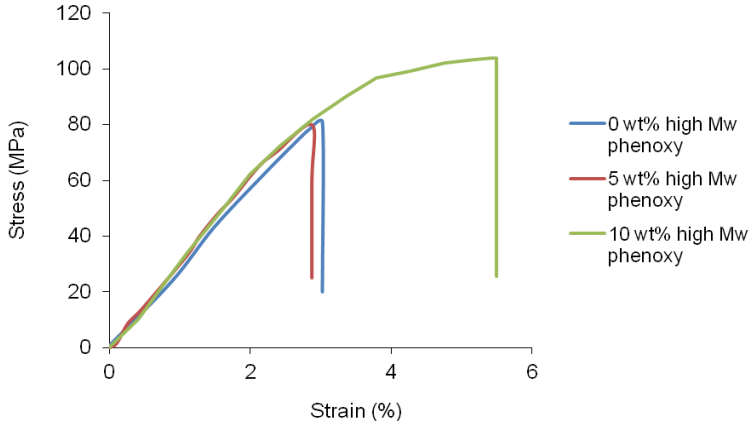

Resin	High M_w phenoxy (wt%)	Modulus (GPa)			Strength (MPa)			Strain (%)		
		Ave	Max	Min	Ave	Max	Min	Ave	Max	Min
DGEBA	0	3.26	3.44	3.11	82.33	95.68	63.25	3.21	3.92	2.54
DGEBA	5	3.28	3.57	3.11	80.29	94.87	66.68	2.80	3.55	2.05
DGEBA	10	3.55	3.89	3.18	99.70	104.12	85.16	4.78	5.74	3.00

Figure 3.10 Tensile properties of DGEBA/high M_w phenoxy neat resin blends.

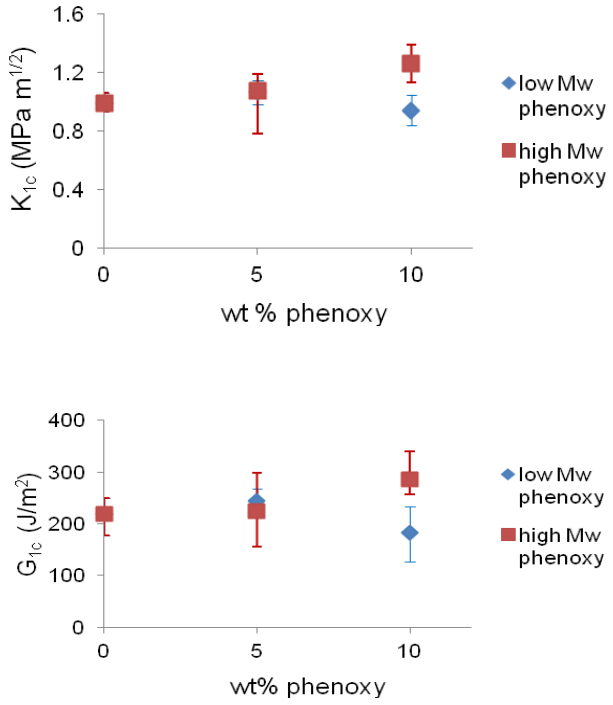

Figure 3.11 Fracture properties of DGEBA/phenoxy neat resin blends.

Table 3.1 Tensile properties of DGEBA/phenoxy blends with data from various studies.

Phenoxy (wt%)	Data taken from *	ΔK_{1c} (%)	ΔG_{1c} (%)	Δ Tensile modulus (%)	Δ Tensile strength (%)	Δ Tensile strain (%)
5	A	**8.8**	**3.1**	**14.7**	**-2.5**	**-12.6**
5	D	25	39.1	3.9	---	---
10	A	**25.4**	**30.3**	**10.4**	**21.6**	**56.1**
10	B	41.3	105.7	-3.3	-2.7	---
10	C	28.6	---	0.0	24.2	47.4
10	D	67.5	182.6	-2.5	---	---
15	D	28.8	45.7	8.1	---	---
20	C	357.1	---	-3.3	124.2	252.6
30	C	228.6	---	-6.7	87.9	194.7
40	C	57.1	---	-16.7	42.4	78.9

*** A – Current study** **C – Siddhamalli and Kyu [94];**
B – Teng and Chang [17] **D – Schauer *et al.* [96]**

For tensile properties of TGDDM/low M_w phenoxy blends (Figure 3.12), modulus was not significantly affected by the addition of phenoxy. Strength and strain were not significantly affected for the 5 wt% blend while an improvement was observed for the 10 wt% blend. Fracture toughness (Figure 3.14) was improved by 8% with a 5 wt% addition of low M_w phenoxy but, at 10 wt%, no significant effect was observed.

For TGDDM /high M_w phenoxy blends (Figure 3.13), the addition of phenoxy had little effect on strength while modulus was slightly decreased. Fracture toughness (Figure 3.14) increased by 12% for the 5 wt% blend but little effect was observed in the 10 wt% blend. This trend is similar to that of the TGDDM/low M_w phenoxy blends, although the toughening effect is more pronounced with the high M_w phenoxy.

The toughness values achieved in this study for both DGEBA and TGDDM blends are rather modest, compared to other more successful rubber (Table 2.1) and thermoplastic blends, such as PBT (Figure 2.12), PEI (Figure 2.18) and PSF (Figure 2.26). However, better improvement can be achieved with phenoxy, as shown by Siddhamalli and Kyu [94], possibly be optimising on the blend chemistry and processing conditions. In this study, phenoxy concentrations of only up to 10 wt% were investigated owning to manufacturing difficulties. Specimens were made by dissolving chopped phenoxy fibres in heated resins and large amount of gas was trapped in the mixture during the process. Degassing was carried out after mixing to release trapped air but it became more and more difficult with increasing phenoxy content as viscosity increased drastically.

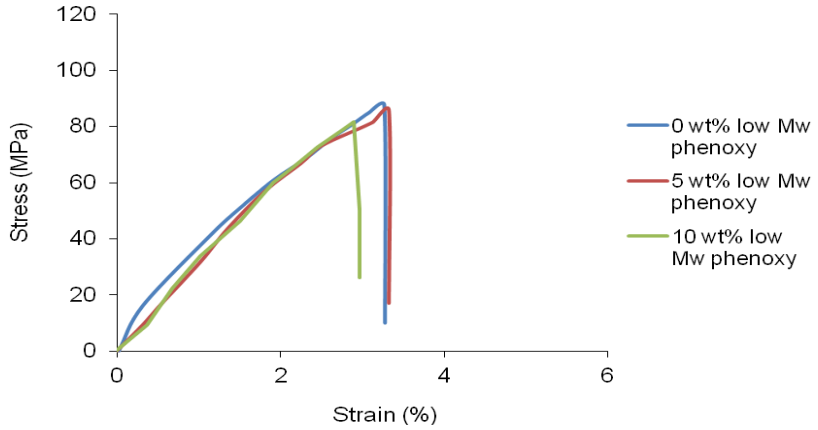

Resin	Low M_w phenoxy (wt%)	Modulus (GPa)			Strength (MPa)			Strain (%)		
		Ave	Max	Min	Ave	Max	Min	Ave	Max	Min
TGDDM	0	3.19	3.58	2.65	80.34	102.14	51.44	3.03	4.40	1.60
TGDDM	5	3.32	3.58	3.25	78.19	97.34	64.38	2.85	3.83	2.09
TGDDM	10	3.38	3.79	3.01	89.08	98.90	74.47	3.51	4.07	2.74

Figure 3.12 Tensile properties of TGDDM/low M_w nphenoxy neat resin blends.

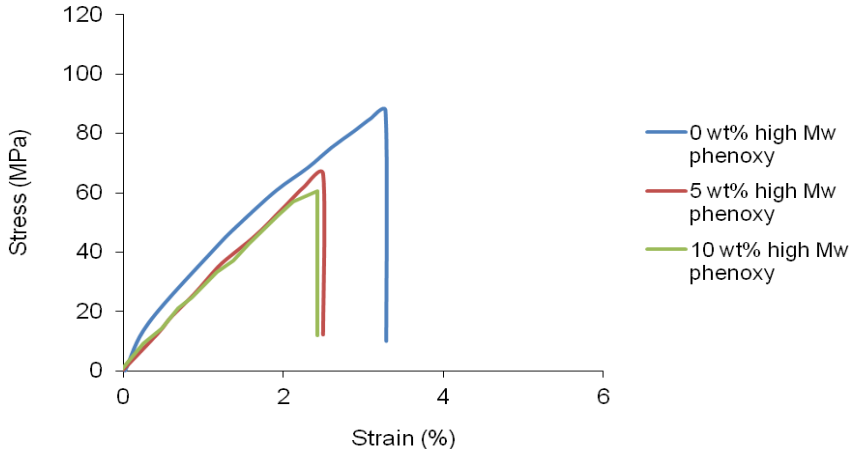

Resin	High M_w phenoxy (wt%)	Modulus (GPa)			Strength (MPa)			Strain (%)		
		Ave	Max	Min	Ave	Max	Min	Ave	Max	Min
TGDDM	0	3.19	3.58	2.65	80.34	102.14	51.44	3.03	4.40	1.60
TGDDM	5	2.86	3.3	2.34	68.15	76.27	62.82	2.59	2.95	2.35
TGDDM	10	3.41	3.6	3.18	68.35	80.99	49.7	2.51	3.28	1.55

Figure 3.13 Tensile properties of TGDDM/high M_w nphenoxy neat resin blends.

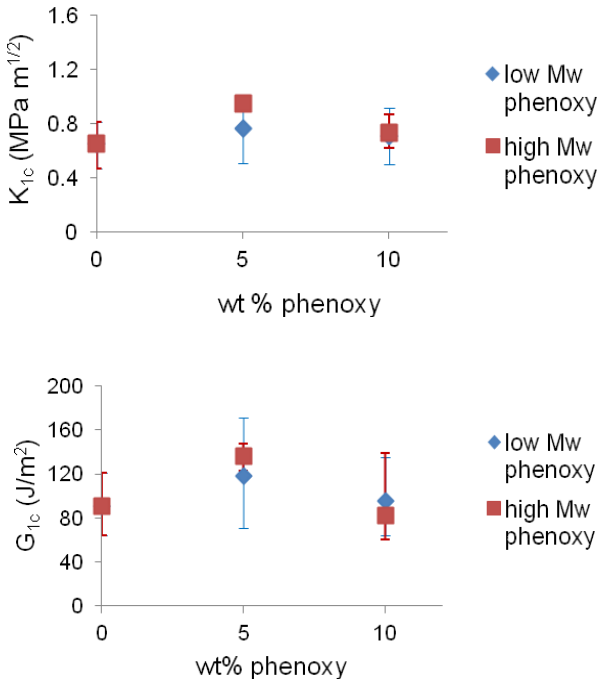

Figure 3.14 Fracture properties of TGDDM/phenoxy neat resin blends.

3.2.3 Glass transition temperature

In this study, the T_g of the blends is defined as the peak of the *tan* δ from DMA. For the DGEBA/low M_w phenoxy blends (Table 3.2), only one T_g was detected, indicating that the blends are homogeneous with no phase separation. Blends with the high M_w phenoxy showed two T_g's, indicating a phase separated blend with the lower T_g corresponding to the phenoxy-rich phase and the high T_g to the epoxy-rich phase. The T_g of the phenoxy-rich phase was lower than that of the pure phenoxy (104°C) which was not expected. On the other hand the T_g of the epoxy phase was slightly raised which again remain to be explained.

For TGDDM/phenoxy blends (Table 3.3), as with the DGEBA blends, one T_g was detected for the low M_w phenoxy blends, indicating that these blends were miscible. The two T_g values detected for the high Mw blends showed the presence of two phases, one being the phenoxy-rich phase and one the cured epoxy phase. In these blends, the T_g of the cured epoxy remained unchanged, which suggests that there was no phenoxy left in the cured epoxy. Similar findings were presented in another study [209], where it was suggested that there was little interaction between phenoxy and epoxy during the early stages of curing, the phenoxy was later expelled from the curing epoxy network and formed a separate phase as the cross-link density of epoxy increased

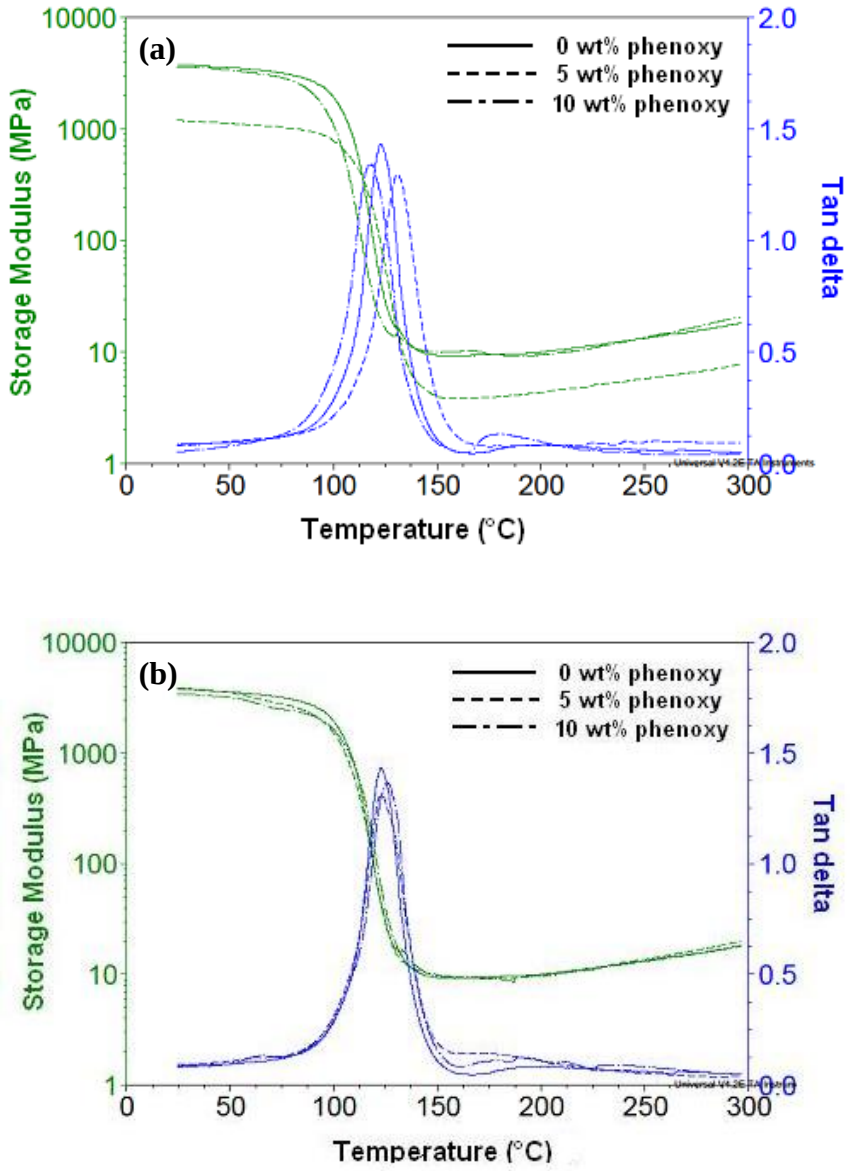

Figure 3.15 DMA curves for DGEBA/phenoxy blends with (a) low M_w phenoxy and (b) high M_w phenoxy.

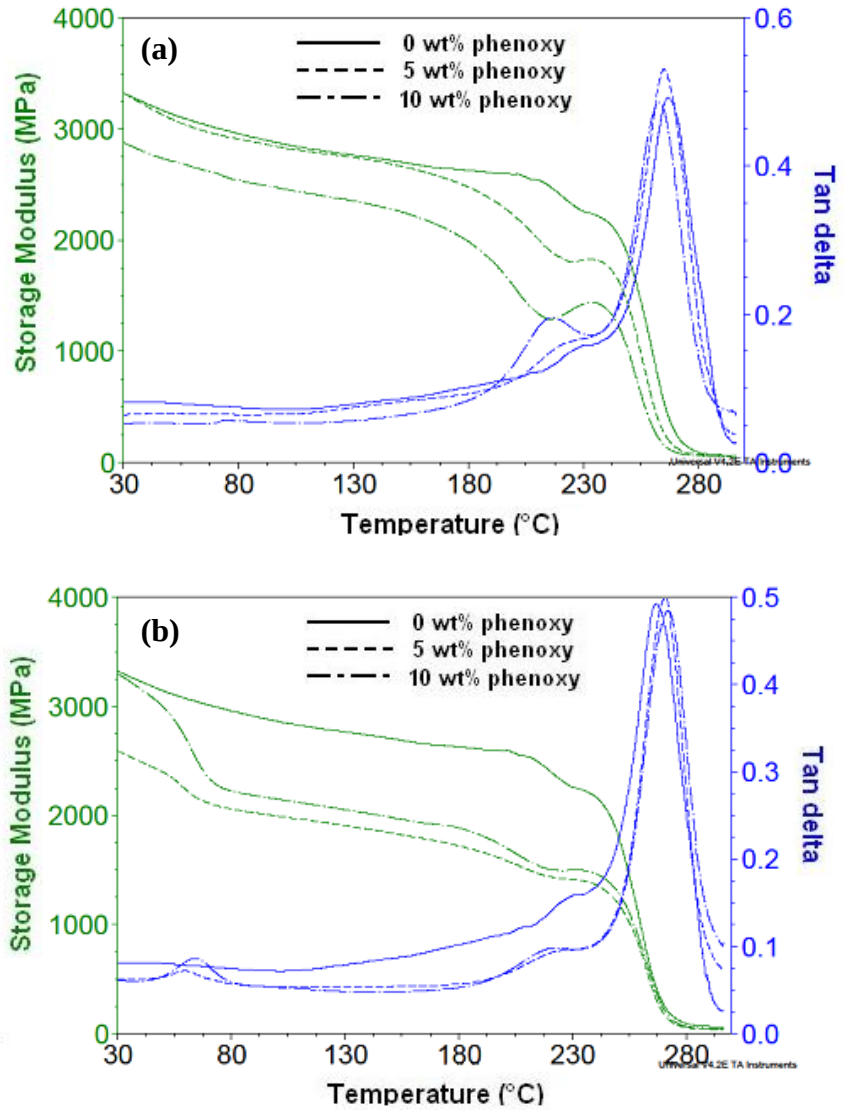

Figure 3.16 DMA curves for TGDDM/phenoxy blends with (a) low M_w phenoxy and (b) high M_w phenoxy.

Table 3.2 T_g of DGEBA/phenoxy blends determined by DMA.

resin	wt% low M_w phenoxy	wt% high M_w phenoxy	T_{g1} (°C)	T_{g2}(°C)
DGEBA	0	0		118
DGEBA	5	0		130
DGEBA	10	0		125
DGEBA	0	5	65	123
DGEBA	0	10	65	125

Table 3.3 T_g of TGDDM/phenoxy blends determined by DMA.

resin	wt% low M_w phenoxy	wt% high M_w phenoxy	T_{g1}(°C)	T_{g2}(°C)
TGDDM	0	0		226
TGDDM	5	0		225
TGDDM	10	0		216
TGDDM	0	5	60	225
TGDDM	0	10	62	223

3.2.4 Morphology

Phase separation and the resulting morphology in thermoset/thermoplastic blends are very complex and involve miscibility, critical viscosity, gelation and vitrification, and both the thermodynamics and kinetics of the system have to be considered. For thermoplastic blends which are uncrosslinkable, morphology is mainly based on a thermodynamically reversible process. For a thermoset/thermoplastic system, the molecular weight of the thermoset component and the resulting viscosity, T_g and crosslink density change continuously as curing progresses.

Epoxy/phenoxy blends were studied by Teng and Chang [17, 92]. It was found that phenoxy is miscible with epoxy resin during the early stages of curing, but tends to separate out when the epoxy resin molecular weight has increased to a critical value and are therefore thermodynamically immiscible. Phase separation then becomes a kinetically controlled diffusion process, and the viscosity increases to a critical level where the diffusion is difficult, and the phase structure is fixed. A schematic phase diagram of epoxy/phenoxy blends is shown in Figure 3.17.

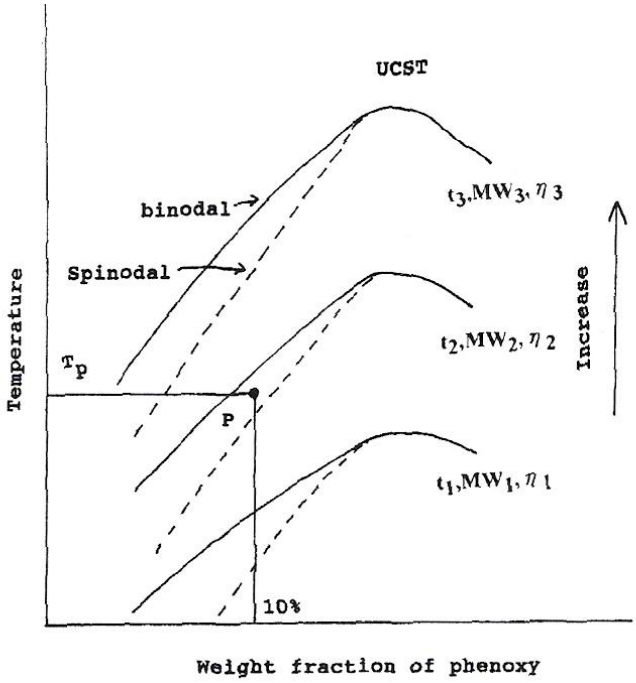

Figure 3.17 Schematic phase diagram illustrating the phase separation mechanisms of an epoxy/phenoxy system [17].

Fracture surfaces of the DGEBA/low M_w phenoxy blends (Figure 3.19 and Figure 3.20) show no special features when compared to those of pure resin (Figure 3.18). Fracture surfaces of the low M_w phenoxy are generally smooth apart from the river lines radiating from the crack front. Figure 3.22 and Figure 3.22 confirm the presence of phase separation in the DGEBA/high M_w phenoxy blends. Phenoxy

fibres are no longer present and have completely dissolved followed by phase-separation into a particulate morphology. The phenoxy-rich phase consists of micron sized spherical particles, with fracture surfaces of the blends generally being rougher in appearance. Plastic deformation of the secondary phase, which is expected to be more ductile than the highly cross-linked epoxy, could be observed in the 5 wt% blend (Figure 3.21) while in the 10 wt% blend (Figure 3.22), there is evidence of epoxy deformation around the phenoxy-rich phase. The secondary phenoxy phase also appears to be larger for the 10 wt% blend. The specimens were immersed in THF at room temperature for a minute and it was expected that the thermoplastic phenoxy phase would be dissolved by the THF, while the more chemical resistant epoxy matrix would remain intact. The etched surface shows cavities previously occupied by phenoxy-rich domains which have been dissolved (Figure 3.23). The smooth surfaces of the cavities indicate that there was little interaction at the interface between the phenoxy-rich and epoxy phases. These observations on the DGEBA/high M_w phenoxy blends are in agreements with a study by Siddhamalli and Kyu [94].

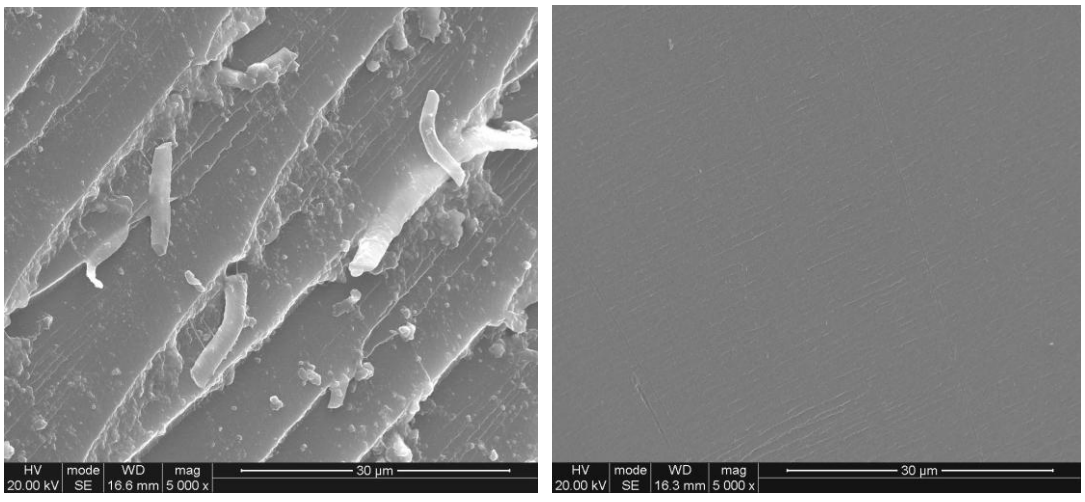

Figure 3.18 Mode-I Fracture surface of DGEBA epoxy: (a) close to crack front and (b) away from crack front.

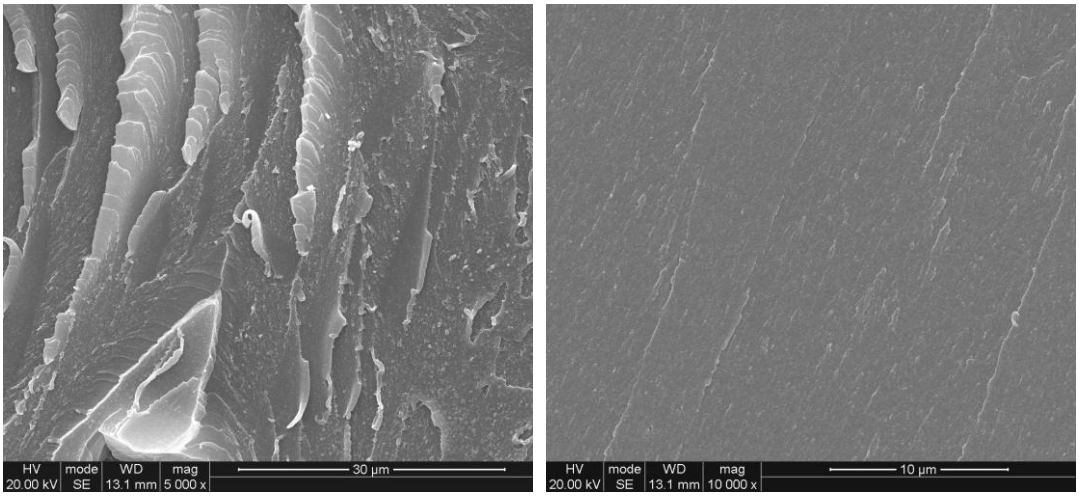

Figure 3.19 Mode-I Fracture surface of DGEBA epoxy + 5 wt% low M_w phenoxy: (a) close to crack front and (b) away from crack front showing no phase separation

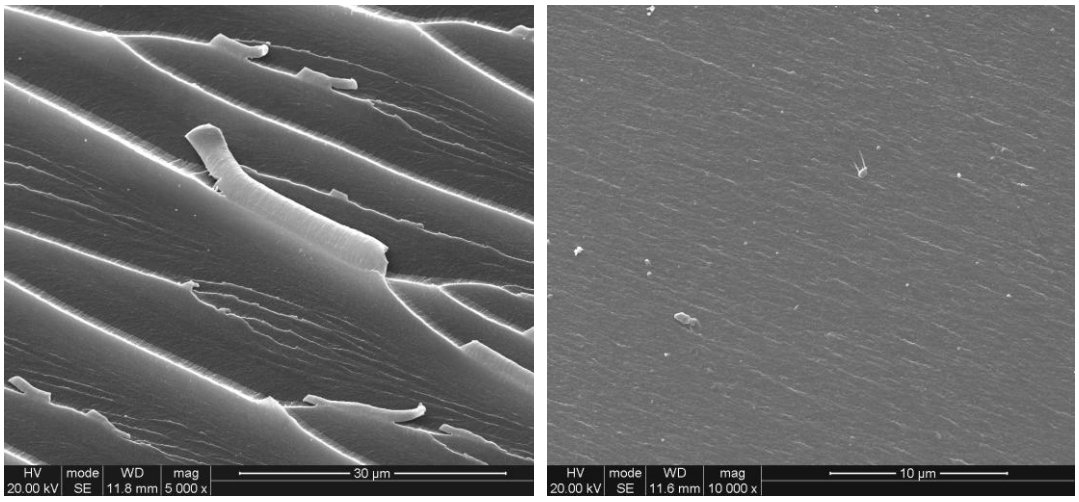

Figure 3.20 Mode-I Fracture surface of DGEBA epoxy + 10 wt% low M_w phenoxy: (a) close to crack front and (b) away from crack front showing no phase separation.

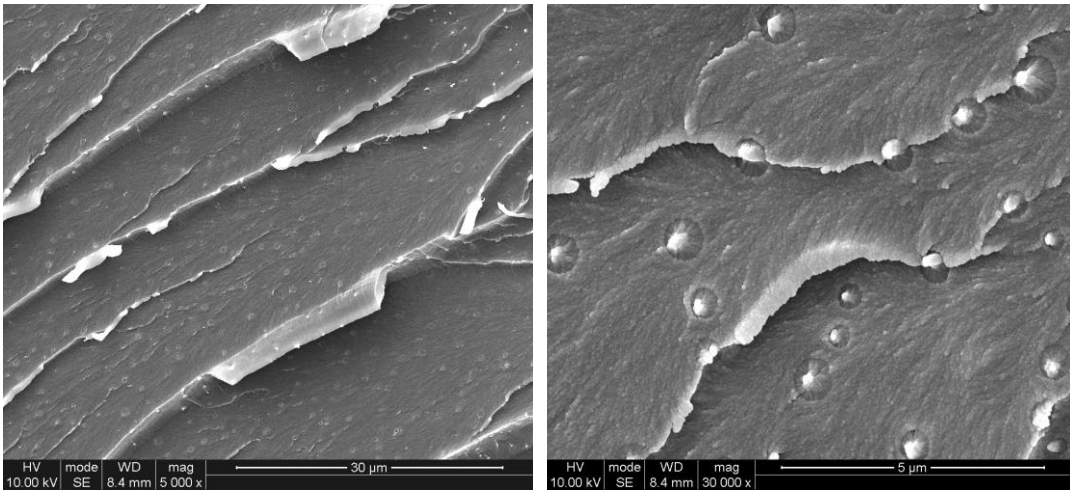

Figure 3.21 Mode-I Fracture surface of DGEBA epoxy + 5 wt% high M_w phenoxy: (a) lower magnification (b) higher magnification, showing phase separation with a droplet phenoxy phase

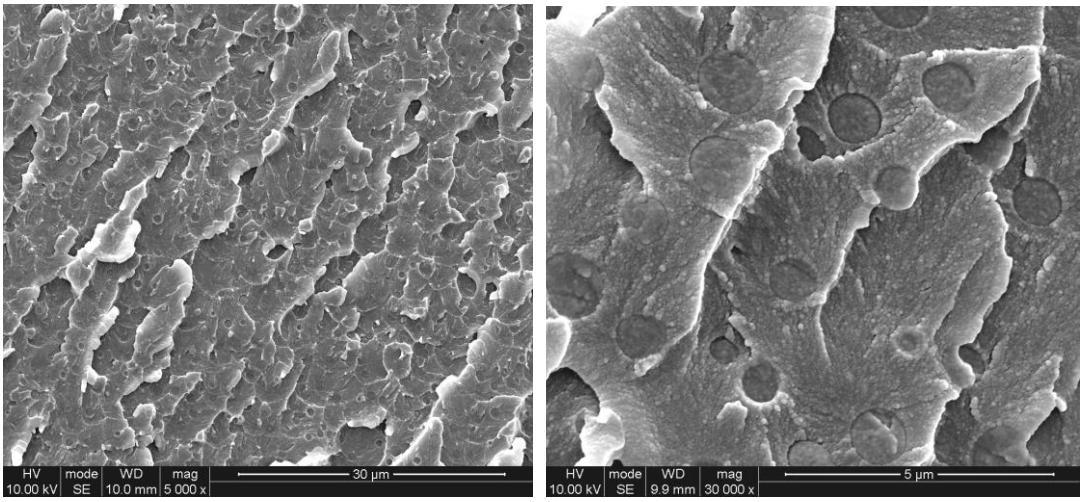

Figure 3.22 Mode-I Fracture surface of DGEBA epoxy + 10 wt% high M_w phenoxy: (a) lower magnification (b) higher magnification, showing phase separation with a droplet phenoxy phase and extensive plastic deformation

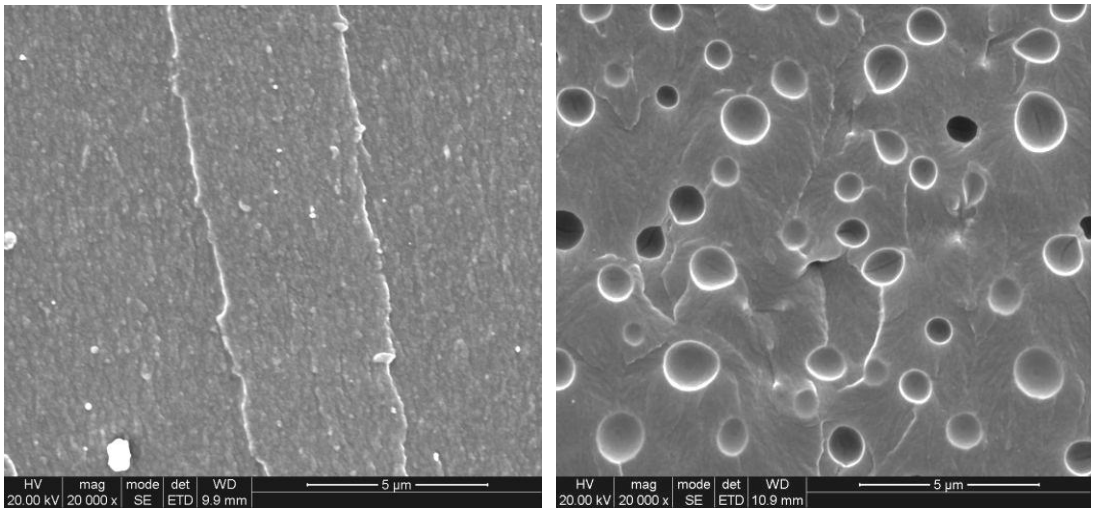

Figure 3.23 Mode-I Fracture surface of etched DGEBA epoxy: (a) 10 wt% low M_w phenoxy with no phase separation; (b) 10 wt% high M_w phenoxy showing hollow spheres after the phenoxy phase was etched away

Similar trends were also observed for the fracture surfaces of the TGDDM/low M_w phenoxy blends (Figure 3.25 and Figure 3.26), in which no phase separation and no special features could be observed. Phase separated morphologies were observed for both high M_w blends (Figure 3.27 and Figure 3.28). Fracture surface of the phase separated blends is rougher, and crack deflection could be observed. Smooth cavities are observed for the etched TGDDM/high M_w phenoxy (Figure 3.29) indicating little interaction between the phenoxy-rich and cured epoxy phases.

The phenoxy-rich phase has lower modulus then the epoxy matrix. This modulus mismatch, particularly in the TGDDM blends, can create a stress concentration and initiate more yielding in the epoxy. Therefore, it was suggested that a particle-induced shear yielding mechanism, similar to that for rubber modified epoxy, could be the key toughening mechanism [17]. Particle-induced yielding can contribute to crack tip blunting prior to crack initiation and localised energy dissipation during crack propagation. Another suggested toughening mechanism is

yielding of the phenoxy-rich phase initiate local yielding in the epoxy matrix [94]. Other toughening mechanisms that operate in a two-phase morphology and mentioned in the literature for epoxy/thermoplastic blends, such as crack bridging, crack pinning, crack deflection, crack tip bifurcation, and micro-cracking, could also contribute to varying, if somewhat more minor degrees to the overall toughness.

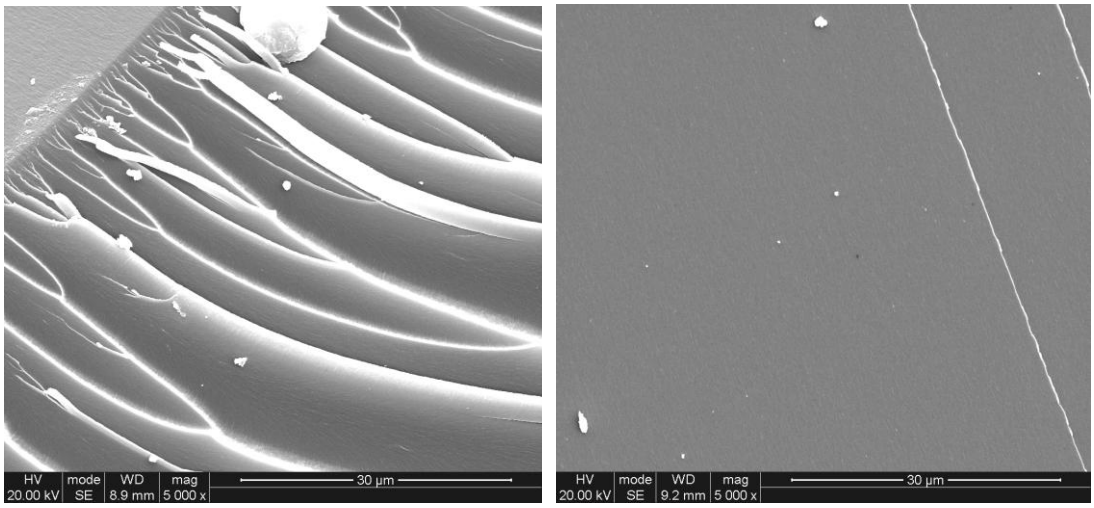

Figure 3.24 Mode-I Fracture surface of TGDDM epoxy: (a) close to crack front and (b) away from crack front.

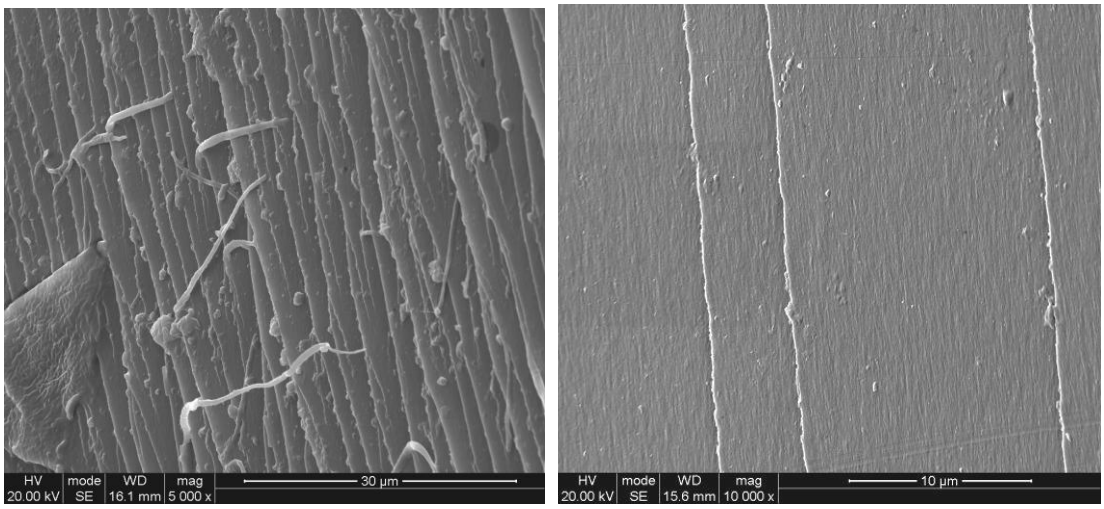

Figure 3.25 Mode-I Fracture surface of TGDDM epoxy + 5 wt% low Mw phenoxy: (a) lower magnification (b) higher magnification, showing no phase separation.

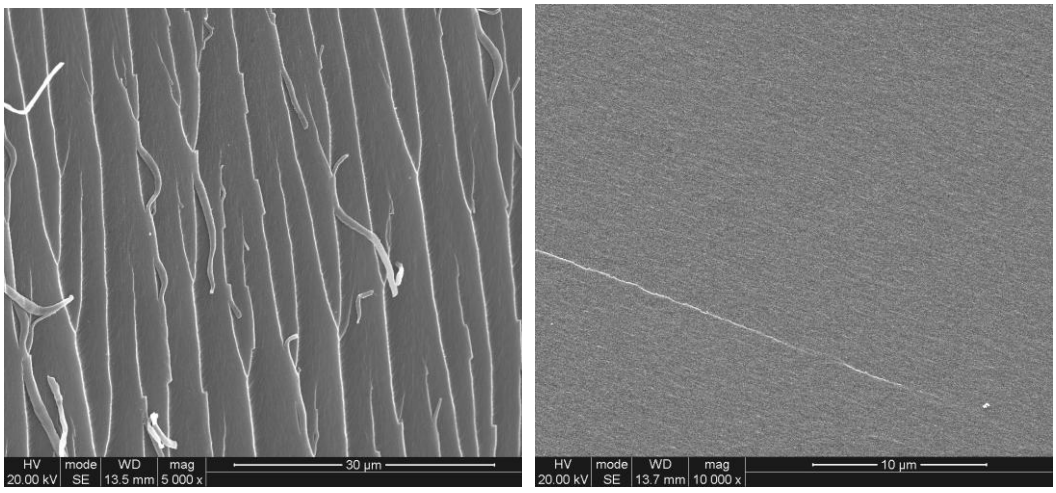

Figure 3.26 Mode-I Fracture surface of TGDDM epoxy + 10 wt% low Mw phenoxy: (a) lower magnification (b) higher magnification, showing no phase separation.

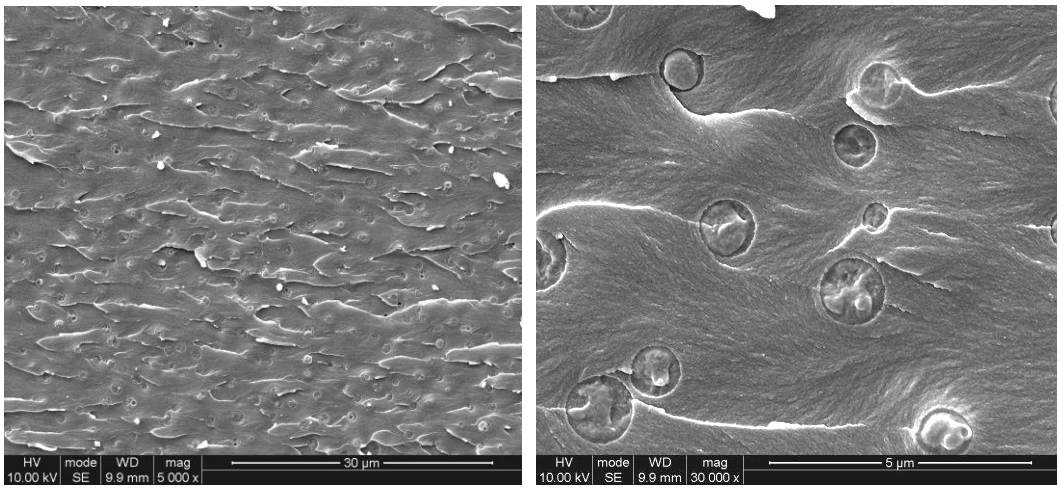

Figure 3.27 Mode-I Fracture surface of TGDDM epoxy + 5 wt% high Mw phenoxy: (a) lower magnification (b) higher magnification, showing phase separation with a droplet phenoxy phase and a more ductile fracture surface than single phased epoxy.

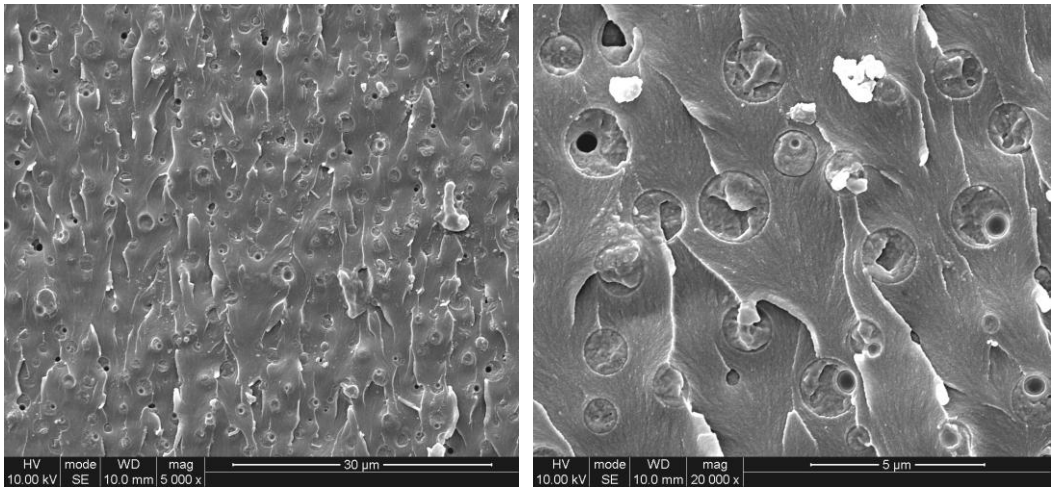

Figure 3.28 Mode-I Fracture surface of TGDDM epoxy + 10 wt% high Mw phenoxy: (a) lower magnification (b) higher magnification, showing phase separation with a droplet phenoxy phase and a more ductile fracture surface than single phased epoxy.

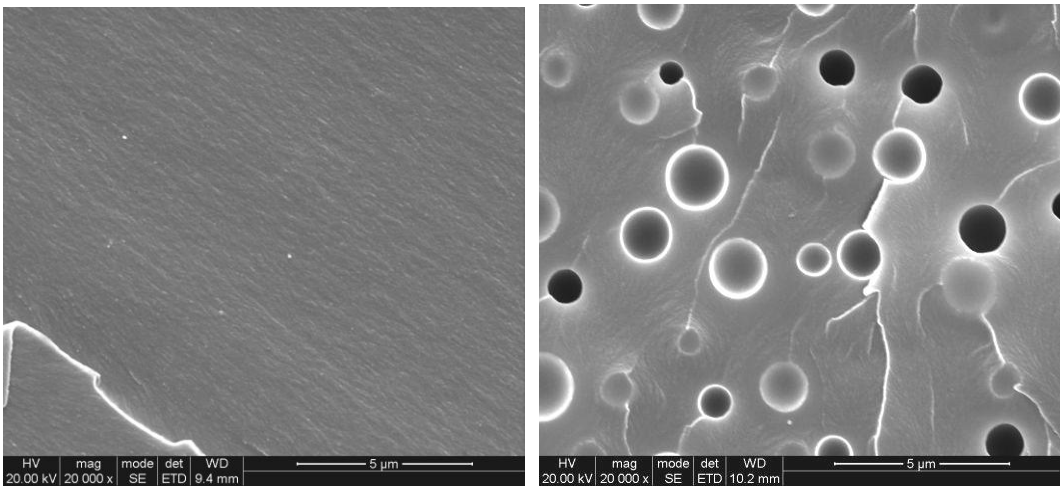

Figure 3.29 Mode-I Fracture surface of etched TGDDM epoxy: (a) 10 wt% low M_w phenoxy with no phase separation; (b) 10 wt% high M_w phenoxy showing hollow spheres after the phenoxy phase was etched away.

3.3 Conclusion

It was found that phenoxy resins can form miscible blends with both DGEBA and TGDDM resins upon mixing, i.e. the blends were initially visibly transparent. Upon curing, the high M_w phenoxy resin phase-separated from both epoxy resins and spherical, phenoxy-rich domains were formed in the crosslinked epoxies at both 5 wt% and 10 wt% loading and the cured specimens were opaque. For both epoxy resin systems, by looking at the etched fracture surfaces, no evidence of chemical reaction between the phenoxy-rich phase and the cured epoxy could be found. The addition of high M_w phenoxy did not appear to have much effect on the cure of either epoxy system as the T_g remained unchanged. However, for the low M_w phenoxy, no evidence of phase separation could be found for either epoxy system, suggesting that the blends remained miscible upon curing.

In terms of fracture toughness, the addition of a low M_w phenoxy resin did not have a positive effect on either epoxy resin systems. On the other hand, the addition of high M_w phenoxy improved the toughness of both epoxy resins to a small extent without adversely affecting the tensile properties. For DGEBA, a loading of 10 wt% was preferred, while for TGDDM 5 wt% was preferred. It was found that the presence of a phase separate morphology on its own was not enough to explain improvement in toughness. This suggests that the size and distribution of the phenoxy-rich phase, as well as the intrinsic toughness of the cured epoxy, are all important factors in determining the final properties.

CHAPTER 4

TOUGHENING OF CARBON FIBRE/EPOXY COMPOSITES WITH DISSOLVABLE PHENOXY FIBRES

The previous chapter studied the properties of bulk epoxy/phenoxy blends. Here we explore a novel toughening concept based on a dissolvable phenoxy fibre as a localised toughening agent for carbon fibre/epoxy composites. The concept is basically a combination of existing toughening concepts based on the inclusion of thermoplastics as fibres, interleafs and as a dispersed phase in the epoxy matrix. The current study uses phenoxy fibres, which are incorporated in solid form into a carbon fibre preform as a chopped fibre interleave. Composite laminates are made by a vacuum infusion process, where the phenoxy fibre was expected to remain in solid form during infusion but then dissolves and subsequently phase separates when the resin is heated during curing.

The main benefits of this approach are that low viscosity resins can be used for infusion, thus ensuring easy resin impregnation and compatibility with other toughening concepts such as 3-D, stitched and non-woven interleaf mats. It also allows for localised toughening by positioning dissolvable thermoplastic fibres in the composite structure where they are most needed; i.e. within the interlaminar region. It is expected that toughening concepts based on dissolvable thermoplastic fibres can

lead to improved damage tolerance for thermoset composites without compromising processability, mechanical or thermal properties of such systems [210].

It should be noted that the use of a dissolvable thermoplastic fibre in epoxy composites has recently been commercialised. This is the basis of the PRIFORM® system developed by Cytec Engineering Materials for liquid resin infusion processes. The Cytec patent claims that a phenoxy fibre can be used as toughening agent [210, 211]. Phenoxy fibre is marketed by EMS-Griltech as a bonding fibre which has a toughening effect [212]. Recently a study of using phenoxy as a stitching yarn for carbon fibre/epoxy composites has been reported [213]. However, so far no detailed study has been reported on the thermal and mechanical properties of phenoxy fibre toughened carbon/epoxy systems.

4.1 Experimental

4.1.1 Materials

Two epoxy resins are used for the composite laminates, one was Araldite™ LY564, a DGEBA (Figure 2.8) type resin developed for resin infusion by Ciba Geigy. The curing agent was 4, 4'-diaminodiphenylsulfone (4-4' DDS) (Figure 3.1) supplied by Sigma Aldrich. A stoichiometric ratio of 0.75 DDS: 1.0 epoxy resin was used throughout the study and the weight ratio was 24.5 DDS: 100 epoxy.

The other was ACG MVR 444, a TGDDM based resin (Figure 2.9) premixed with polyamines curing agent, it is designed for resin infusion and was supplied by Advanced Composites Group UK.

The phenoxy fibre used was Grilon® MS phenoxy yarn, 500 dtex, supplied by EMS-Griltech. Phenoxy is a high molecular weight linear thermoplastic made by reacting bisphenol A with the diglycidyl ether of bisphenol A making it chemically similar to DGEBA epoxy resin, but with no terminal epoxide groups (Figure 2.11). These phenoxy fibres, with an individual filament diameter of 48 μm, were chopped to approximately 5 cm lengths to enable specimen manufacturing.

Plain weave carbon fibre fabric (300 g/m^2) based on high-strength carbon fibre Pyrofil® TR30S-6K from Mitsubishi Rayon Co., was supplied by Carr Reinforcements, UK.

4.1.2 Specimen manufacturing

A steel plate was used as a mould and was coated with Frekote mould release agent. Six layers of plain weave carbon fibre fabric were cut to size (400 mm x 370 mm) and the lay-up was $[0]_6$. An insert film of 12 μm thick PTFE was placed in the mid-plane of the lay-up for the double cantilever beam (DCB) specimens. The fabric was sealed in a vacuum bag and the mould was heated to 80ºC before resin infusion. The DGEBA epoxy resin and curing agent was heated to 130ºC and the mixture was stirred until the curing agent was fully dissolved. The mixture was then degassed for 15 min. The vacuum bag was placed under a vacuum of ~1 bar for the resin infusion process. The infused laid-up specimen was then cured by heating to 180ºC at 3°C/min, followed by a dwell at 180ºC of 2 hr before cooling to room temperature at 3ºC/min.

For DGEBA phenoxy modified composite laminates, the phenoxy fibre was added as a chopped fibre mat between each layer of carbon fibre fabric. The amount of phenoxy fibre corresponded to around 5 wt% and 10 wt% of the total matrix content of the composite. The phenoxy fibre was weighed and randomly distributed by hand between the carbon fibre plies. The distribution of phenoxy fibre in terms of areal density was around 12.5 g/m^2 and 25 g/m^2 for the 5 wt% and 10 wt% specimens, respectively. Upon impregnation and subsequent curing these phenoxy fibres are expected to dissolve and phase separate to form a secondary (spherical) phase that toughens the epoxy matrix at the inter-ply region. The preparation of the mould, sealing of the vacuum bag, mixing of the resin and curing agent, and the resin infusion process were all as described above. The curing cycle was 80 to 125 °C at 3°C/min, with a dwell time of 1 hr at 125°C, followed by heating to 180°C at 3C/min and hold at 180°C for 2 hr, before cooling to room temperature at 3°C.

For TGDDM specimens, the same bagging procedures were followed. The premixed resin was heated up to 80C for resin infusion. The curing cycle was 80 to 120°C at 3°C/min, hold at 120°C for 4 hr, before cooling to room temperature at 3°C/min. A post-curing cycle was carried out in which the specimens was heated from room temperature to 180°C at 3°C/min, hold at 180°C for 2 hr before cooling to room temperature at 3°C/min.

Figure 4.1(a) shows a schematic diagram of a general set up of a vacuum bag and a more detailed layup of the fabric is shown in Figure 4.1(b) without phenoxy and Figure 4.1(c) with chopped phenoxy fibre. The volume fraction, $V_{f,}$ of all the laminates made was in the range of 0.5 with a laminate thickness of around 2.2 mm ± 0.4mm. V_f was calculated using the weight of the different components.

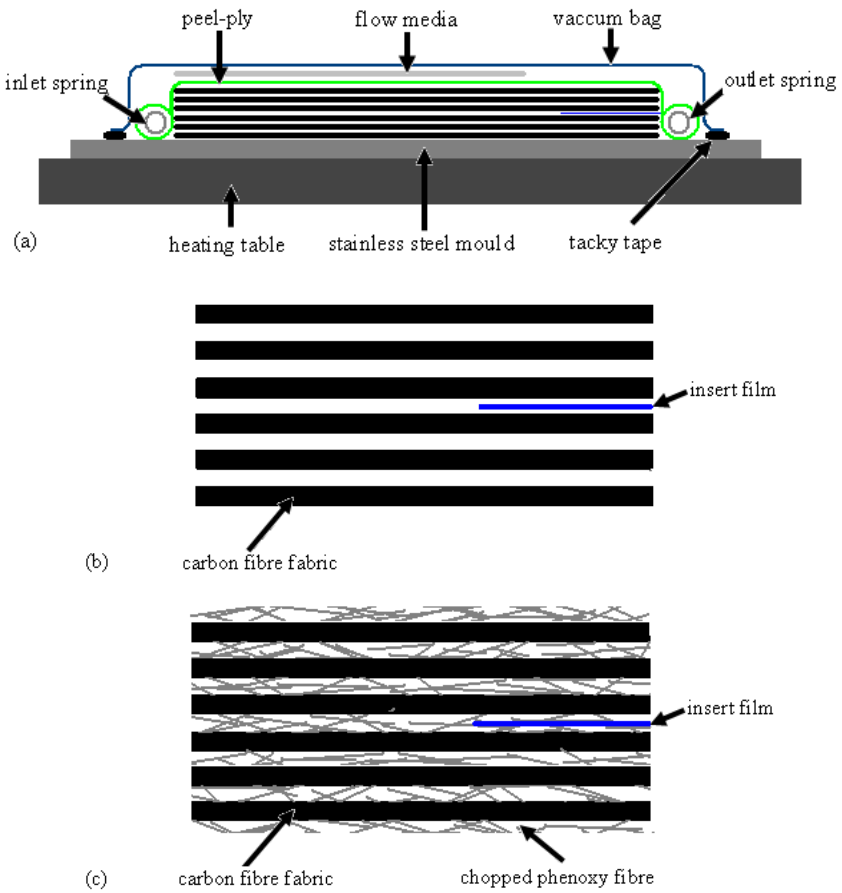

Figure 4.1 Schematic diagram of the composite laminate layup, (a) a general vacuum bag setup, (b) layup without phenoxy (c) layup with chopped phenoxy fibre.

4.1.3 Characterisations

4.1.3.1 Tensile testing

The tensile properties of a continuous fibre composite are largely determined by the fibre as it is the load carrying component. However, the fibre/matrix interface also plays an important role as it affects load transfer between matrix and fibre, with good interfacial bonding being preferred for optimum strength. For composites with brittle matrices, such as epoxy, tensile failure generally starts with matrix cracking. As matrix cracking continues, a majority of the load is transferred to the fibres and fibres carry the load until complete failure occurs.

The composite specimens were cut to size (200 mm x 20 mm) with end-tabs (38 mm x 20 mm) adhesively bonded to both ends and tested according to ASTM D3039 (Figure 4.2) [214]. For strain measurement, a strain gauge with a length of 6 mm was bonded to the centre of each specimen using an adhesive. The tests were performed with an Instron 5505 universal testing machine at a testing rate of 2 mm/min.

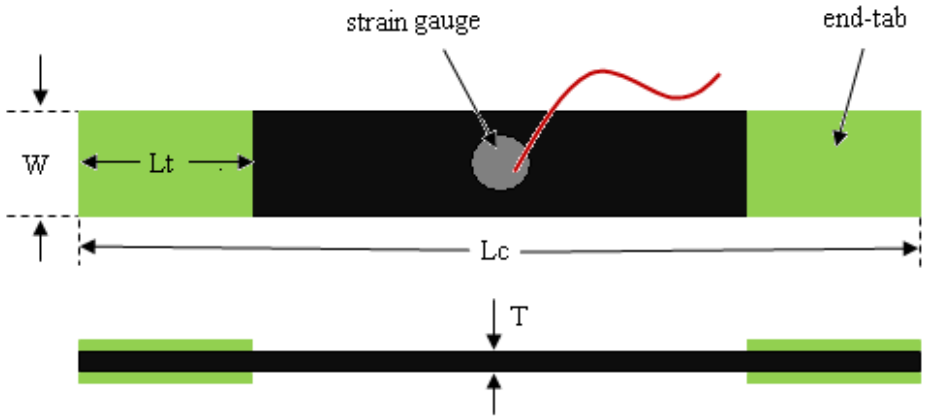

Figure 4.2 Schematic diagram of tensile test specimens.

4.1.3.2 Mode-I delamination toughness

Laminated fibre-reinforced composites are susceptible to delamination. The initiation and propagation of a delamination is controlled by the interlaminar fracture toughness of the composite material. Interlaminar fracture toughness of laminated composites is normally expressed in terms of critical energy release rate, G_c, and it is the energy consumed by the material as the delamination front advances through a unit area.

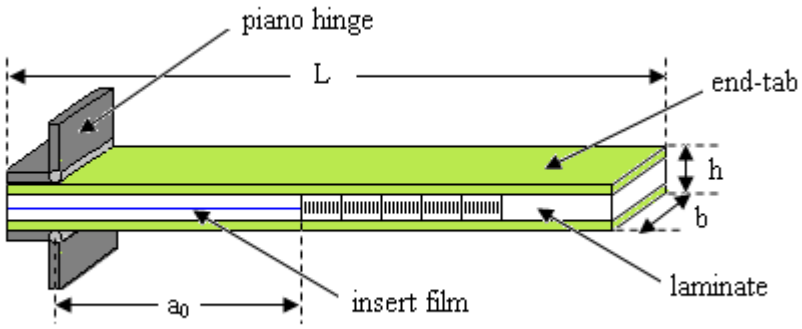

Figure 4.3 Schematic diagram of Mode-I DCB specimens.

For the composite laminates, double cantilever beam (DCB) specimens were prepared for Mode-I fracture toughness tests according to ASTM D5528 (Figure 4.3) [215]. The composite specimens were cut to size (130 mm x 20 mm) and a composite material made of glass fabric and epoxy (commonly used for end-tabs) was cut to size (130 mm x 20 mm) and bonded to both sides of the specimen surface to increase flexural stiffness, making the total thickness of the specimens around 6 mm . Piano hinges were bonded to the ends of the specimens, and the distance between the loading points and the end of the insert film (i.e. the beginning of the crack) was 50 mm. The sides of the specimens were spray painted with a white paint primer and markers were drawn on the primer for every 1 mm interval. Each sample was loaded in tensile Mode-I with a Hounsfield universal testing machine, at 1 mm/min. Crack growth was observed using a digital microscope and the measurements of load and displacement at corresponding crack length were

recorded. The G_{1c} values in this study were calculated using the modified beam theory (MBT) and refer to the propagation G_{1c} value. MBT was selected since it yielded most conservative values in a majority of cases in round robin tests carried out by the ASTM [216].

Expression of the G_{Ic} by MBT is as follows:

$$G_{Ic} = \frac{3P\delta}{2b(a+|\Delta|)} \tag{4.1}$$

where P = load

δ = displacement

b = specimen width

a = delamination length

$|\Delta|$ = correction factor for delamination length

Determination of $|\Delta|$:

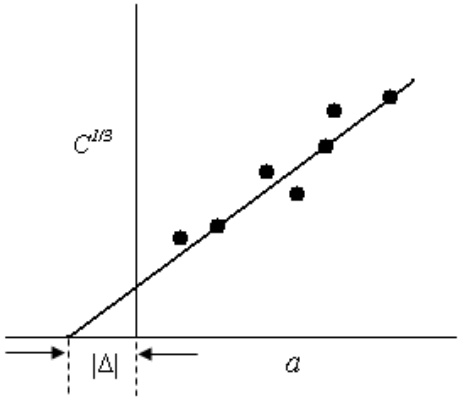

4.1.3.3 Short beam shear strength

In composite materials, a low resistance to shear deformation, particularly in material planes dominated by matrix properties, is a severe weakness in fibre

composites. Relatively low shear stiffness and strength often compromise material performance. Interlaminar shear stress (ILSS) is dependent on the interfacial bonding at the fibre/matrix interface and thus sometimes used as an indicator of the interfacial bonding in composite. Composites with low ILSS are prone to delamination and have poor resistance to environmental degradation, which is detrimental to many applications. However, composites with too high ILSS may have a low toughness, as some of the toughening mechanisms such as fibre/matrix debonding, and crack deflection cannot be triggered.

Considerable experimental and analytical effort has been made in the development of shear testing methods. One of the major difficulties is the provision of a pure shear stress state in the specimen. A number of shear tests have been developed, which includes Iosipescu shear test (ASTM D5379), two-rail shear tests (ASTM D4255), [±45°] tensile shear tests (ASTM D3518) and short beam shear test (ASTM D2344) among others. However, there is no universal method suitable for the accurate evaluation of the shear properties for the extensive range of material geometries existing in composite technology. All the shear test methods, standardised or otherwise, have their own physical and geometrical limitations.

Short beam shear (SBS) test was chosen for this study, which is an interlaminar shear test method. A specimen with a low support span-to-depth ratio is subjected to three-point loading. Both bending and interlaminar shear stresses are induced, the axial bending stresses are compressive on the loading surface and tensile on the opposite surface. The neutral axis is where the bending stress passes through zero, and the interlaminar stress is at its maximum. For a shear test, by keeping the span-to-depth ratio low, the bending stresses can be kept low, promoting shear failures at the neutral plane. However, the concentrated loadings on the beam at the loading and support points create stress concentrations, complicating the stress state. No strain or displacement measurements are made because the span-to-depth ratio is too small. This means the shear modulus cannot be determined and a shear stress-strain curve is not obtained. Despite of the serious limitations, the test is in common

use owning to the ease of sample preparation. The sample can be very small, the text fixture can be relatively simple and a test can be performed very quickly. The SBS test is used extensively as a materials screening and quality control test in the composite field.

In this study SBS strength of the laminates was measured according to ASTM D2344 (Figure 4.4) [217] using an Instron universal testing machine. The width to thickness ratio of the specimen was 2, the span to depth ratio was 4 and the test rate was 1 mm/min. The average dimensions of the SBS specimens were 25 mm x 4.4 mm x 2.2 mm. The diameter of the loading roller was 6mm and diameter of the support rollers was 3 mm.

Expression for SBS strength:

$$\tau_{13} = 0.75\frac{P}{A} \qquad (4.2)$$

where P = maximum load

A = cross-sectional area

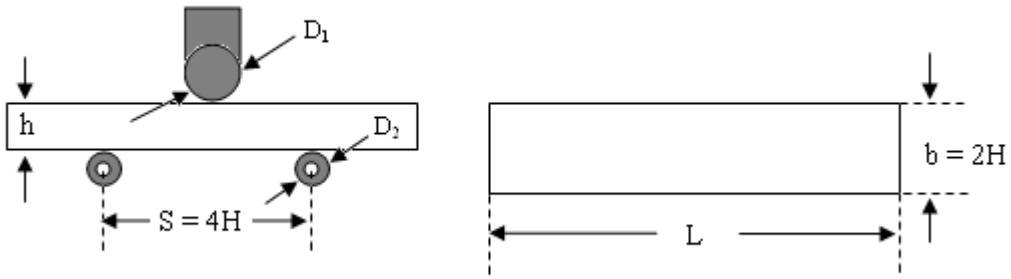

Figure 4.4 Schematic diagram of short beam shear specimens.

4.1.3.4 Compression after impact

It is thought that during service, composite structures are subjected to minor impacts and other damages, which are sometimes not visible on the surface. It is important to understand how a composite will perform after being damaged. The CAI test for composite laminates generally involves subjecting a plate to an out-of – plane low energy impact to introduce damage but not complete failure. The damaged plate was then loaded until failure by in-plane compression. The most common form of internal damage after impact is delamination. Delamination can lead to premature failure during compression loading caused by ply buckling and Mode-I dominated crack growth [218]. Tensile properties are fibre dominated and less affected by this type of damage unless the impact energy is high enough to cause fibre damage, hence compression test is carried out.

The test has been developed within the composite industry as a test method for damage tolerance assessment of composite laminated and is routinely carried out for materials developments, screening and quality control. There is no ISO or ASTM standard, although numerous studies have been done by companies and institution such as Boeing, National Aeronautics and Space Adminstration (NASA), Suppliers of Advanced Composite Materials Association (SACMA), and Royal Space Establishments (RAE) [218].

In this study CAI specimens were cut from composite laminates to size (89 mm x 55 mm) and impacted at 2 J, 4 J and 6 J, using a CEAST impact tester (Figure 4.5). Each specimen was clamped in a 40 mm diameter support and the dart diameter was 20 mm. Internal damage of the impacted specimens was examined using ultrasonic C-scan (Figure 4.6). The maximum width and length of the damage area was measured. The non-impacted and impacted specimens were then placed in a miniaturised Boeing CAI rig (Figure 4.7) [219] and loaded in compression at a rate of 0.5 mm/min. Five specimens were tested for each impact energy. The maximum compressive strength was recorded and the ratio of maximum compressive strength

for each impacted specimen to that of a non-impacted control specimen was presented as residual compressive strength.

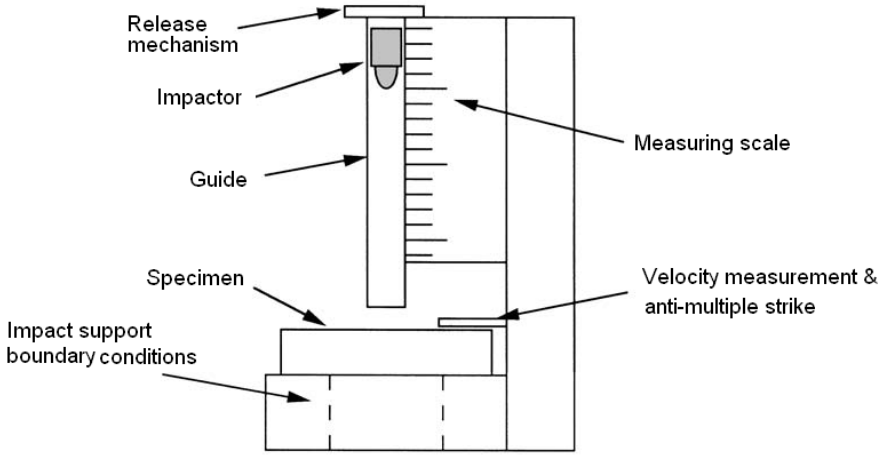

Figure 4.5 Schematic diagram of an impact tester.

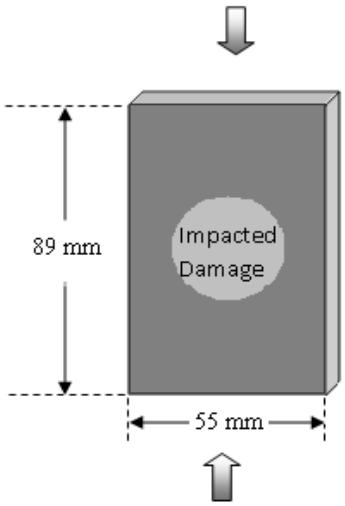

Figure 4.6 Schematic diagram of impacted specimen for CAI test.

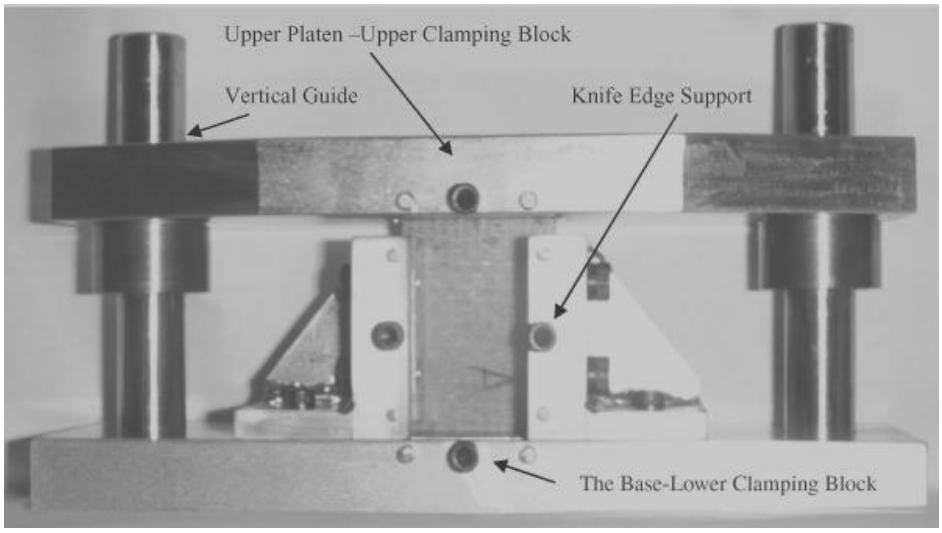

Figure 4.7 Miniaturised CAI rig used in this study.

4.1.3.5 Dynamic mechanical analysis

In this study DMA was carried out in a Q800, by TA Instruments in 3-point bending mode and the specimens were simply supported. For composite laminates, sample size was (60 mm x 10 mm x 2.2 mm) and span length was 50 mm. Specimens were heated from 30°C to 250°C at 3°C/min with an amplitude of 25 µm at a frequency of 1 Hz. Values of storage modulus (*E'*), loss modulus (*E''*) and tan delta (*tan δ*) were recorded. Glass transition temperature, *Tg*, was taken as the *tan δ* peak. Three specimens of each type were tested,

4.1.3.6 Fractography

Mode-I Fracture surfaces of specimens were examined in a scanning electron microscope (SEM), Inspect F by FEI Company. The specimen was coated with gold and an electron beam of 20kV was used. Fracture surfaces were obtained from Mode-I interminar toughness tests.

4.2 Results and Discussion

4.2.1 Tensile properties

Tensile properties of DGEBA composites are shown in Figure 4.8. Tensile modulus and strength remained largely unchanged with the addition of phenoxy. In contrast with bulk resin specimens (Figure 3.10), modulus and strength of the composites did not increase with increasing amount of phenoxy and the strain to break decreased slightly instead of increased. This indicates that the addition of the more ductile phenoxy phase actually made the composite more brittle in tensile loading. Failure modes of the specimens differed greatly (Figure 4.10). The unmodified specimen showed delamination, resulting in 'brooming' and 'brush-like' failure, whereas the ones with 10 wt% phenoxy did not show extensive delamination and the specimen failed in a fairly brittle manner across its width. The 5 wt% specimen failed by delamination, but at a lesser extent with less 'brooming'.

For TGDDM composites (Figure 4.9), modulus dropped slightly, while strength remained largely unchanged and strain increased with increasing amount of phenoxy. This is in contrast to bulk resin TGDDM specimens (Figure 3.13) in which phenoxy lowered the strength and strain. Failure modes of the specimens were similar to DGEBA specimens in which the unmodified and the 5 wt% specimens showed more extensive delamination than the 10 wt% specimen (Figure 4.11).

The change in failure mode of phenoxy modified laminates is interesting. Since there was no evidence of significant changes to fibre/matrix interface (Section 4.3.3), the change was assumed to be down to modification of the matrix, with phenoxy modified laminates showing less delamination.

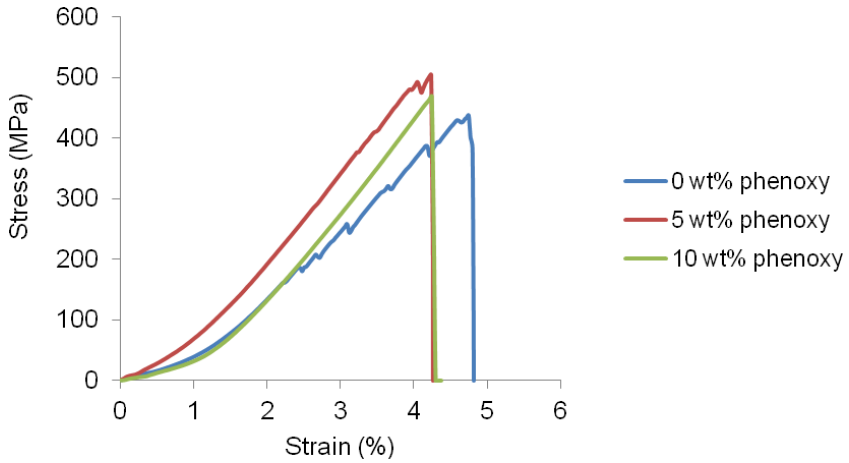

Phenoxy (wt%)	Modulus (GPa)			Strength (MPa)			Strain (%)		
	Ave	Max	Min	Ave	Max	Min	Ave	Max	Min
0	48.47	50.43	44.21	475.47	493.67	437.24	5.45	5.81	5.16
5	51.86	53.33	49.35	498.74	536.76	467.27	4.59	5.13	3.96
10	49.29	52.83	46.63	489.10	537.36	420.17	4.79	5.04	4.42

Figure 4.8 Tensile properties for carbon fibre/DGEBA laminates.

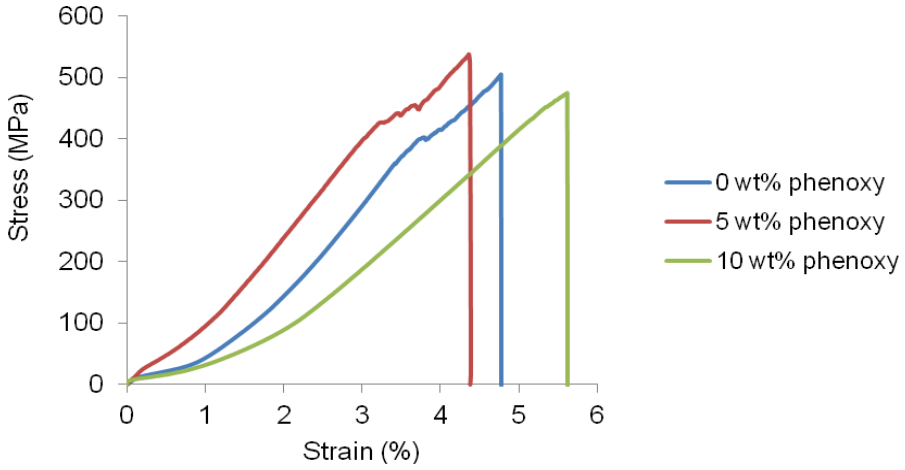

Phenoxy (wt%)	Modulus (GPa)			Strength (MPa)			Strain (%)		
	Ave	Max	Min	Ave	Max	Min	Ave	Max	Min
0	54.14	55.77	52.06	441.61	464.29	416.15	4.35	4.91	3.7
5	48.70	52.52	46.31	489.28	537.28	439.92	4.78	5.61	4.5
10	51.00	51.41	50.77	453.95	508.86	418.78	5.14	5.94	4.61

Figure 4.9 Tensile properties for carbon fibre/TGDDM laminates.

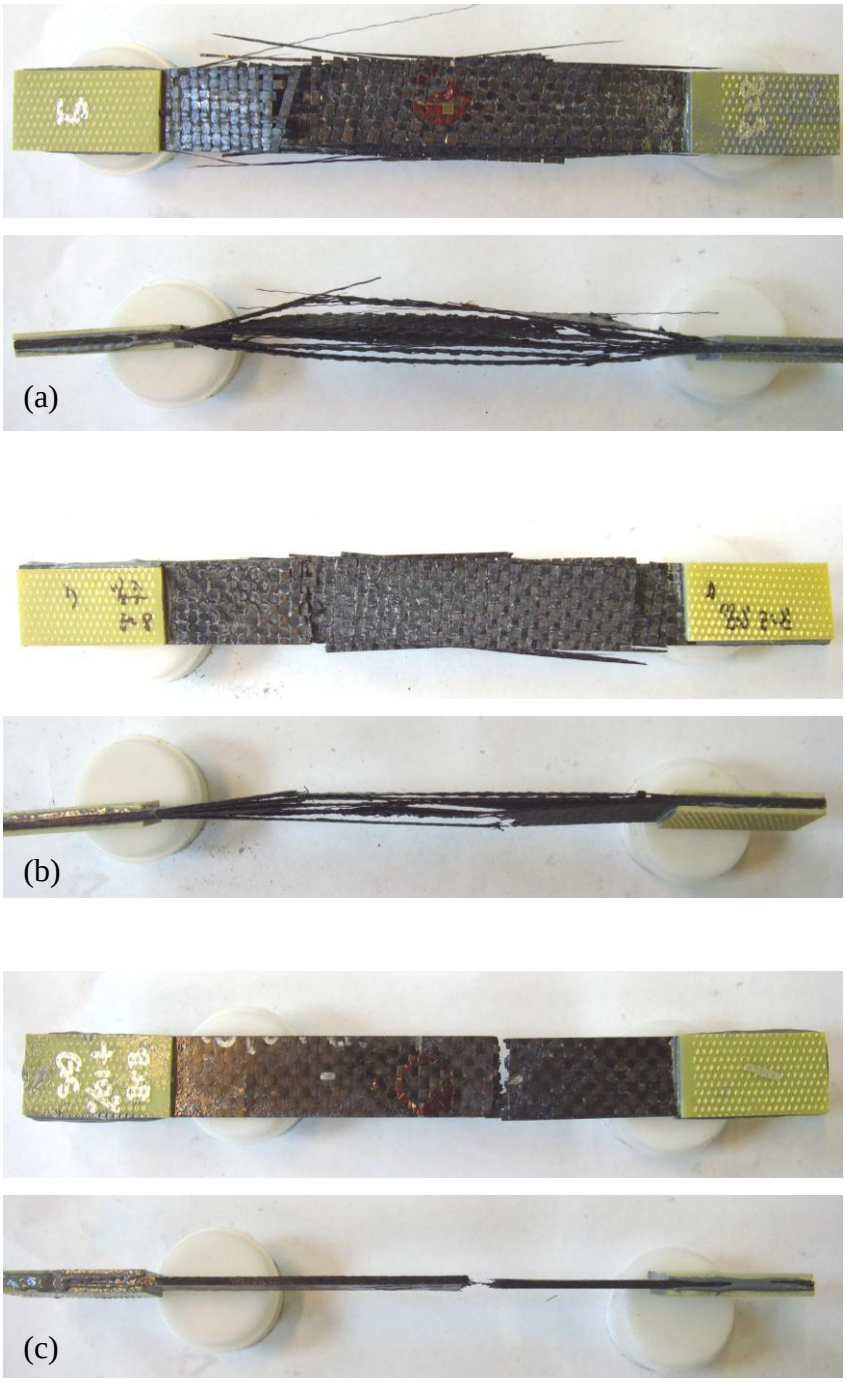

Figure 4.10 Tested tensile specimens of carbon/fibre DGEBA laminates with (a) 0 wt% (b) 5 wt% and (c) 10 wt% phenoxy, showing less delamination in the 10 wt% phenoxy specimen.

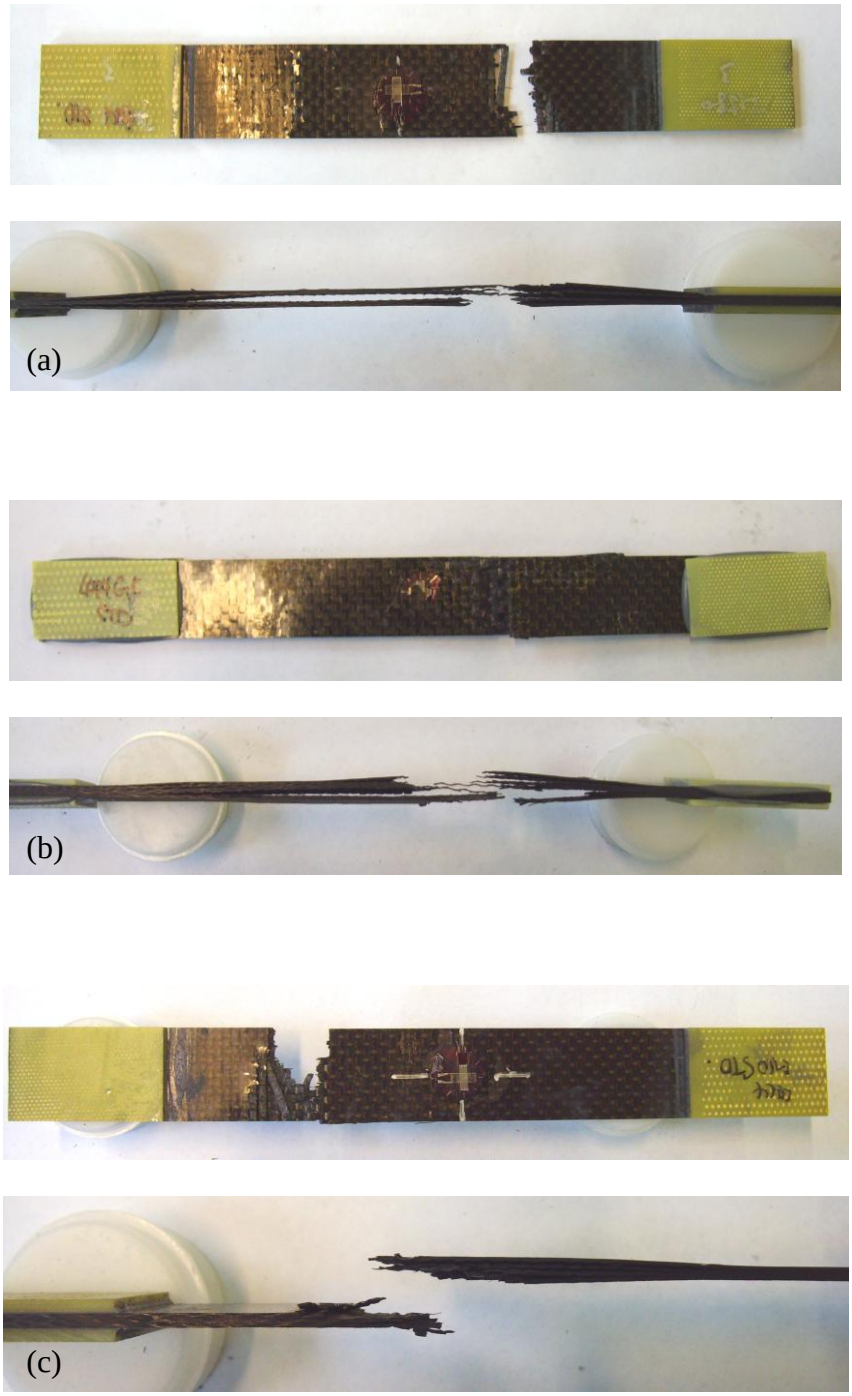

Figure 4.11 Tested tensile specimens of carbon fibre/TGDDM laminates with (a) 0 wt% (b) 5 wt% and (c) 10 wt% phenoxy, showing less delamination in the 10 wt% phenoxy specimen.

4.2.2 Mode-I delamination toughness

Figure 4.12 and Fig 4.15 show the load-displacement curves of Mode-I DCB tests for DGEBA and TGDDM specimens respectively. The curves follow stick-slip behaviour common in composite laminates based on epoxy matrix and woven fabrics. The data points highlighted on the curves were used to calculate G_{Ic}. It was found that while the propagation G_{Ic} fluctuated as the crack grew, no general trend could be drawn and no fibre bridging was observed for all the specimens, and thus R-curves are not presented. In this study as plain weave carbon fibre fabric was used, only crack propagation G_{Ic} was presented. Crack initiation values would be affected by the weaving pattern and makes initiation G_{Ic} values invalid. Upon unloading specimens after testing, the displacement did not always go back to zero, which indicates inelastic deformation. It should be noted that care had already been taken to minimise such effect by making the specimens thicker and stiffer.

Figure 4.14 and Figure 4.17 shows the G_{Ic} results of Mode-I DCB test. In the DGEBA specimens, the G_{Ic} values doubled with 5 wt% of phenoxy fibre but increased nearly ten-fold when 10 wt% phenoxy fibre was added. In TGDDM specimens, little change in G_{Ic} was observed for the 5 wt% specimen, and at 10 wt% phenoxy G_{Ic} increased by more than 100%. In a study in which phenoxy powder was added in the interlaminar region of a carbon fibre/TGDDM composite, an areal density of 21.5 g/m^2 phenoxy led to a 170% increase in G_{1c} [13].

For both resins the increase in G_{1c} is a lot more significant than that observed for bulk resins (Figure 3.11 and 3.14), in contrast to other liquid rubber and thermoplastic systems. Yan *et al.* showed that for CTBN rubber modified epoxy, while the matrix toughness increased by four-fold, the laminate toughness only increased by two-fold [85]. Turmel and Partridge found that for a PEI modified system, toughness improvement for the glass fibre laminate lagged behind that for bulk resin, as shown in Figure 2.21 [11]. Mujika *et al*. showed that for PSF modified systems a 10 wt% of PSF resulted in a 38% increase in G_{1c} for DGEBA and 36% for TGDDM bulk resins, however, only an improvement of 23% was achieved for the

corresponding laminates. Similar finding was also shown by Verry *at al.* on HBP modified system in which a 100% increased in bulk resin toughness only translated to 32% increase in laminate toughness [110]. It is generally suggested that fibres in the laminates suppressed the development of a plastic zone ahead of the crack tip, thus lowering toughness.

In this study the significant increase in toughness for laminates could be due to the fact that phenoxy fibres were not homogeneously distributed in the matrix. Since most of the phenoxy fibres were localised within the interlaminar region between carbon plies, this could result in a more pronounced toughening effect due to an increased phenoxy loading in this region. As such, the actual phenoxy concentration in the interlaminar region was higher than the overall stated 5 or 10 wt%. In other studies of epoxy/phenoxy resin blends, it was found that a phenoxy content of more than 10 wt% achieved greater toughness improvement in some blends (Table 3.1). For example, Siddhamalli and Kyu [94] reported an improvement in toughness of nearly 30% with 10 wt% phenoxy, which is similar to the finding in this study. However, greater improvement of more than 300% was achieved with 20 wt% phenoxy and although improvement in toughness decreased with further increase in phenoxy, the toughness achieved was still better than that for 10 wt% phenoxy. Unfortunately the local concentration is not known in our specimens. Moreover,the addition of phenoxy could also affect the fibre/matrix interface and improved toughness.

Similar to film based interleafing concepts, phenoxy fibres can be positioned within damage prone zones such as interlaminar regions, leading to highly efficient toughening effects at low overall concentrations of thermoplastic. Unfortunately, the unknown higher local phenoxy concentrations in the composite laminates do make a direct comparison between bulk resin and laminate data difficult. It should also be noted that G_{1c} values for specimens based on 10 wt% phenoxy show large scatter, presumably due to the inhomogeneous distribution of the chopped phenoxy fibres.

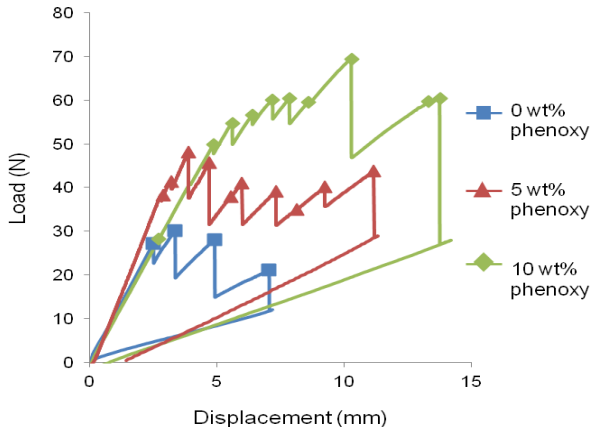

Figure 4.12 DCB load-displacement curve for carbon fibre/DGEBA laminates.

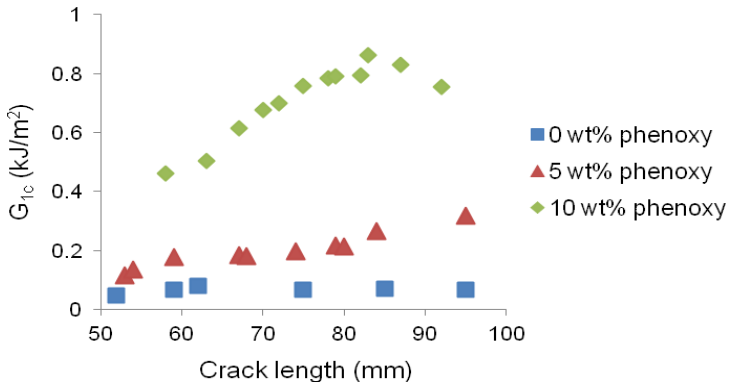

Figure 4.13 DCB G_{Ic} vs crack length graph for carbon fibre/DGEBA laminates.

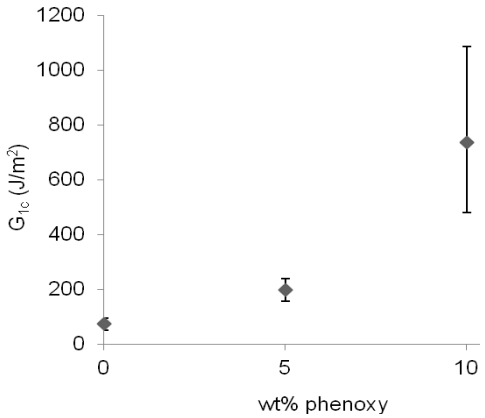

Figure 4.14 Mode-I G_{1c} fracture toughness values for carbon fibre/DGEBA laminates modified with phenoxy.

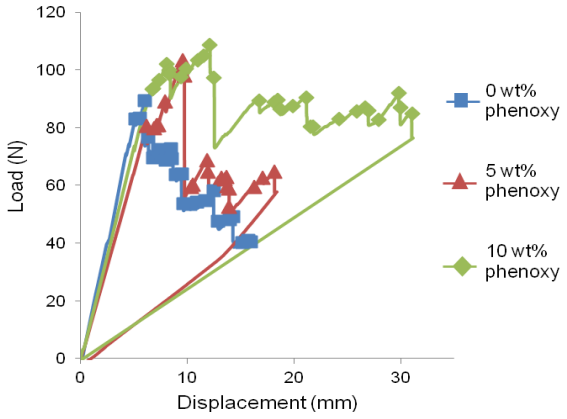

Figure 4.15 DCB load-displacement curve for carbon fibre/TGDDM laminates.

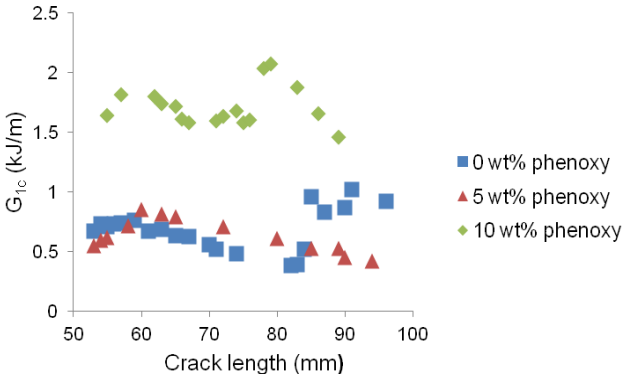

Figure 4.16 DCB G_{Ic} vs crack length graph for carbon fibre/TGDDM laminates.

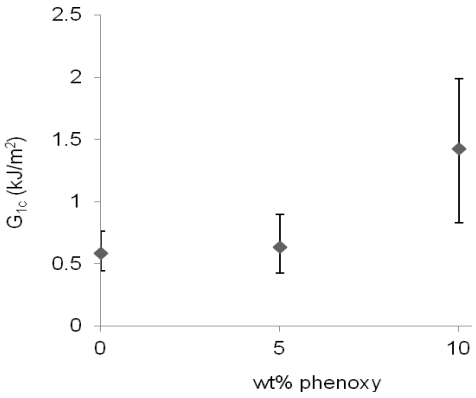

Figure 4.17 Mode-I G_{Ic} fracture toughness values for carbon fibre/TGDDM laminates modified with phenoxy.

4.2.3 Short beam shear strength

In order to assess the effect of phenoxy on other interlaminar properties of composites, short beam shear tests were carried out and the results are shown in Figure 4.18 and 4.19. The range of values indicated that short beam shear strength was not significantly affected by the addition of phenoxy fibre for both resins. This suggests that the interface between carbon fibres and phenoxy modified epoxy matrix was neither strengthened nor weakened by the phenoxy.

From tensile test specimens, it was found that phenoxy modified lamimates showed less delamination Figure 4.10 and Figure 4.11. It was thought that the addition of phenoxy could altered the fibre/matrix interface which led to less delamination, however, SBS test results did not support such claims.

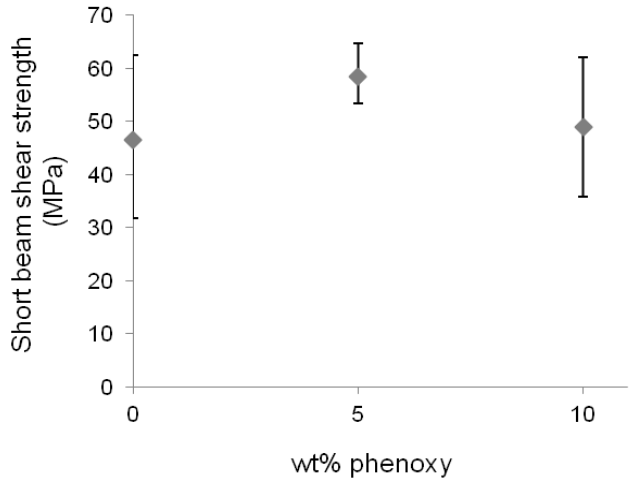

Figure 4.18 Short beam results for carbon fibre/DGEBA laminates showing no significant change in short beam shear strength.

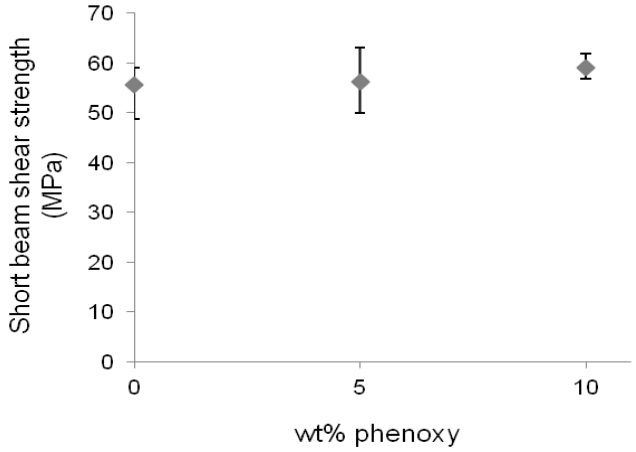

Figure 4.19 Short beam results for carbon fibre/TGDDM laminates, showing no significant change in short beam shear strength.

4.2.4 Compression after impact

CAI tests were carried out to study the impact damage resistance and tolerance of the composites. Impact damage resistance measures the ability of composite materials to resist the ultimate failure or load-bearing capability. The extent of damage can be reported in terms of damage area after a drop weight impact. Damage tolerance, by contrast, measures the changes of the performance of composite structures in the presence of damage while continuously surpassing the requirements of safety, structural efficiency, and maintenance. It is based on the retention rate of residual strengths with reference to strength values of undamaged composite structures. The residual compressive strength measured using the compression after impact (CAI) test is considered to be the most important way to assess impact damage tolerance.

Figure 4.20 and Figure 4.22 show damage to specimens after impact and CAI results are plotted in Figure 4.21 and Figure 4.23. It was found that for DGEBA specimens, the 10 wt% phenoxy sample provided improved damage resistance and damage tolerance. Figure 4.21a shows reduced damage areas for the 10 wt% sample,

particularly at higher impact energy. Higher residual compressive strengths were reported for the 10 wt% sample (Figure 4.20c). On the other hand, the 5 wt% specimen actually showed a reduced damage tolerance compared to the control sample. Figure 4.21b shows for undamaged specimens that the addition of phenoxy reduced the compressive strength.

For TGDDM specimens, phenoxy modified specimens showed improved damage resistance as damage width was reduced (Figure 4.23a). Phenoxy modified specimens also showed improvement in damage tolerance (Figure 4.23(c)) with the most improvement achieved for the 5 wt% specimens. However, compressive strength was lowest for 5 wt% specimens (Figure 4.23b).

In general TGDDM specimens had a smaller damage size than DGEBA specimens after impact, which suggest they had higher overall damage resistance. For both resins damage resistance was increased for the 10 wt% specimens, while 10 wt% was preferred for DGEBA and 5 wt% was preferred for TGDDM in terms of damage tolerance improvement. Based on the improvement in G_{Ic} (Section 4.3.2), CAI performance of the laminates was expected to improve, however, this was found not to be the case. This could be due to uneven distribution of phenoxy fibres during layout, which leads to fluctuations of phenoxy concentration across the specimens. CAI fracture is a mixture of crack opening (Mode-I) and shear (Mode-II) fracture, therefore G_{1c} only account for a fraction of the CAI improvement. It was found by Masters that Mode-I interlaminar toughness showed poor correlation to CAI strength, with G_{IIc} showing better correlation [168, 169]. However, other studies by Kim *et al.* [182] and Kuwata [220] have found linear relationship between G_{1c} and CAI strength for epoxy blends. However, it was also suggested that the correlation depended on the resin and fabric system [220].

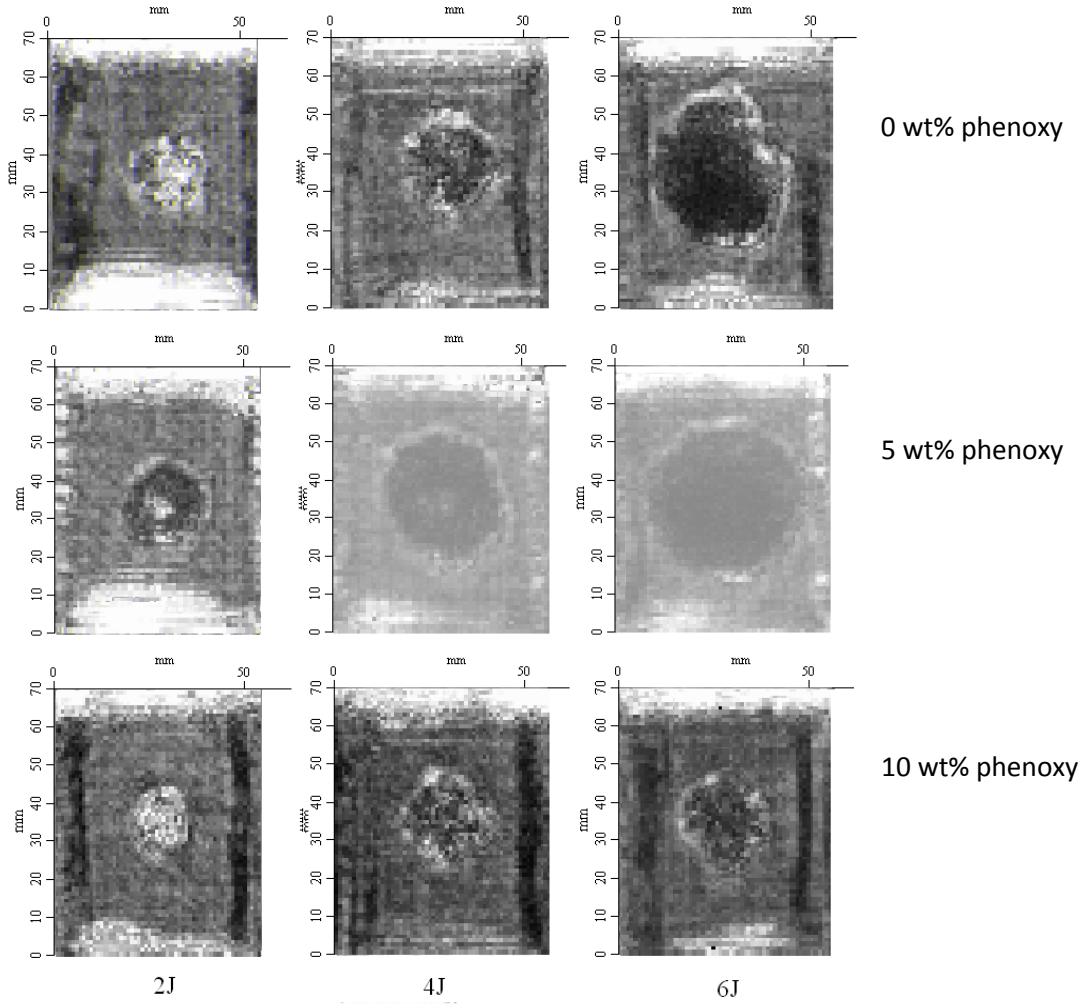

Figure 4.20 C-scan image for impacted carbon fibre/DGEBA laminates showing impact damage at 2J, 4J and 6J.

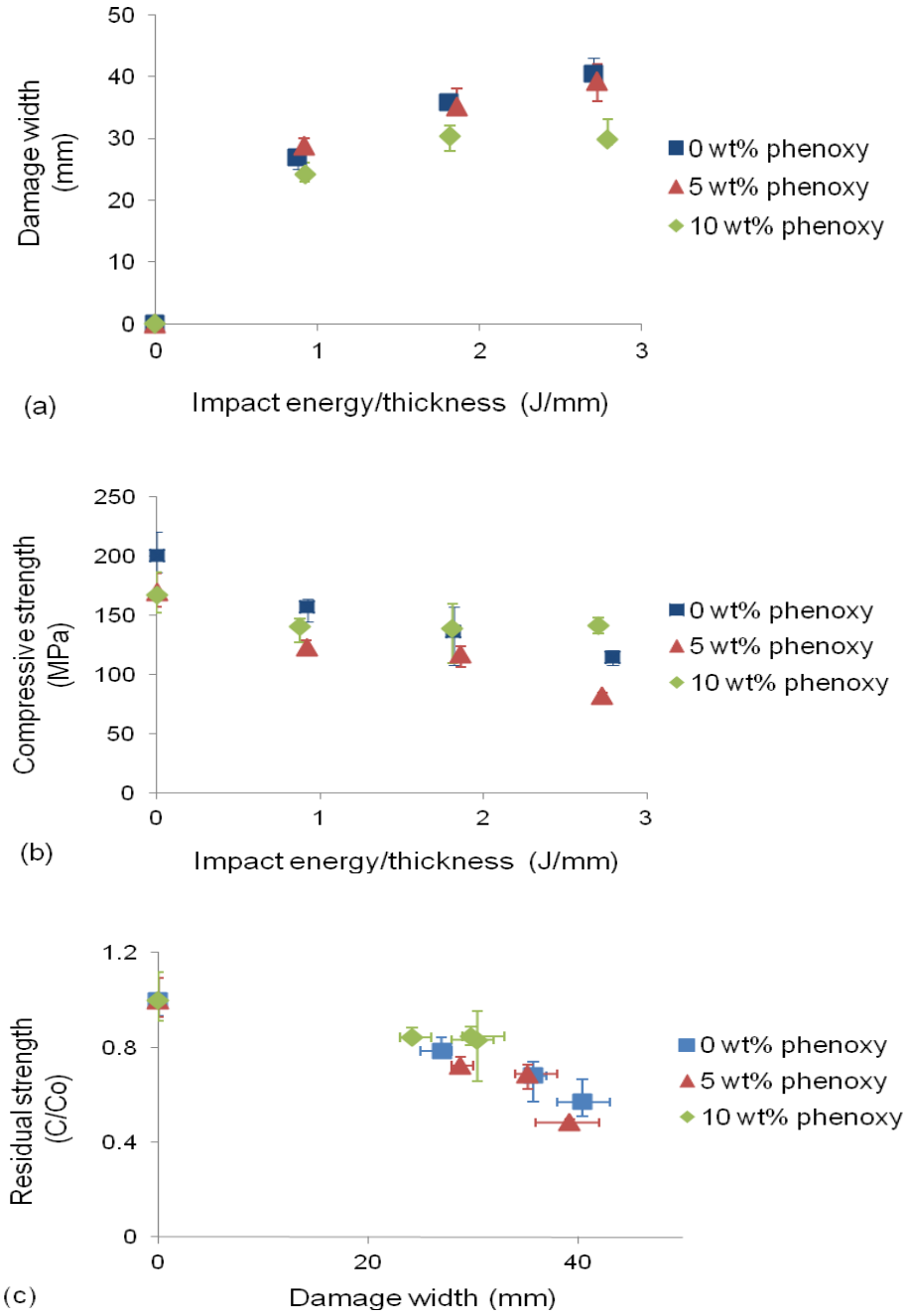

Figure 4.21 CAI results for carbon fibre/DGEBA laminates.

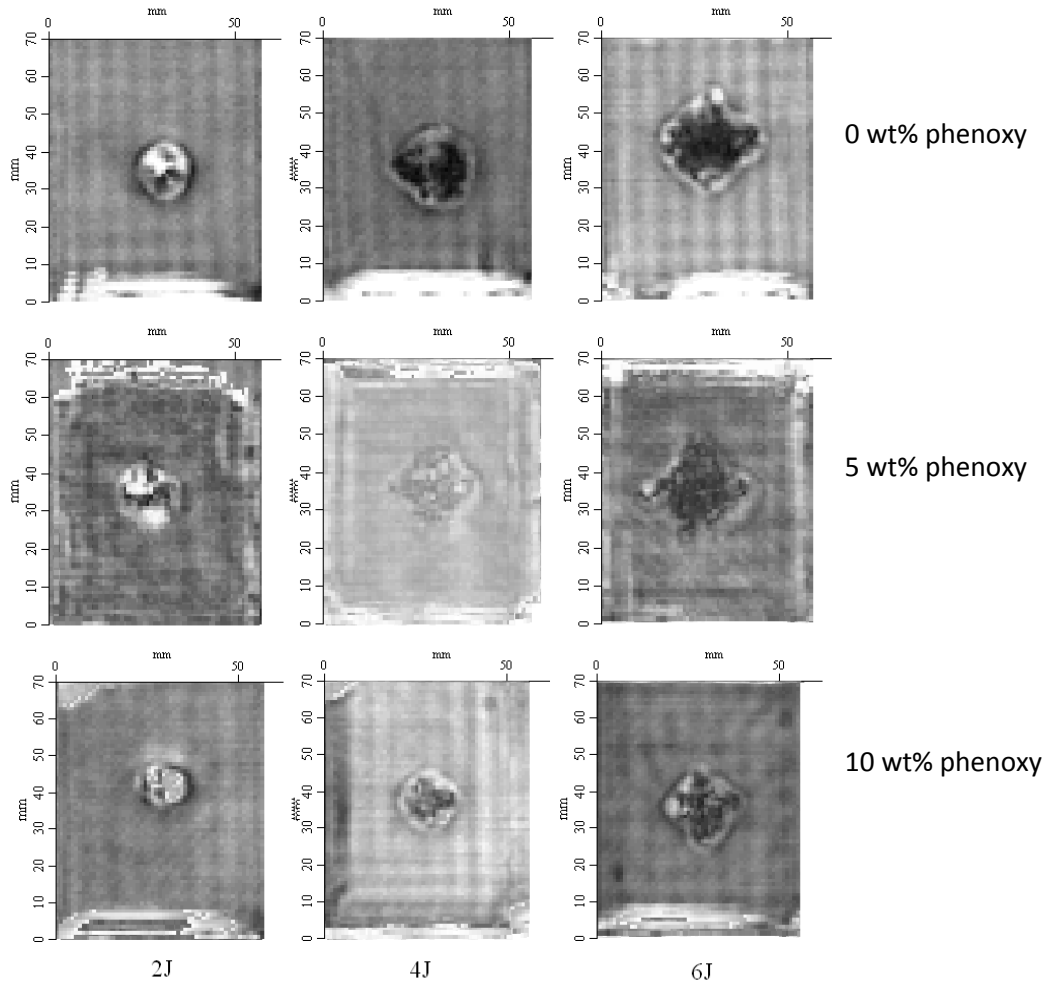

Figure 4.22 C-scan image for impacted carbon fibre/TGDDM laminates, showing impact damage at 2J, 4J and 6J.

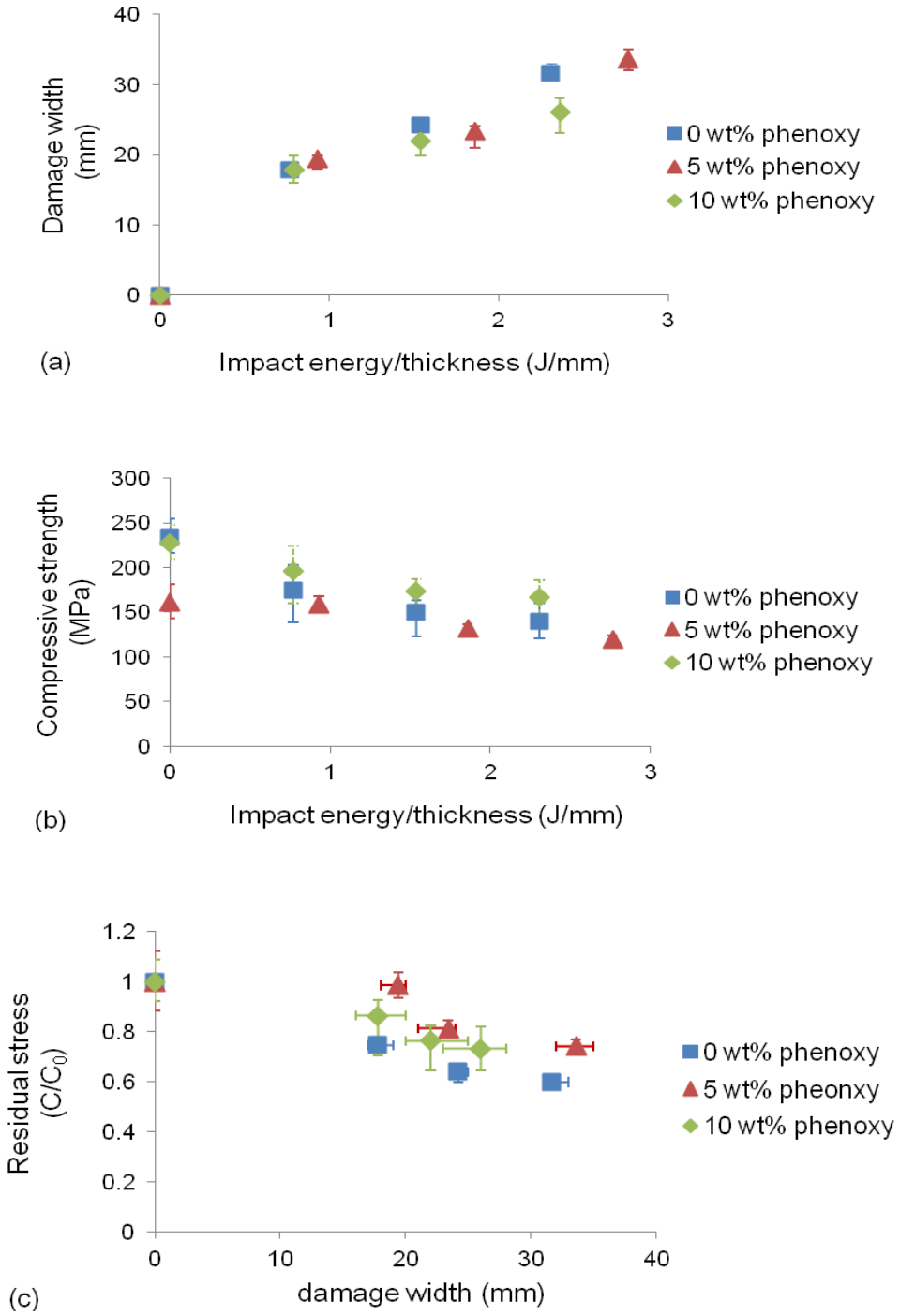

Figure 4.23 CAI results for carbon fibre/TGDDM laminates.

4.2.5 Glass transition temperature

Figure 4.24 shows the *E'* and *tan δ* results from the DMA tests for DGEBA specimens. Similar to bulk resin specimens the T_g of the epoxy matrix in the composites increased with phenoxy content (Table 3.2). The T_g of the phenoxy phase in the 10 wt% sample could be observed as a slight change of gradient in the *tan δ* curve and by studying the *E'* curve. However, the T_g for the 5 wt% specimen was not so obvious from the tan δ curve, and the E' increased as the specimen went through the T_g of the phenoxy phase.

Figure 4.25 shows the DMA results for TGDDM specimens. Similar to the DGEBA specimens, at 10 wt% a slight change in slope in *tan δ* could be detected around 90°C which corresponds to the T_g of the phenoxy-rich phase in the matrix. No such feature could be detected for the 5 wt% specimen. The T_g of the phenoxy-rich phase in the TGDDM resin is closer to the neat phenoxy (104°C) than the phenoxy-rich phase in the DGEBA resin. It suggests that there was less dissolved epoxy monomer in the phenoxy-rich phase for the TGDDM resin, as this was not observed for bulk TGDDM resin (Figure 3.16). However, the resin used for the composite laminates was not the same as the one used for the bulk resin, and the change in resin chemistry could affect phase separation [92, 93]. The T_g of the epoxy phase was not significantly altered by the addition of phenoxy, indicating that curing of the epoxy phase was not affected. In this case, the onset of the first major change of slope of the *E'* was a more accurate measurement for T_g. It was found that there was a second change in slope after the first major drop in modulus which affected the *tan δ* peak values. The second change in slope could be related to further curing action of the resin as the specimens were heated during testing. The *tan δ* peak values are therefore not representative for the as-manufactured conditions of the specimens.

The DMA curves of both resins show that for some specimens the *E'* increased with temperature before finally dropping. This is unexpected and remains to be explained.

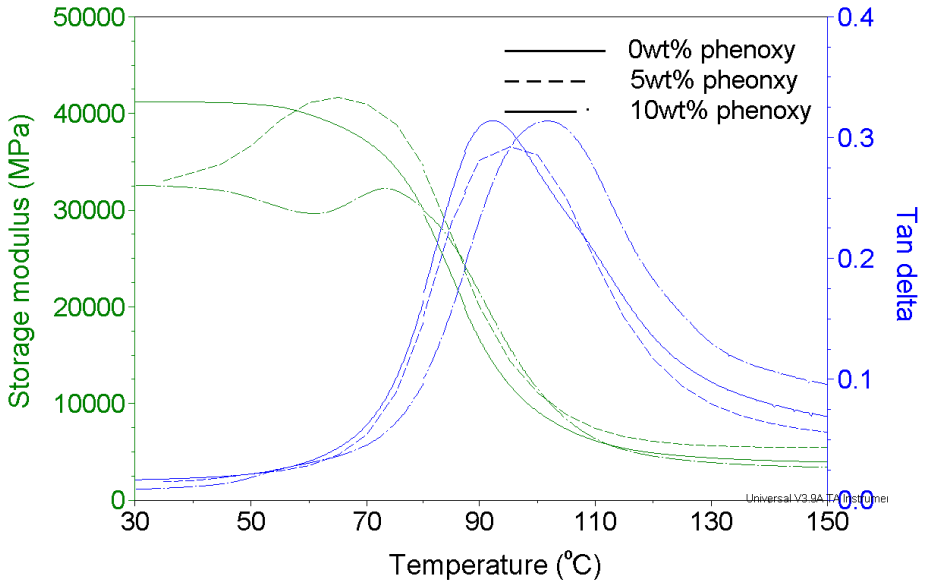

Figure 4.24 DMA results for carbon fibre/DGEBA laminates.

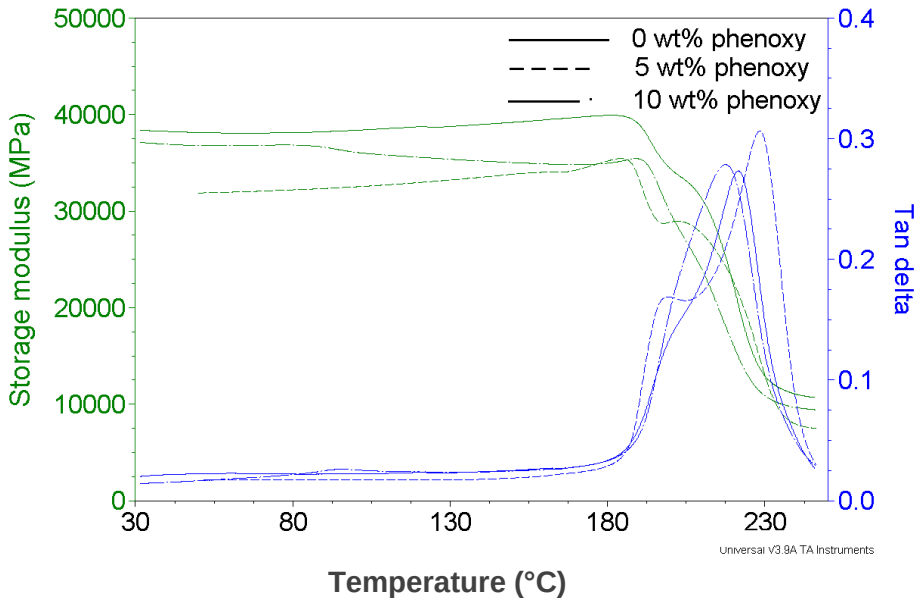

Figure 4.25 DMA results for carbon fibre/TGDDM laminates.

4.2.6 Morphology

The fracture surfaces of the DGEBA composites showed brittle fracture when no phenoxy was added (Figure 4.26a). Figure 4.26b and 4.26c show a phase separated blend morphology with all the fibres dissolved and no solid fibre remaining after curing of the laminate. For the 5 wt% specimen (Figure 4.26b, a phase separated, droplet morphology was prominent in which the spherical phenoxy phase was distributed throughout the continuous epoxy phase and some drawing of the phenoxy phase could be seen. However there were also areas in which no phase separation could be observed. Figure 4.26c shows the morphology of the 10 wt% specimen. It was found that in areas with a high loading of phenoxy fibre phase inversion occurred (Fig, 4.26c right), in which epoxy spheres were surrounded by phenoxy matrix. In areas of lower phenoxy loading, a phenoxy droplet morphology occurred (Figure 4.26c left). Different morphologies could be found across the same specimen owning to the fact that the phenoxy fibres were not perfectly distributed, leading to concentration fluctuations. It was found in another study [94] on DGEBA/phenoxy blends that while a droplet morphology was formed when phenoxy content was below 10 wt%, at 20 wt% phenoxy a co-continuous morphology was observed and above 30 wt%, phase inversion occurred. The fracture surface of the 10 wt% specimen was a lot rougher, indicating more ductile fracture and more energy was dissipation during fracture.

For TGDDM sample (Figure 4.27), the 10 wt% specimen (Figure 4.27c) shows a phase separated droplet morphology. The phenoxy-rich domains were found dispersed in epoxy and drawing of the more ductile phenoxy-rich phase could be observed. Fracture surfaces of the 10 wt% specimens were also rougher. For the 5 wt% specimens (Figure 4.27b) no phase separation was observed for the area studied. It did seem that phase separation did not happen as readily as it was for the DGEBA resin. However, there would be local fluctuations of phenoxy concentration throughout the laminates, and different morphologies could be present but not observed.

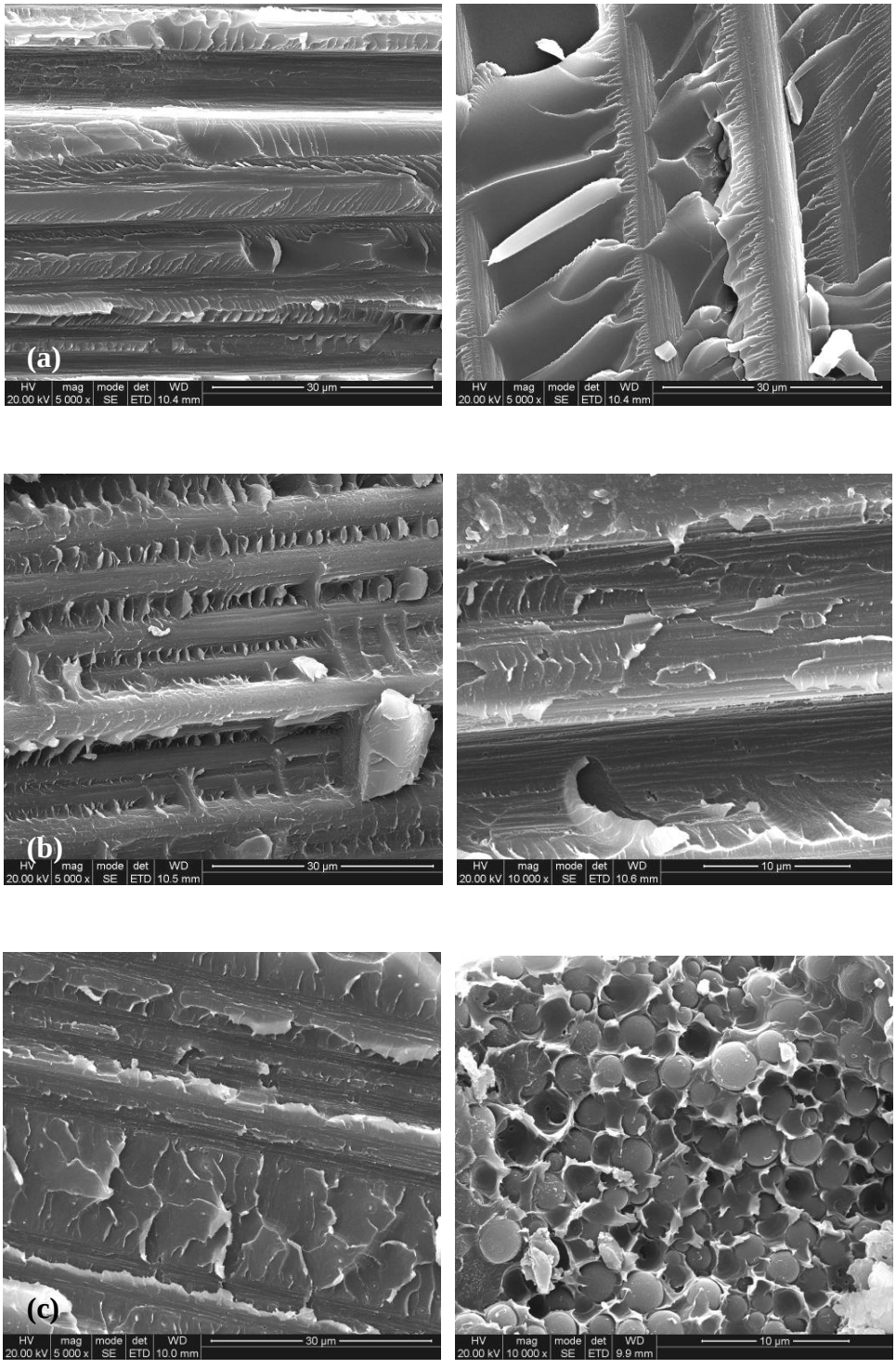

Figure 4.26 Mode-I SEM fractography of carbon fibre/DGEBA laminates with (a) 0 wt% phenoxy, (b) "5" wt% phenoxy and (c) "10" wt% phenoxy at low (left) and high (right) magnification, showing phase separation in the "5" and "10" wt% specimen.

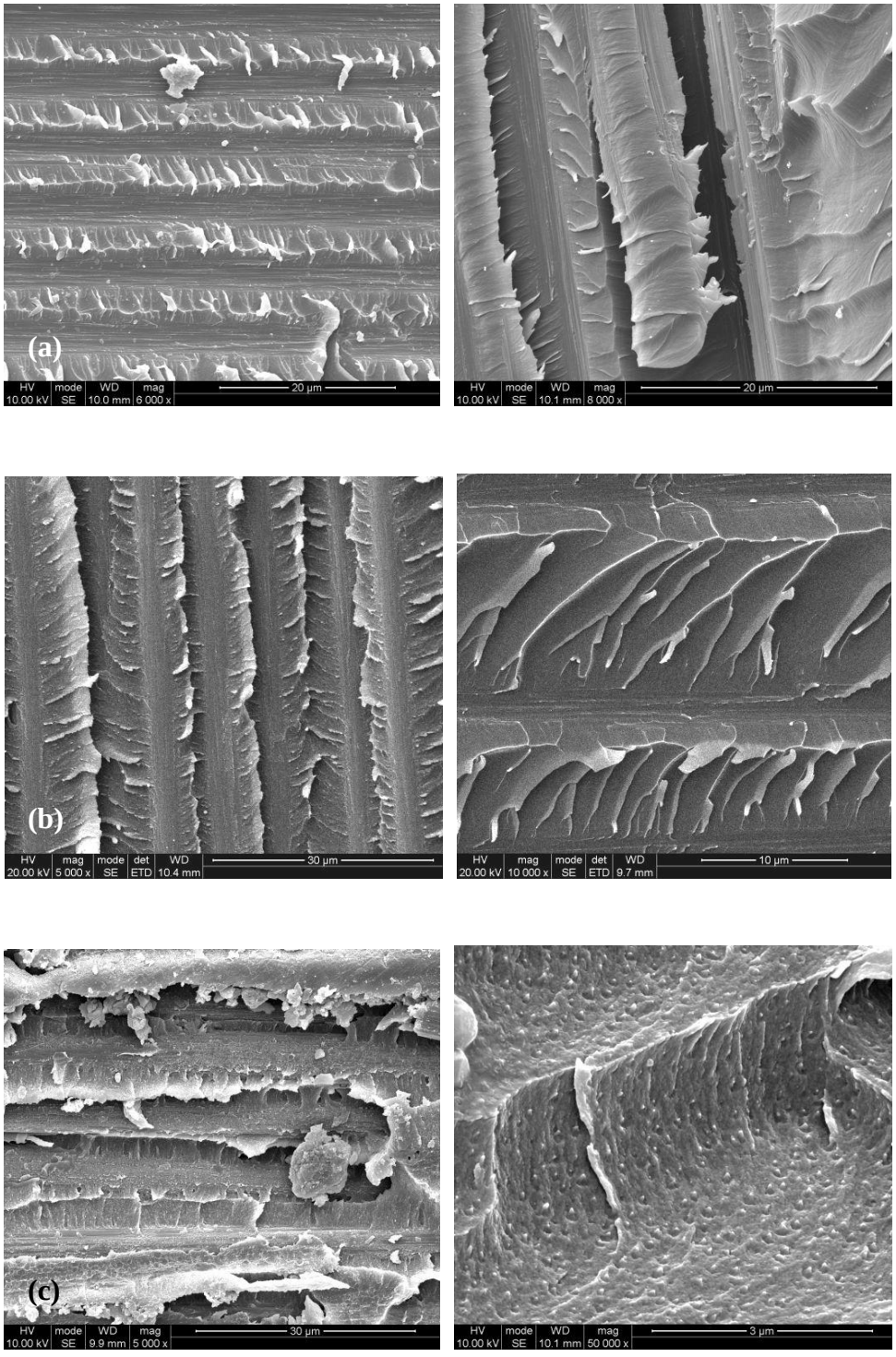

Figure 4.27 Mode-I SEM fractography of carbon fibre/TGDDM laminates with (a) 0 wt% phenoxy, (b) "5" wt% phenoxy and (c) "10" wt% phenoxy, at low (left) and high (right) magnification, showing phase separation in the "10" wt% specimen.

4.3 Conclusion

In this chapter the effects of introducing phenoxy to carbon fibre/epoxy composites were studied. The phenoxy was introduced as chopped solid fibres in the interlaminar region of dry lay-ups. The phenoxy fibres remained in solid form during resin infusion and later dissolved and phase separated during curing. No solid fibre remained after curing and various phase separated morphologies were achieved. For DGEBA specimens a droplet morphology was observed at lower phenoxy loading in which discrete phenoxy-rich domains were dispersed in an epoxy continuous phase. At higher loading, phase inverted morphology occurred in which spherical epoxy domains were surrounded by phenoxy. In TGDDM specimens, only a droplet morphology was observed for the 10 wt% specimen.

In both of the DGEBA and TGDDM matrix, the toughness of the composites improved with phenoxy content. For a loading of 10 wt%, DGEBA specimens had a ten-fold increase in Mode-I G_{1c} while the TGDDM specimens improved by more than 100%, while no drastic changes were observed in tensile properties and T_g for both matrices. As for the bulk resin samples, the phenoxy employed was more effective in toughening the DGEBA resin. The toughness improvement for laminates far exceeded that for bulk resins. This could be due to the fact that the dissolved phenoxy was mainly located in the interlaminar region, thus the actual concentration of phenoxy was much higher in the region, leading to a higher $G_{1c.}$ The addition of phenoxy could also affect the fibre/matrix interface, although no evidence for this was found by the short beam shear test.

CAI tests were carried out to study the damage resistance and tolerance of the specimens. It was found that damage resistance and tolerance could be improved for the phenoxy modified specimens for both matrices. The improvement in damage resistance was more profound for the DGEBA specimens, while damage tolerance improvement was more profound for the TGDDM specimens.

Since the phenoxy fibre was simply chopped and randomly distributed between carbon plies by hand it led to phenoxy concentration fluctuations within the interlaminar region, which can lead to property variations. In future this problem could however be overcome by using non-woven mats made of phenoxy fibres which are currently already under development by EMS Griltech.

CHAPTER 5

TOUGHENING OF CARBON FIBRE/EPOXY COMPOSITES WITH ARAMID INTERLEAVES AND DISSOLVABLE PHENOXY FIBRES

In the previous chapter, addition of dissolvable phenoxy fibres has been found to improve toughness of carbon fibres/epoxy composites. In this chapter, the idea of toughening in the interlaminar region was further developed with the introduction of an additional tough, heat resistant interleaf layer in combination with phenoxy modification. The interleaf was expected to remain intact throughout processing unlike the dissolved phenoxy fibres. The aim was to study whether the combination of these two different types of toughening approaches would result in some synergetic effects.

Interleaving involves the insertion of thin, tough polymer layers between selected plies of the composite laminate. This approach has shown significant improvement in the residual compressive strength after impact and delamination resistance of composites. There are different types of interleaves, including thermosetting adhesive films [28], non-woven fibres mats [29, 30], chopped fibres mats [31, 32] and thermoplastic particles [33] or films [34]. The term interleaf sometimes refers only to thermosetting or thermoplastic films applied in the

interlaminar region of laminates. In this work, however, interleaf refers to a layer of material in the interlaminar region that remains intact before and after laminate manufacture, and is in the form of a non-woven veil made with staple aramid fibres. As with the previous chapter (Chapter 4), two different epoxies were studied.

5.1 Experimental

5.1.1 Materials

The epoxy resins, curing agents, phenoxy fibres and carbon fibres fabrics used are described in section 4.1.1. The interleaf used was an Optimat® aramid veil with a crosslinked polyester binder, by PFR Composite Materials. It is a non-woven veil made with chopped para-aramid fibres (6 mm length and 12 μm diameter) with an areal weight of 26 g/m^2.

5.1.2 Specimen manufacturing

Composite laminates were manufactured as described in section 4.1.2., with the addition of one ply of the aramid interleaf placed at the mid-plane. For phenoxy modified composite laminates, distribution of phenoxy fibres in terms of areal density was around 11.4 g/m^2 and 22.9 g/m^2 for the 5 wt% and 10 wt% specimens, respectively. Figure 5.1(a) shows a schematic diagram of a general set up of a vacuum bag and a more detailed look at the lay-up of fabrics is shown in Figure 5.1(b) with no phenoxy and Figure 5.1(c) with chopped phenoxy fibres. Volume fraction, $V_{f,}$ of all the laminates made was in the range of 0.45 with a laminate thickness of 2.5 ± 0.4 mm.

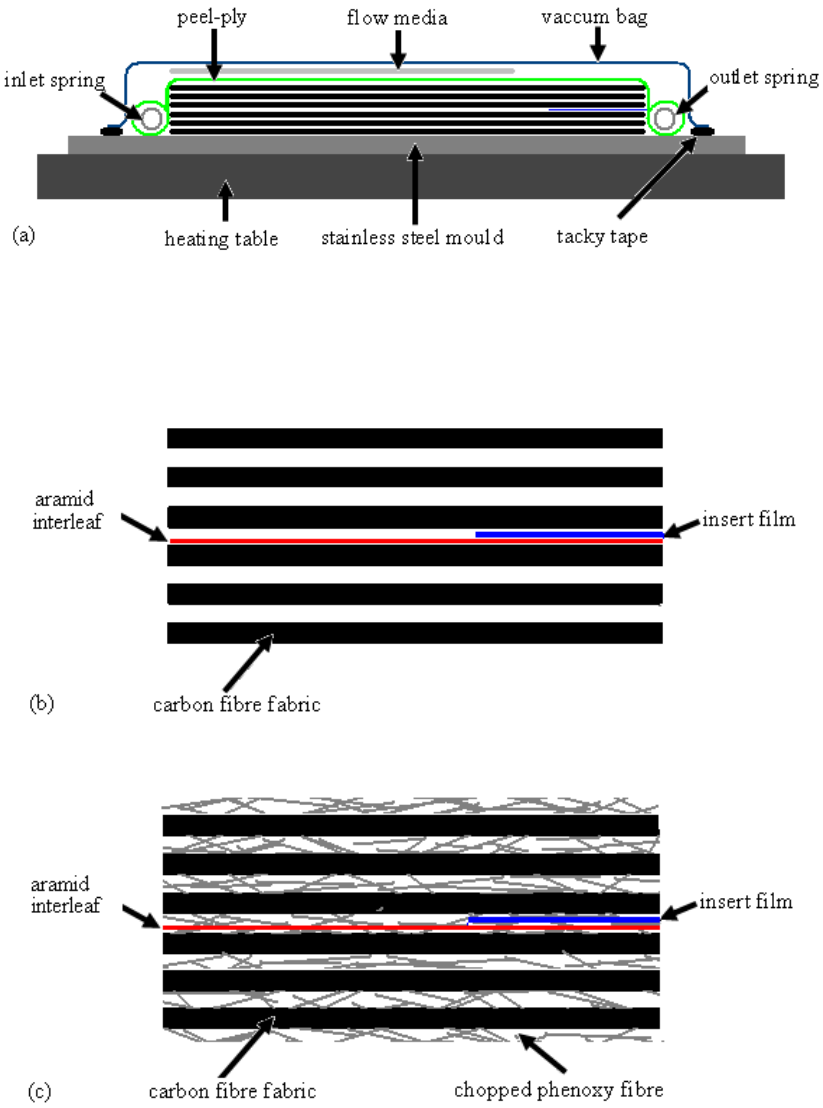

Figure 5.1 Schematic diagram of the composite laminate layup with interleaf, (a) a general vacuum bag setup, (b) layup without phenoxy (c) layup with chopped phenoxy fibres.

5.1.3 Characterisations

Tensile tests, Mode-I delamination test, short beam shear stress (SBS) test, compression after impact (CAI) test, dynamic mechanical analysis (DMA) and fractography were carried out as described in section 4.1.3.

5.2 Results and Discussion

5.2.1 Tensile properties

In the case of DGEBA resin composites (Figure 5.3), addition of phenoxy had detrimental effects on modulus and strength of aramid interleaved laminates, while strain was not significantly affected. Failure mode of the specimens (Figure 5.6) was similar to that of non-interleaved specimens (Figure 4.10), in which 10 wt% specimens showed less delaminations and failed across the width. 'Brooming' occurred more readily for 0 wt% and 5 wt% specimens, similar to that of non-interleaved specimens (Figure 4.10) however it should be noted that aramid interleaves remained intact for the two specimens.

For TGDDM resin composites (Figure 5.5), addition of aramid interleaves lowered modulus and strength for laminates without phenoxy, while strain at break was not significantly affected. Addition of phenoxy in interleaved laminates had little effect on modulus and strain, while strength improved slightly. Failure mode (Figure 5.7) of all the interleaved specimens was similar, with specimens failing across the width of the specimens with little delamination observed, regardless of phenoxy modification. This is in contrast to non-interleaved specimens where 0 wt% and 5 wt% specimens showed delamination (Figure 4.11).

Introduction of an interleaf layer decreases the effective V_f of a composite, and as there are less load carrying fibres per unit area, tensile modulus and strength are expected to reduce. However, this expected trend was more profound in phenoxy modified DGEBA specimens. This suggests that apart from V_f, resin chemistry also affects tensile properties, which could be due to changes on fibres/matrix interface with the addition of phenoxy.

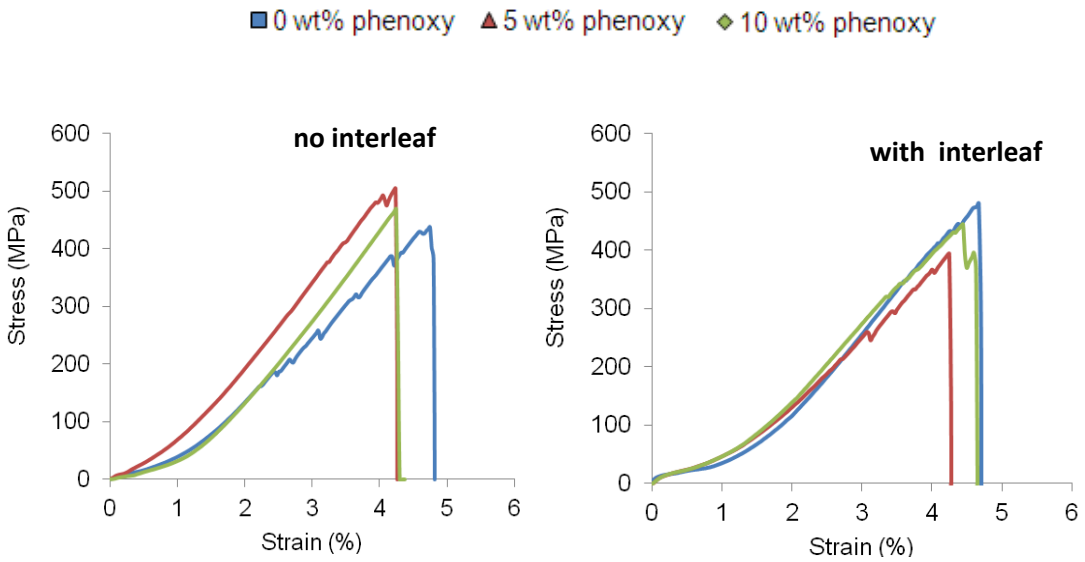

Figure 5. 2 Tensile stress-strain curves for carbon fibre/DGEBA composite laminates with and without aramid interleaf.

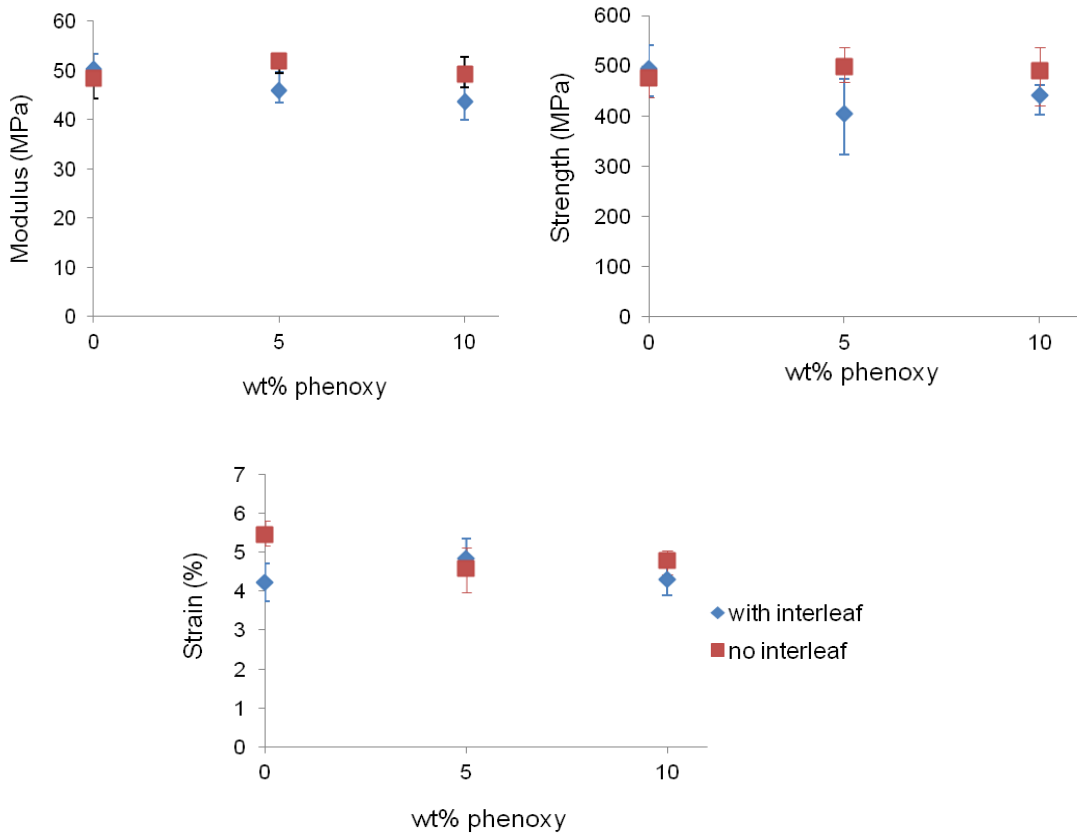

Figure 5.3 Tensile properties for carbon fibre/DGEBA laminates with and without aramid interleaf.

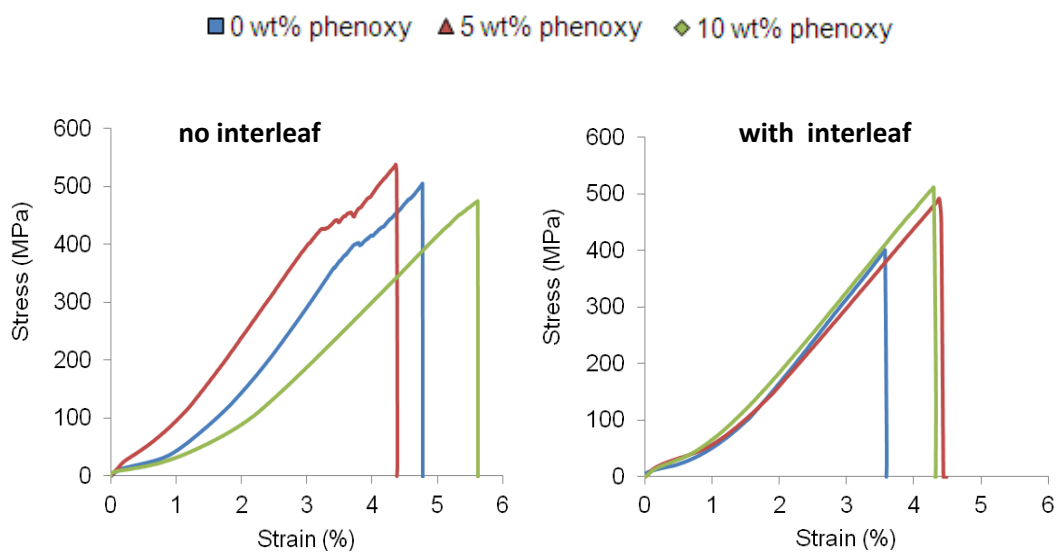

Figure 5. 4 Tensile stress-strain curves for carbon fibre/TGDDM composite laminates with and without aramid interleaf.

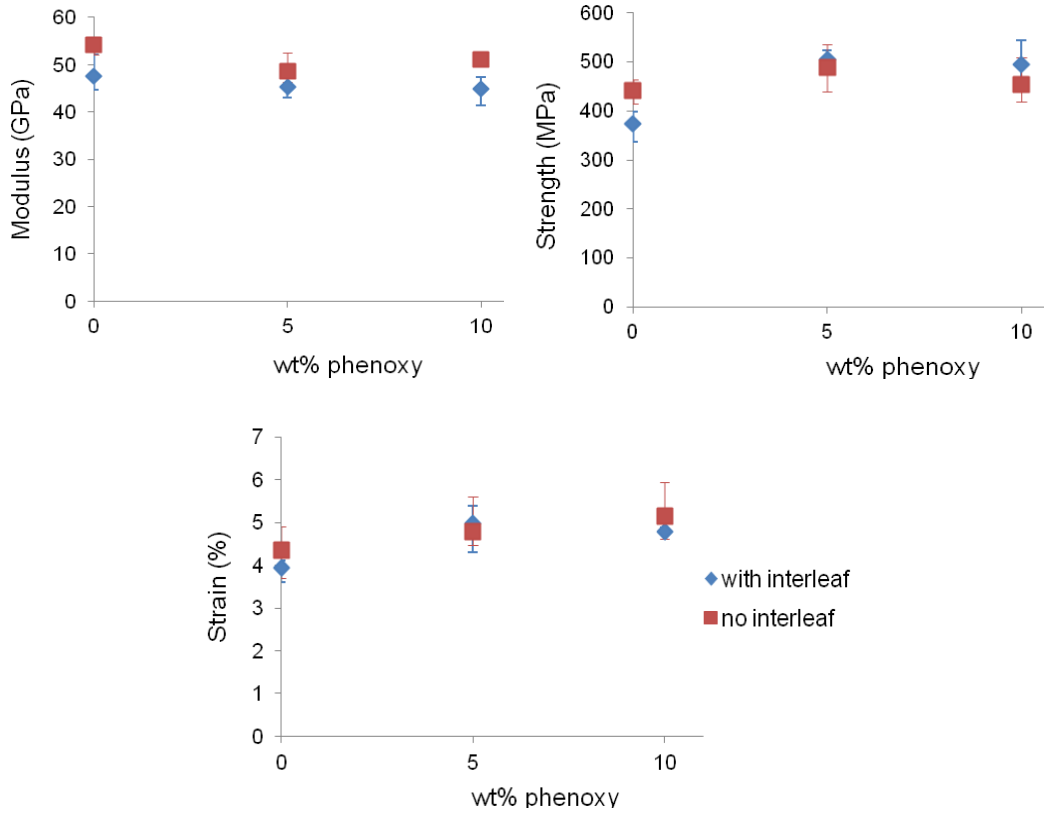

Figure 5.5 Tensile properties for carbon fibre/TGDDM laminates with and without aramid interleaf.

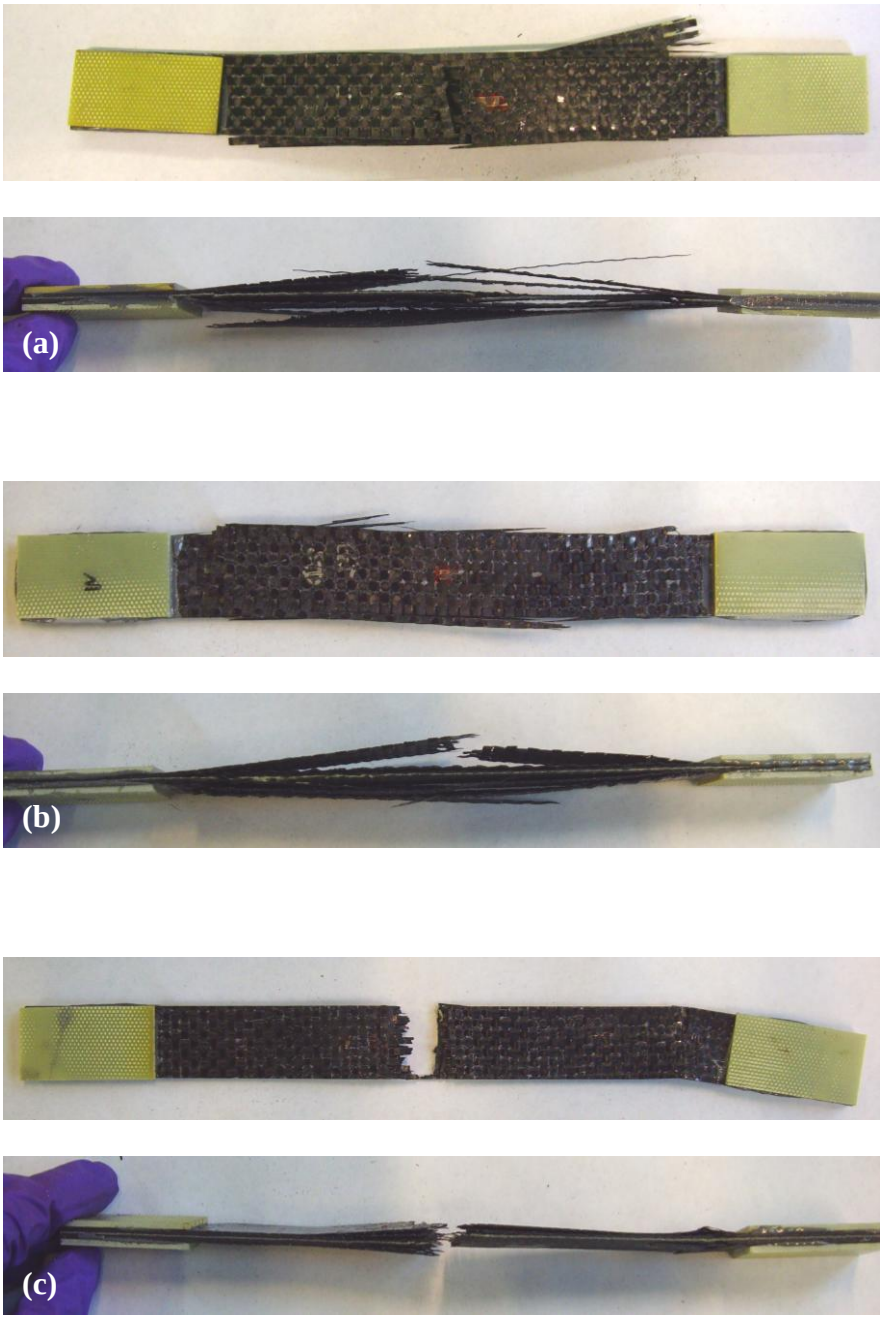

Figure 5.6 Tested tensile specimens of carbon fibre/DGEBA laminates with aramid interleaf, with (a) 0 wt% (b) 5 wt% and (c) 10 wt% phenoxy, showing less delamination for the 10 wt% specimen

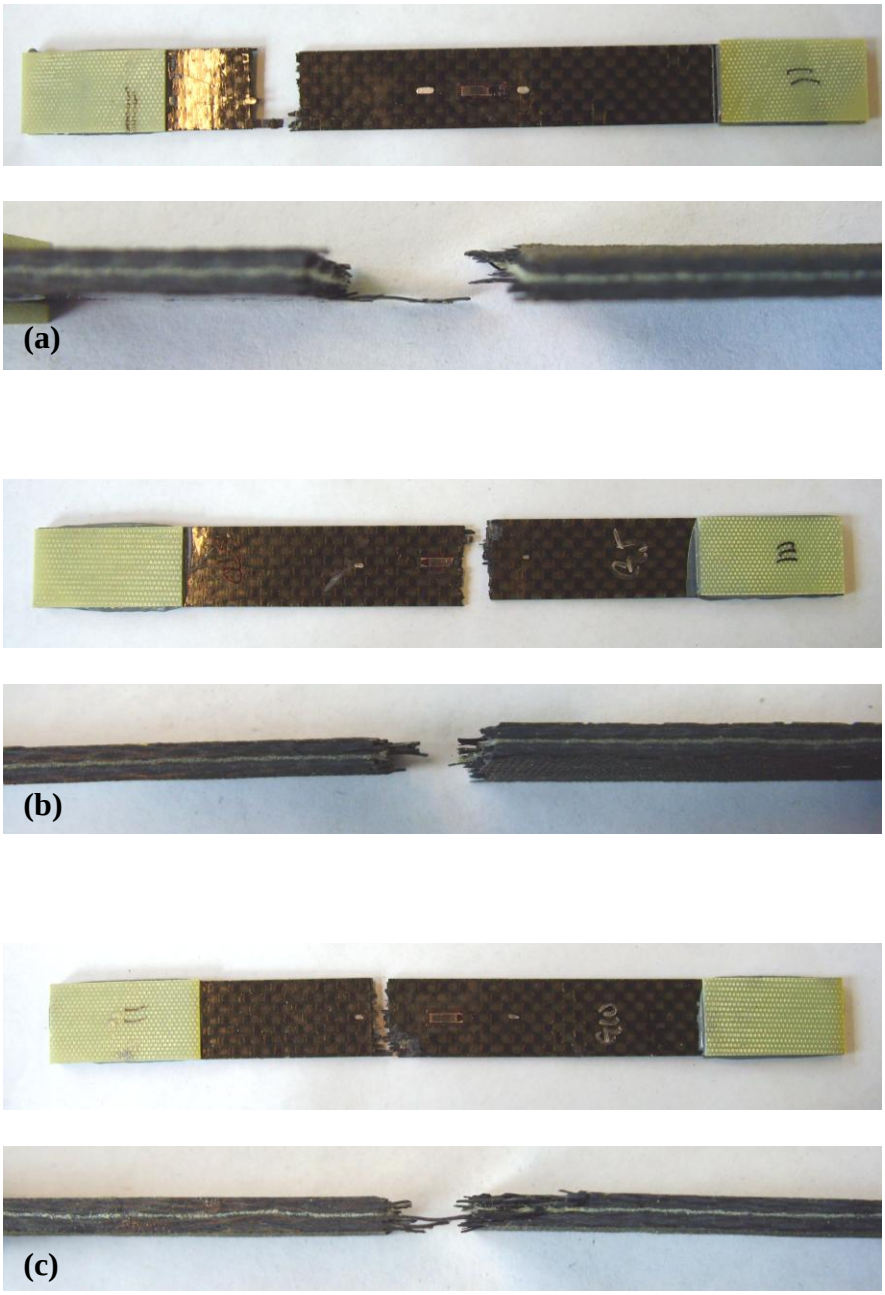

Figure 5.7 Tested tensile specimens of carbon fibre/TGDDM laminates with aramid interleaf, with (a) 0 wt% (b) 5 wt% and (c) 10 wt% phenoxy, showing similar tensile fracture for the different specimens.

5.2.2 Mode-I delamination toughness

For DGEBA specimens without phenoxy, aramid interleaves improved G_{1c} by more than 100% (Figure 5.10). Toughness improvement could be attributed to fibres bridging, fibres pull-out, and fibres deformation of aramid fibres which were observed by SEM (Figure 5.20). R-curve behaviour was observed for all the specimens, which could be the result of fibres bridging in interleaved specimens (Figure 5.9). However, G_{1c} was found to be similar in all the specimens and further improvement was found when phenoxy was added, in contrast to non-interleaved specimens in which addition of phenoxy increased G_{1c} significantly. Looking at fracture surfaces of 0 wt% (Figure 5.20), 5 wt% (Figure 5.21) and 10 wt% (Figure 5.22) specimens, they all share the same features that delamination occurred within the interleaving region, and no carbon fibres were exposed. The only toughening came from aramid fibres for all the specimens and therefore whether there was phenoxy or not did not make much difference to the overall composite toughness. This could be due to fact that the aramid fibre/matrix interface is weaker than the carbon fibre/matrix layer, and crack grows along the weaker interface. For interleaved specimens, as the carbon fibre/matrix interface was not involved in delamination, the effect of phenoxy toughening became redundant. Addition of phenoxy did not strengthen aramid fibre/matrix interface as G_{1c} did not increased. Therefore in terms of Mode-I delamination toughness, the two interlaminar toughening methods were not compatible with each other for the DGEBA used. Regardless of matrix toughness, the overall toughness of aramid interleaved composites remained the same and was limited by properties of the aramid/DGEBA interface.

A different trend was observed for the TGDDM resin, where the interleaves did not toughen the specimens without phenoxy, while G_{1c} improved for a combination of aramid interleaf and phenoxy, particularly for 5 wt% phenoxy specimens (Figure 5.13). No R-curve was observed for 0 wt% phenoxy but this was observed for specimens with phenoxy (Figure 5.12). This suggests that addition of

phenoxy encouraged fibre bridging of the specimens for this resin. Comparing fracture surfaces of 0 wt% (Figure 5.23), 5 wt% (Figure 5.24) and 10 wt% (Figure 5.25) specimens, it is found that for specimens without phenoxy, delamination occurred at the carbon fibre /matrix interface with little involvement of aramid fibres. Both 5 wt% and 10 wt% showed fracture features involving carbon and aramid fibres. Fibre debonding, fibre pull-out occurred for both fibres, with fibre fracture for carbon fibres, and fibre fibrillation, plastic deformation and fracture for aramid fibres. This indicates a favourable match between the toughness of carbon fibre/matrix and aramid fibre/matrix layers for phenoxy modified systems, which allowed toughening mechanisms to be operated by both fibres. This indicates that carbon fibre/unmodified TGDDM interface was the weaker phase, in contrast to DGEBA. Addition of phenoxy to TGDDM improved the toughness of the carbon fibre/TGDDM interface to a level close to the aramid fibre/TGDDM interface.

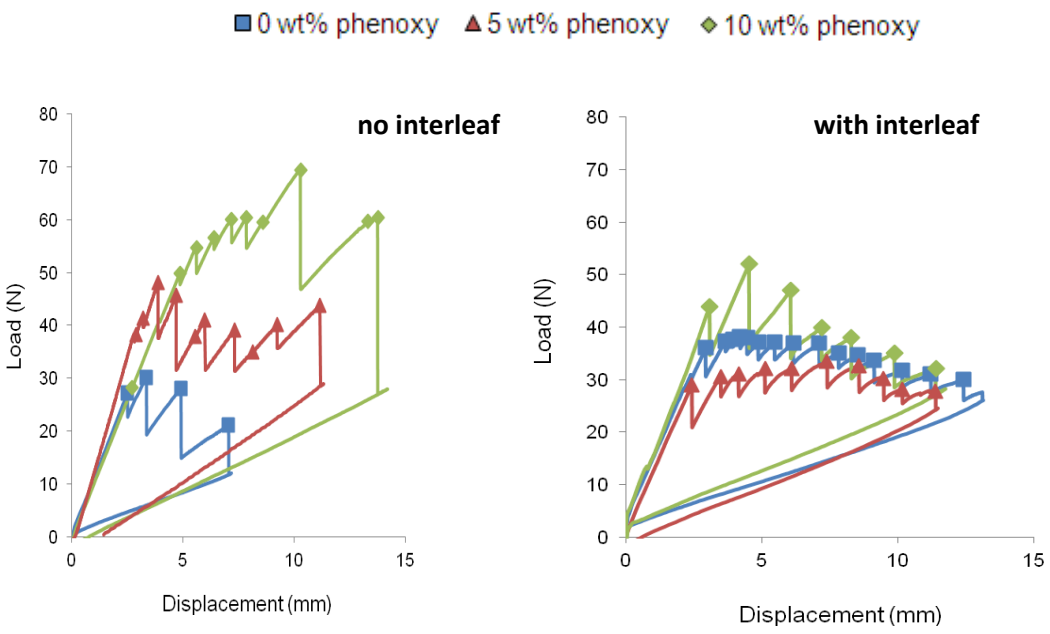

Figure 5.8 DCB load-displacement curve for carbon fibre/DGEBA laminates with and without aramid interleaf at different phenoxy contents.

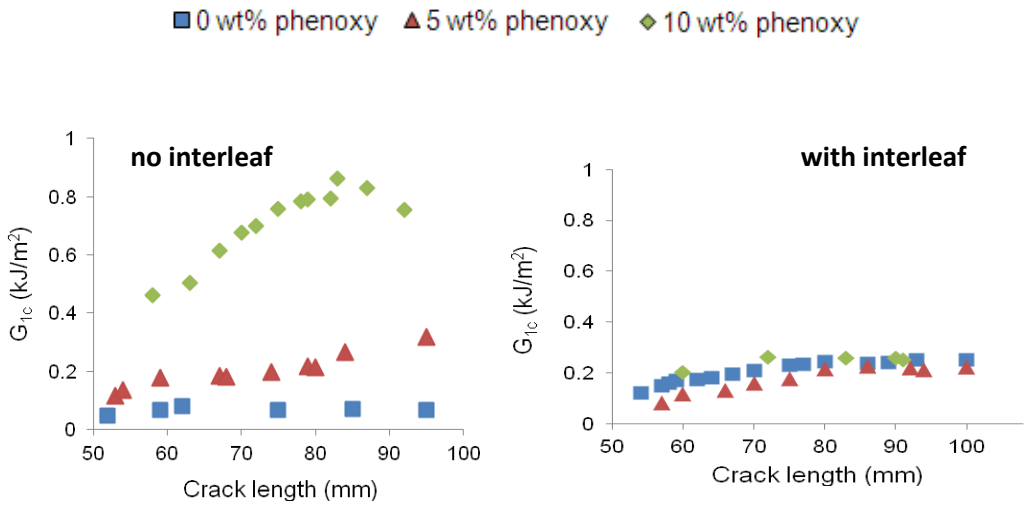

Figure 5.9 Mode-I DCB G_{1c} vs crack length for DGEBA laminates with and without aramid interleaf at different phenoxy contents.

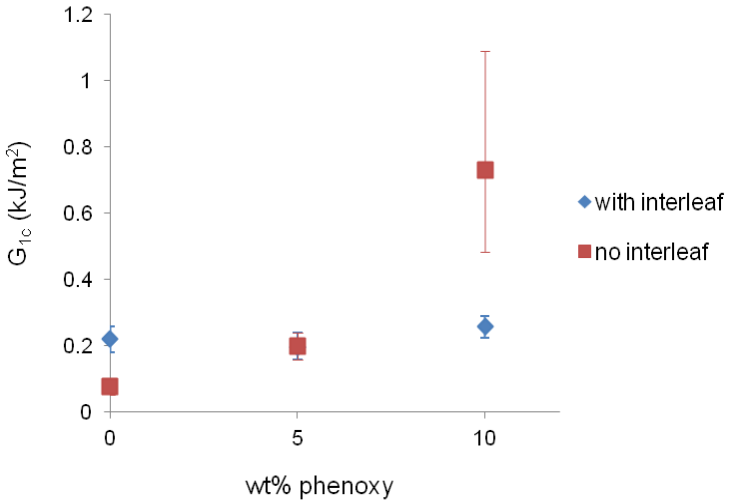

Figure 5.10 Mode-I DCB G_{1c} fracture toughness values for carbon fibre/DGEBA laminates modified with phenoxy, with and without aramid interleaves.

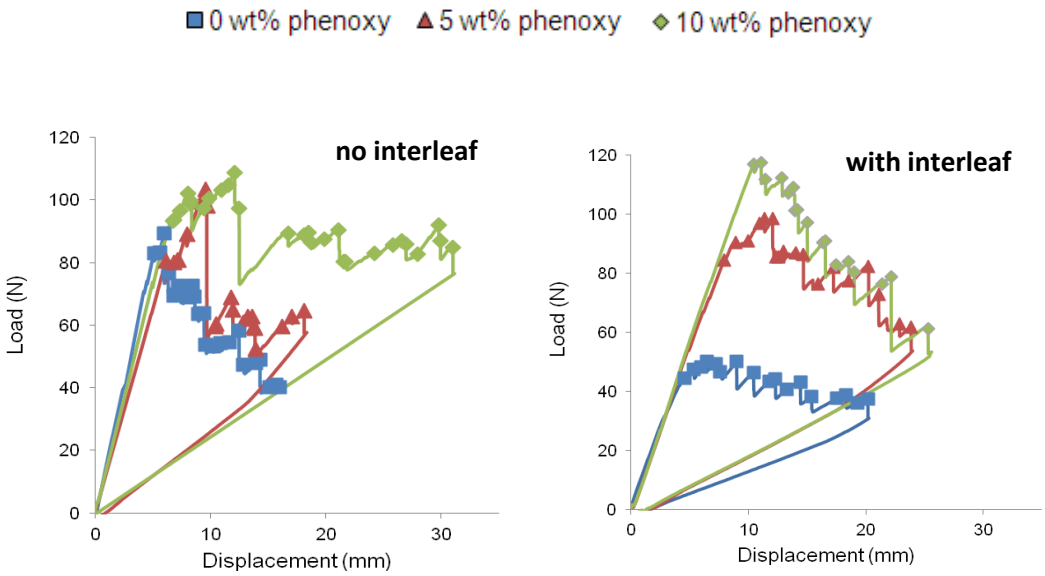

Figure 5.11 DCB load-displacement curve for carbon fibre/TGDDM laminates with and without aramid interleaf.

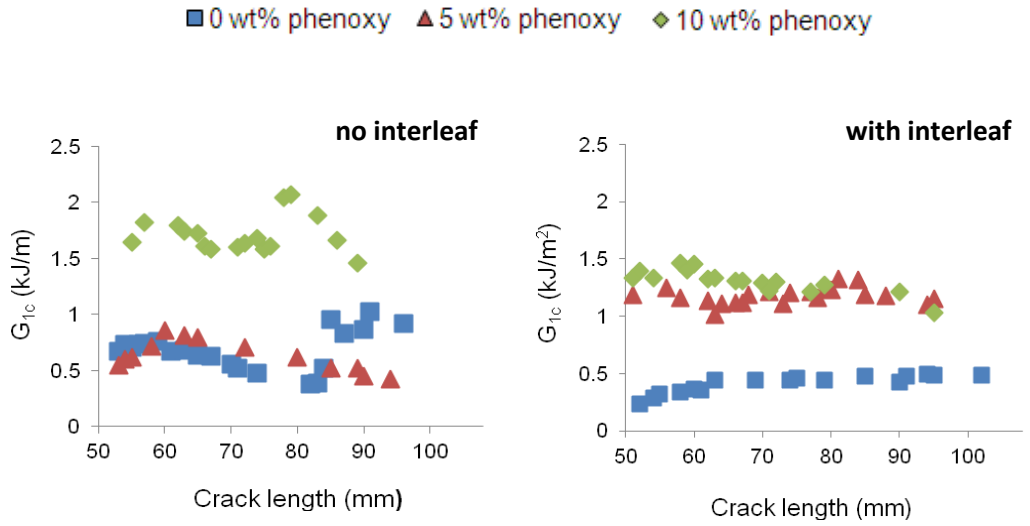

Figure 5.12 Mode-I DCB G_{1c} vs crack length for TGDDM laminates with and without aramid interleaf.

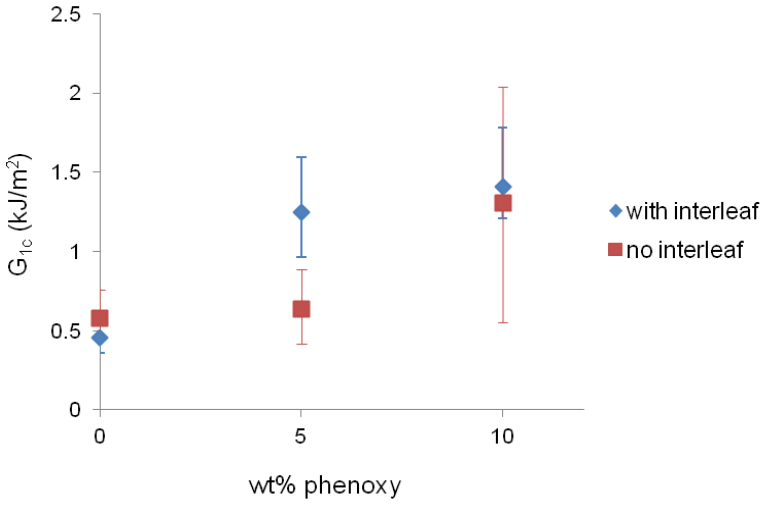

Figure 5.13 Mode-I DCB G_{1c} fracture toughness values for carbon fibre/TGDDM laminates modified with phenoxy, with and without aramid interleaves.

5.2.3 Short beam shear strength

For DGEBA interleaved specimens (Figure 5.14), the combination of aramid interleaf and phenoxy modification was detrimental to the shear strength. Aramid interleaved specimens had a lower short beam shear strength in the presence of phenoxy. This suggests that the interface between phenoxy-modified resin and aramid fibres is weak.

For TGDDM aramid interleaved specimens (Figure 5.15), an opposite trend was observed compared to DGEBA specimens. Here the shear strength of specimens without phenoxy decreased while the ones with 5 wt% phenoxy increased. In general, the addition of phenoxy improved shear strength of interleaved specimens.

As with the Mode-I G_{1c} values, different trends were observed for the two resins. However, both resins showed that 5 wt% phenoxy specimens with interleaves gave the most profound changes, while no such trend was observed for specimens

without interleaves. The results show that phenoxy can alter the shear strength of interleaved laminates, however, effects can either be positive or negative depending on resin system used.

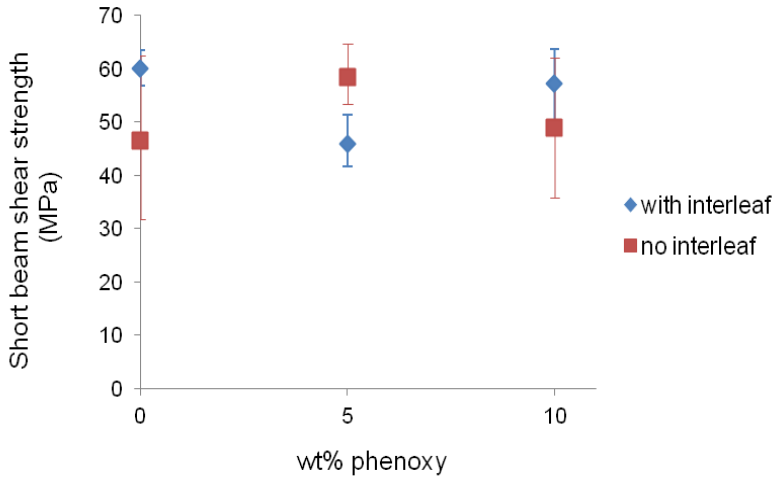

Figure 5.14 Short beam results for carbon fibre/DGEBA laminates with and without aramid interleaves.

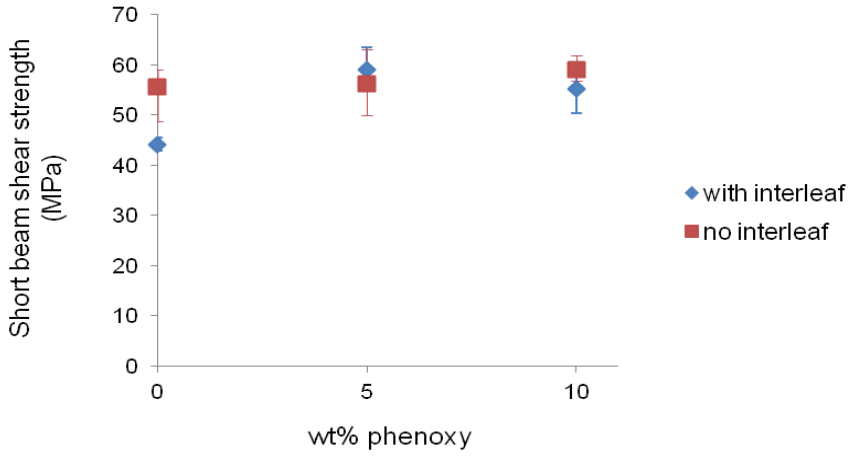

Figure 5.15 Short beam results for carbon fibre/TGDDM laminates with and without aramid interleaves.

5.2.4 Compression after impact

For DGEBA laminates, addition of aramid interleaves decreased damage resistance of laminates. Damage widths of aramid interleaved lamimates were greater than their non-interleaved counterparts for all matrices (Figure 5.17a). Addition of phenoxy further decreased damage resistance for aramid interleaved laminates, especially for 5 wt% phenoxy modified aramid interleaved specimens which showed increased damage width. Damage tolerance of interleaved laminates only improved for the 5 wt% sample, with the 0 wt% and 10 wt% aramid interleaved laminates either had similar or lowered residual strength when compared to their non-interleaved counterpart (Figure 5.17c). Compressive strength, however, was higher for undamaged aramid interleaved specimens (Fig, 5.17b), compressive strength also became stable for all phenoxy concentrations at higher impact energy. There was no clear trend between G_{1c} (Figure 5.10) and CAI properties for DGEBA. As explained in the previous chapter (section 4.2.4). CAI properties are dependent on both delamination and shear, and G_{1c} only accounted for a fraction of CAI performance.

For TGDDM laminates, aramid interleaves did not provide positive effect on damage resistance in the presence of phenoxy but improved for laminates with unmodified matrix (Figure 5.19a). In terms of damage tolerance, increasing phenoxy content had a positive effect for aramid interleaved specimens. 0 wt% and 10 wt% aramid interleaved specimens performed better than non-interleaved specimens (Figure 5.19c), while 5 wt% specimen had a lower tolerance. This shows an opposite trend to DGEBA specimens in which 5 wt% phenoxy aramid interleaved laminates provided better non-interleaved laminates. Figure 5.19b showed that addition of phenoxy improved compressive strength of interleaved laminates. However, addition of aramid interleaves drastically reduced the compressive strength of laminates with unmodified TGDDM compared to its non-interleaved counterpart. 5 wt% phenoxy aramid interleaved laminates had higher compressive strength than non-interleaved specimens, but a higher concentration of phenoxy did not result in further improvement. Comparing G_{1c} (Figure 5.13) to CAI properties, aramid interleaved

laminates show with increasing G_{1c}, damage resistance reduced, while damage tolerance and compressive strength increased.

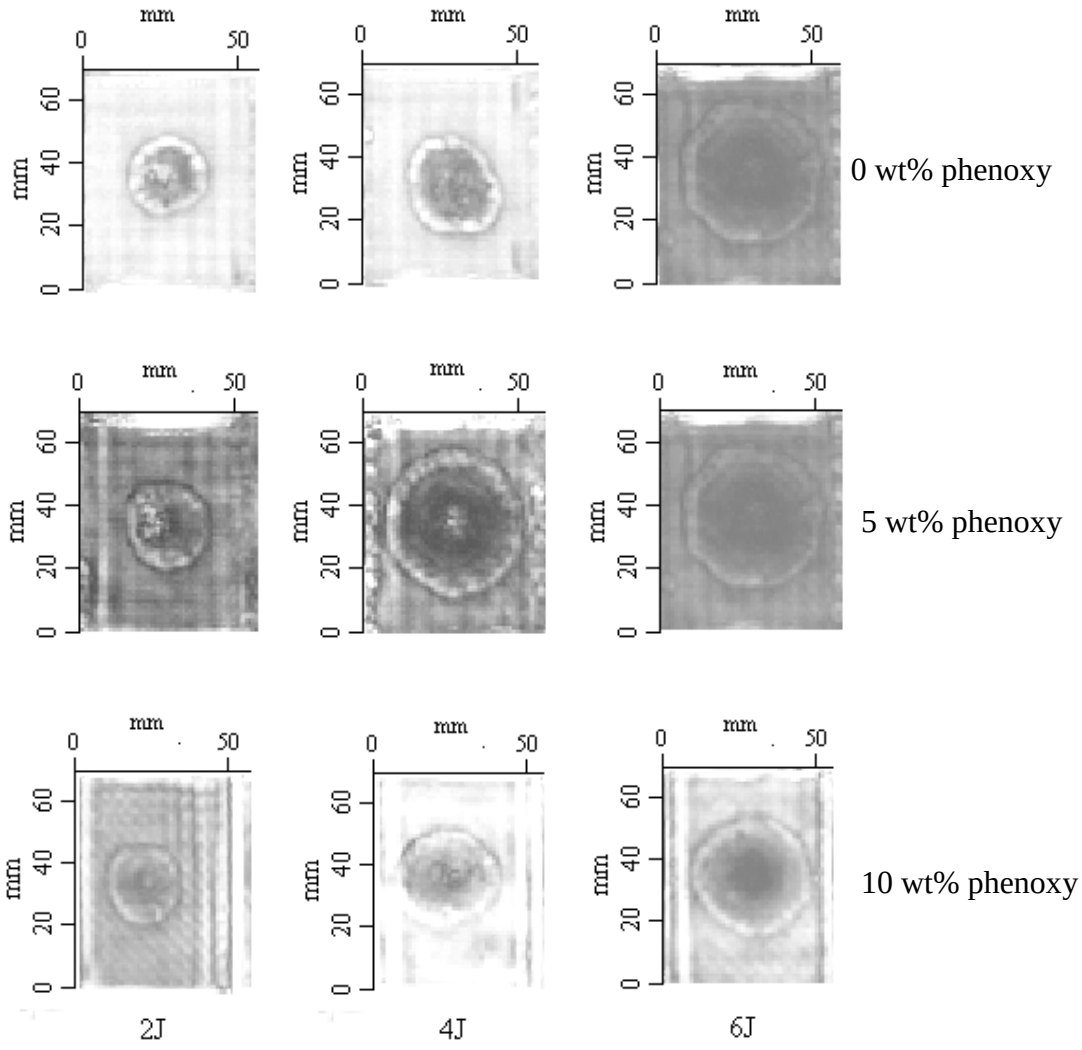

Figure 5.16 C-scan image for impacted carbon fibre/DGEBA laminates with aramid interleaves.

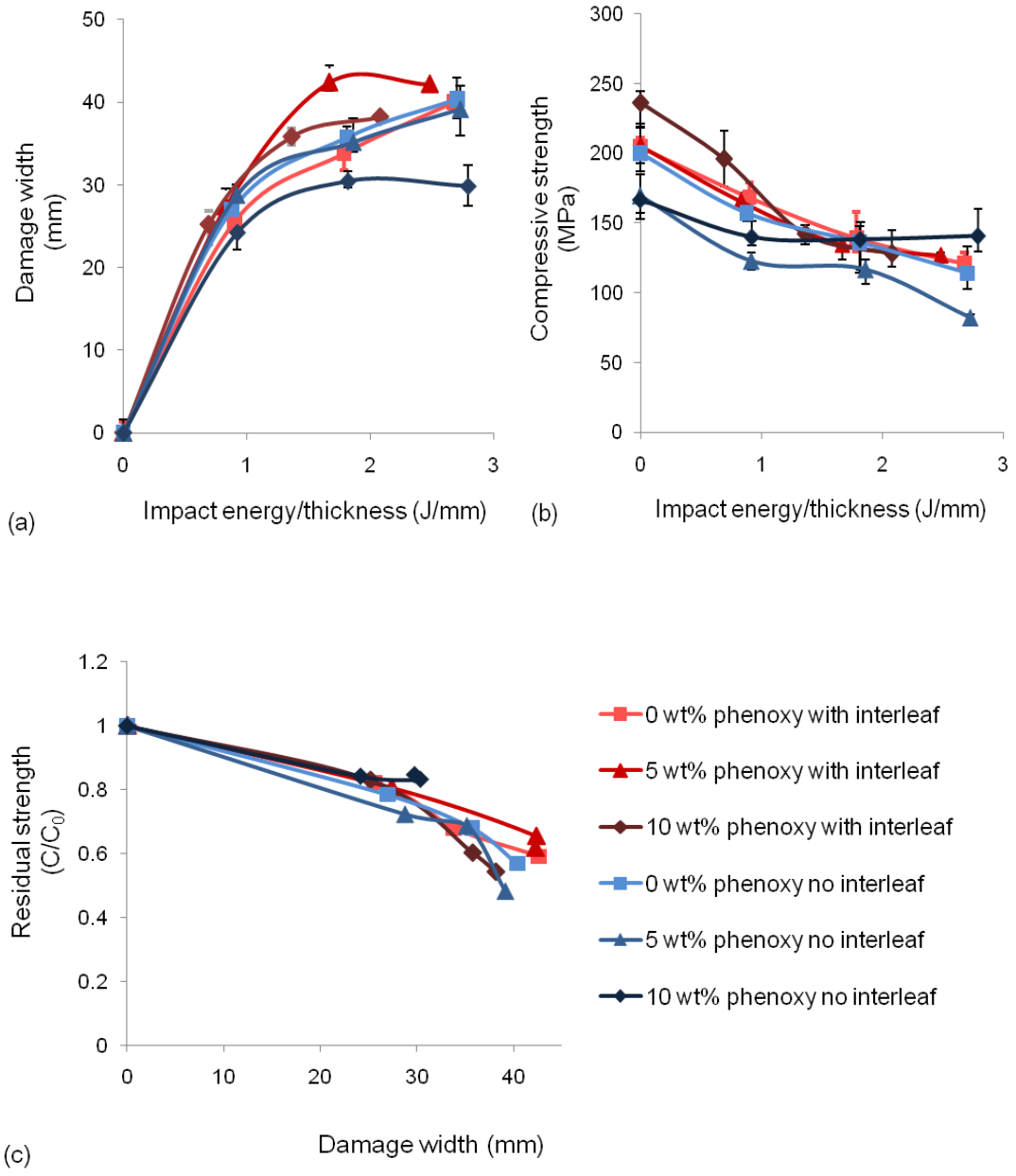

Figure 5.17 CAI results for carbon fibre/DGEBA laminates with and without aramid interleaves.

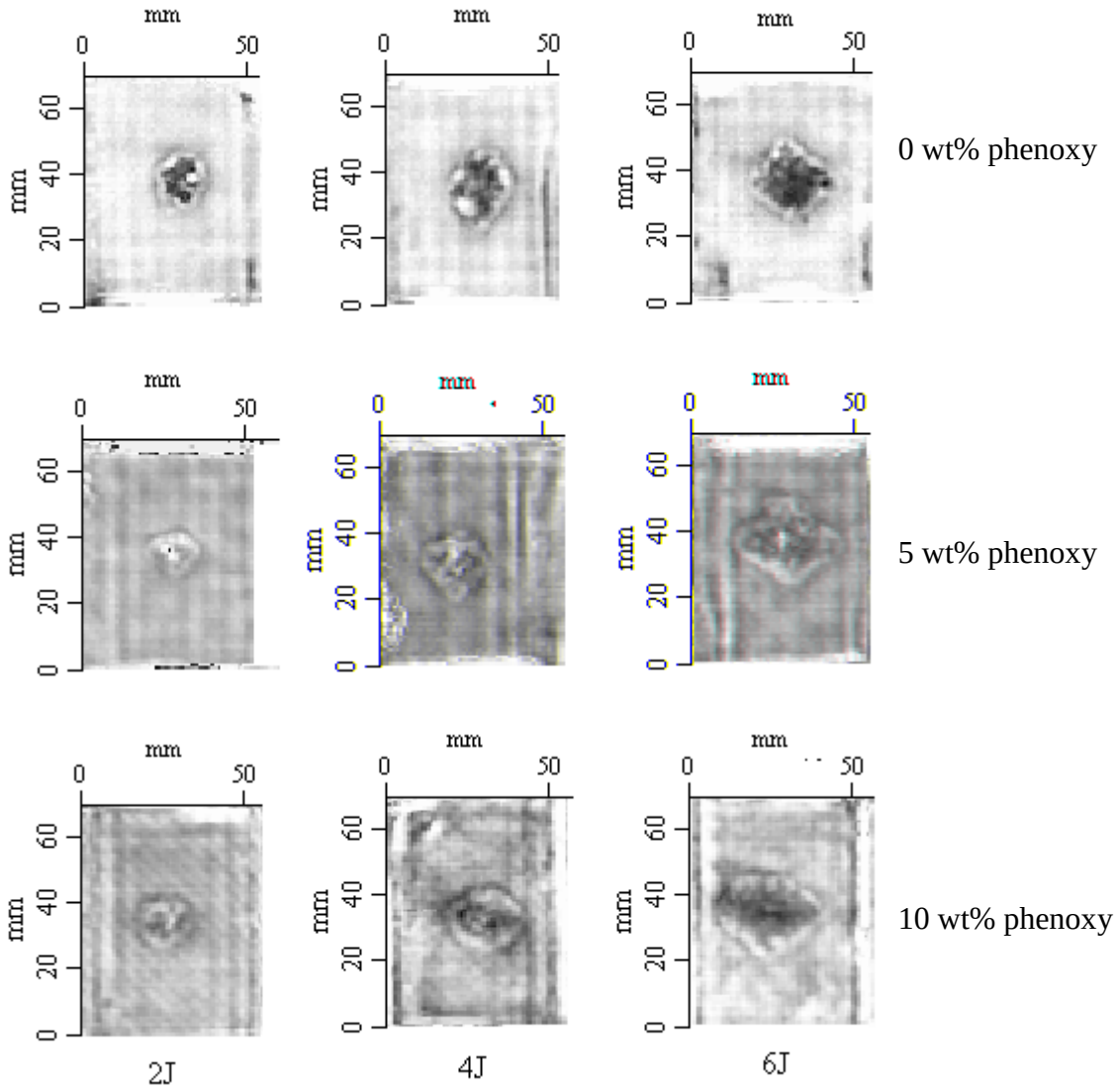

Figure 5.18 C-scan image for impacted carbon fibre/TGDDM laminates with aramid interleaves.

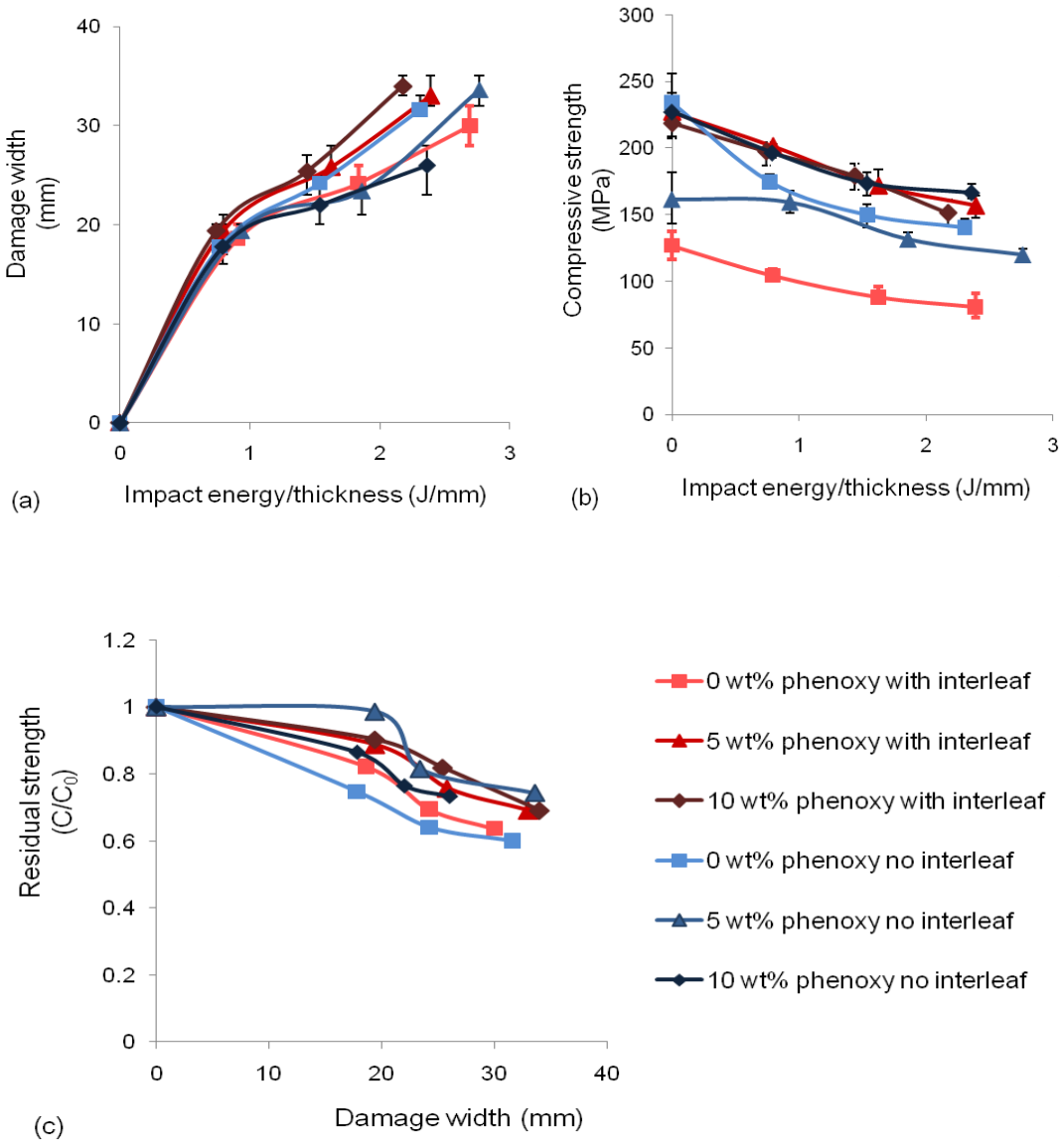

Figure 5.19 CAI results for carbon fibre/TGDDM laminates with and without aramid interleaves.

5.2.5 Morphology

Mode-I fracture surfaces of aramid interleaved DGEBA specimens at 0 wt% (Figure 5.20), 5 wt% (Figure 5.21) and 10 wt% show (Figure 5.22) that the major toughening mechanisms were generated by aramid fibres. Fibre bridging, fibre pull-out, fibre/matrix debonding and fibre damage of aramid fibres were all observed. Aramid fibres were stretched and broken, and fibrillation occurred. For all the specimens, fracture occurred within the resin-rich interleaf layer, and carbon fibres were not exposed. This indicated that the interleaving layer had a lower toughness and was more prone to fracture than carbon fibres/phenoxy-modified epoxy interlaminar region, and the carbon fibre/DGEBA interface was not involved in the toughening. Phase separation was observed for 5 wt% and 10 wt% specimens, however, fracture surfaces look similar for all phenoxy concentrations, suggesting the same toughening mechanisms responsible for overall toughness.

In contrast to DGEBA, Mode-I fracture surfaces of aramid interleaved TGDDM specimens without phenoxy show that fracture occurred mostly at the carbon fibre/matrix interface (Figure 5.23a) with only little involvement from aramid interleaves (Figure 5.23b). The fracture surfaces are clean with no fibre bridging. Specimens with 5 wt% (Figure 5.24) and 10 wt% (Figure 5.25) phenoxy show toughening mechanisms generated by aramid interleaves as well as those by carbon fibres. Aramid fibre pull-out, fibre/matrix debonding, fibrillation, fibre stretching and fracture were all observed. Carbon fibre/matrix debonding and carbon fibre fracture were also observed in the 5 wt% and 10 wt% specimens and they also contributed to overall toughness.

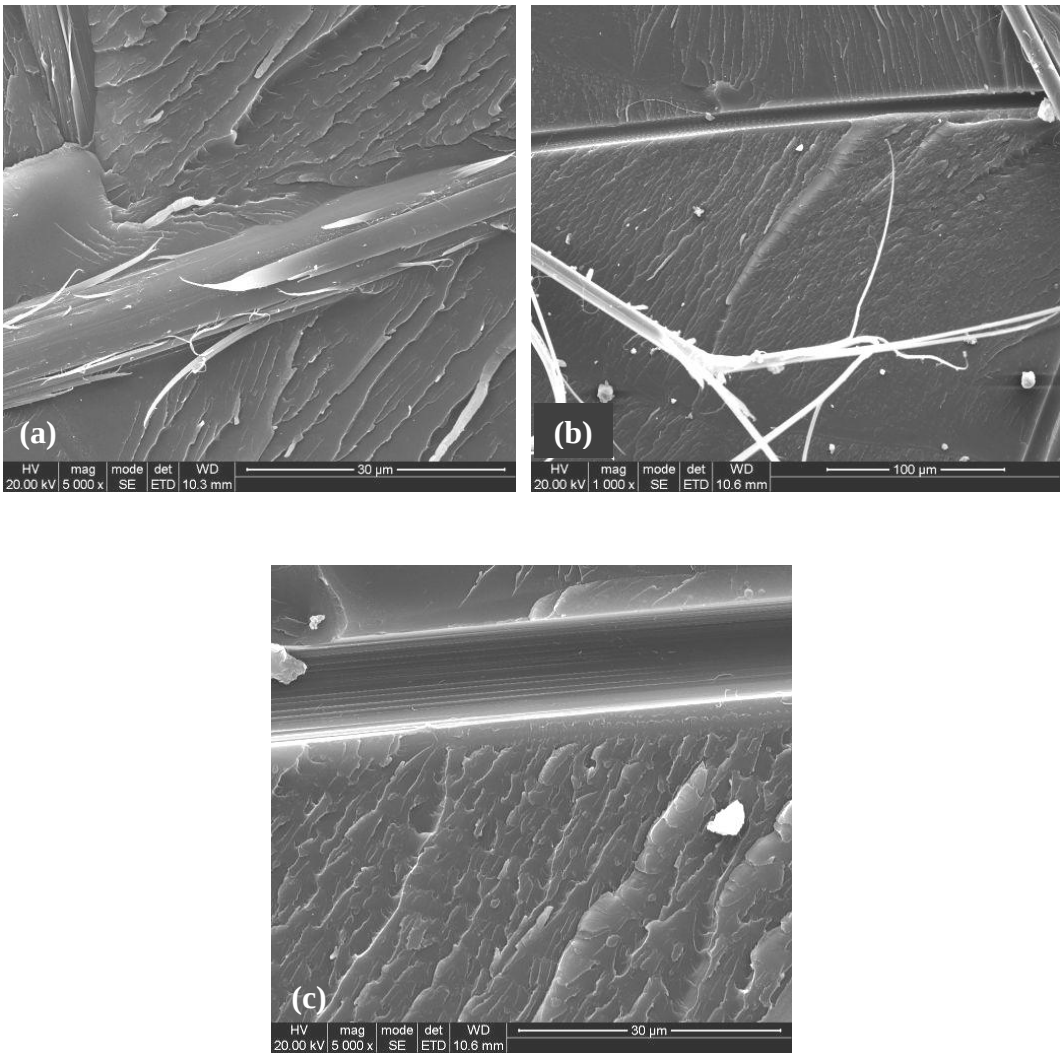

Figure 5.20 Mode-I SEM fractography of carbon fibre/DGEBA laminates with aramid interleaf and no phenoxy, showing: (a) fracture occurring within the interleaving region; (b) aramid fibre fibrillation; (c) aramid fibre stretching and fracture and (d) debonding of aramid fibres.

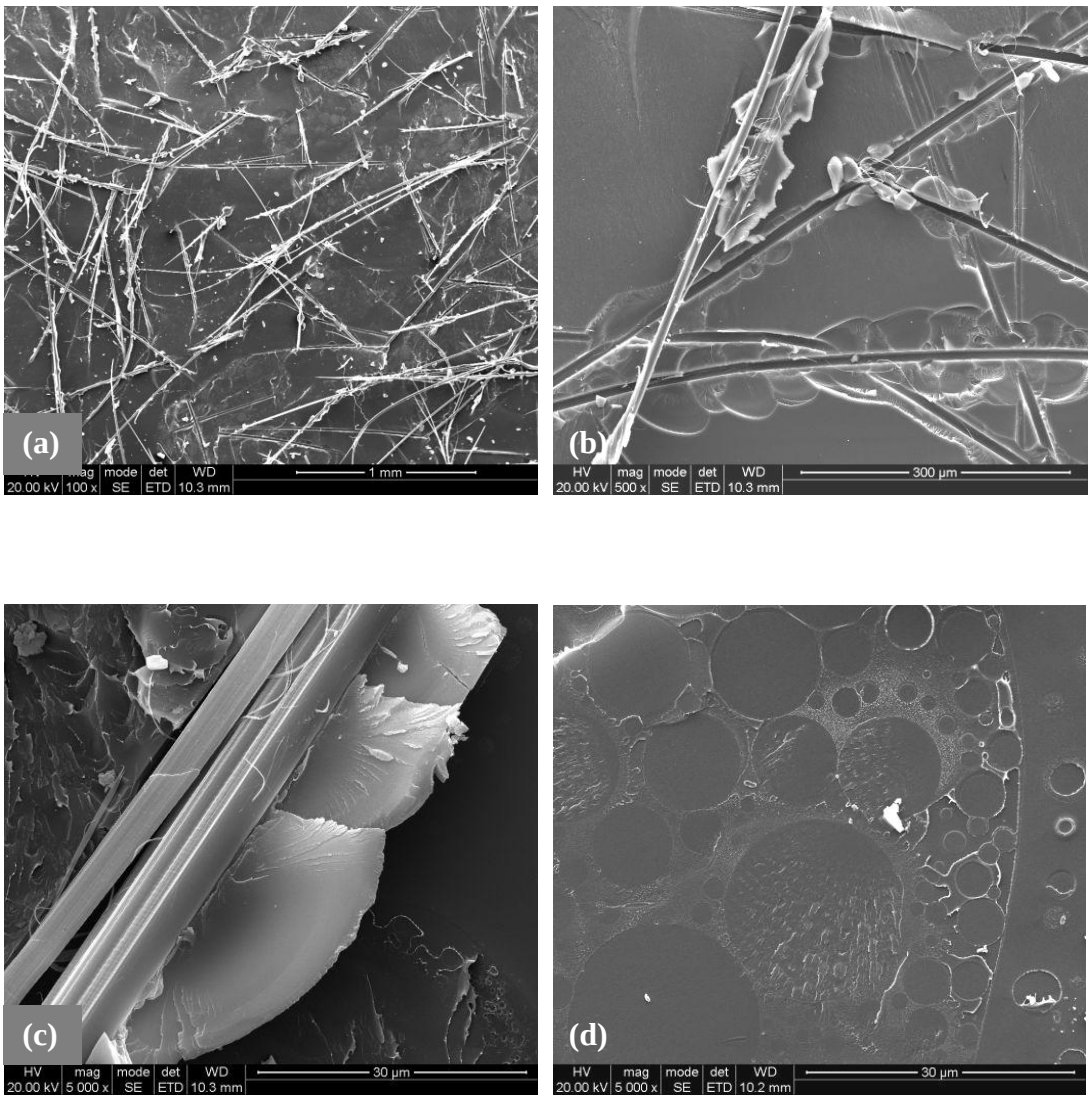

Figure 5.21 Mode-I SEM fractography of carbon fibre/DGEBA laminates with aramid interleaf and "5 wt%" phenoxy showing: (a) fracture occurring within the interleaving region; (b) debonding of aramid fibres; (c) aramid fibrillation and (d) matrix phase separation.

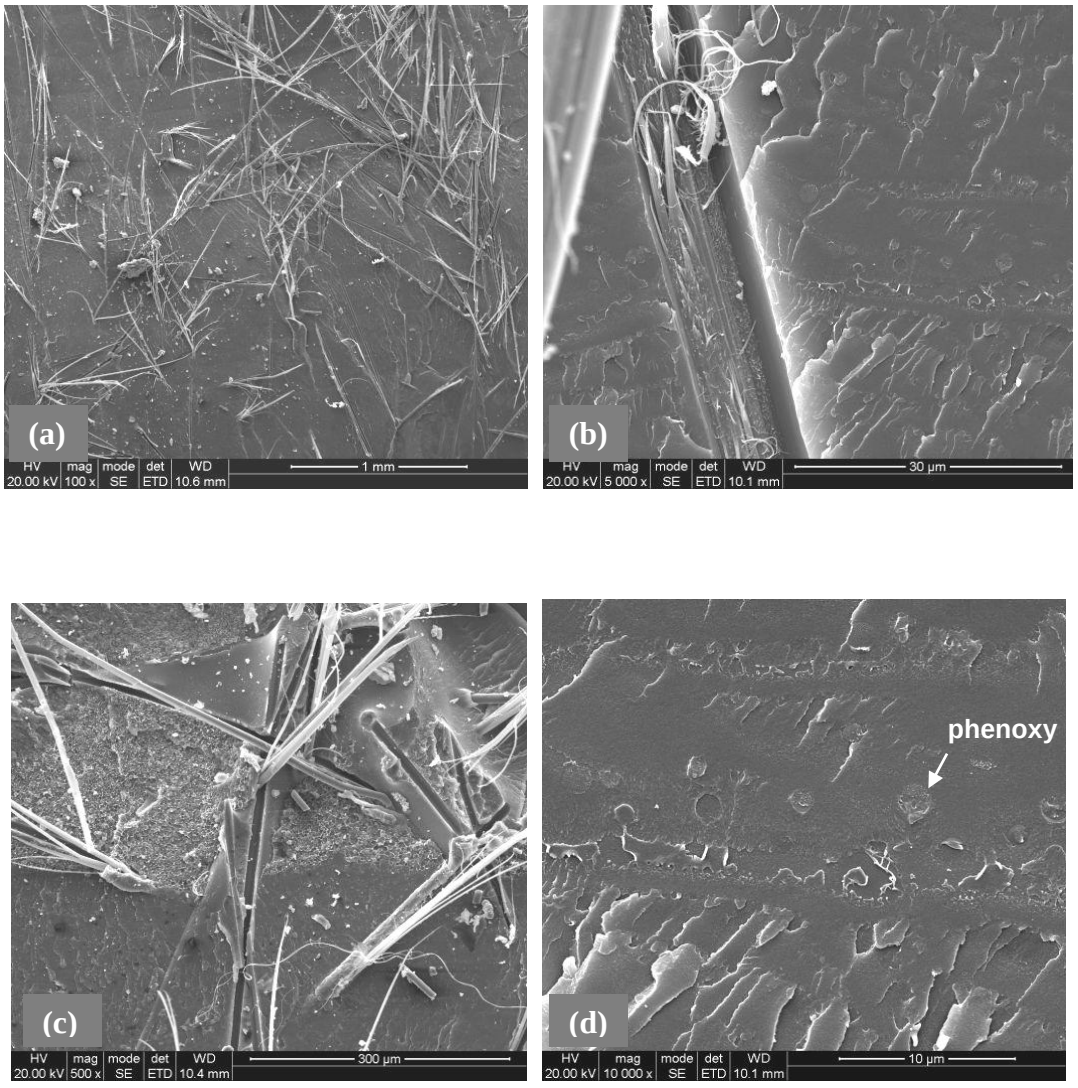

Figure 5.22 Mode-I SEM fractography of carbon fibre/DGEBA laminates with aramid interleaf and "10 wt%" phenoxy showing: (a) fracture occurring within the interleaving region; (b) debonding of aramid fibres; (c) aramid fibre stretching, fibrillation and fracture; and (d) matrix phase separation.

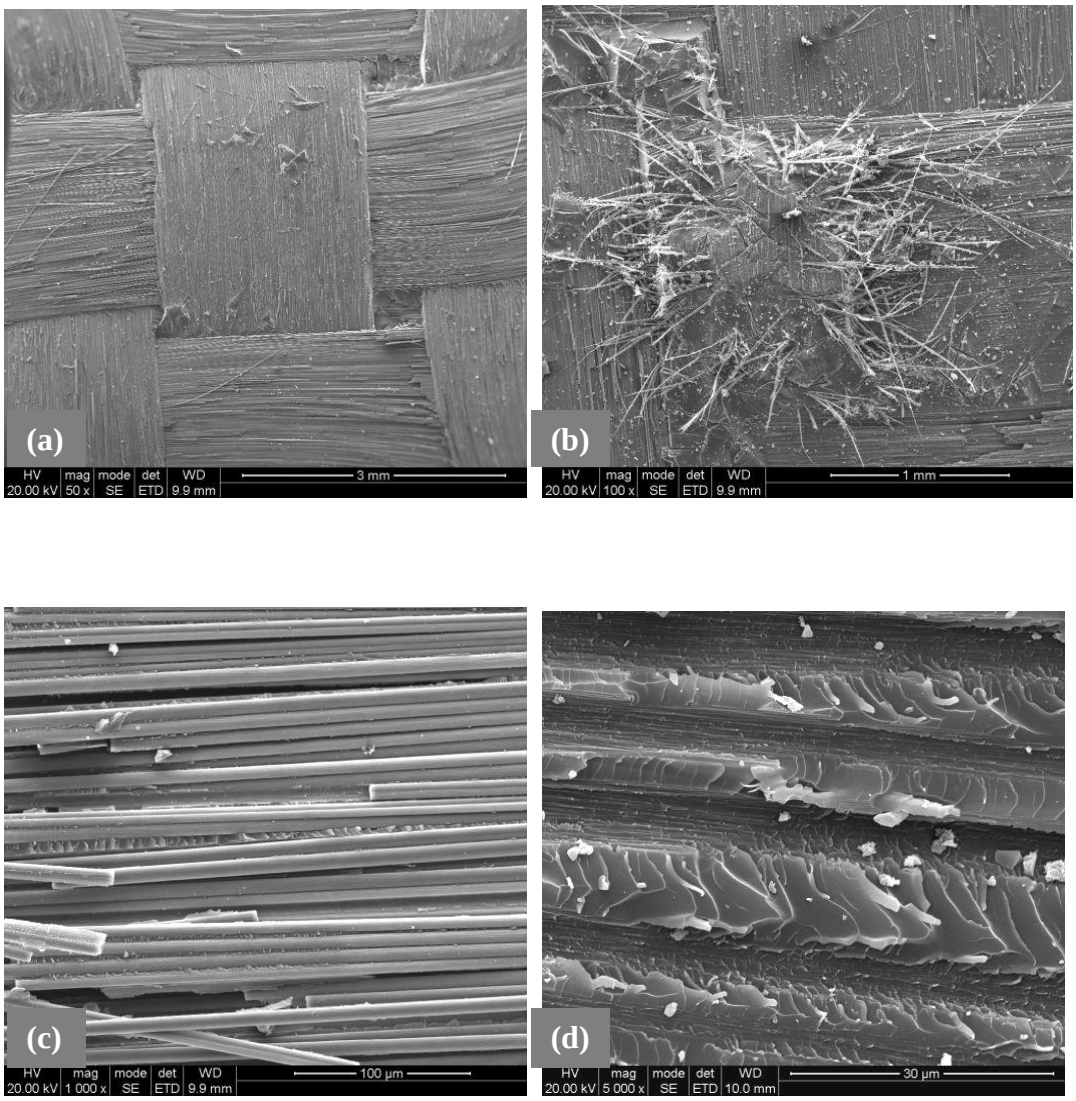

Figure 5.23 Mode-I SEM fractography of carbon fibre/TGDDM laminates with aramid interleaf and no phenoxy showing (a) fracture occurring mostly along carbon fibres/matrix region; (b) aramid fibre deformation; (c) carbon fibre fracture and (d) debonding of carbon fibres.

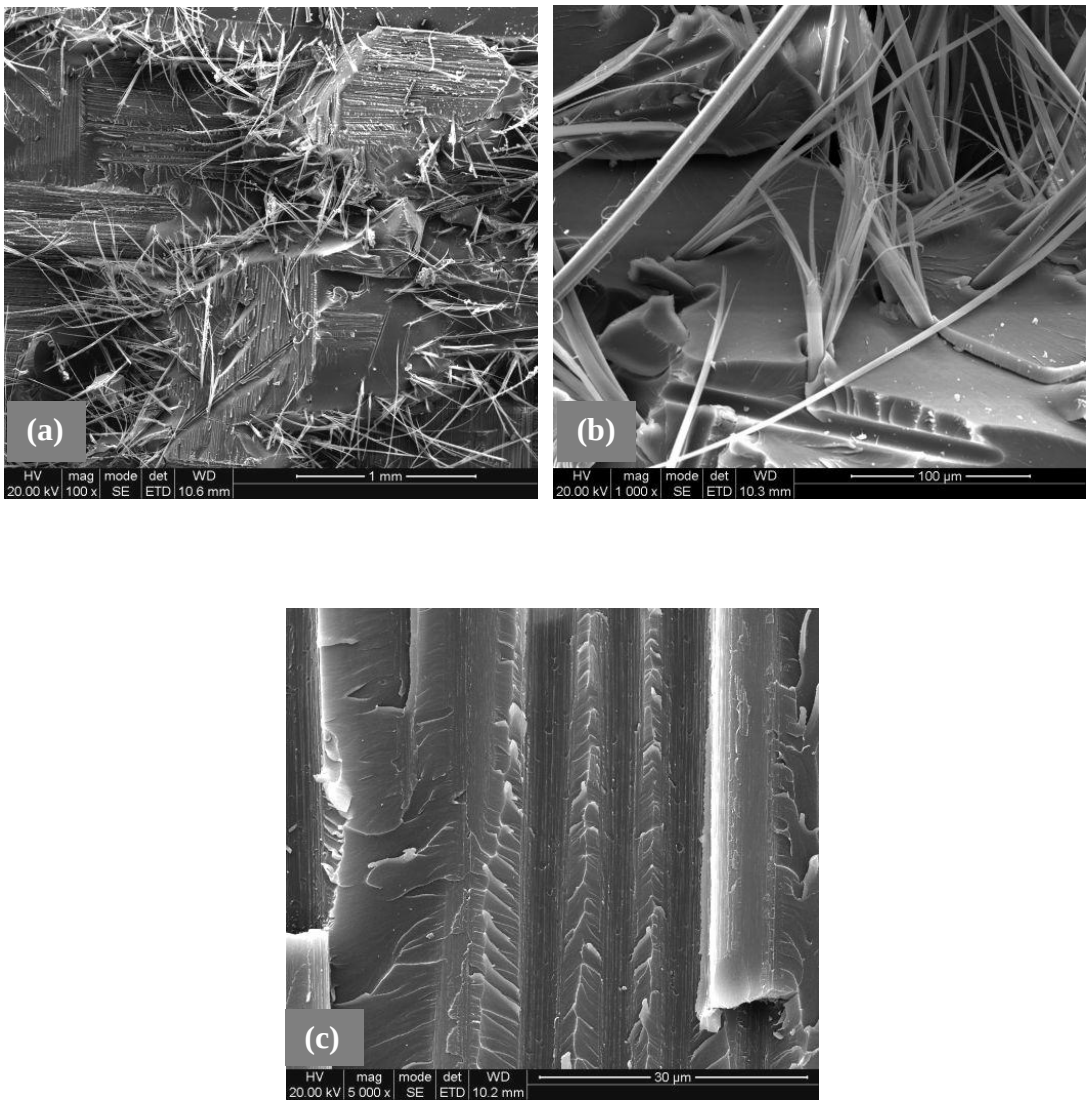

Figure 5.24 Mode-I SEM fractography of carbon fibre/TGDDM laminates with aramid interleaf and "5 wt%" phenoxy showing: (a) deformation of aramid fibres; (b) aramid fibre stretching, fibrillation and fracture and (c) carbon fibre debonding.

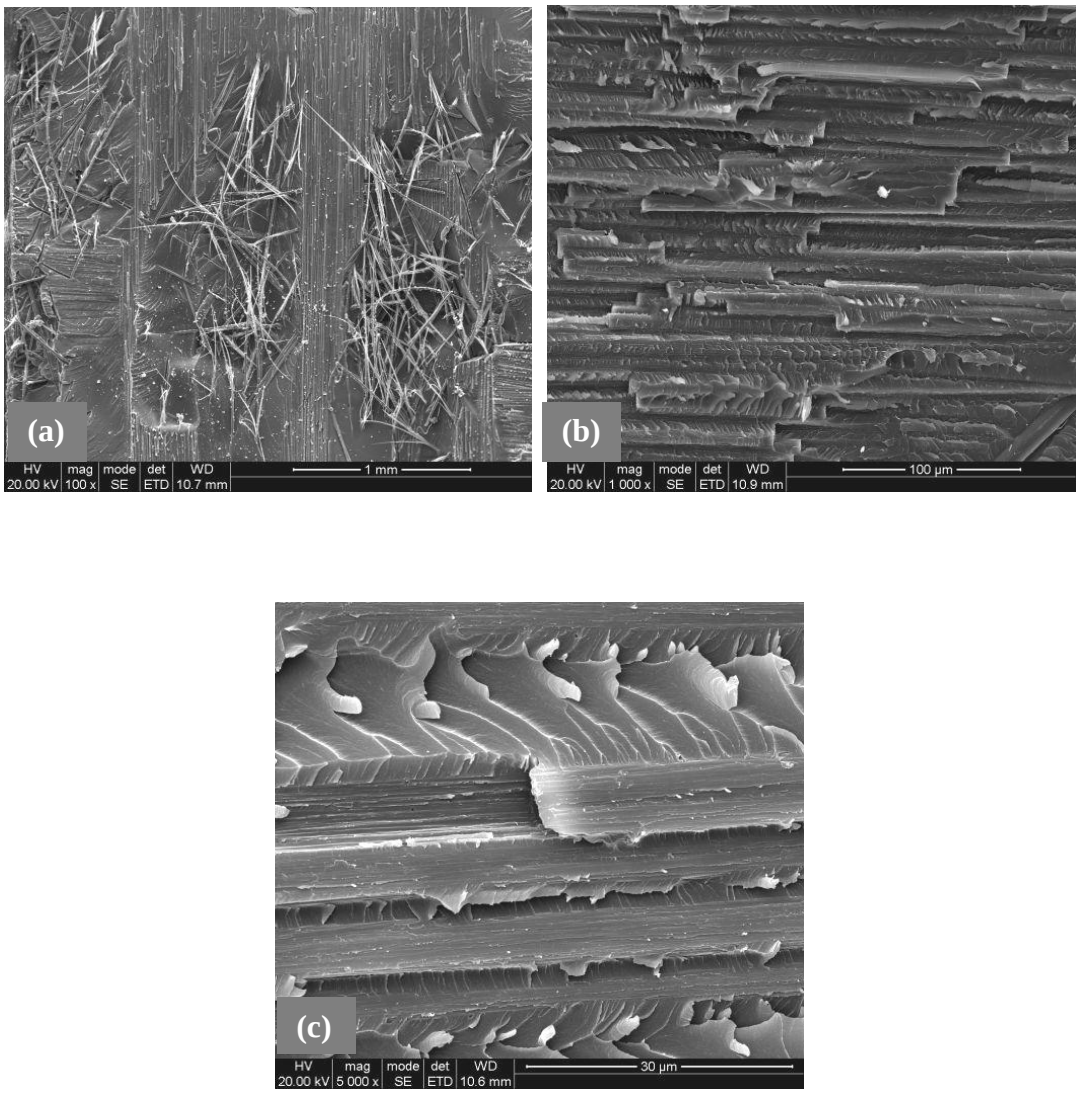

Figure 5.25 Mode-I SEM fractography of carbon fibre/TGDDM laminates with aramid interleaf and "10 wt%" phenoxy showing: (a) deformation of aramid fibres; (b) carbon fibre fracture; and (c) carbon fibre debonding.

5.3 Conclusion

A combination of two interlaminar toughening techniques was investigated for two epoxy resin systems. One technique was the use of dissolvable phenoxy fibres in the interlaminar region which in the previous chapter had shown to improve the toughness of carbon fibres/epoxy laminates. The second technique was the use of an aramid non-woven veil as an interleaf layer at mid-plane.

The effects of interleaving plus phenoxy-modification were different for the two resins, with the effects on the TGDDM resin being in general more favourable. For both resins however, changes in properties were generally more profound for the 5 wt% phenoxy modified interleave laminates, which is in contrast to non-interleaved laminates for which the 10 wt% phenoxy laminates showed a stronger response. In terms of fracture toughness and CAI properties, a combination of an aramid interleave on phenoxy modification did not show significant positive effects for DGEBA laminates, while for the TGDDM laminates, some improvements were observed. This showed that it is possible to improve toughness and damage properties by combining the two techniques, depending on the resin systems used.

The toughening mechanism for aramid interleaved DGEBA laminates was dominated by aramid fibres, with little involvement from carbon fibres, with and without phenoxy. Fibre pull-out, debonding, fibrillation and fracture of aramid fibres were the main failure features in these materials. For aramid interleaved TGDDM laminates with phenoxy, in addition to toughening by aramid fibres, carbon fibre/matrix debonding and carbon fibre fracture also played a major part in the overall toughness.

CHAPTER 6

EFFECTS OF ENVIRONMENTAL CONDITIONING ON CARBON FIBRE/EPOXY COMPOSITES MODIFIED WITH DISSOLVABLE PHENOXY FIBRES

In Chapter 4, carbon fibre/epoxy composites were modified using dissolvable phenoxy fibres in order to achieve thermoplastic toughening of epoxy matrix. The addition of phenoxy has been found to improve toughness of carbon fibre/epoxy composites. While phenoxy modified systems showed improvement in fracture toughness, it is important to investigate whether stability and durability of these composites are compromised when subjected to solvent attack and hot-wet conditions. In this chapter, we will therefore look into the effect on environmental properties of such systems.

A polymer composite structure could be subjected to moisture, heat, chemical attack and radiation during its operation. This can cause changes in the microstructure and/or chemical structure of the materials, which in turn can alter properties such as tensile properties and toughness. Typical consequences include matrix swelling, fibre-matrix debonding, microcracking and chain scission of polymer molecules [221].

Environmental testing involves an assessment of a material's properties and microstructure before and after exposure to some aggressive environment. The chosen test procedure will depend on the motive for having the tests. The aim may be to simply compare the merits of two competing candidate materials, or to subject a single material to pass/fail criteria. More complicated procedures can also be designed for the research and development of materials. There are a number of important national and international tests related to the environmental performance of composites materials [222]. There are also tests for individual constituents of fibrous composites, such as matrix resins [223, 224] and fibre reinforcements [225].

In this chapter, as with the previous chapters, two different epoxy resins were studied. Two simple environmental conditions were chosen to compare the durability and stability of the composite systems. One was a hot-wet treatment, in which specimens were placed in a hot water bath. This is to evaluate the performance of the composites in hydrothermal conditions. The second test involved solvent resistance, in which specimens were exposed to an organic solvent. It should be noted that rather than investigating fundamental parameters of environmental conditioning, the tests carried out in this work were mainly for comparison purposes and aimed to give a general idea about the stability and durability of the phenoxy modified epoxy systems.

6.1 Experimental

The epoxy resins, curing agents, phenoxy fibres and carbon fibre fabric used were as described in Section 4.1.1. Composite laminates were manufactured as described in Section 4.1.2.

6.1.1 Environmental conditioning

Prior to conditioning, the specimens were first cut to size with a water cooled diamond/silicon carbide saw. Dimensions of the various types of specimens are summarised in Table 6.1. The thickness of the specimens is 2.2mm ± 0.4

6.1.1.1 Hot-wet

A water bath was filled with distilled water and heated to 90°C. Specimens were weighed before being placed in the water bath. The specimens were submerged in the bath at 90°C for 72 hr. After 72 hr, the specimens were taken out of the bath, tissue-dried and weighed. The weight of specimens was recorded before and after hot-wet treatment and the weight change calculated.

6.1.1.2 Solvent resistance

Specimens were weighed before being placed in a glass dish. Methyl ethyl ketone (MEK) was then poured into the dish, making sure the specimens were completely immersed in the solvent. The dish was then covered and kept in a fume cupboard for 24 hr at room temperature. The specimens were taken out of the solvent after 24 hr, tissue-dried and put in a vacuum oven for 24 hr to extract the solvent. Pressure of the vacuum oven was kept at 1 bar and at a temperature of 40°C. The specimens were weighed once removed from the oven and weight change was calculated.

Table 6.1 Dimensions of specimens subject to environmental conditioning.

Type	Dimensions	
	Length (mm)	Width (mm)
Tensile	200	20
DCB	130	20
SBS	25	4.4
DMA	60	10

6.1.2 Characterisations

Tensile tests, Mode-I delamination toughness test, short beam shear stress (SBS) test, dynamic mechanical analysis (DMA) and fractography were carried out on the conditioned samples as described in Section 4.1.3.

6.2 Results and Discussion

6.2.1 Effect of hot-wet treatment

Moisture diffuses into all organic matrix composites to varying extents and at various rates, leading to changes in their mechanical and physical properties [221]. It is more common for the matrix to have a greater sensitivity to moisture than the fibre, especially in the case of carbon fibres. Therefore matrix dominated properties will be most affected. For epoxy resins, the differing degree of water absorption arises from variation in the molecular structure of the network of the cured epoxy resin. Thus the nature of the base epoxy resin and the curing agent employed plays an important role [226]. It is found that the TGDDM systems in this study absorbed less moisture than the DGEBA systems (Table 6.2). Resin blends containing modifiers are sometimes employed to reduce the sensitivity of the matrix to moisture, and both thermosetting and thermoplastic modifiers are used [227]. In this study, the addition of phenoxy did not seem to have a large effect on the overall amount of water absorption in both resins (Table 6.2). However, effect of the hydrothermal treatment was visible for some DGEBA specimens (Figure 6.4a), as whitening was observed for phenoxy modified specimens. This could be due to plasticization and swelling of the phenoxy phase. No such effects were observed for TGDDM specimens (Figure 6.6b), because less water was absorbed by the specimens.

It is generally suggested that water absorption plasticizes epoxy resins and results in a reduction in modulus and T_g of the matrix [226]. As tensile properties of fibre composites are largely fibre dominated, the tensile properties of composite specimens were not expected to be significantly altered. This is generally found to be the case for DGEBA specimens, regardless of whether the specimens were phenoxy

modified or not (Figure 6.2). In TGDDM specimens, tensile strength increased with hot-wet conditioning in the unmodified sample, while the addition of phenoxy lowers the hydrothermal stability of the composites in terms of strain to failure (Figure 6.2).

Mode-I interlaminar toughness was not adversely affected by the hot-wet treatment for specimens without phenoxy for both resins (Figure 6.10 and Figure 6.12). In fact, interlaminar toughness of unmodified DGEBA laminated increased significantly, possibly due to matrix plasticisation. All of the DGEBA hot-wet treated specimens had similar toughness regardless of phenoxy concentrations and G_{1c} reduced after treatment for the 10 wt% phenoxy specimens. For TGDDM specimens, G_{1c} reduced after the hot-wet treatment for all the specimens. While phenoxy modification improved interlaminar toughness for both resins before hot-wet treatment, the toughness improvement was not sustained after treatment.

Water absorption can alter interfacial properties and reduce fibre/matrix adhesion, which could be reflected in reduced short beam shear strength [228]. However, Figure 6.15 and Figure 6.16 did not show significant effects of the hot-wet treatment and doubts have been raised about the validity of the SBS test for ductile matrix composites. As mentioned earlier, water absorption induces matrix swelling, which could lead to inelastic deformation during the short beam test, making the assumption of elastic deformation invalid. The reduced fibre/matrix adhesion can sometimes be reflected in the clean fibre surfaces in a fractured specimen [229]. Figure 6.17 and Figure 6.21 show fracture surfaces of treated DGEBA and TGDDM specimens without phenoxy. The fracture surfaces were found to be clean and smooth compared to untreated specimens (Figure 4.26a and Figure 4.27a), indicating reduced interfacial bonding. Similar features can also be observed for the phenoxy modified specimens (Figure 6.19 and Figure 6.23) clean and smooth fibre/matrix interface was observed, indicating that fibre/matrix debonding was the major failure mechanism for all the hot-wet treated specimens.

The most important environmental effect of a resin exposed to moisture is the reduction in T_g. Moisture plasticizes epoxy resins and lowers T_g and reduces their

maximum service temperature significantly [228]. Table 6.3 shows the T_g of the systems as determined by DMA. T_{g1} is associated with the phenoxy-rich phase and T_{g2} with the epoxy phase. T_g was reduced in most cases after hot-wet conditioning apart from the 5 wt% phenoxy specimens. As such, the addition of phenoxy did not seem to affect the hydrothermal degradation of the specimens in terms of T_g.

6.2.2 Effect of solvent treatment

The durability of a fibre reinforced composite is largely dependent on the individual components. Carbon fibres are resistant to almost all chemical reactions, notably to alkalis, non-oxidizing acids, although some carbon fibres can be degraded by oxidation and intercalation. Therefore the chemical resistant of carbon fibre/epoxy composites is largely matrix and interphase dominated. As with moisture absorption, solvent diffuses into the matrix and swelling occurs. The chemical resistance of epoxy resins is determined by the chemical structure of the solvent and the cured epoxy. It is generally agreed that a high crosslink density results in better chemical resistance. In this study it was difficult to determine the absorption of solvent in the different composite systems (Table 6.2). The reason for this being that besides swelling (weight gain), leaching (weight lost) also occurs in the case of solvent exposure. However, it was obvious from visual inspection that the DGEBA specimens were more adversely affected by solvent attack, with the specimens going 'soft' after being immersed in solvent prior to drying. The phenoxy modified specimens were more susceptible to solvent attack. For the DGEBA specimens, whitening and severe blistering was observed (Figure 6.6(b)) and surfaces of the specimens became rough after drying. For the phenoxy modified TGDDM specimens (Figure 6.8(b)), swelling and blistering occurred to a lesser extent and no whitening was observed. One thing to note is that the tensile modulus (Figure 6.2) of the solvent treated unmodified specimens was unexpectedly low.

Mode-I interlaminar toughness of specimens without phenoxy did not decrease after exposure to solvent treatment and actually increased for the DGEBA specimens (Figure 6.10 and Figure 6.12). This could be due to the fact that the solvent created defects in the matrix, thus providing a tortuous path for crack growth, leading to increased energy absorption. However, as for hot-wet treatments, the improvement achieved by the phenoxy modification could not be maintained after solvent treatment.

The fibre/matrix interface is expected to alter significantly by exposure to solvent, however, no effects on SBS strength were reported (Figure 6.15 and Figure 6.16). As mentioned in the earlier section, the validity of the test was questioned due to non-linearity effects where testing requirements were no longer met.

The results of T_g (Table 6.3) showed that solvent exposure to MEK did not change the T_g significantly for all TGDDM specimens. No results could be obtained for DGEBA since the specimens were degraded by the solvent and no meaningful results could be obtained once the specimens were heated to the elevated temperatures required for T_g measurements.

The fracture surface of the solvent treated specimens was quite different to that of untreated or hot-wet treated specimens. For the specimens without phenoxy (Figure 6.18 and Figure 6.22), the fracture surfaces appeared to be more ductile and flat, as there were no sharp and clean features. Similar features were observed for phenoxy modified specimens, whereas modified specimens showed rougher surfaces (Figure 6.20 and Figure 6.24).

Table 6.2 Weight change of specimens after environmental conditioning. Five specimens were tested for each type of sample.

Type	Resin	wt% phenoxy	Weight change (%)	
			Hot-wet	Solvent
Tensile	DGEBA	0	2.20 (0.02)	-3.17 (0.37)
Tensile	DGEBA	5	2.08 (0.04)	0.51 (0.17)
Tensile	DGEBA	10	2.12 (0.05)	-0.85 (0.30)
Tensile	TGDDM	0	0.43 (0.004)	-0.07 (0.002)
Tensile	TGDDM	5	0.41 (0.24)	0.22 (0.07)
Tensile	TGDDM	10	0.77 (0.01)	0.41 (0.09)

(a)

Type	Resin	wt% phenoxy	Weight change (%)	
			Hot-wet	Solvent
DCB	DGEBA	0	2.67 (0.09)	-2.31 (0.4)
DCB	DGEBA	5	2.46 (0.31)	1.59 (0.17)
DCB	DGEBA	10	3.34 (0.14)	-0.85(0.30)
DCB	TGDDM	0	0.60 (0.10)	0.19 (0.01)
DCB	TGDDM	5	0.67 (0.02)	0.1 (0.01)
DCB	TGDDM	10	0.60 (0.16)	0.28 (0.14)

(b)

Type	Resin	wt% phenoxy	Weight change (%)	
			Hot-wet	Solvent
SBS	DGEBA	0	1.99 (0.11)	-2.14 (1.78)
SBS	DGEBA	5	2.06 (1.08)	-0.02 (0.27)
SBS	DGEBA	10	2.22 (0.07)	0.44 (1.43)
SBS	TGDDM	0	0.34 (0.02)	-0.13 (0.006)
SBS	TGDDM	5	0.66 (0.01)	0.14 (0.02)
SBS	TGDDM	10	0.32 (0.10)	-0.33 (0.15)

(c)

Type	Resin	wt% phenoxy	Weight change (%)	
			Hot-wet	Solvent
DMA	DGEBA	0	2.22 (0.05)	2.72 (0.15)
DMA	DGEBA	5	2.03 (0.01)	0.64 (0.43)
DMA	DGEBA	10	2.21 (0.06)	0.86 (0.88)
DMA	TGDDM	0	0.38 (0.01)	-1.37 (1.80)
DMA	TGDDM	5	0.71 (0.001)	-2.44 (0.04)
DMA	TGDDM	10	0.45 (0.06)	-1.21 (1.66)

(d)

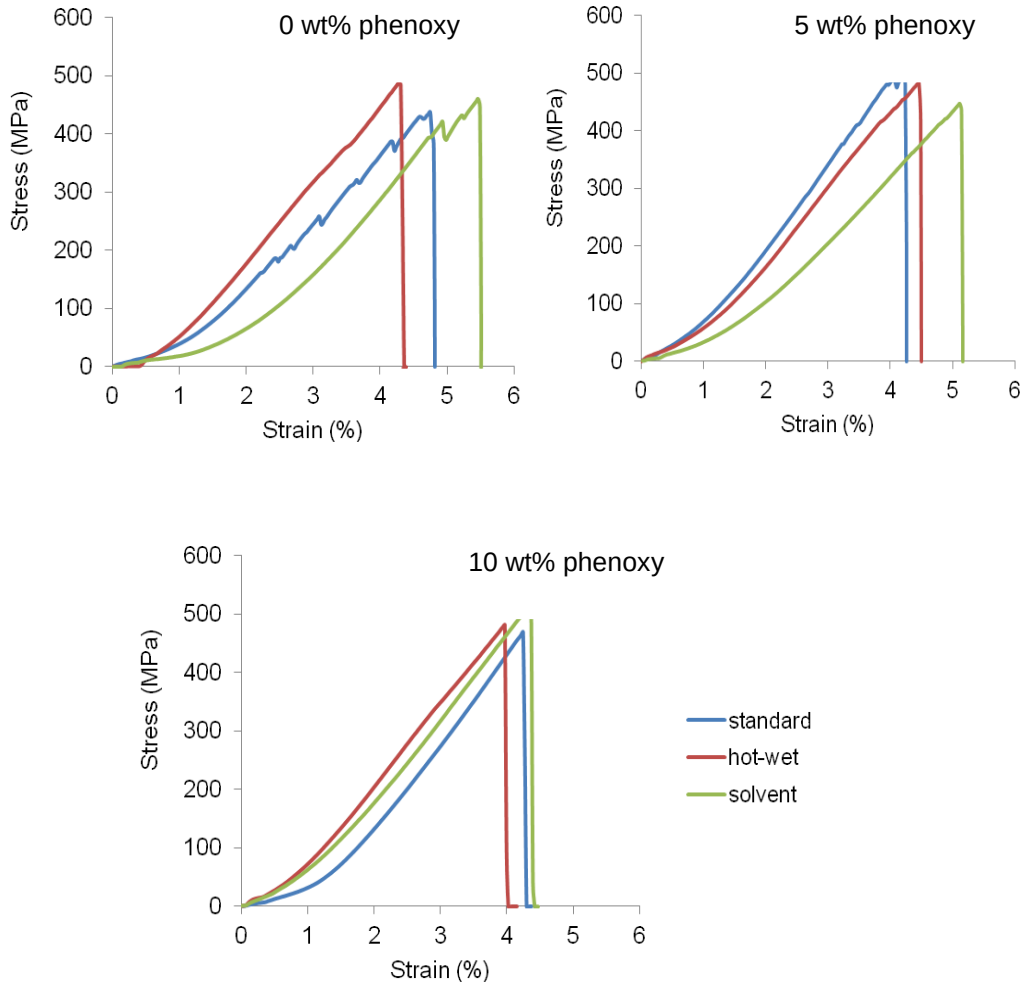

Figure 6. 1 Tensile stress-strain curves for carbon fibre/DGEBA laminates after environmental conditioning.

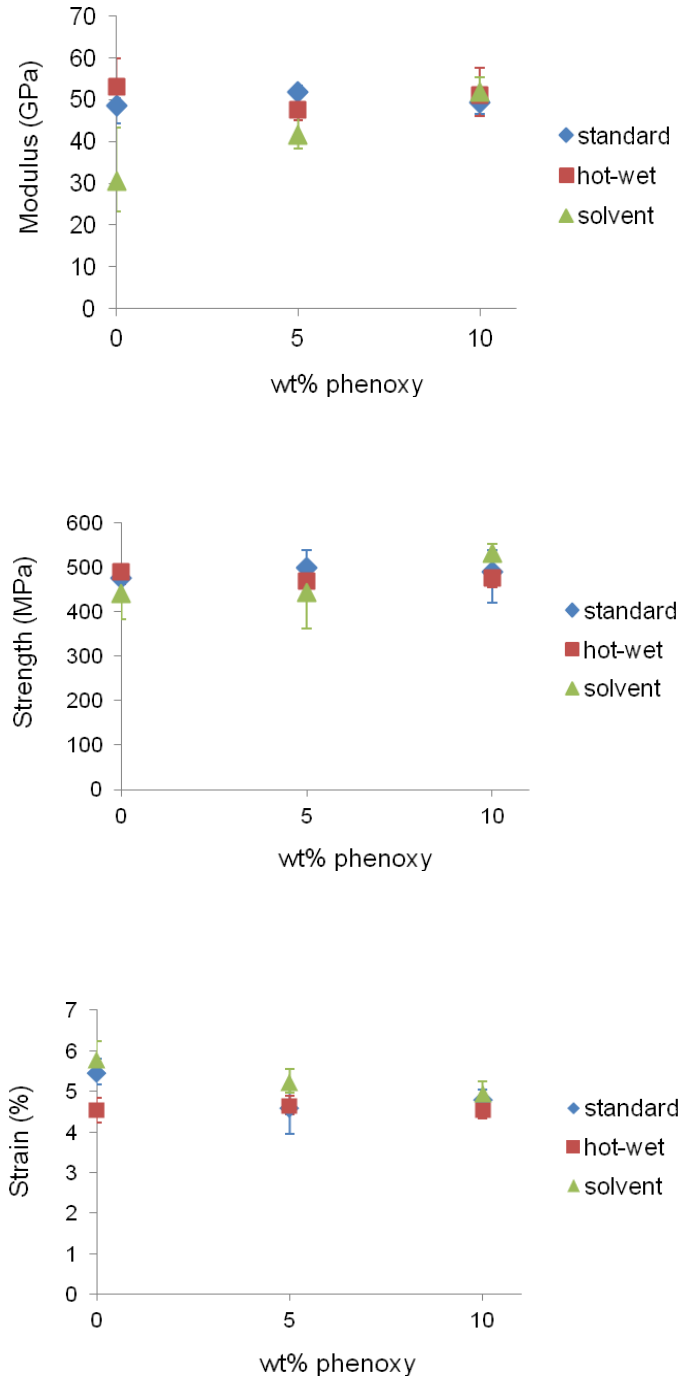

Figure 6.2 Tensile properties for carbon fibre/DGEBA laminates after environmental conditioning.

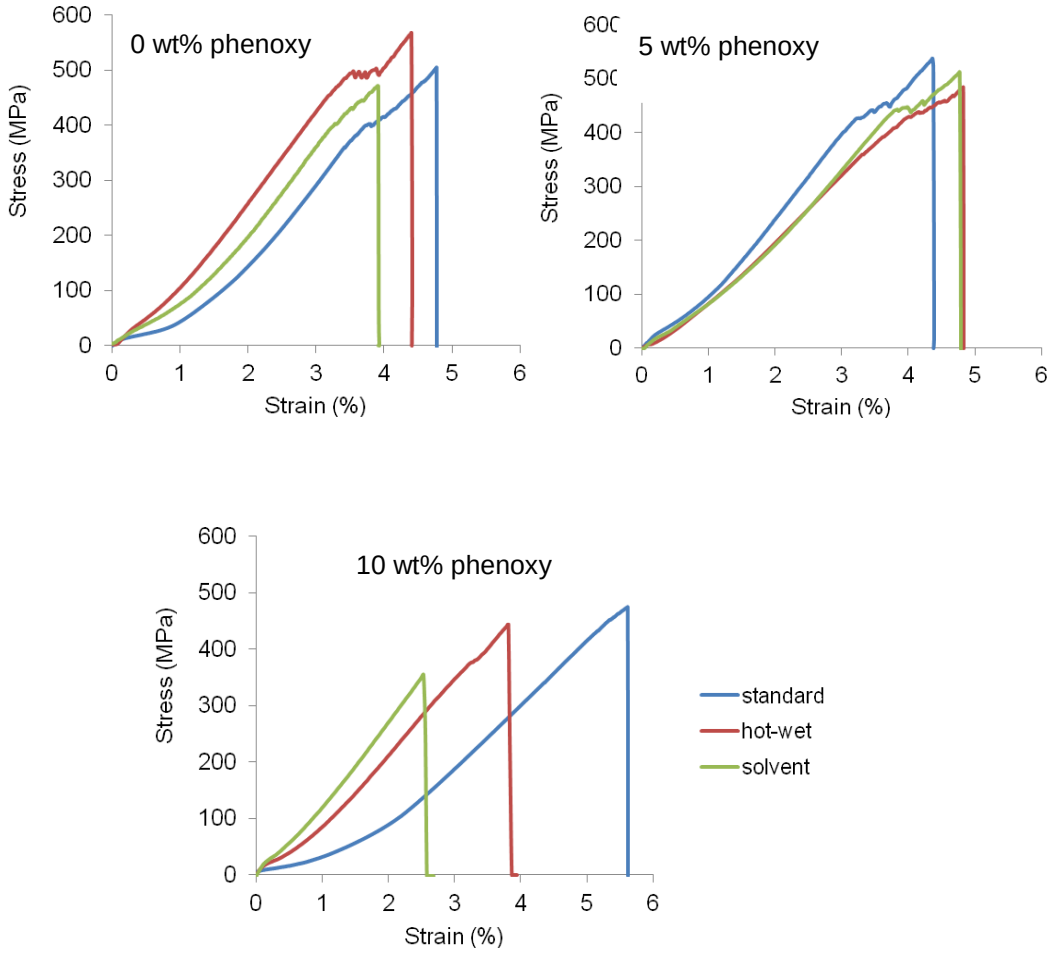

Figure 6. 3 Tensile stress-strain curves for carbon fibre/TGDDM laminates after environmental conditioning.

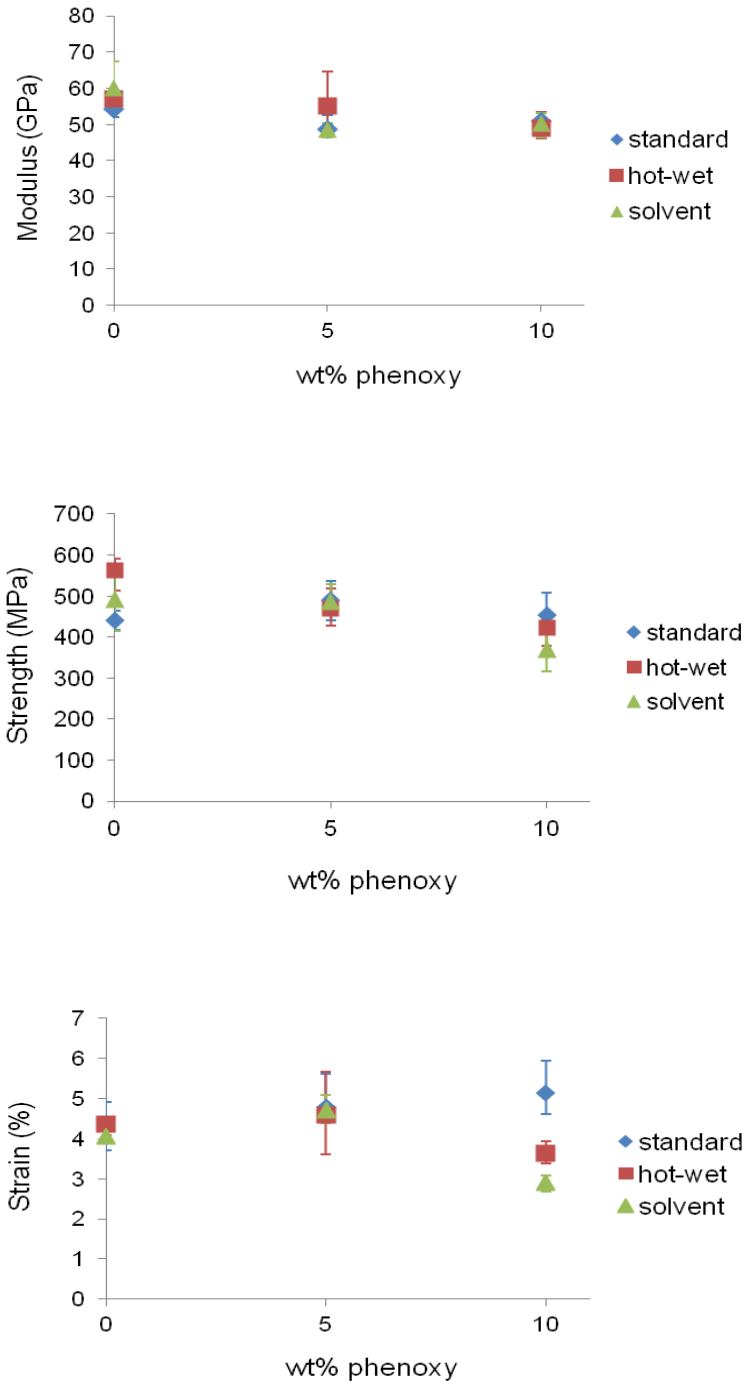

Figure 6.4 Tensile properties for carbon fibre/TGDDM laminates after environmental conditioning.

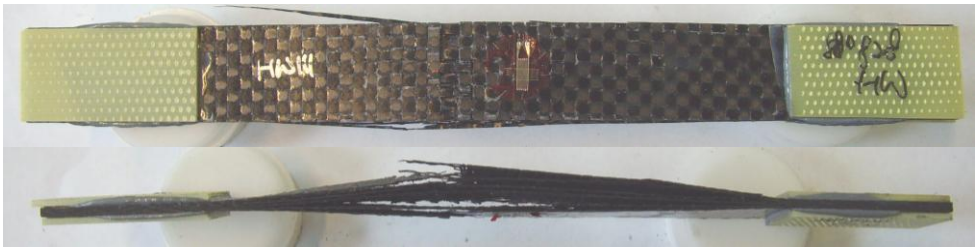

(a) Hot-wet

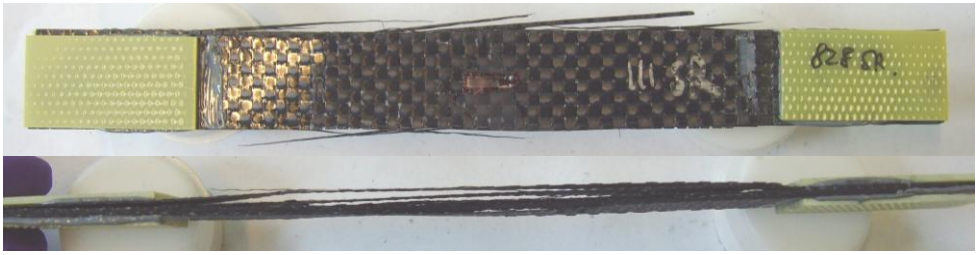

(b) Solvent resistant

Figure 6.5 Tested tensile specimens of carbon fibre/DGEBA laminates with 0 wt% phenoxy after environmental conditioning showing extensive delamination

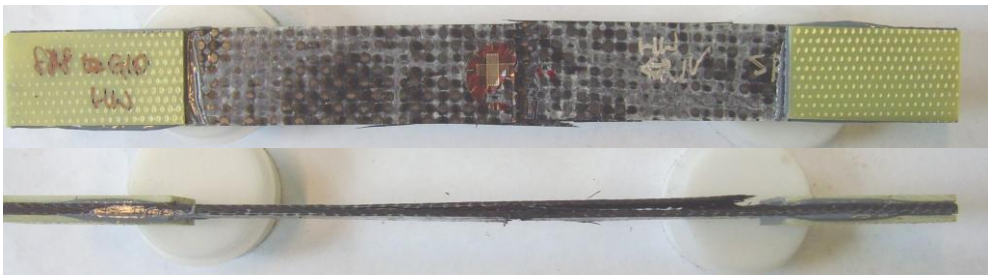

(a) Hot-wet

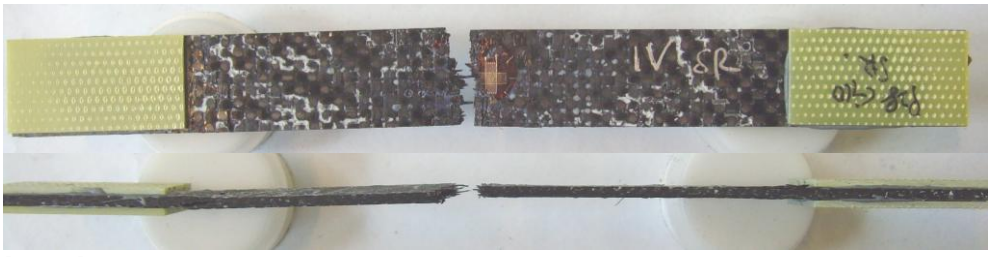

(b) Solvent resistant

Figure 6.6 Tested tensile specimens of carbon fibre/DGEBA laminates with 10 wt% phenoxy after environmental conditioning showing (a) matrix whitening treatment and (b) white blisters in matrix

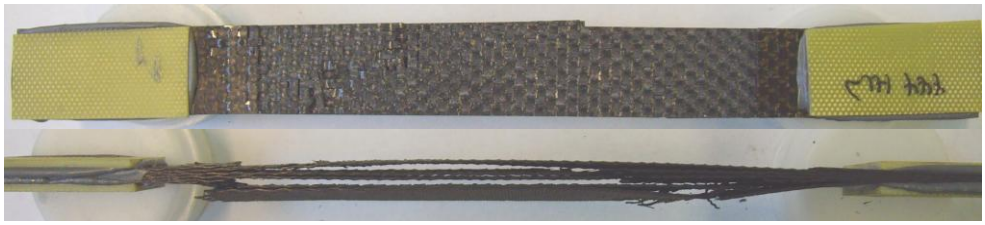

(a) Hot-wet

(b) Solvent resistant

Figure 6.7 Tested tensile specimens of carbon fibre/TGDDM laminates with 0 wt% phenoxy after environmental conditioning showing (a) extensive delamination and (b) delamination and through-thickness fracture.

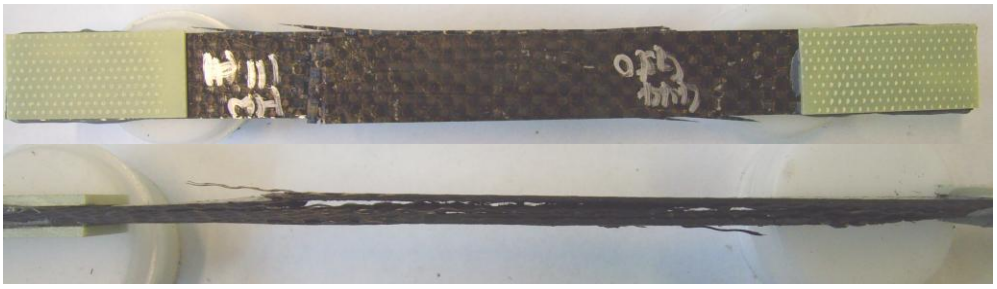

(a) Hot-wet

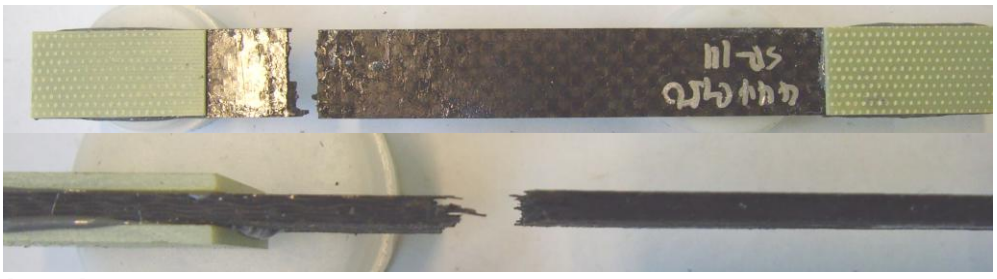

(b) Solvent resistant

Figure 6.8 Tested tensile specimens of carbon fibre/TGDDM laminates with 10 wt% phenoxy after environmental conditioning showing (a) extensive delamination and (b) through-thickness fracture.

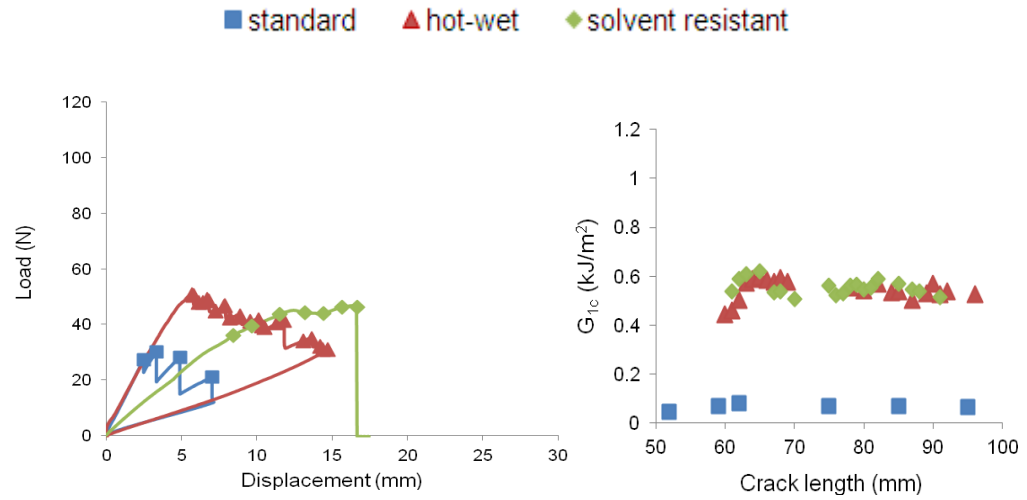

(a) 0 wt% phenoxy

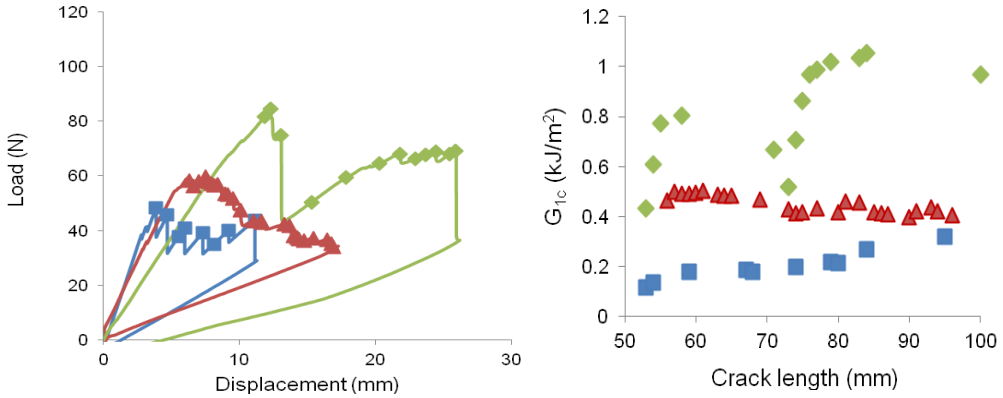

(b) 5 wt% phenoxy

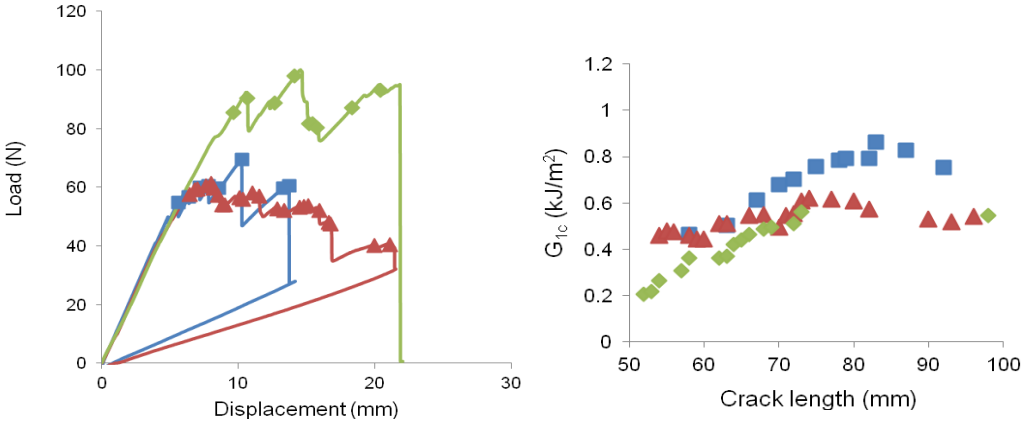

(c) 10 wt% phenoxy

Figure 6. 9 DCB Load-displacement curves and G_{1c} vs crack length for DGEBA composites after environmental conditioning.

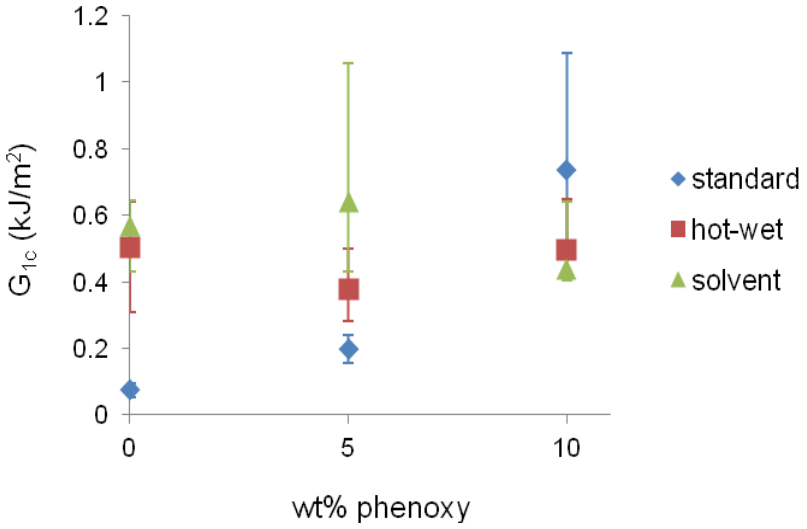

Figure 6. 10 Mode-I interlaminar toughness of carbon fibre/DGEBA laminates after environmental conditioning.

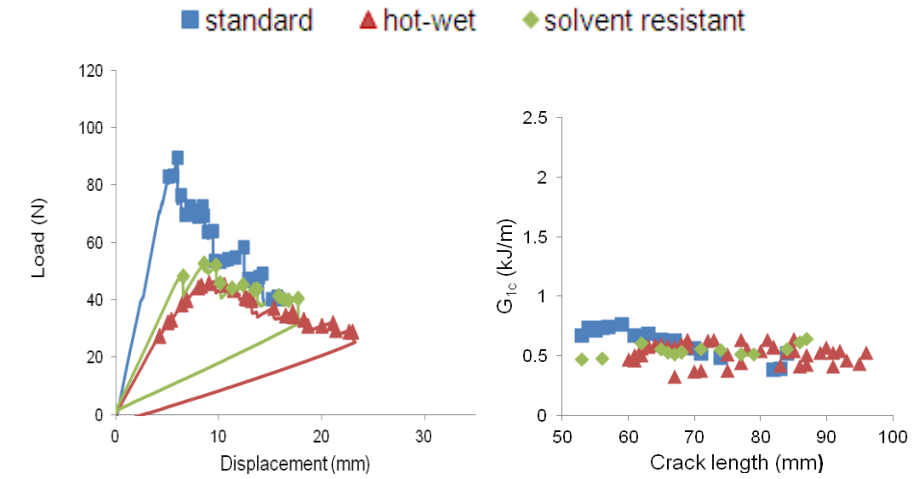

(a) 0 wt% phenoxy

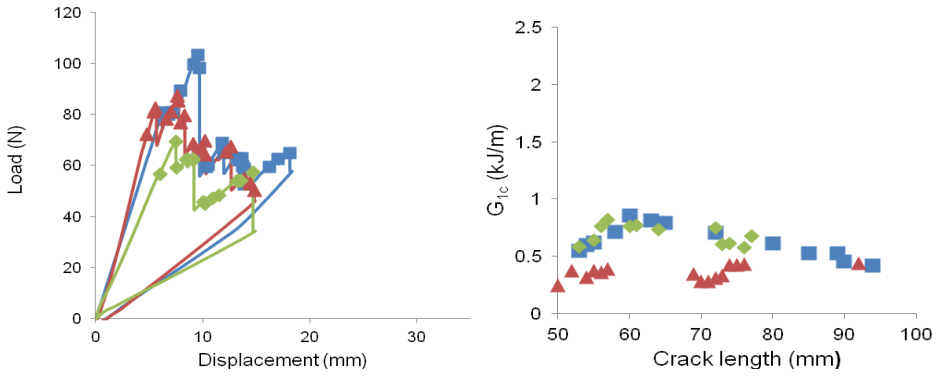

(b) 5 wt% phenoxy

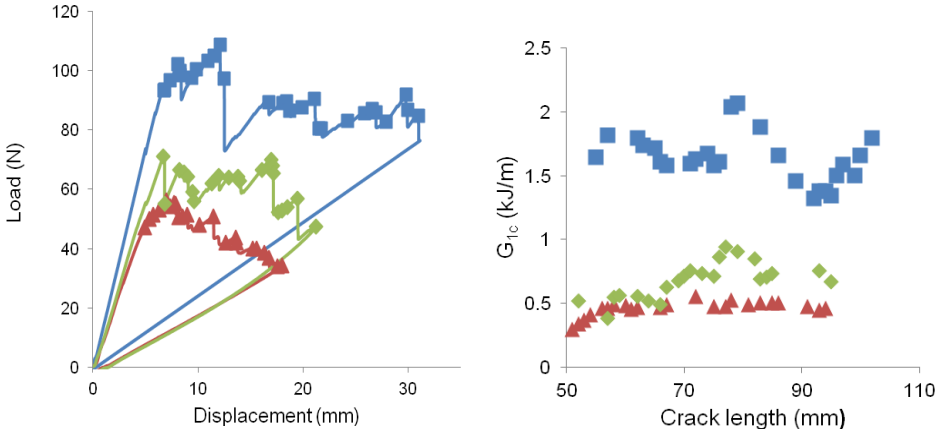

(c) 10 wt% phenoxy

Figure 6. 11 DCB Load-displacement curves and G_{1c} vs crack length for DGEBA composites after environmental conditioning.

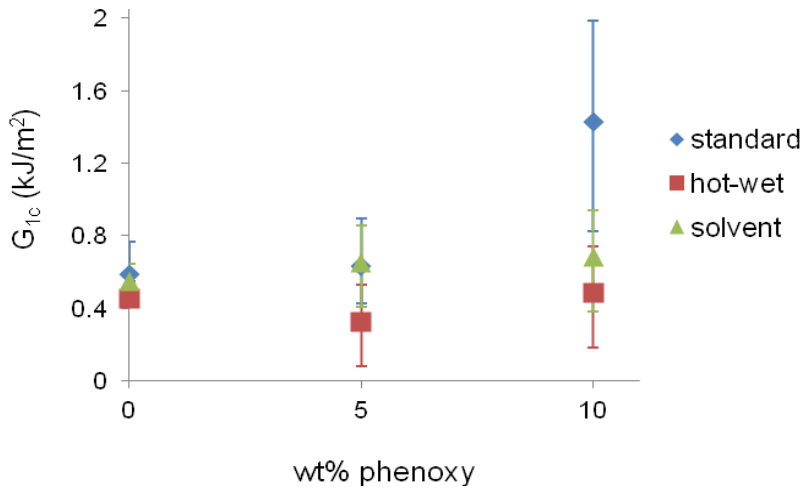

Figure 6.12 Mode-I interlaminar toughness of carbon fibre/TGDDM laminates after environmental conditioning.

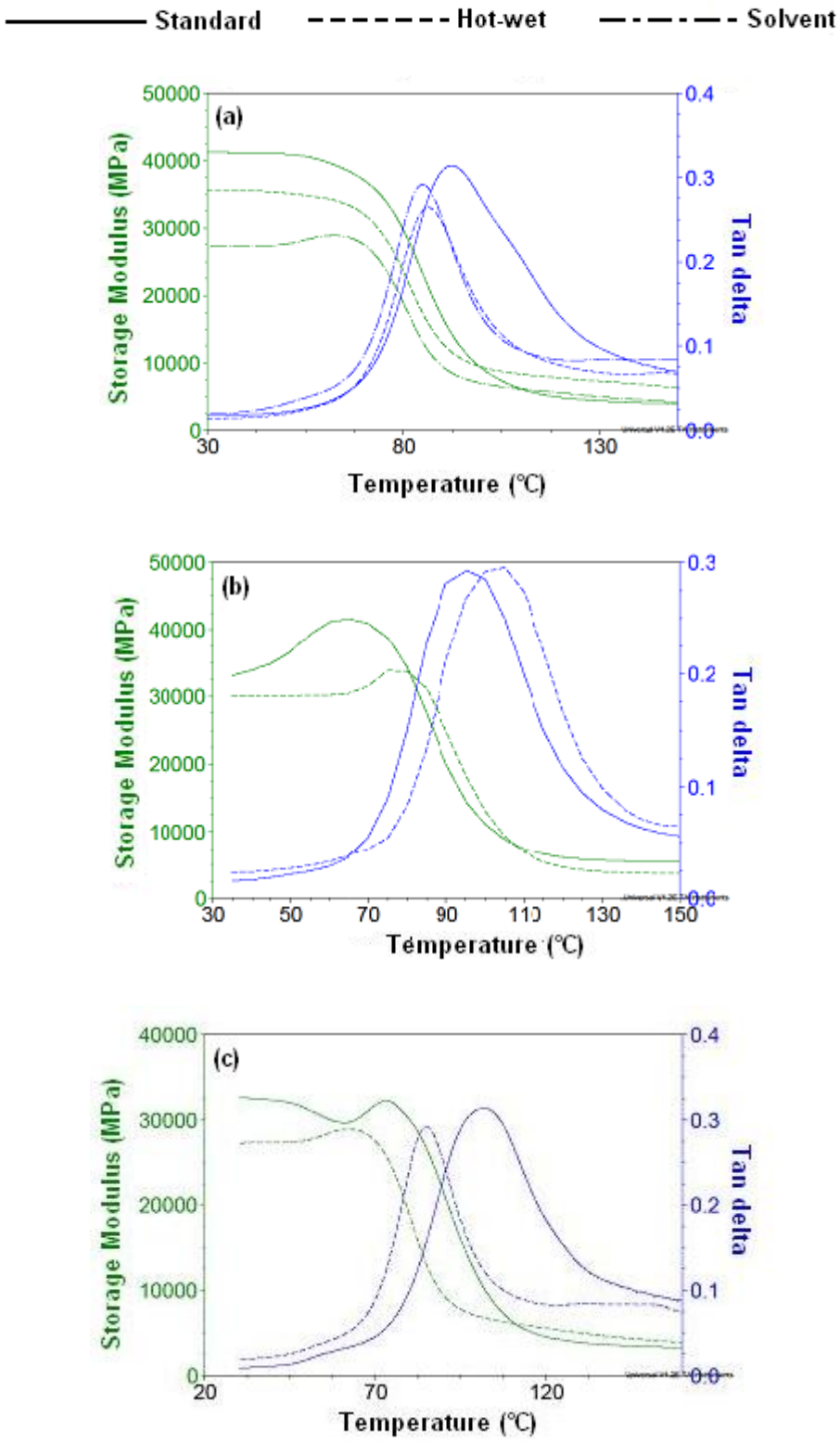

Figure 6.13 DMA results of DGEBA composite laminates after environmental conditioning: (a) 0 wt% phenoxy, (b) 5 wt% phenoxy and (c) 10 wt% phenoxy.

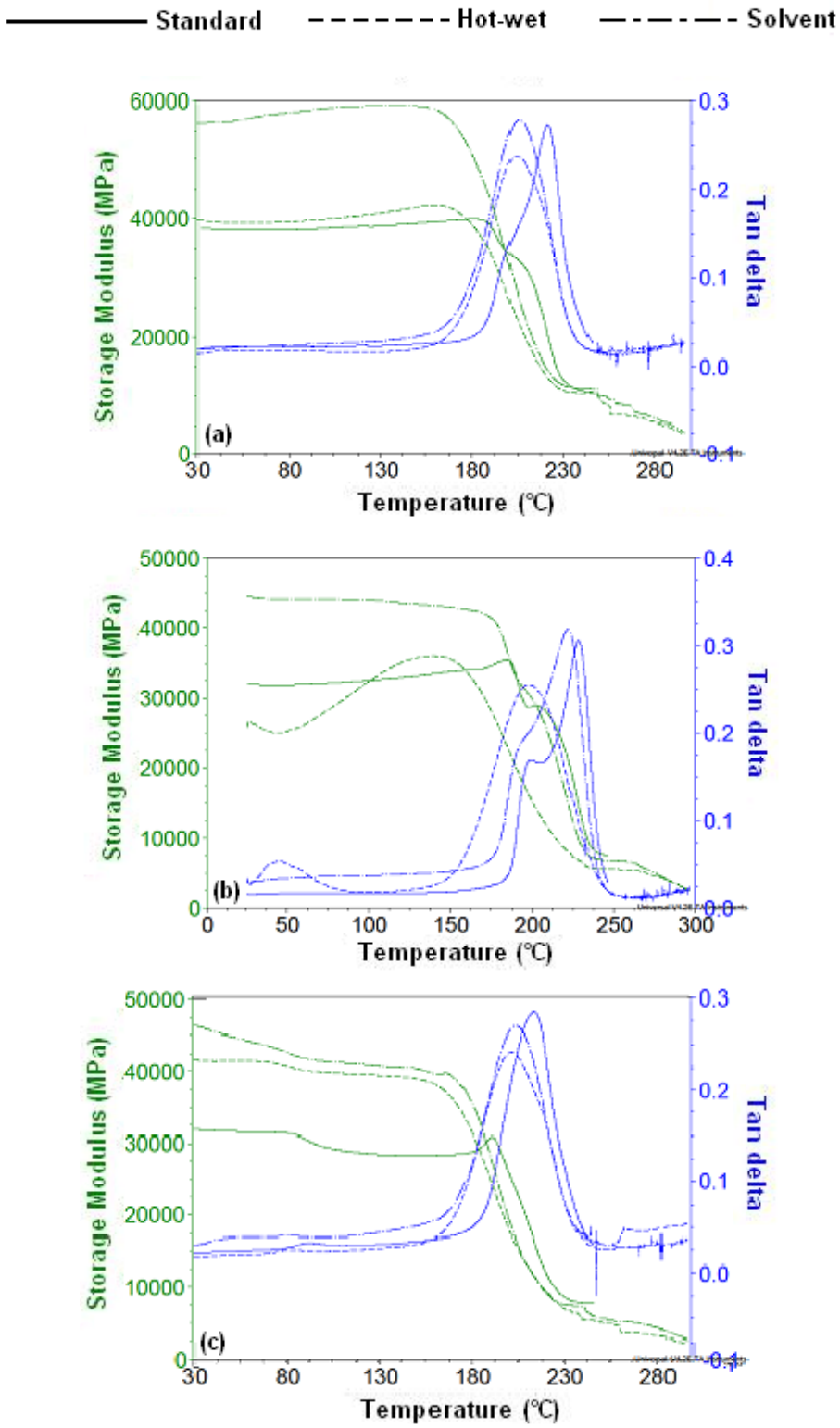

Figure 6.14 DMA results of TGDDM composite laminates after environmental conditioning: (a) 0 wt% phenoxy, (b) 5 wt% phenoxy and (c) 10 wt% phenoxy.

Table 6.3 T_g of composite laminates after environmental conditioning.

Composite laminate		Standard		Hot-wet		Solvent resistance
resin	wt% phenoxy	T_{g1}(°C)	T_{g2}(°C)	T_{g1}(°C)	T_{g2}(°C)	T_{g2}(°C)
DGEBA	0	---	92	---	86	---
DGEBA	5	---	95	---	103	---
DGEBA	10	58	101	---	85	---
TGDDM	0	---	221	---	204	206
TGDDM	5	---	199	45	198	196
TGDDM	10	93	214	83	202	204

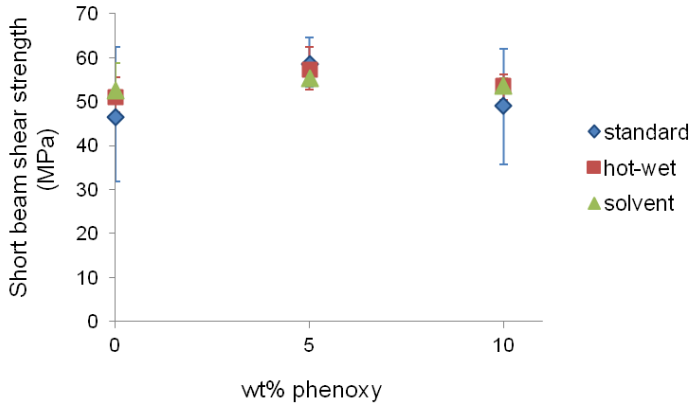

Figure 6.15 Short beam shear test results for carbon fibre/DGEBA laminates after environmental conditioning.

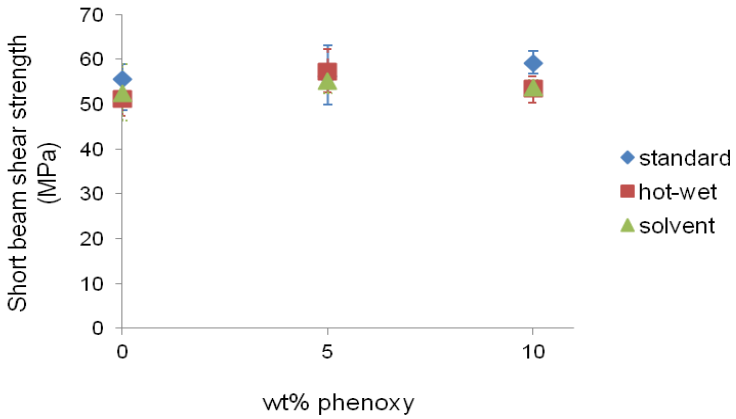

Figure 6.16 Short beam shear test results for carbon fibre/TGDDM laminates after environmental conditioning.

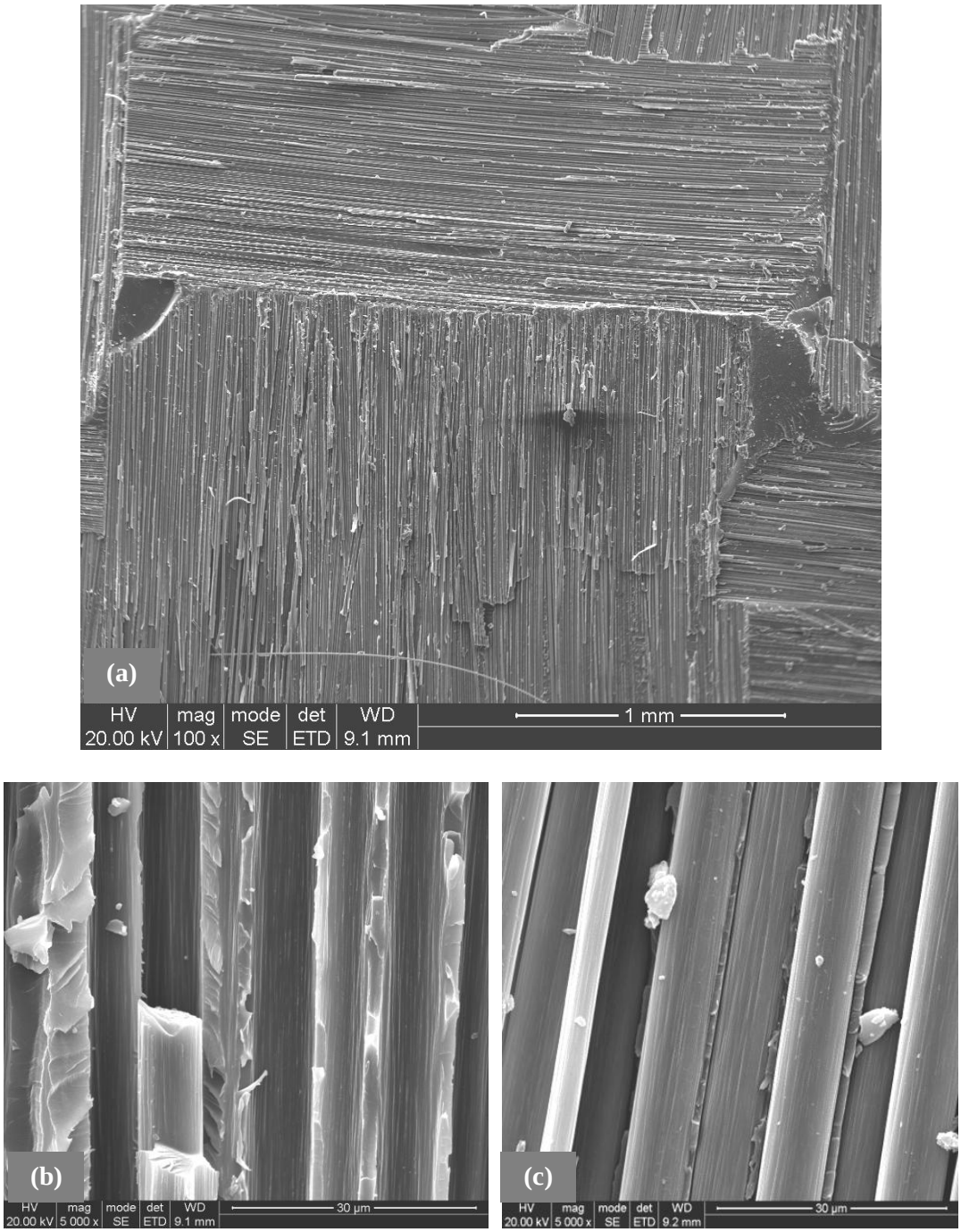

Figure 6.17 Mode-I SEM fractography of carbon fibre/DGEBA laminates with 0 wt% phenoxy after hot-wet conditioning showing clean fracture surfaces indicating fibre/matrix debonding.

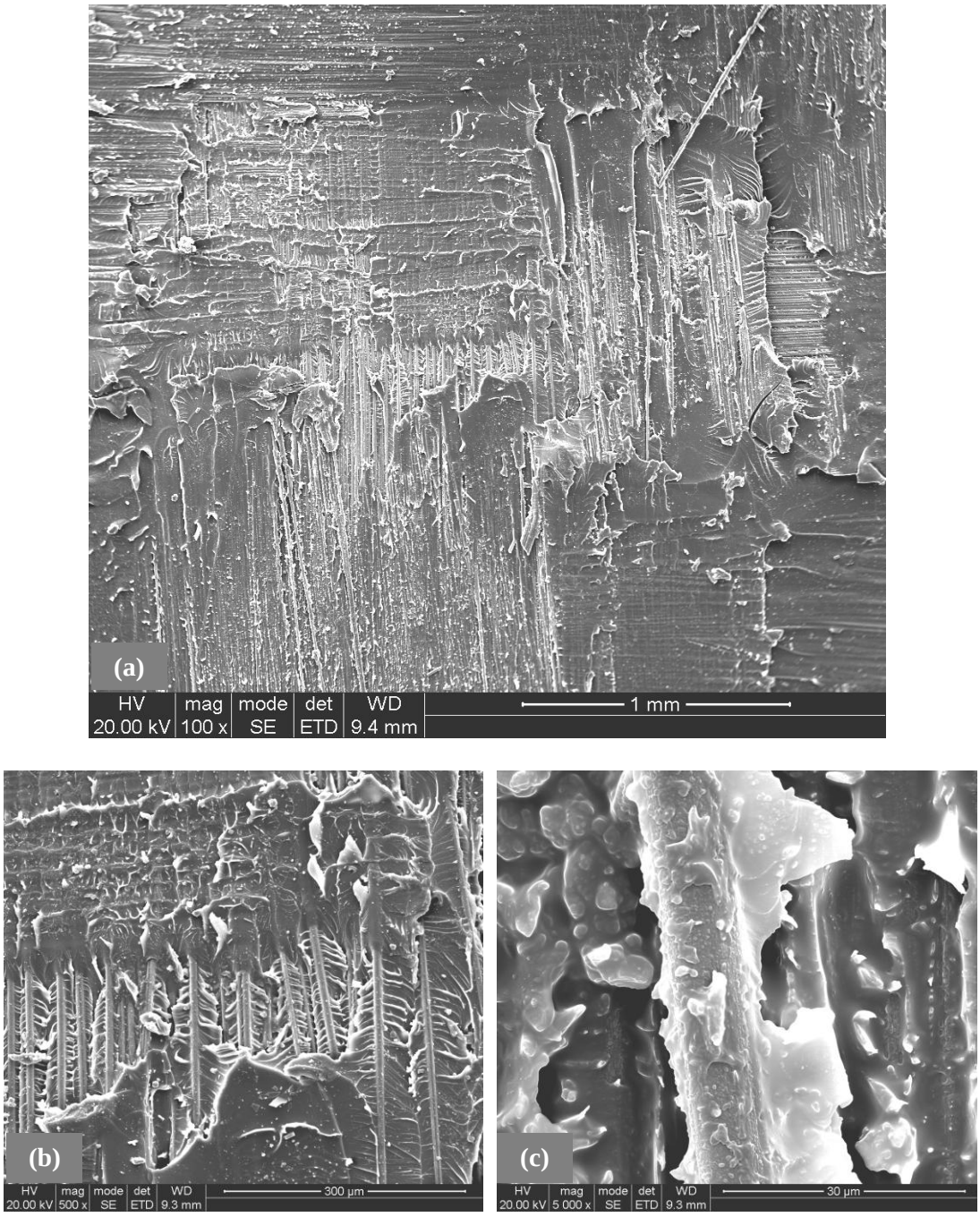

Figure 6.18 Mode-I SEM fractography of carbon fibre/DGEBA laminates with 0 wt% phenoxy after solvent conditioning showing (a) rough fracture surfaces, and (b) and (c) extensive matrix deformation.

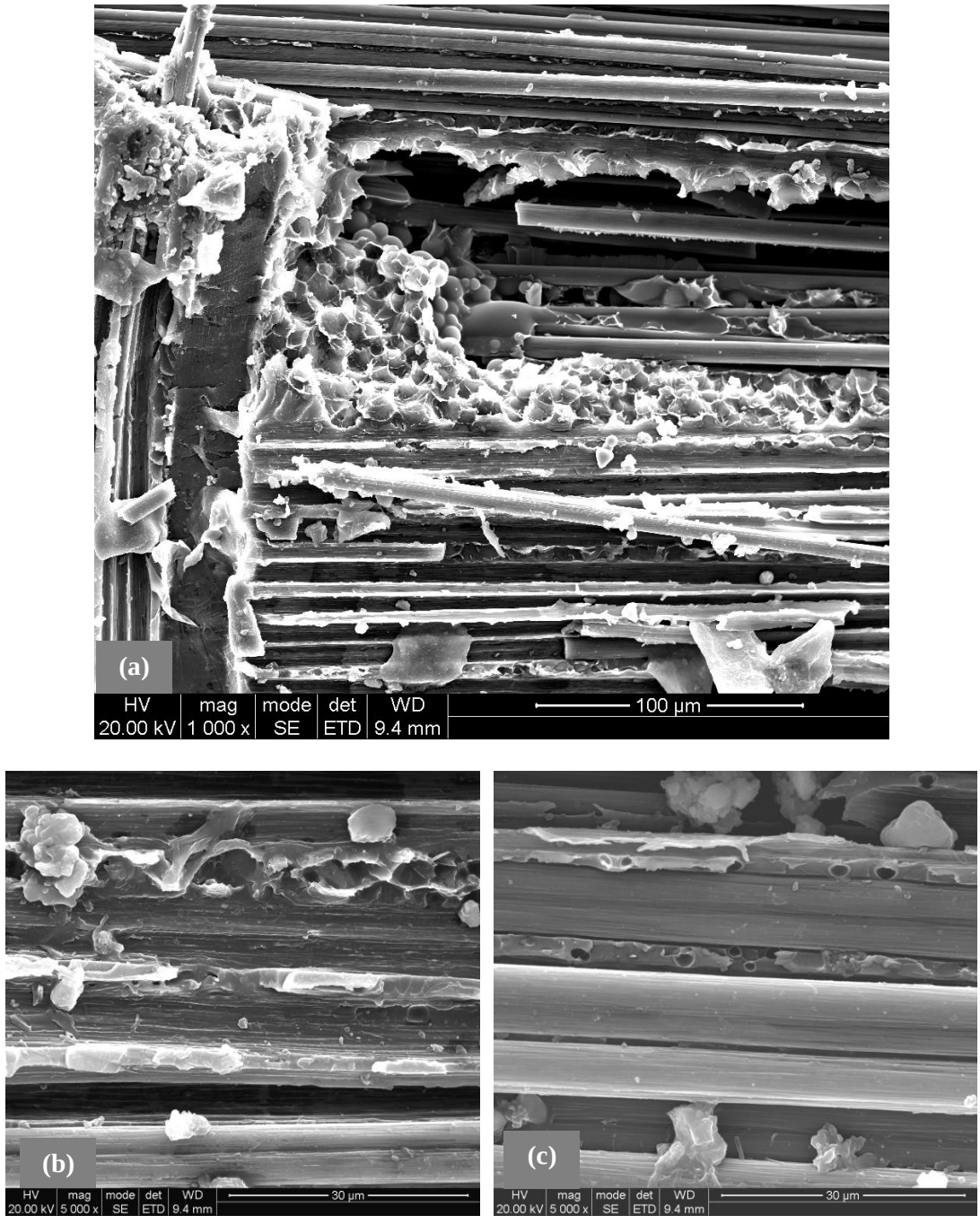

Figure 6.19 Mode-I SEM fractography of carbon fibre/DGEBA laminates with 10 wt% phenoxy after hot-wet conditioning showing (a) phase separation, and (b) and (c) fibre/matrix debonding.

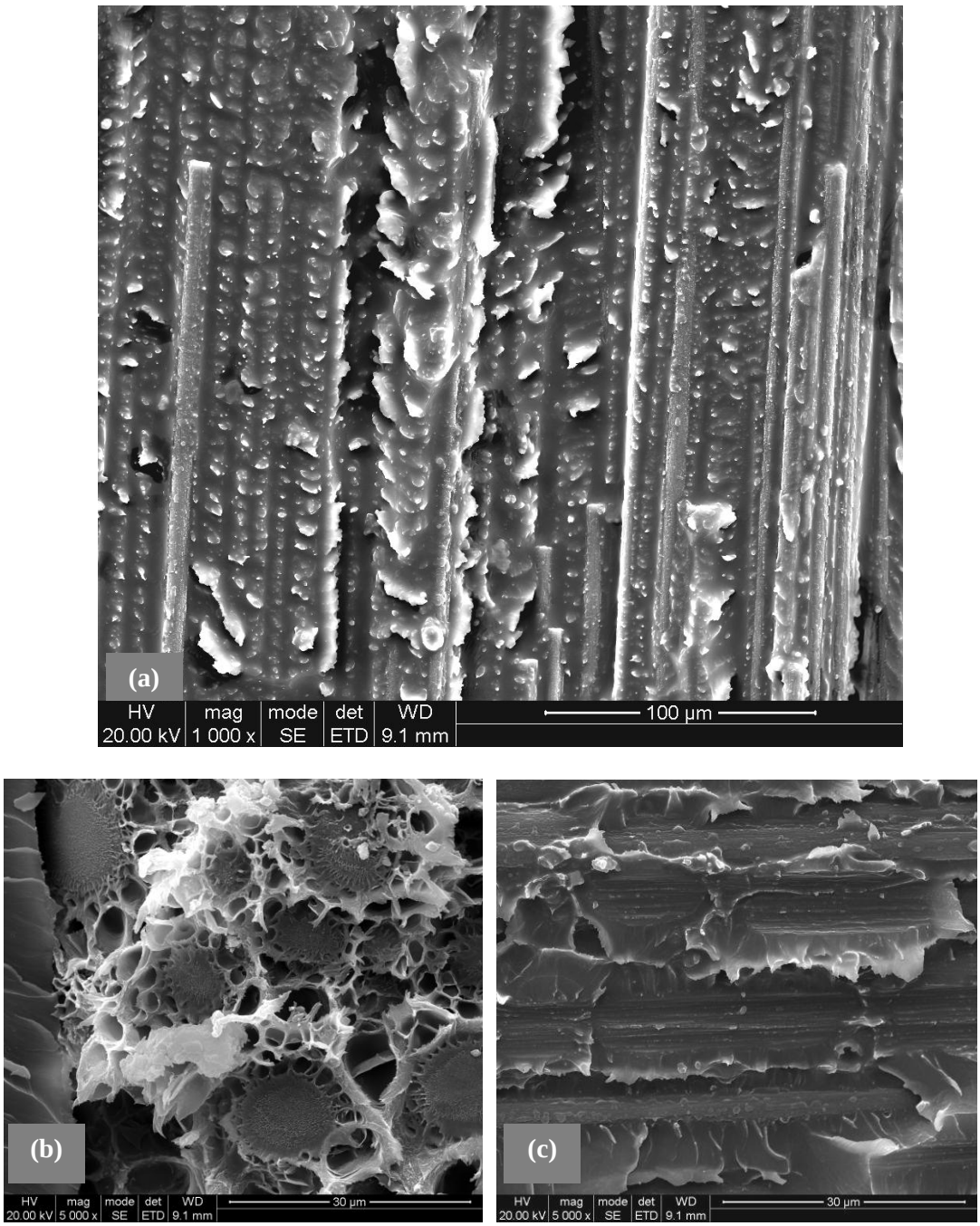

Figure 6.20 Mode-I SEM fractography of carbon fibre/DGEBA laminates with 10 wt% phenoxy after solvent conditioning showing (a) rough fracture surfaces, (b) phase separation and (c) extensive matrix deformation.

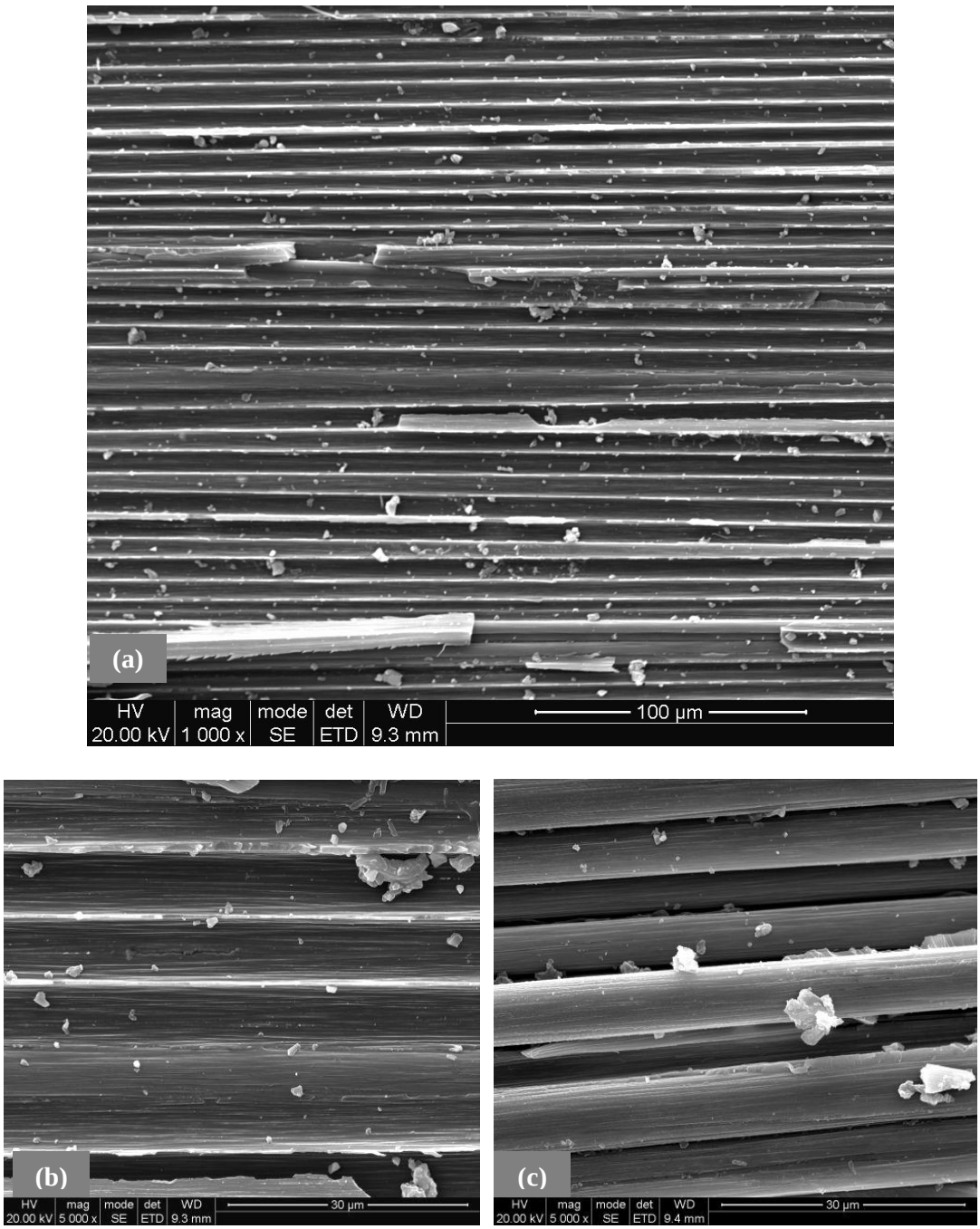

Figure 6.21 Mode-I SEM fractography of carbon fibre/TGDDM laminates with 0 wt% phenoxy after hot-wet conditioning showing clean fracture surface and fibre/matrix debonding.

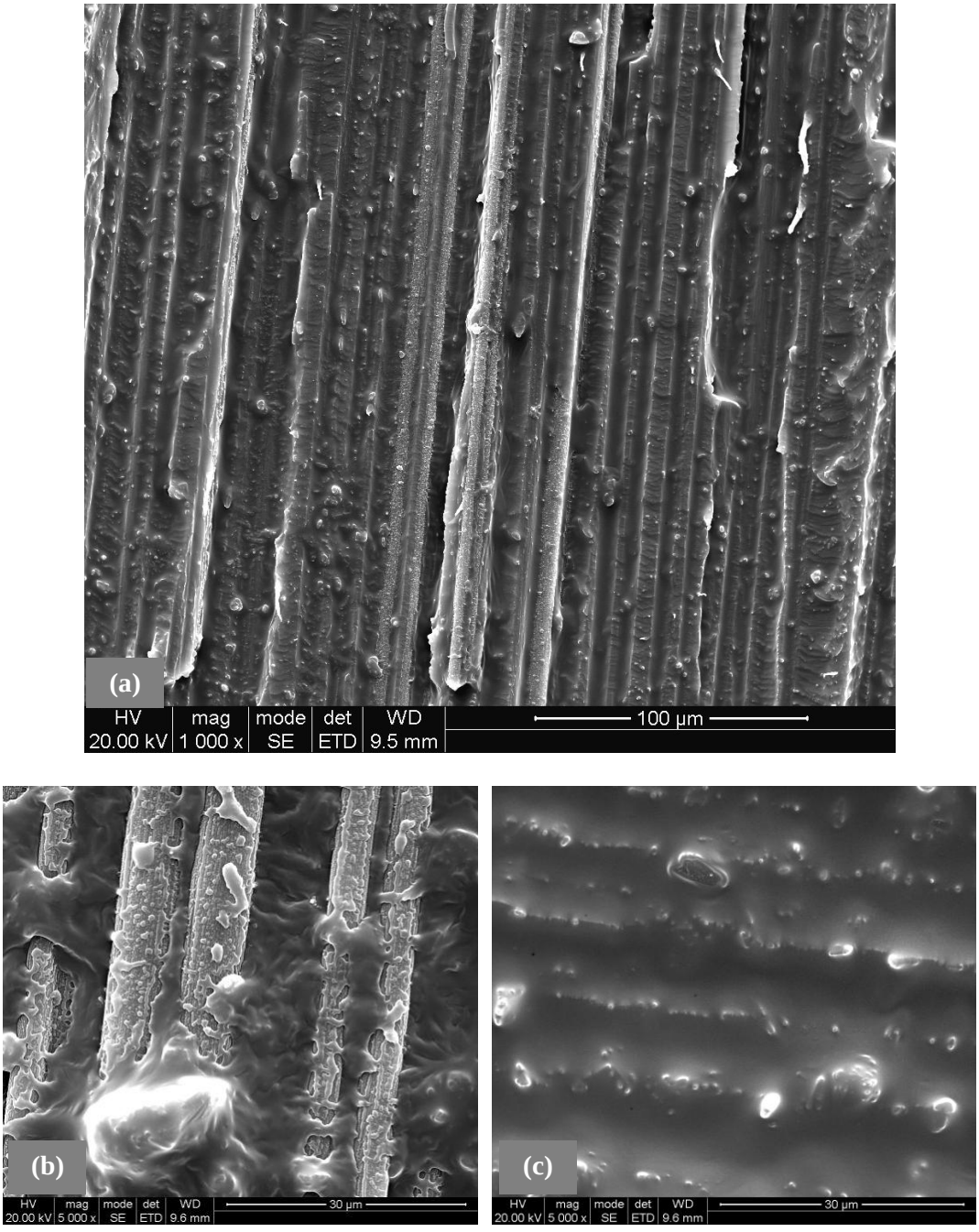

Figure 6.22 Mode-I SEM fractography of carbon fibre/TGDDM laminates with 0 wt% phenoxy after solvent conditioning showing rough fracture surfaces.

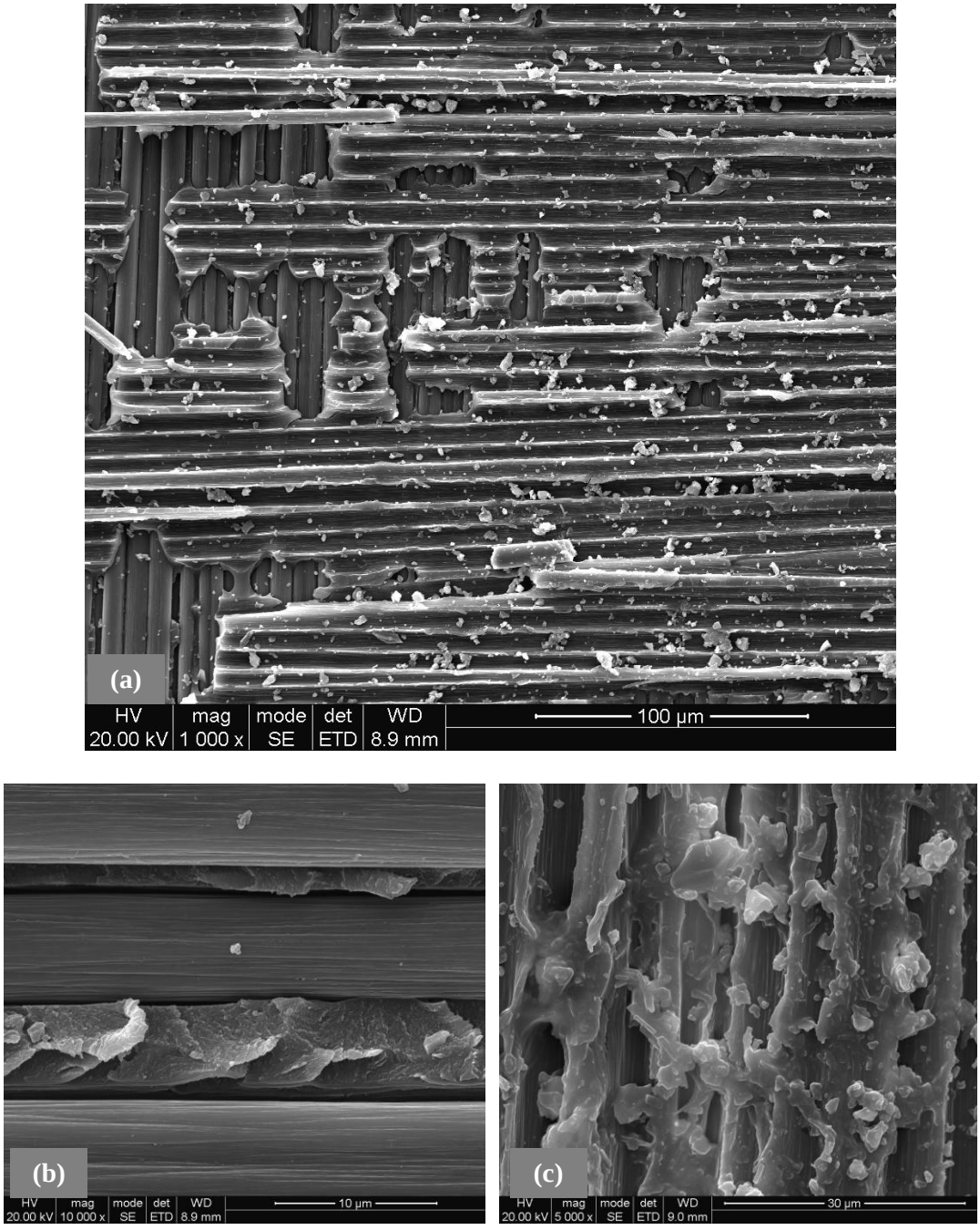

Figure 6.23 Mode-I SEM fractography of carbon fibre/TGDDM laminates with 10 wt% phenoxy after hot-wet conditioning, showing (a) and (b) fibre/matrix debonding, and (b) and (c) matrix deformation in some areas.

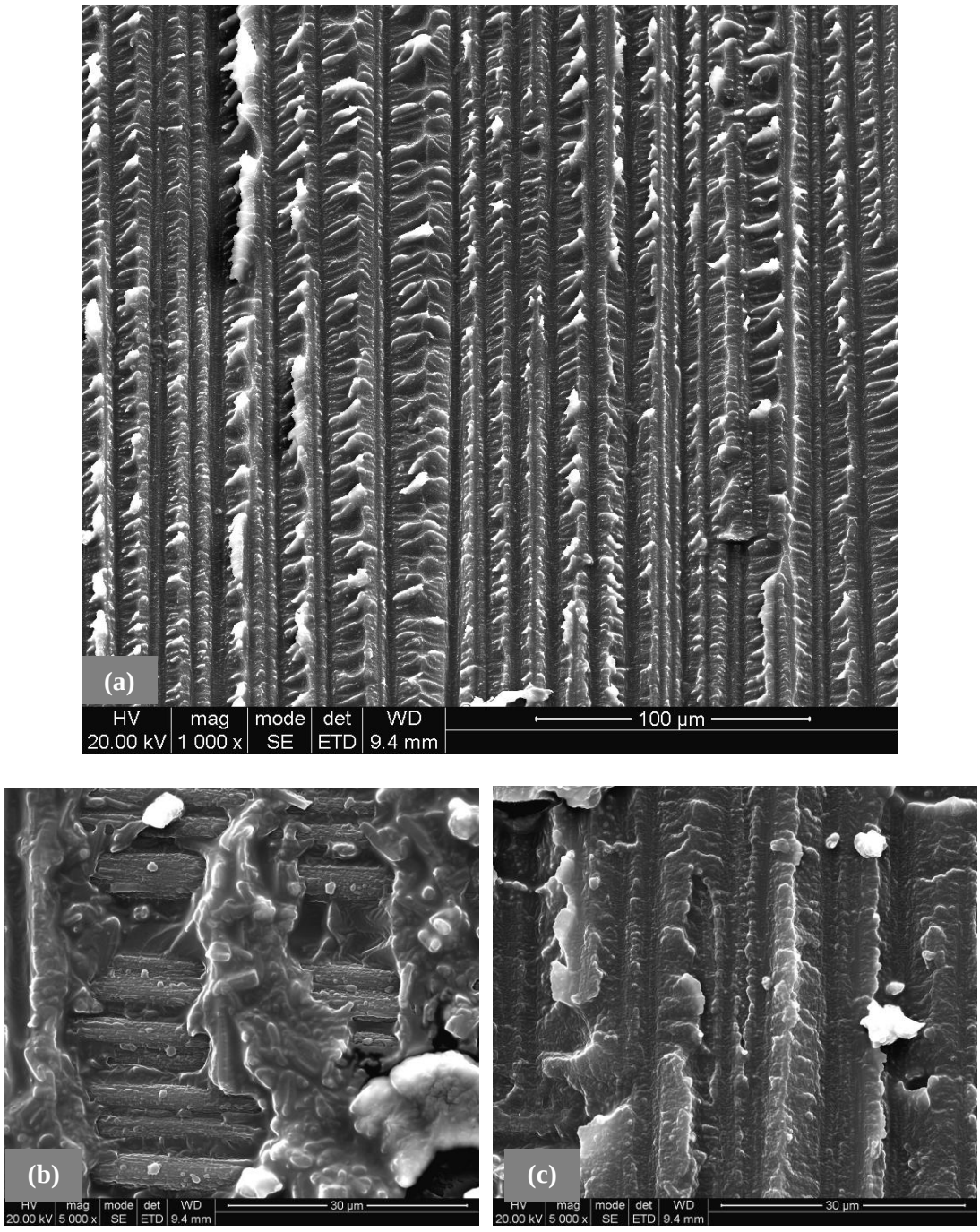

Figure 6.24 Mode-I SEM fractography of carbon fibre/TGDDM laminates with 10 wt% phenoxy after solvent conditioning showing extensive matrix deformation.

6.3 Conclusion

In this chapter the effects of hot-wet and organic solvent (MEK) treatments on phenoxy modified carbon fibre/epoxy composites were investigated. It was found that generally the addition of phenoxy made the composite more susceptible to environmental degradations. Visible effects of degradation could be observed, especially for DGEBA specimens, in which whitening and severe blisters occurred after hot-wet and solvent treated specimens, respectively. It was concluded that the improvement in Mode-I interlaminar toughness achieved by phenoxy modification could not be maintained after environmental conditioning.

CHAPTER 7

MULTISCALE HYBRID MICRO-NANOCOMPOSITES BASED ON CARBON NANOTUBES AND CARBON FIBRE

The previous chapters have concentrated on thermoplastic toughening of epoxy carbon fibre composites with dissolvable phenoxy fibres. In this chapter, nano-scale toughening was attempted through the use of carbon nanotubes. Amino-modified double wall carbon nanotube (DWCNT-NH_2) / carbon fibre (CF) / epoxy hybrid micro- nanocomposite laminates were prepared by a resin infusion technique. DWCNT-NH_2 / epoxy nanocomposites and carbon fibre / epoxy composites were made for comparison.

From virtually the moment carbon nanotubes (CNTs) were discovered it was expected that they would display superior mechanical properties as compared to carbon fibres. It has been shown that CNTs can significantly strengthen polymer matrices if the nanotubes are well dispersed, bonded and aligned [230, 231]. A number of reports have however also shown positive effects of the incorporation of randomly dispersed nanotubes on the crack resistance of polymer resins [23, 25, 232-235] . Gojny et al. [232], for example, reported a 43% increase in the fracture toughness of a standard epoxy resin with the addition of 0.5 wt% amine-functionalized double wall carbon nanotubes. Besides, the (often modest) mechanical property improvements, CNTs have been especially successful in improving the electrical properties of polymers. Their combination of good intrinsic conductivity

and high aspect-ratio makes them very interesting fillers for the creation of conductive polymer composites with low percolation thresholds [150, 236-239]. The introduction of such CNT modified resins into already matured carbon fibre reinforced plastics (CFRP) opens the possibility for the creation of new multifunctional multiscale materials with optimized mechanical, thermal as well as electrical properties.

Nature is full of interesting hybrid micro-nanocomposites. Bone is a fascinating multiscale composite, the basic constituents of which are the fibrous protein collagen; the mineral, carbonated apatite, close to dahllite in structure and water [240]. Bone has a hierarchical structure that contains micro as well as nano features, which are responsible for imparting unique mechanical characteristics such as high stiffness and high toughness. The purpose of hybridization in composites is to extend the concept of tailoring properties to suit requirements, and to offset the disadvantages of one component by the addition of another [39, 200, 241]. Multiscale composites offer a route by which multifunctionality, such as enhanced thermal stability, lower coefficient of thermal expansion, high thermal and electrical conductivity, can be imparted to the fibre reinforced composites. While fibre dominated properties of such multiscale hybrid micro-nanocomposites may benefit to some extent from the incorporation of nanoparticles, it is expected that especially resin dominated properties will benefit the most.

Recent research efforts in this field have focused on properties of hybrid micro-nanocomposites in which dispersed second phase nanoparticles are added to the epoxy matrix [27, 156, 159, 242-253]. Mahrolz et al. [244] reported a significant enhancement in mechanical performance including improvements in stiffness and tensile strength, delamination resistance and safety factors of their epoxy based multiscale composites. Mode II fracture behavior of the laminates was examined by Karapappas et al. [242] and an increase was reported in fracture energy of the CFRP doped with 0.5% and 1% CNTs (about 45% and 75%, respectively). Chen et al. [246, 247] prepared an epoxy-silicate nanocomposite using an aerospace grade epoxy resin

and carbon fibres and showed higher storage modulus as compared to neat resin properties. Gojny et al. [27] made glass fibre/CNT/epoxy composites and reported an increase in interlaminar shear strength by 20%. Tsantzalis et al. [248, 249] doped carbon fibre reinforced epoxy laminates with carbon nanofibres (CNFs) and titanate piezoelectric (PZT) particles and reported a 100% increase in fracture energy of laminates with the addition of 1 wt% CNFs. Wichmann et al. [159] developed fumed silica/glass fibre/epoxy, carbon black/glass fibre/epoxy and CNT/glass fibre/epoxy micro-nanocomposites by resin transfer moulding technique (RTM) and reported a 16% increase in interlaminar shear strength and superior electrical properties as a result of a smalls addition (0.3 wt%) of CNTs. Chowdhury et al. [250] investigated the effects of nanoclay on the mechanical and thermal properties of woven carbon fibre reinforced epoxy and reported an 18% and 9% improvement in flexural strength and modulus, respectively with the addition of 3 wt% nanoclay. Dean et al. reported on the synthesis and fabrication of glass fibre reinforced composites based on vinyl ester and epoxy nanocomposites, respectively [251, 252]. Qiu et al. [253] improved electrical conductivity and mechanical properties of CFRPs by effective infiltration of CNTs using vacuum assisted resin transfer molding technique.

Thostenson et al. [254] and Kepple et al. [255] grew CNTs on carbon fibres and embedded these fibres into an epoxy matrix and reported superior interfacial bond strength between the polymer and the CNT-modified carbon fibre. Gou et al. [256] worked on the fabrication of carbon nanofibre modified glass fibre reinforced polyester matrix. Vlasveld et al. [257, 258] showed a more than 40% increase in flexural and compressive strength at elevated temperatures with the incorporation of 10 wt% nanoclay in continuous fibre reinforced thermoplastics. Additional interesting properties of nanocomposite resins for advanced composites reported in literature are a reduced creep rate [258] and coefficient of thermal expansion [259], improved barrier properties for gasses and vapours [260, 261] and reduced flammability [258, 262, 263]. Micro-sized carbon fibres coated with aligned CNTs and their derivatives provide an effective means to connect nanoscale entities to the macroscopic world and were shown to possess interesting electrochemical properties

attractive for a wide range of potential applications, including methanol direct fuel cells and highly sensitive chemical and biological sensors [264]. Frankland et al. [265] modeled multiscale hybrid micro-nanocomposites based on CNT / carbon fibre / epoxy and indicated that the presence of nanotubes near the surface of carbon fibres can have a small, but positive, effect on the properties of the lamina.

The use of the nanotube modified epoxies as a matrix system for carbon fibre reinforced composites has been a challenge, and this is the aim of this study. It is not the aim of this study to replace any continuous carbon fibre with CNTs. However, dispersing them in small amounts in the polymer resin can potentially enhance matrix-dominated properties of these carbon fibre composites (Figure 7.1). In this work, we prepared multiscale hybrid micro-nanocomposites, based on amino-functionalized double wall carbon nanotubes (DWCNT-NH_2), carbon fibre fabrics and epoxy matrix.

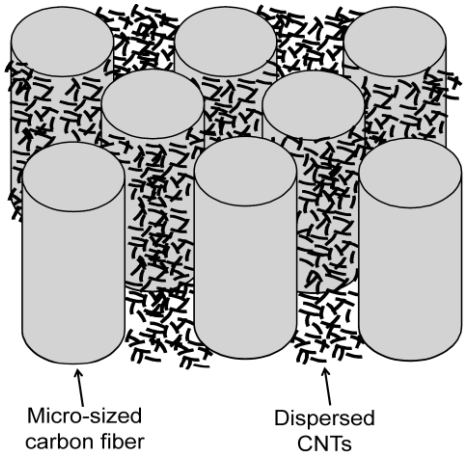

Figure 7. 1 Multi-scale hybrid micro/ nanocomposite based on CNTs and CF. Adapted from [36].

7.1 Experimental

7.1.1 Materials

The epoxy matrix used in this study consists of a CYCOM 823® RTM liquid epoxy resin with an aromatic anhydride hardener, supplied by Cytec Engineering Materials Ltd., UK. This epoxy system is a standard resin for the aerospace industry and infusion processes [266]. Plain weave carbon fibre fabric (P1726, 0/90^o), with an aerial density of 0.445 kg/m^2, was also obtained from Cytec. Cadek et al. [267] showed that DWCNTs-polymer composites, as compared to other CNTs, give potentially the best balance of properties in terms of dispersibility and mechanical properties for use as reinforcement of polymers. The interfacial bonding between carbon nanotubes and the epoxy matrix in the case of composites containing DWCNT-NH2 can be expected to be significantly higher than for composites containing non-functionalized DWCNTs, because the DWCNT-NH_2 may be covalently bonded to the epoxy matrix. The other aspect is the improved dispersibility of the amino-functionalized CNTs, which leads to a more homogeneous distribution in the matrix and a reduced risk for agglomerates [25, 233]. DWCNT-NH_2 (Nanocycl® 2152) was supplied by Nanocyl S.A., Belgium. As per supplier, these CNTs were synthesized by CVD method, having diameters of around 4.7 nm, lengths up to several microns, a carbon purity of more than 90% and a functionalization of less than 0.5%.

7.1.2 Specimen manufacturing

7.1.2.1 Dispersion procedure

Three compositions (0.025, 0.05 and 0.1 wt%) of DWCNT-NH_2 were homogenized in the epoxy matrix using a high power bath ultrasonication (Decon Ultrasonics Ltd, FS Minor, 75 Watts) for five hours. Shown in previous work by Inam and Peijs [268], this method is highly effective for lower concentrations of CNTs and results in a good level of dispersion. As per supplier, anhydride hardener (20 wt%) was added. After degassing (at 50^{o}C/30 mm Hg) the suspension for 30 min

in a vacuum oven, one batch of materials was used to make DWCNT-NH_2/ epoxy nanocomposites by an open mould casting method, while a second batch was used for the manufacturing of the hybrid micro-nanocomposites by vacuum infusion technique.

7.1.2.2 Neat resin casting

The homogenized suspensions were slowly poured between two mirror-polished stainless steel plates at an angle (~30^o) in a vertical position. Frekote mould release agent was applied to the plates before casting. The resin was heated at 1^oC/min to 125°C and cured for an hour and cooled slowly in and oven cooled. The thickness of the epoxy nanocomposite plates was 3 ± 0.25 mm. No voids and shrinkage marks were observed by naked eye. The same procedure was employed to make neat epoxy plates.

7.1.2.3 Composite laminates manufacturing

Table 7. 1 CNT/epoxy neat resin and CNT/epoxy composites samples prepared for this study.

Sample Description	Method of preparation	Sample ID	Fibre volume fraction V_f
Neat epoxy	Open mould casting	A	-
0.025 wt% DWCNT-NH_2 + epoxy	Open mould casting	B	-
0.05 wt% DWCNT-NH_2 + epoxy	Open mould casting	C	-
0.1 wt% DWCNT-NH_2 + epoxy	Open mould casting	D	-
CF + epoxy	Vacuum infusion	E	0.6
0.025 wt% DWCNT-NH_2 + CF + epoxy	Vacuum infusion	F	0.6
0.05 wt% DWCNT-NH_2 + CF + epoxy	Vacuum infusion	G	0.6
0.1 wt% DWCNT-NH_2 + CF + epoxy	Vacuum infusion	H	0.6

Composite laminates were made by resin infusion using neat epoxy and DWCNT-NH_2 dispersed mixtures, details of the procedures were described in Section 4.1.2. The only differences were that the steel mould was heated to 50°C and the infused lay-ups were cured by heating to 125°C at 1°C/min, followed by a dwell at 125°C for 1 hr before oven cooled to room temperature. The thickness of the laminates was 3 ± 0.30 mm and the fibre volume fraction was 0.6, by calculation.

7.1.3 Characterisations

Flexural strength was measured according to ASTM D 790-03 [269] in a 3-point bend test using an Instron 6025 screw-driven universal tensile testing machine at a cross-head speed of 5 mm/min at room temperature. Sample size was 127 mm x 12.7 mm x 3 mm, span-to-depth ratio was 16 for neat resin specimens and 32 for composite specimens. At least five specimens were tested for each composition.

Double cantilever beam (DCB) specimens were prepared for Mode I fracture toughness tests according to ASTM D5528-01 [215] (Fig. 4.3). See Section 4.1.3.2 for details.

Dynamic mechanical analysis was carried out in a DMA Q800 by TA Instruments in 3-point bending mode at a frequency of 1 Hz. Heating occurred at a rate of 5 °C/min and in a temperature range between 30 and 200 °C. Sample size was 68 mm x 12.7 mm x 3 mm, span length was 50 mm.

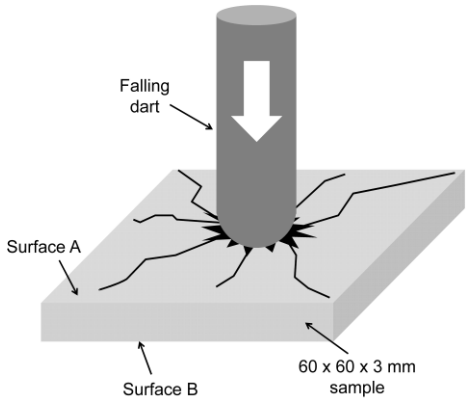

Figure 7. 2 Schematics of falling dart impact testing.

Energy absorption during impact was measured on flat plates (sample size = 60 x 60 x 3 mm) using a Ceast instrumented dart impact tester (Dart Vis, diameter = 18 mm) fitted with a data acquisition system (Figure 7.2). The laminates were clamped between two plates. At least five samples were tested for each composition and were impacted at a fixed initial impact energy level of 6 joules. Ultrasonic C-scan was performed using a jet probe inspection system (Midas-ndt) to measure the damaged area in laminates.

Fractography was carried out as described in Section 4.1.3.6

7.2 Results and Discussion

7.2.1 SEM characterisation

Using SEM analysis, the inter-ply resin (between 3rd and 4th ply) of the cured laminate was studied to evaluate the level of impregnation of the nanotube modified resin within the carbon fibre plies as well as in between the plies. Figure 7.4 shows the inter-ply region in the centre of the woven fabric laminate (between 3rd and 4th ply). No clear filtering effect of the carbon fabric on the DWCNT-NH_2 for samples F and G was observed, as was reported in earlier studies [159]. However, for sample H, which contains 0.1 wt% DWCNT-NH_2 there was a clear difference in the clearness of the resin coming out of the suction line, indicating lower nanotube content due to filtering of larger agglomerates present in this resin system by the carbon fabric. It should be noted, that due to the large difference in scale, it is not possible to directly observe both DWCNTs-NH_2 and carbon fibres in the same image (Figure 7.3a and 7.3b). Agglomerates of DWCNT-NH_2 are visible in Figure 7.3b and 7.3c for sample F. The lower viscosity may lead to better wetting of the carbon fibres and dispersion of the DWCNT-NH_2 but a non-uniform distribution of CNT aggregates is observed in Figure 7.3b. The non-uniform dispersion of DWCNT-NH_2 (Figure 7.3a, 7.3b and 7.3c) in between carbon fibre layers should be due to the aggregate nature of CNTs because of their high specific surface area and strong interaction forces between them. Key failure mechanisms in continuous fibre reinforced composites like fibre

fracture, fibre pull-out, fibre/matrix debonding, crack bridging (Figure 7.3d) and matrix cracking have also been observed in CNT modified polymer composites as demonstrated by Thostenson and Chou [270, 271] and the same is expected for these hybrid micro-nanocomposites.

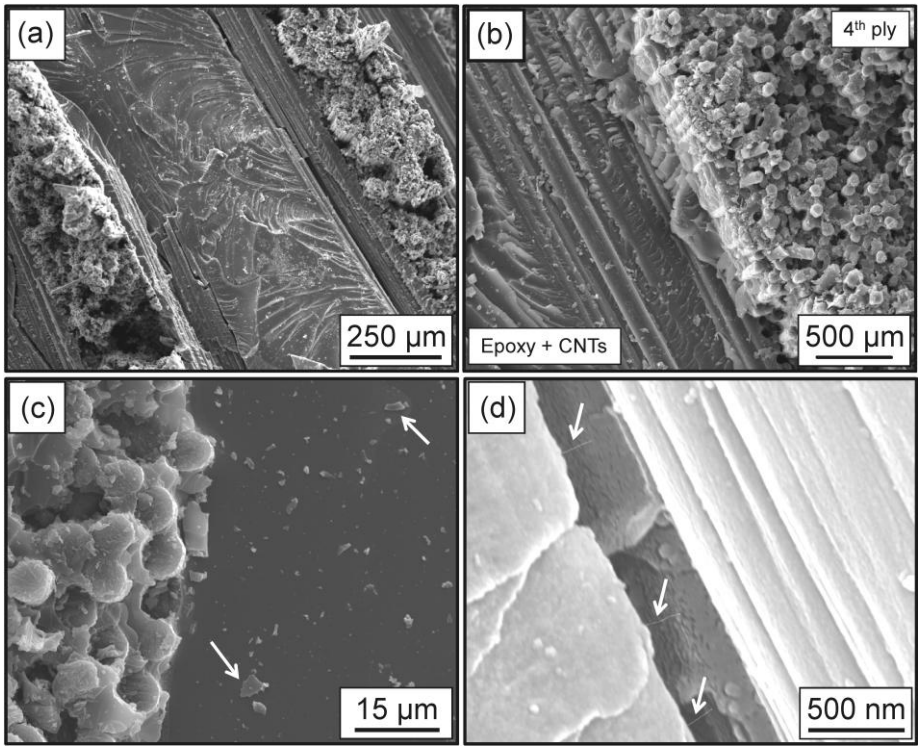

Figure 7. 3 SEM images of hybrid (0.025 wt% DWCNT-NH_2) micro-nanocomposites: a,b) middle of cured laminate (between 3rd and 4th plies); c) agglomerates of DWCNT-NH_2 (pointed); and d) individual DWCNT-NH_2 bridging epoxy matrix (pointed).

7.2.2. Flexural testing

So far nanotube-filled polymers have not had many industrial successes in which they showed a mechanical property advantage over traditional carbon fibres [272], even though the potential reinforcing properties, notably strength, of CNTs are superior to those of carbon fibres [273]. The low loadings of CNTs often employed in epoxy resins imply less inhomogenities but also less positive perturbations of

mechanical properties [274]. Previous attempts to combine nanocomposites with micron-size fibres often resulted in a strong decrease in strength, presumably caused

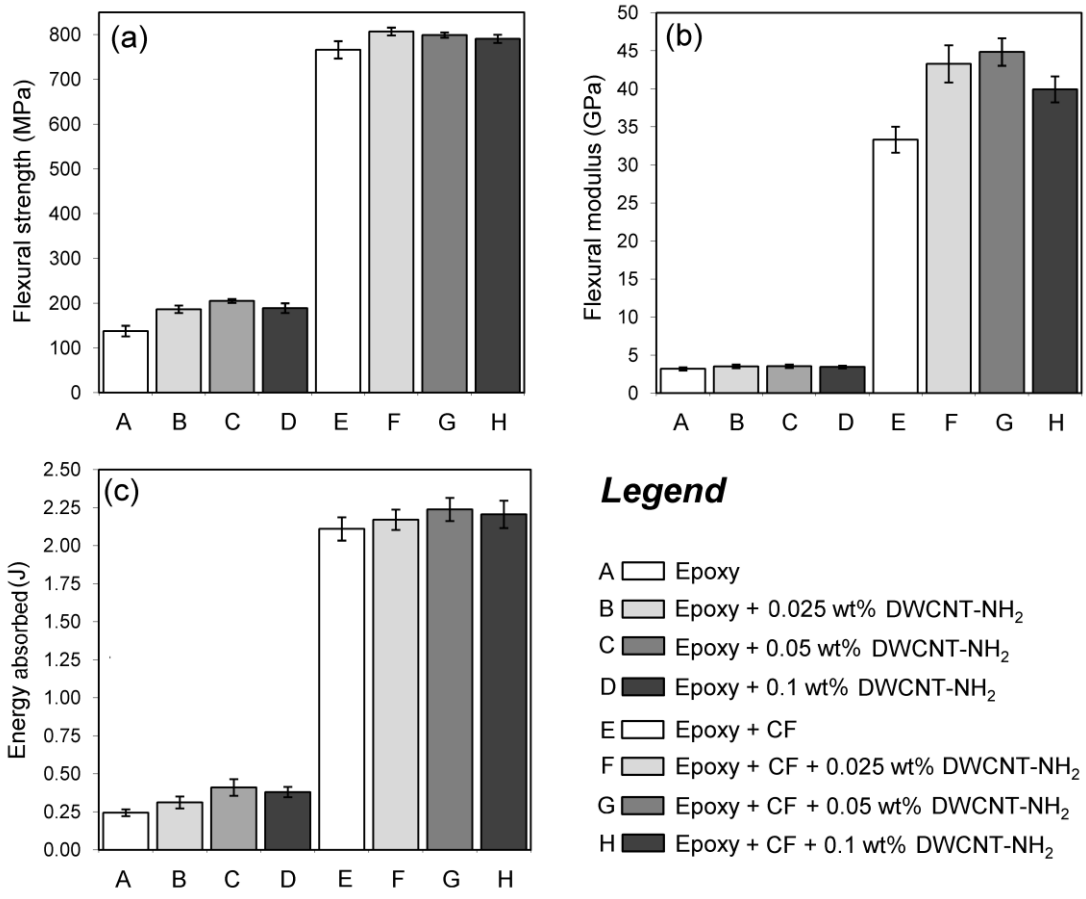

Figure 7.4 Mechanical characterizations (three-point bend test and drop-weight impact test): a) flexural strength; b) flexural modulus; and c) energy absorbed (area under the curve of force vs displacement).

by poor adhesion [258]. In this case, adding CNTs to CFRP imparted a small increase in flexural strength (Figure 7.4a) of around 5% for sample F, indicating a good bonding between the CNT-modified epoxy matrix and the carbon fibres. Nanotube modification of the pure epoxy resin showed an increase in flexural strength of nearly 50% for sample C, but this is still significantly below the theoretically predicted values [275]. Flexural strength of the CNT/ epoxy nanocomposites increased up to a loading of 0.05 wt% of DWCNT-NH_2 (sample C)

and then decreased, presumably due to agglomeration at higher nanotube concentrations. For hybrid micro-nanocomposites flexural strength only increased up to 0.025 wt% of DWCNT-NH_2 (sample F). As compared to sample A, a very small improvement in flexural stiffness (Figure 7.4b) for samples B (10%), C (11%) and D (8%) was observed. However, the introduction of DWCNT-NH_2 in CFRP, resulted in a near 35% improvement in flexural modulus for sample G. Flexural modulus increased up to 0.05 wt% of DWCNT-NH_2 (sample G) and then decreased.

7.2.3. Impact testing

Falling-weight impact testing has potential for evaluating the damage tolerance of composite materials. This type of testing gives significant information about failure mechanisms and behavior of materials under low velocity impact [187, 241]. Post processing of the measured impact parameters, force, time and impact velocity, results in the complete energy history and the energy absorbed during impact by the composite laminate. Upon impact the total impact energy can be divided into two parts: First, the elastically stored energy in the composite plate, which is released after maximum deflection by rebouncing of the laminate. This rebouncing energy is successfully transferred back to the impactor. Secondly, the energy absorbed in the composite laminate available for damage that consequently controls the extent of damage and residual strength [39, 187, 241].

To study the impact damage tolerance of the micro-nanocomposites, only the 'absorbed energy' of the composite laminates was report here. It should be noted that the neat resin based samples A, B, C and D cannot be compared with the CFRP based samples E, F, G and H. The first four samples were too brittle and shattered upon impact (full-penetrating impact); whereas the latter four containing carbon fibre did not penetrate. The energy absorbed, calculated by the area under the force-displacement curve is presented in Figure 7.4c. CNTs improved the impact strength by up to 30% (sample C) for the nanotube modified epoxy resin. In the case of hybrid micro-nanocomposites, carbon fibres were expected to absorb most of the energy during impact because of their large volume. After hybridization, slightly

more energy was absorbed by the hybrid micro-nanocomposites. However, no significant effect on damage area was observed in the ultrasonic C-scans (Figure 7.5). Hybridized (0.1 wt% CNTs) and non-hybridized CFRP laminates both showed similar damage areas (~254 mm^2) on the impacted surface (Figure 7.5). At the initial impact energies of 6 Joules, no damage was detected at the non-impacted surfaces (surface B, Figure 7.2) of the laminates. Results in Figure 7.4c, show a negligible enhancement in the energy absorbed by samples F (3% improvement) and G (6% improvement) as a result of the presence of DWCNT-NH_2. This small increase was rather disappointing given the large increase in surface area offered by the CNTs. Regarding the enormous surface area of nanofillers, only small volume fractions of CNTs are needed to modify a large volume of the matrix, resulting in a high interphase fraction [159]. Energy absorbed by the hybrid micro-nanocomposites increased only up to loadings of 0.05 wt% DWCNT-NH_2 (sample G) and then decreased for sample H. A similar trend was also observed for epoxy nanocomposites in which the maximum energy was absorbed by sample C (0.33 J, 30% enhancement as compared to neat epoxy). However, compared to standard rubber or thermoplastic toughened epoxy systems these enhancements in impact toughness of CFRP through the introduction of CNTs are not all that significant. Significantly higher improvements in toughness can be achieved using more traditional methods such as polymer blends [276] or hybridization with other more ductile fibres [39, 106, 241, 277].

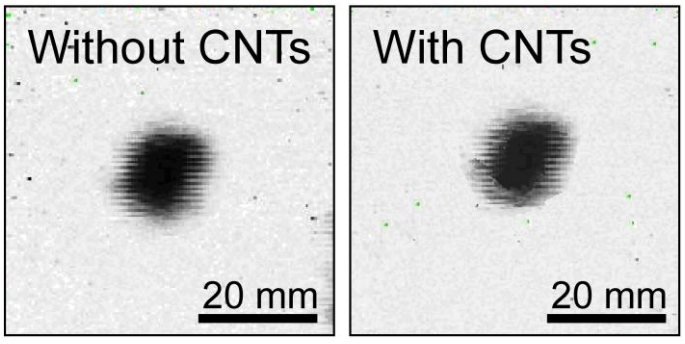

Figure 7.5 C-scan images of non-hybridized CFRP and hybridized (0.1 wt% CNTs) micro-nanocomposite.

7.2.4. Mode-I delamination toughness

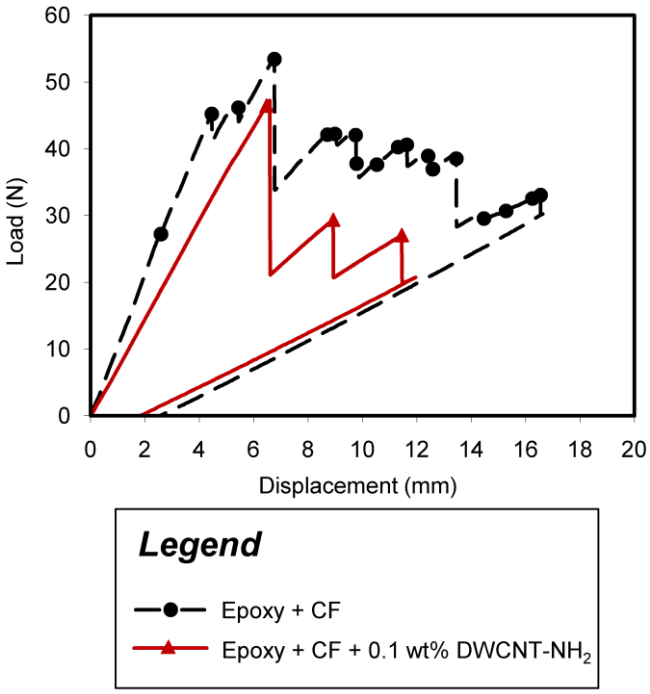

Figure 7. 6 Mode-I interlaminar fracture toughness analysis of non-hybridized CFRP and hybridized (0.1 wt% DWCNT-NH_2) micro-nanocomposite. Data points represent stick-slip fracture mode.

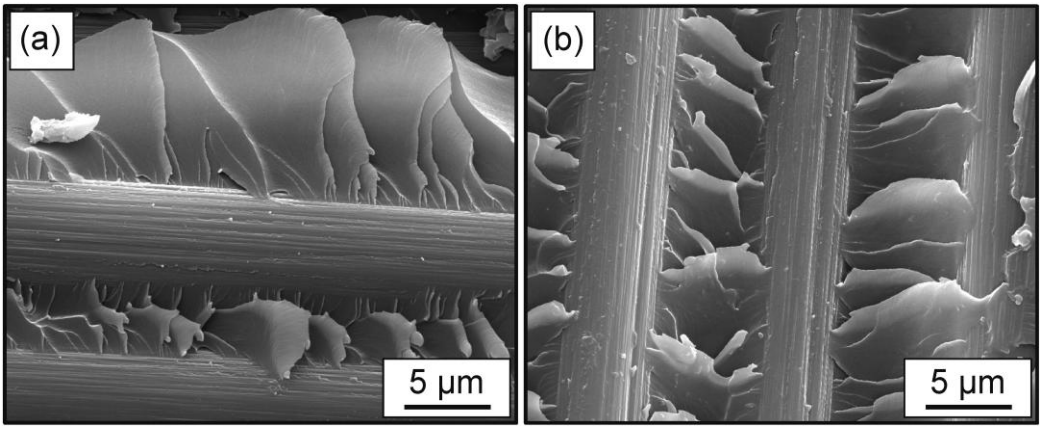

Figure 7. 7 SEM images of Mode-I fractured surface: a) non-hybridized CFRP; and b) hybrid micro-nanocomposite (0.1 wt% DWCNT-NH_2).

The load-displacement curve (Figure 7.6) of the CFRP laminate without CNTs shows a stick-slip failure mode which is common for epoxy laminates. Stick-slip fracture follows a crack propagation and crack arrest behaviour which indicates unstable crack growth. In neat CFRP composites the crack propagated gradually and only a small drop in load was recorded (Figure 7.6). The laminate with 0.1 wt% CNTs also shows a stick-slip fracture mode. However, as there are less drop steps in the load-displacement curve (Figure 7.6) for the hybrid micro-nanocomposite, fracture was fast and more catastrophic, as compared to cracking in the neat CFRP composite. Consequently, load decreases significantly during propagation of the crack for hybrid micro-nanocomposites. Average G_{Ic} values for non-hybridized CFRP microcomposites and hybridized micro-nanocomposites are 0.38 kJ/m^2 and 0.31 kJ/m^2, respectively. Hence the mode I interlaminar fracture toughness remained largely unchanged. FE-SEM images of fractured surfaces are shown in Figure 7.7. Both fracture surfaces show hackle formation as the predominant failure mode for both matrices.

7.2.5. Dynamic mechanical analysis

As expected from the three-point bending results, CNTs improved the storage modulus of the nanocomposites and the hybrid micro-nanocomposites, as evidenced from Figure 7.8a and 7.8b. It can be seen in Figure 7.8a, that sample D (0.1 wt% CNT/ epoxy) possessed a lower storage modulus as compared to neat epoxy and other nanocomposites (having lower concentrations) over the temperature range (30-130^{o}C). Above 130^{o}C neat epoxy and all the epoxy nanocomposites possessed the same storage modulus, indicating that the presence of nano-reinforcement was not significant above T_g. A similar trend was observed for the micro-nanocomposites as shown in Figure 7.8 b. Sample H (0.1 wt% CNT/ CF/ epoxy) possessed an inferior storage modulus as compared to other lower compositions of hybrid micro-nanocomposites over the temperature range 30 to 115^{o}C. At high temperatures, the loss modulus of the nanocomposites and the hybrid micro-nanocomposites decreased with increasing CNT content, shifting the T_g peak downward (Figure7.8c and 7.8d).

Higher concentrations possessed lower energy dissipation ability as well. This effect is very clear at higher temperature (above 90°C). Hence, it can be concluded that dampening characteristics (*tan δ*) of nanocomposites and hybrid micro-nanocomposites start to improve above 90-100°C, because of increased energy dissipation ability of the matrix. There are concerns with increasing storage modulus values for the hybrid composites samples as temperature increased, as this is unexpected and remained to be explained.

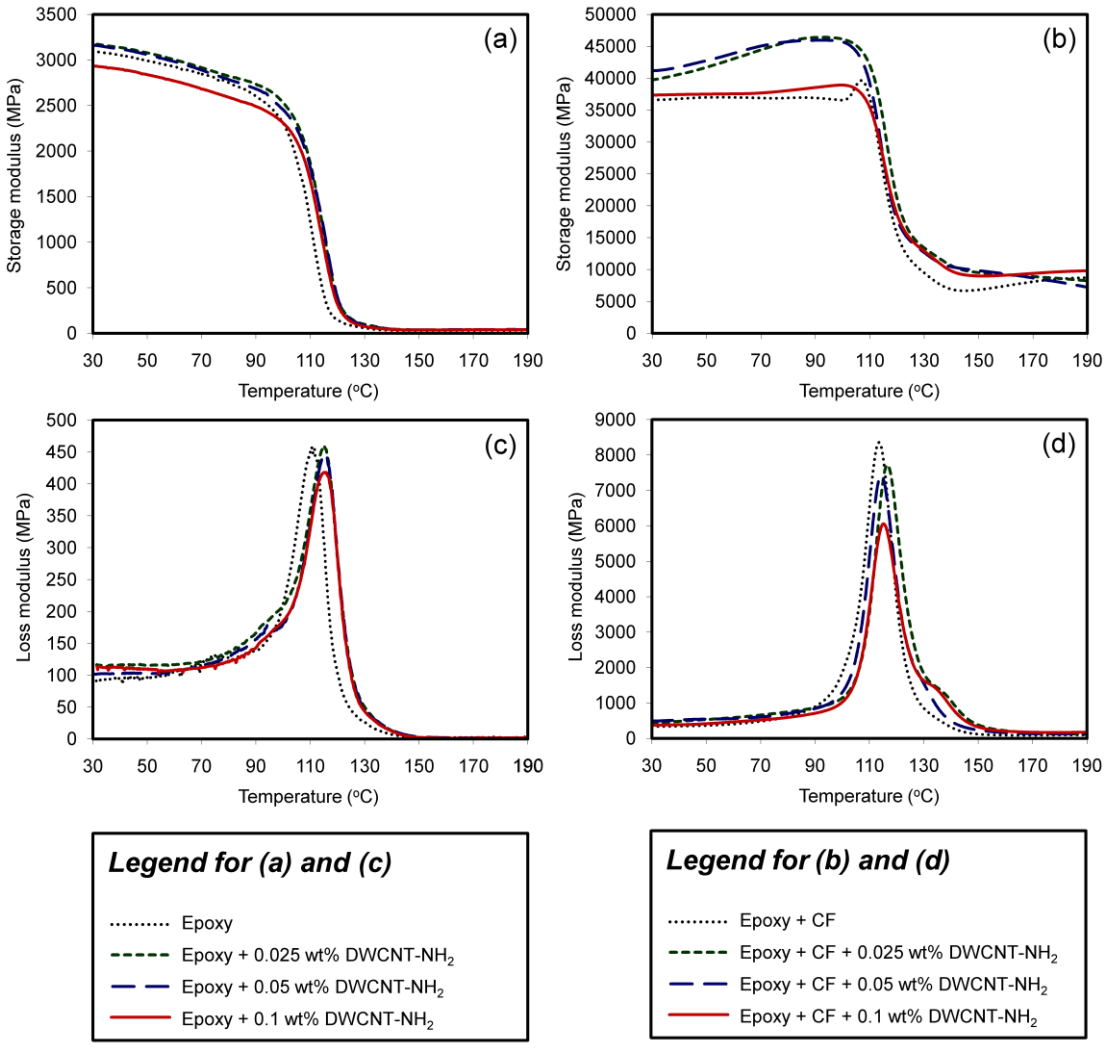

Figure 7. 8 Dynamic mechanical analysis: a) storage modulus for neat epoxy and nanocomposites; b) storage modulus for CFRP and hybrid micro-nanocomposites; c) loss modulus for neat epoxy and nanocomposites; and d) loss modulus for CFRP and hybrid micro-nanocomposites

Based on the *tan δ* peak, the T_g for all samples are given in Table 7.2. At least five samples were tested for each condition. According to table 2, CNTs slightly enhanced the T_g of epoxy nanocomposites up to 5% (sample C, T_g = 122 ^{o}C). T_g was decreased for sample D due to the presence of aggregates. Furthermore, instead of having a positive effect on T_g, hybridization (Table 7.2) resulted in a reduction in T_g, possibly due to a more non-uniform distribution of CNT's in the CFRP laminates as a result of filtering effects by the carbon fabrics [278]. These results are consistent with the work performed by Lee at al. [278]. It is interesting to note that micro-nanocomposites and epoxy nanocomposites showed inferior dampening properties (at room temperature) as compared to CFRP and neat epoxy, respectively (Table 7.2). Here it can be concluded that hybridization with CNTs, results in a significant reduction (22% in case of sample G) in dampening properties of these composites at room temperature. More work needs to be done to explain this reduction in properties and the non-uniform behaviour in Table 7.2. On the other hand, lower values for loss modulus at higher temperatures (near T_g, 110-130^{o}C) in Figure 7.8c and 7.8d suggest higher dampening characteristics of hybrid micro-nanocomposites and nanocomposites containing higher CNT concentrations.

Table 7.2 Effect of CNTs on glass transition temperature and tan-delta for nanocomposites and hybrid micro/nano-composites.

Sample Description	Sample ID	T_g(^{o}C)	Tan-delta*
Neat epoxy	A	116 ± 3	34 ± 2
0.025 wt% DWCNT-NH_2 + epoxy	B	122 ± 4	27 ± 3
0.05 wt% DWCNT-NH_2 + epoxy	C	122 ± 5	31 ± 4
0.1 wt% DWCNT-NH_2 + epoxy	D	122 ± 3	26 ± 4
CF + epoxy	E	118 ± 5	108 ± 4
0.025 wt% DWCNT-NH_2 + CF + epoxy	F	118 ± 3	89 ± 3
0.05 wt% DWCNT-NH_2 + CF + epoxy	G	118 ± 6	84 ± 4
0.1 wt% DWCNT-NH_2 + CF + epoxy	H	118 ± 4	100 ± 3

** at room temperature*

Most of the mechanical features of hybrid micro-nanocomposite started to decrease above 0.05 wt% CNT, mainly because of three reasons: i) filtering of CNTs by the carbon fabric, leading to reduced dispersion and inhomogeneous CNT dispersions throughout the laminate; ii) higher CNT contents in epoxy reducing the wetting and bonding between carbon fibres and the nanotube modified resin [279]; and iii) agglomeration, which has a significant effect on the strength, stiffness and toughness of the CNT modified epoxy [278, 280]. The presence of large agglomerates decreases the effective surface area of CNTs or in other words, reduces the efficiency of the nano-reinforcement. For pure nanocomposites (samples *B*, *C* and *D*) the latter reason is more appropriate, explaining the drop in mechanical properties with the addition of 0.05 wt% CNTs. CNTs need to be separated from the bundles and dispersed uniformly in a polymer matrix to maximize their interaction with the matrix [271]. In a CNT / polymer composite, aggregation of CNTs may become a defect that causes the mechanical properties of the resin and hence the composite to deteriorate. Therefore, the primary problem in fabricating a nanocomposite is to ensure a homogeneous dispersion of CNTs in the polymer matrix. So far, only ultrasonic, three-roll milling and high-speed mechanical stirring have been verified to be effective methods for the dispersion of CNT in epoxy resin [281]. But from this study, it appeared that bath ultrasonication is a good way to disperse lower concentrations of CNT in epoxy. Better homogenizing techniques should be employed for dispersing higher contents of CNTs in epoxy. The results of Allaoui *et al*. [151] suggest that it would not be helpful to use high CNTs concentrations to improve the mechanical properties of composites if they are in random distribution. The upper limit, for the addition of CNTs, is governed by the distribution and topology (aspect ratio) of the CNTs. Similar to short fibre composites, the orientation of the nanofibres plays an important role and the higher the degree of alignment of CNTs, the higher their reinforcing efficiency [282].

7.3 Conclusion

Multiscale hybrid micro-nanocomposites offer a route by which multifunctionality can be introduced in fibre reinforced composites. DWCNT-NH_2/ carbon fibre/ epoxy micro-nanocomposites were prepared and their mechanical properties were compared with their respective pure micro- and nanocomposites. Apart from flexural modulus, fracture toughness, T_g and *tan δ,* CNTs imparted a very minor enhancement in mechanical properties of woven fabric based CFRP. The addition of small amounts of CNTs (0.025, 0.05 and 0.1 wt%) to epoxy resins for the fabrication of multiscale carbo n fibre composites resulted in a maximum enhancement in flexural modulus by 35%, a 5% improvement in flexural strength, a 6% improvement in absorbed impact energy, and no improvement in the mode I interlaminar toughness. Hybridization of carbon fibre reinforced epoxy using CNTs also resulted in a reduction in T_g and dampening characteristics, owing to the presence of micron-sized agglomerates. However, even without these aggregates, it was concluded that DWCNT-NH_2 achieved only a limiting toughening effects in the CFRP. Especially compared to standard rubber or thermoplastic toughened epoxy the enhancements were not all that significant. These results are especially disappointing considering the large surface-to-volume ratio of CNTs compared to other fillers, including carbon fibres, and the effect this - in theory - can have on energy absorption mechanisms such nanotube debonding or pull-out [64]. Therefore, a careful future optimization of processing parameters such as nanotube dispersion at higher concentrations, nanotube alignment and localization, should lead to further improvements in mechanical properties of these multiscale composites.

Chapter 8
Summary, Reflection & Future work

8.1 Summary

This study mainly focused on the toughening of carbon fibre epoxy composites using dissolvable phenoxy fibres. Two epoxy systems were selected to investigate the effect of resin properties on toughening. DGEBA is a bifunctional resin with a chemical structure close to that of phenoxy and is widely used in many general engineering applications. TGDDM is a tetrafunctional resin with a high crosslink density in its cured state. It has higher T_g and is more brittle than DGEBA and is used for high temperature applications. Different resins were used to prepare neat resin and composite laminate specimens, i.e. for Epon™ 828 and Araldite™ LY 721 for neat resin, and Araldite™ LY 564 and ACG MVR 444 for laminates, which could make direct comparison between the two types of specimen difficult. While the Epon 828 and LY 721 are pure DGEBA and TGDDM resins respectively, LY 564 and MVR 444 are low viscosity resins suitable for resin infusion which is the reason they were chosen. For the case of TGDDM resin in particular, LY 721 resin mixed with DDS curing agent has high viscosity and makes infusion impossible, and an alternative has to be found. MVR 444 resin is a proprietary blend of mainly tetrafunctional epoxy resins premixed with polyamine curing agents and the exact chemistry is unavailable. While this is not ideal, it is the case with most supplied resins.

Dissolvable phenoxy fibres were chopped and distributed between carbon fibre fabrics during dry lay-up. These lay-ups were then vacuum bagged and resin infusion took place. The phenoxy fibres remained solid and stayed in place during infusion and subsequently dissolved after infusion was completed. Therefore the viscosity of the epoxy resin system remained low during infusion which allowed impregnation and wet-out of carbon fibres. The phenoxy fibres later dissolved as the laminates were heated to their curing temperature, and no phenoxy fibre was observed in cured laminates. It was suggested that the dissolved phenoxy formed a miscible blend with epoxy resins and then phase separated as curing progressed. This toughening approach is a combination of thermoplastic toughening and interleaf concepts, as it involved polymer blending and an interleaving layer.

The benefits of this approach are that the viscosity of resin can remain low, as no thermoplastic or rubber is needed prior to moulding, which makes liquid resin infusion possible. No solution or melting blending is required and this saves manufacturing costs and time. It also allows for higher concentrations of thermoplastics as it is generally the increase in viscosity in the modified epoxy blend that limits the amount of thermoplastics that can be added. Selective and localized toughening can be achieved as well as phenoxy fibres can be placed only where they are needed, without having too great an impact on other properties of the laminates, such as V_f and tensile modulus and strength.

In terms of Mode-I toughness, the addition of phenoxy improved G_{1c} for both resins. With 10 wt% phenoxy, DGEBA specimens had a ten-fold increase in G_{1c} while the TGDDM specimens improved by more than 100%, while no drastic changes were observed in tensile properties and T_g for both matrices. As for the bulk resin samples, the phenoxy was more effective in toughening the DGEBA resin. The toughness improvement for laminates far exceeded that for bulk resins. This is due to the fact that the dissolved phenoxy was mainly located in the interlaminar region, thus the actual concentration of phenoxy was much higher in that region, leading to a higher $G_{1c.}$ The addition of phenoxy could also affect the fibre/matrix interface, although no evidence was found by the short beam shear tests. It should be noted that

a low molecular weight phenoxy was also used for comparison, but no phase separation and toughness improvement was observed in bulk epoxy blends.

CAI tests were carried out to study damage resistance and damage tolerance of the specimens. It was found that damage resistance and tolerance could be improved for phenoxy modified specimens for both matrices. The improvement in damage resistance was more profound for the DGEBA specimens, while damage tolerance improvement was more profound for the TGDDM specimens. However there was no general trend between phenoxy concentration to CAI properties and changes in properties are specific to the resin system.

A combination of dissolvable phenoxy fibres and interleaving with non-woven aramid veils was also investigated. The effects of interleaving plus phenoxy-modification were different for the two resin systems, In terms of fracture toughness and CAI properties, the combination of an aramid interleave on phenoxy modification did not show significant positive effects for DGEBA laminates, while for the TGDDM laminates, some improvements were observed. This shows that it is possible to improve toughness and damage properties by combining these two techniques, depending on the resin system used. The toughening mechanism for aramid interleaved DGEBA laminates was dominated by aramid fibres, with little involvement from carbon fibres, with and without phenoxy. Fibre pull-out, debonding, fibrillation and fracture of aramid fibres were the main failure features in these materials. For aramid interleaved TGDDM laminates with phenoxy, in addition to toughening by aramid fibres, carbon fibre/matrix debonding and carbon fibre fracture also played a major part in the overall toughness.

In order to study the environmental stability of the phenoxy modified composites, the effects of hot-wet and organic solvent (MEK) treatments on phenoxy modified carbon fibre/epoxy composites were investigated. It was generally found that the addition of phenoxy made the composite more susceptible to environmental degradations. Visible effects of degradation could be observed, especially for DGEBA specimens, in which whitening and severe blisters occurred after hot-wet

and solvent treated specimens, respectively. It was concluded that the improvement in Mode-I interlaminar toughness achieved by epoxy modification could not be maintained after environmental conditioning.

Finally, the combination modification of laminates using carbon nanotubes was studied by mixing CNTs with epoxy resin prior to resin infusion. The toughening effects here were disappointing, which could be due to the presence of micron-sized agglomerates. Therefore a careful future optimization of processing parameters such as nanotube dispersion at higher concentrations, nanotube alignment and localization, should lead to improvements in mechanical properties of these multiscale composites. As outlined in the next section, it is hoped the use of CNTs in combination with dissolvable phenoxy fibres can be combined in the future to localize CNTs at specific areas in the composite.

Table 8.1 A summary of changes in mechanical properties of epoxy composite laminates modified with dissolvable phenoxy fibres.

	DGEBA		**TGDDM**	
wt % phenoxy	**5%**	**10%**	**5%**	**10%**
Tensile modulus	—	—	—	—
Mode-I fracture toughness G_{1c}	⇧	⇧	—	⇧
Short beam shear stress	—	—	—	—
Damage resistance	—	⇧	⇧	⇧
Damage tolerance	—	⇧	⇧	⇧

8.2 Reflection

The idea of this project came from previous work by a colleague in the research group, in which hybrid fabrics made with different thermoplastic fibres commingled with glass fibre were studied. Similar to this project, the epoxy composites were manufactured by resin infusion with the aim to improve interlaminar fracture toughness. It was found that one of the thermoplastic fibres dissolved during processing and although it did not improve toughness, it gave us an idea about thermoplastic toughening by introducing a dissolving fibre. At around the same time, Cytec Engineered Materials Ltd. was marketing the PRIFORM system in which a phenoxy fibre, Grilon® MS by EMS-Griltech, is weaved into carbon fibre fabric. It was claimed that the phenoxy fibre acts as a toughening agent and can provide the properties achieved by other toughened prepreg system, without the penalty of increased resin viscosity. The Grilon® MS fibre is also marketed as a bonding fibre and stitch thread for epoxy composites and received a JEC Composites award in 2007, and a non-woven mat version was later developed. However, little detail is available about how the modification affects composite mechanical and physical properties. There is also little information on how the phenoxy concentration and the type of epoxy resin used would affect the final properties. It was decided then to study phenoxy modified epoxy systems further in order to gain better understanding with a view to develop the idea further.

In general, the aim set out in the thesis has been achieved. It is felt that the techniques employed in manufacturing and characterization are successful in investigating phenoxy modified epoxy systems which leads to a better understanding. Improvement can be made on phenoxy fibre distribution during laminates manufacturing. The phenoxy fibre was simply chopped and sprinkled which led to local concentration fluctuations. It would be better to spin our own fibre and make non-woven mat or weave the phenoxy fibre into the fabric, however it was not possible with the resources available. Instead of tensile test, compression could be used as this is more appropriate for brittle materials such as epoxy, and sample

preparation is also a lot easier. The dog-boned neat resin tensile specimens were difficult and very time consuming. However, compression test was not chosen as there was little technical support available at the time.

This study has confirmed that phenoxy modification can indeed toughen epoxy composites, but there are doubts about the stability of such systems. The improvement on toughness is cancelled out by hot-wet treatment and the specimens degraded badly after solvent attack, especially for the DGEBA specimens. This raises serious questions about application of such systems, and extra care has to be taken when incorporating phenoxy fibre into composite components. No such information is available from the manufacturer or in the literature. It has shown that it can be worthwhile to carry out your own study rather than relying on supplied information.

8.3 Future work

Toughening with dissolvable phenoxy fibres is dependent on resin chemisty, with the two epoxy systems behaving very differently. Different curing agents and curing cycles can be studied to achieve the most desirable properties. The use of catalysts and accelerated can also be investigated.

In the current thesis, the dissolvable phenoxy fibres used are available as a yarn and was chopped and sprinkled in-between plies of carbon fibre fabric. The phenoxy fibre was weighed and the volume in wt% with regard to the total matrix content was calculated. However, owing to the hand sprinkling process, and the fibres being bundled into yarn, the distribution of the phenoxy was not uniform and led to local concentration variations. This makes a direct comparison of the specimens difficult. The use of non-woven veils would be preferred as this will lead to a more uniform interlaminar region. Other ways of incorporating phenoxy fibre into fibre composites, such as commingled yarn and stitching can also be studied.

As mentioned earlier, the phenoxy fibre concentrations studied was 5 wt% and 10 wt% with regard to the overall matrix. Phenoxy fibres were located between

carbon fabric and most of them were expected to remain in the region even after fibre dissolution, therefore phenoxy concentration in the interlaminar region was much higher than the 5 wt% or 10 wt% stated. Neat resin samples of higher phenoxy concentrations can be made for comparison. There were plans to prepare samples with higher phenoxy concentration but they could not be made due to viscosity related manufacturing problems that occurred at the time.

The use of dissolvable phenoxy fibres or films together with CNTs can also be investigated as a mean to specifically localize CNTs in composite laminates. CNTs can be added to the phenoxy fibre, either by mixing with phenoxy fibre prior to fibre spinning, or as a coating to the phenoxy fibre, or in the form of thin film or tapes. The manufacturing and properties of polymer tapes containing CNTs have been reported [283, 284]. The CNTs carrying phenoxy fibres can then be added to laminates during dry lay-up. The phenoxy fibres dissolve in the epoxy matrix which releases the CNTs into the matrix, as shown in Figure 8.1. Incorporating CNTs in this way eliminates the need of mixing CNTs with epoxy resin and prevents the increase in resin viscosity, thus making composite manufacturing easier. It also allows a selective and localised CNT distribution, positioning CNTs there where they are needed. As outlined in Chapter 8, CNTs can improve mechanical properties of laminates, even though the mechanical properties of the CNT modified composites studied was disappointing. However, a potentially more interesting application of CNTs in composites is in electrical property enhancement with possible application in damage sensing. CNTs can be selectively positioned in the interlaminar region to form a conductive layer which can be used as sensors for strain monitoring and damage detection [27]. The electrical properties of CNT modified epoxy composites have been studied by Wichmann *et al.* [159] and it was found that even a low loading of CNTs (0.3 wt%) was enough to imply conductivity into composites. Matrix cracks on delaminations will alter the electrical conductivity of such a CNT network and this could be used for damage monitoring [285]. In the damage monitoring system mentioned above, the whole matrix is modified by CNT. In the proposed concept this modification is only needed at critically loaded areas, which can lead to large reduction in the overall CNT loadings needed for this kind of application.

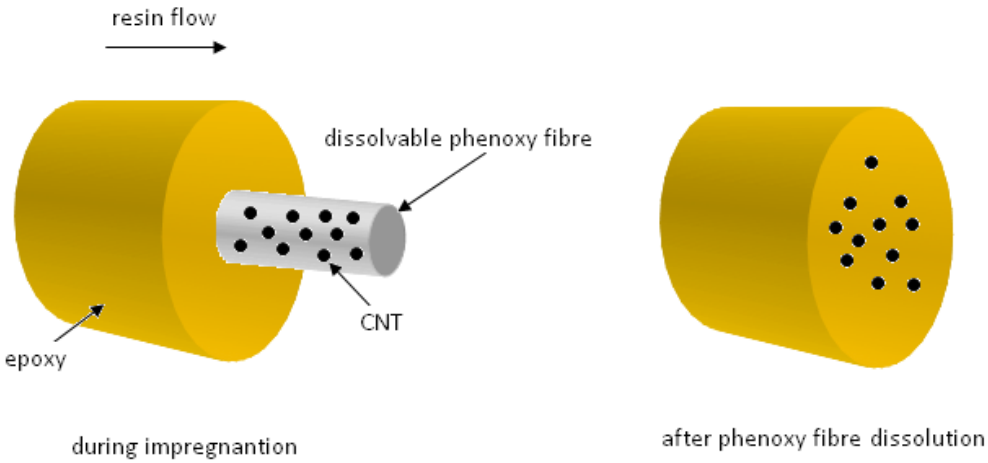

Figure 8.1 A schematic diagram showing the use of dissolvable phenoxy fibres as carriers of CNTs. CNTs could either be coated on or embedded within phenoxy fibres and CNTs are then released into epoxy matrix as phenoxy fibres dissolve.

References

[1] C. B. Bucknall and T. Yoshii, *Relationship between structure and mechanical properties in rubber-toughened epoxy resins*, British Polymer Journal, 1978, 10, p.53.

[2] C. B. Bucknall, *Toughened Plastics* (Applied Science Publishers Limited, London, 1977).

[3] F. J. McGarry, *Building Design with Fibre Reinforced Materials*, Proceedings of Royal Society London, 1970, A319, p.59-68.

[4] C. K. Riew and J. K. Gillham, eds., Rubber Modified Thermoset Resins (American Chemical Society, 1984).

[5] G. Di Pasquale, O. Motta, A. Recca, J. T. Carter, P. T. McGrail and D. Acierna, *New high-performance thermoplastic toughened epoxy thermosets*, Polymer, 1997, 38(17), p.4345-4348.

[6] E. van Overbeke, J. Devaux, R. Legras, J. T. Carter, P. T. McGrail and V. Carlier, *Phase separation in epoxy-copolyethersulphone blends: morphologies and local characterisation by micro-Raman spectroscopy*, Polymer, 2003, 44, p.4899-4908.

[7] G. Y. Nam, G. W. Yong and C. K. Sung, *Toughening of carbon/fibre composites by inserting polysulfone film to form morphology spectrum* Polymer, 2004, 45, p.6953-6958.

[8] F. Mujika, A. D. Benito, B. Fernández, A. Vázquez, R. Llano-Ponte and I. Mondragon, *Mechanical properties of carbon woven reinforced epoxy matrix composites. A study on the influence of matrix modification with polysulfone*, Polymers Composites, 2002, 23(23), p.372-382.

[9] H. S. Min and S. C. Kim, *Fracture toughness of polysulfone/epoxy semi-IPN with morphology spectrum* Polymer Bulletin, 1999, 42, p.221-227.

[10] C. B. Bucknall and I. K. Partridge, *Phase separation in epoxy resins containing polyethersulphone*, Polymer, 1983, 24(5), p.639-644.

[11] D. J. P. Turmel and I. K. Partridge, *Heterogeneous phase separation around fibres in epoxy/PEI blends and its effect on composite delamination resistance*, Composites Science and Technology, 1997, 57(8), p.1001-1007.

[12] L. Bonnaud, J. P. Pascault, H. Sautereau, J. Q. Zhao and D. M. Jia, *Effect of reinforcing glass fibers on morphology and properties of thermoplastic modified epoxy-aromatic diamine matrix*, Polymer Composites, 2004, 25(4), p.368-374.

[13] E. M. Woo and K. L. Mao, *Interlaminar morphology effects on fracture resistance of amorphous polymer-modified epoxy/carbon fibre composites*, Composites Part A: Applied Science and Manufacturing, 1996, 27(8), p.625-631.

[14] R. W. Venderbosch, T. Peijs, H. E. H. Meijer and P. L. Lemstra, *Fibre-reinforced composites with tailored interphases using PPE/epoxy blends as a matrix system*, Composites Part A, 1996, 27, p.895-905.

[15] A. Saalbrink, A. Lorteije and T. Peijs, *The influence of processing parameters on interphase morphology in polymer composites based on phase-separation thermplastic/epoxy blends*, Composites Part A, 1998, 29, p.1243-1250.

[16] A. Saalbrink, M. Mureau and T. Peijs, *Blends of poly(ethylene terepthalate) and epoxy as matrix material for continuous fibre reinforced composites*, Plastics, Rubber and Composites, 2001, 30(5), p.213-221.

[17] K.-C. Teng and F.-C. Chang, *Single-phase and multiple-phase thermoplastic/thermoset polyblends: 2. Morphologies and mechanical properties of phenoxy/epoxy blends*, Polymer, 1996, 37(12), p.2385-2394.

[18] E. M. Woo and K. L. Mao, *Evaluation of interlaminar-toughened poly(ether imide)-modified epoxy/carbon fibre composites*, Polymer Composites, 1996, 17, p.799-805.

[19] J. Kim and R. E. Robertson, *Preparation of poly(butylene terephthalate)-toughened epoxies*, Toughened Plastics I, 1992, Advances in Chemistry Series 233, p.427.

[20] Brian S. Hayes and J. C. Seferis, *Modification of thermosetting resins and composites through preformed polymer particles: A review*, Polymer Composites, 2001, 22(4), p.451-467.

[21] R. J. Day, P. A. Lovell and A. A. Wazzan, *Toughened carbon/epoxy composites made by using core/shell particles*, Composites Science and Technology, 2001, 61(1), p.41-56.

[22] A. Kinloch, K. Masania, A. Taylor, S. Sprenger and D. Egan, *The fracture of glass-fibre-reinforced epoxy composites using nanoparticle-modified matrices*, Journal of Materials Science, 2008, 43(3), p.1151-1154.

[23] B. Wetzel, P. Rosso, F. Haupert and K. Friedrich, *Epoxy nanocomposites - fracture and toughening mechanisms*, Engineering Fracture Mechanics, 2006, 73(16), p.2375-2398.

[24] B. C. Kim, S. W. Park and D. G. Lee, *Fracture toughness of the nano-particle reinforced epoxy composite*, Composite Structures, 2008, 86(1-3), p.69-77.

[25] F. H. Gojny, M. H. G. Wichmann, U. Kopke, B. Fiedler and K. Schulte, *Carbon nanotube-reinforced epoxy-composites: enhanced stiffness and fracture toughness at low nanotube content*, Composites Science and Technology 2004, 64(15), p.2363-2371.

[26] F. Inam, D. W. Y. Wong and T. Peijs, *Multiscale hybrid micro-nanocomposites based on carbon nanotubes and carbon fibers*, Journal of Nanomaterials, 2010(Article ID 453420), p.12 pages.

[27] F. H. Gojny, M. H. G. Wichmann, B. Fiedler, W. Bauhofer and K. Schulte, *Influence of nano-modification on the mechanical and electrical properties of conventional fibre-reinforced composites*, Composites Part A: Applied Science and Manufacturing, 2005, 36(11), p.1525-1535.

[28] N. Sela and O. Ishai, *The effect of adhesive thickness on interlaminar fracture toughness of interleaved CFRP specimen*, Composites, 1989, 20(3), p.257-264.

[29] S.-H. Lee, J.-H. Lee, S.-K. Cheong and H. Noguchi, *A toughening and strengthening technique of hybrid composites with non-woven tissue*, Journal of Materials Processing Technology, 2008, 207(1-3), p.21-29.

[30] P. J. Hogg, *Toughening of thermosetting composites with thermoplastic fibres*, Materials Science and Engineering: A, 2005, 412(1-2), p.97-103.

[31] M.-S. Sohn and X.-Z. Hu, *Processing of carbon-fibre/epoxy composites with cost-effective interlaminar reinforcement*, Composites Science and Technology, 1998, 58(2), p.211-220.

[32] M. S. Sohn, X. Z. Hu, J. K. Kim and L. Walker, *Impact damage characterisation of carbon fibre/epoxy composites with multi-layer reinforcement*, Composites Part B: Engineering, 2000, 31(8), p.681-691.

[33] M. Hojo, S. Matsuda, M. Tanaka, S. Ochiai and A. Murakami, *Mode I delamination fatigue properties of interlayer-toughened CF/epoxy laminates*, Composites Science and Technology, 2006, 66(5), p.665-675.

[34] W. H. Lu, F. S. Liao, A. C. Su, P. W. Kao and T. J. Hsu, *Effect of interleaving on the impact response of a unidirectional carbon/epoxy composite*, Composites, 1995, 26(3), p.215-222.

[35] E. Greenhalgh and M. Hiley, *The assessment of novel materials and processes for the impact tolerant design of stiffened composite aerospace structures*, Composites Part A: Applied Science and Manufacturing, 2003, 34(2), p.151-161.

[36] K. A. Dransfield, L. K. Jain and Y.-W. Mai, *On the effects of stitching in CFRPs--I. mode I delamination toughness*, Composites Science and Technology, 1998, 58(6), p.815-827.

[37] B. V. Sankar and S. K. Sharma, *Mode II delamination toughness of stitched graphite/epoxy textile composites*, Composites Science and Technology, 1997, 57(7), p.729-737.

[38] A. A. J. M. Peijs and J. M. M. De Mok, *Hybrid composites based on polyethylene and carbon fibres*, Composites, 1993, 24(1), p.19-31.

[39] A. A. J. M. Peijs and R. W. Venderbosch, *Hybrid composites based on polyethylene and carbon fibres Part IV Influence of hybrid design on impact strength*, Journal of Materials Science Letters, 1991, 10, p.1122-1124.

[40] C. Thanomsilp and P. J. Hogg, *Interlaminar fracture toughness of hybrid composites based on commingled yarn fabrics*, Composites Science and Technology, 2005, 65(10), p.1547-1563.

[41] R. Van Eijk and T. Peijs, *Impact behaviour of glass/aramid hybrid composites*, Proceedings of the 10th International Conference on Composites Materials (ICCM/10), ed. A., 1995, 5, p.599.

[42] C. K. H. Dharan, *Fracture mechanics of composite materials*, Journal of Engineering Materials and Technology, 1978, 100, p.233-247.

[43] F. F. Lange and K. C. Radford, *Fracture energy of an epoxy composite*, Journal of Materials Science, 1970, 6, p.1197.

[44] R. A. Pearson, *Toughening epoxies using rigid thermoplastics particles*, Toughened Plastics I, 1992, Advances in Chemistry Series 233.

[45] P. Davies, W. Cantwell, C. Moulina and H. H. Kausch, *A study of the delamination resistance of IM6/PEEK composites*, Composites Science and Technology, 1989, 36(2), p.153-166.

[46] K. R. Hirschbuehler, *A comparison of several mechanical tests used to evaluate the toughness of composites, in Toughened Composites*, ASTM STP 937, edited by N. J.Johnston,(American Society for Testing and Materials, Philadelphia, 1987) p. p. 61-73.

[47] J. A. Sayre, R. A. Assink and R. R. Lagasse, *Characterization of the phase structure of an amine cured rubber modified epoxy*, Polymer, 1981, 22(1), p.87-94.

[48] S. Kunz-Douglass, B. P.W.R. and M. F. Ashby, *A model for the tougheness of epoxy-rubber particulate composites*, Journal of Materials Science, 1980, 15, p.1109-1123.

[49] S. Kunz and P. W. R. Beaumont, *Low temperature behaviour of epoxy-rubber particulate composites*, Journal of Materials Science, 1981, 16, p.3141-3152.

[50] M. Frounchi, M. Mehrabzadeh and M. Parvary, *Toughening epoxy resins with solid acrylonitrile-butadiene rubber*, Polymer International, 2000, 49(2), p.163-169.

[51] S. J. Shaw, in "*Toughened Engineering Plastics*", edited by A. A. Collyer (Chapman & Hall, London, 1994).

[52] A. J. Kinloch and S. J. Shaw, *Deformation and fracture behaviour of a rubber-toughened epoxy: 2. Failure criteria*, Polymer, 1983, 24, p.1355-1363.

[53] R. A. Pearson and A. F. Yee, *The preparation and morphology of PPO-epoxy blends*, Journal of Applied Polymer Science, 1993, 48, p.1051-1060.

[54] W. D. Bascom, R. Y. Ting, R. J. Moulton, C. K. Riew and A. R. Siebert, *Fracture of an epoxy polymer containing elastomeric modifiers*, Journal of Materials Science, 1981, 16, p.2657.

[55] B. J. Cardwell and A. F. Yee, *Rate and temperature effects on the fracture toughness of a rubber-modified epoxy*, Polymer, 1993, 34, p.1695.

[56] Y. Huang and A. J. Kinloch, *Modelling of the toughening mechanisms in rubber modified epoxy polymers*, Journal of Materials Science, 1992, 27, p.2763-2769.

[57] R. A. Pearson and A. F. Yee, *Influence of particel size and particle size distribution on toughening mechanisms in rubber-midified epoxies*, Journal of Materials Science, 1991, 26, p.3828-3844.

[58] A. G. Evans and K. T. Faber, *Crack growth resistance of microcracking brittle materials*, Journal of American Ceramic Society, 1984, 67, p.255.

[59] W. Cantwell and J. Morton, *The significance of damage and defects and their detection in composites materials - a Review*, Journal of Strain Analysis for Engineering Design 1992, 27(1), p.29-42.

[60] P. W. R. Beaumont, *Fracture mechanisms in fibrous composites* (Pergamon Press, Oxford, 1979).

[61] A. Kelly and W. R. Tyson, *Tensile properties of fibtr-reinforced metals: copper/tungsten and copper/molybdenum*, Journal of the Mechanics and Physics of Solids, 1965, 13, p.329-350.

[62] L. T. Drzal and M. J. Rich, in "*Advances in Composites in*

The United States and Japan, ASTM STP 864", edited by J. R. Vinson and M. Taya (American Society for Testing and Materials, Philadelphia, 1985) p. 16-26.

[63] P. Davies, in "*Advanced Composites*", edited by I. K. Partridge (Elsevier Applied Science, 1989) p. 303-329.

[64] H. S. Schwartz and J. T. Hartness, in "*Toughened Composites*", edited by N. J. Johnston (American Society for Testing and Materials, Philadelphia, 1987) p. 150-165.

[65] S. Abrate, *Low-velocity imapct damage* (Cambridge University Press, 1998).

[66] P. Davies and M. L. Benzeggagh, in "*Composite Materials Series: Application of Fracture Mechanics to Composite Materials*", edited by K. Friedrich (Elsevier Science Publishers, 1989) p. 81-112.

[67] A. A. Aliyu and I. M. Daniel, in "*Delamination and debonding of materials*", edited by W. S. Johnson (ASTM International, Philadelphia, 1985) p. 336-348.

[68] D. H. Liu, *Impact-Induced Delamination - a View of Bending Stiffness Mismatching*, Journal of Composite Materials, 1988, 22(7), p.674-692.

[69] V. M. A. Calado and S. G. Advani, in "*Processing of Composites*", edited by R. S. Dave and A. C. Loos (Hanser/Gardner Publications, Inc., 1999) p. 33-107.

[70] C. K. Riew, E. H. Rowe and A. R. Siebert, *Rubber Toughened Thermosets*, Advance Chemistry Series, 1976, 154, p.326.

[71] C. K. Riew and A. J. Kinloch, eds., Toughened Plastics I (American Chemical Society, 1993).

[72] S. Sankaran and M. Chanda, *Chemical toughening of epoxies. II. Mechanical, thermal, and microscopic studies of epoxies toughened with hydroxyl-terminated poly(butadiene-co-acrylonitrile)*, Journal of Applied Polymer Science, 1990, 39, p.1635-1647.

[73] C. Kaynak, C. Celikbilek and G. Akovali, *Use of silane coupling agents to improve epoxy-rubber interface*, European Polymer Journal, 2003, 39(6), p.1125-1132.

[74] L. T. Manzione and J. K. Gillham, *Rubber-modified epoxies. II. Morphology and mechanical properties*, Journal of Applied Polymer Science, 1981, 26, p.907-919.

[75] J. N. Sultan and F. J. McGarry, *Effect of rubber particle size on deformation mechanisms in glassy epoxy Polymer Engineering and Science*, Polymer Engineering and Science, 1973, 13, p.29-34.

[76] A. J. Kinloch and D. L. Hunston, *Effect of volume fraction of dispersed rubbery phase on the toughness of rubber-toughened epoxy polymers*, Journal of Materials Science Letters, 1987, 6, p.137-139.

[77] A. Lazzeri and C. B. Bucknall, *Dilatational bands in rubber-toughened polymers*, Journal of Materials Science, 1993, 28, p.6799-6808.

[78] R. A. Pearson and A. F. Yee, *Toughening mechanisms in elastomer-modified epoxies. Part 3. The effect of cross-link density*, Journal of Materials Science, 1989, 24, p.2571-2580.

[79] D. Verchere, J. P. Pascault, H. Sautereau and S. M. Moschiar, *Rubber-modified epoxies. IV. Influenece of Morphology on Mechanical Properties*, Journal of Applied Polymer Science, 1991, 43, p.293-403.

[80] D. Verchere, H. Sautereau and J. P. Pascault, *Rubber-modified epoxies. I. Influence of carboxyl-terminated butadiene-acrylonitrile random copolymers (CTBN) on the polymerisation and phase separation processes*, Journal of Applied Polymer Science, 1990, 41, p.467-485.

[81] J. F. Hwang, J.-A. E. Manson, R. W. Herszberg, G. A. Miller and J. H. Sperling, *Structure-property relationships in rubber-toughened epoxies*, Polymer Engineering & Science, 1989, 29, p.1466.

[82] S. L. Kirshenbaum, S. Gazit and J. P. Bell, *Rubber Modified Thermoset Resins*, Advances in Chemistry Series, 1984, 208.

[83] M. Ochi and J. P. Bell, *Rubber-mofifiled resins containing high functionality acrylic elastomers*, Journal of Applied Polymer Science, 1984, 29, p.1381-1391.

[84] S. L. Kirshenbaum and J. P. Bell, *Matrix viscoelasticity: Controlling factor in the rubber toughening of epoxy resins*, Journal of Applied Polymer Science, 1985, 30, p.1875-1891.

[85] C. Yan, K. Xiao, L. Ye and Y.-W. Mai, *Numerical and experimental studies on the fracture behaviour of rubber-toughened epoxy in bulk specimen and laminated composites*, Journal of Materials Science., 2002, 37(5), p.921-927.

[86] B. G. Min, Z. H. Stachurski, J. H. Hodgkin and G. R. Heath, *Quantitative analysis of the cure reaction of DGEBA/DDS epoxy resins without and with thermoplastic polysulfone modifier using near infra-red spectroscopy*, Polymer, 1993, 34(17), p.3620-3627.

[87] C. D. Wincard and C. L. Beatty, *Crosslinking of an epoxy with a mixed amine as a function of stoichiometry. I. Cure kinetics via dynamic mechanical spectroscopy*, Journal of Applied Polymer Science, 1990, 40, p.1981-2005.

[88] L. T. Manzione and J. K. Gillham, *Rubber-modified epoxies. I. Transitions and morphology*, Journal of Applied Polymer Science, 1981, 26, p.889-905.

[89] K. Yamanaka, Y. Takagi and T. Inoue, *Reaction-induces phase separation in rubber-modified epoxy resins*, Polymer, 1989, 30, p.1839-1844.

[90] J. L. Hedrick, I. Yilgor, G. L. Wilkes and J. E. McGrath, *Chemical modification of matrix resin networks with engineering thermoplastics. 1. Phenolic hydroxyl terminated poly(aryl ether sulfone)-epoxy systems*, Polymer Bulletins, 1985, 13, p.201.

[91] R. A. Pearson, *Sources of toughness in modified epoxies*, Polymer Material Science and Engineering, 1990, 26, p.311-314.

[92] K.-C. Teng and F.-C. Chang, *Single-phase and multiple-phase thermoplastic/thermoset polyblends: 1. Kinetics and mechanisms of phenoxy/epoxy blends*, Polymer, 1993, 34(20), p.4291-4299.

[93] Q. Guo, *Effect of curing agent on the phase behaviour of epoxy resin/phenoxy blends*, Polymer, 1995, 25(25), p.4753-4760.

[94] S. K. Siddhamalli and T. Kyu, *Toughening of thermoset/thermoplastic composites via reaction-induced phase separation: epoxy/phenoxy blends*, Journal of Applied Polymer Science, 2000, 77, p.1257-1268.

[95] G. Pena, A. Eceiza, A. Valea, P. Remiro, P. Oyanguren and I. Mondragon, *Control of morphologies and mechanical properties of thermoplastic-modified epoxy matrices by addition of a second thermoplastic*, Polymer International, 2003, 52, p.1444-1453.

[96] E. Schauer, L. Berglund, G. Pena, C. Marieta and I. Mondragon, *Morphological variations in PMMA-modified epoxy mixtures by PEO addition*, Polymer, 2002, 43(4), p.1241-1248.

[97] Y. Cao, Y. Shao, J. Sun and S. Lin, *Mechanical Properties of an Epoxy Resin Toughened by Polyester*, Journal of Applied Polymer Science, 2003, 90, p.3384-3389.

[98] S. Japon, L. Boogh, Y. Leterrier and J.-A. E. Manson, *Reactive processing of poly(ethylene terepthalate) modified with multifunctional epoxy-based additives*, Polymer, 2000, 41, p.5809-5818.

[99] F. Fenouillot, C. Hedreul, J. Forsythe and J.-P. Pascault, *Reaction and miscibility of two diepoxides with poly(ethylene terephthalate)*, Journal of Applied Polymer Science, 2003, 87, p.1995-2003.

[100] P. Huang, Z. Zhong, S. Zheng, W. Zhu and Q. Guo, *Miscibility and interchange reactions in blends of bisphenol-A-type epoxy resin and poly (ethylene terephthalate)*, Journa of Applied Polymer Science, 1998, 73, p.639-647.

[101] P. A. Oyanguren, P. M. Frontini, R. J. J. Williams, G. Vigier and J. P. Pascault, *Reaction-induced phase separation in poly(butylene terephthalate)-epoxy systems: 1. Conversion-temperature transformation diagrams*, Polymer, 1996, 37, p.3079-3085.

[102] P. Oyanguren, P. M. Frontini, R. J. J. Williams and J. P. Pascault, *Phase separation in PBT-epoxy systems: 2. Morphologies generated and resulting properties*, Polymer, 1996, 37(14), p.3087-3092.

[103] H. S. Kim and P. Ma, *Mode II Fracture mechanisms of PBT-modified brittle epoxies*, Journal of Applied Polymer Science, 1998, 69, p.405-415.

[104] S. Kim, H. J. Won, J. Kim, H. L. Soon and R. C. Chul, *The effect of crystalline morphology of poly(butylene terephthalate) phases on toughening on poly(butylene terephthalate)/epoxy blends*, Journal of Materials Science, 1999, 34, p.161-168.

[105] S. T. Kim , J. Y. Kim , S. Lim , C. R. Choe and S. I. Hong *The phase transformation toughening and synergism in poly(butylene terephthalate)/poly(tetramethyleneglycol) copolymer-modified epoxies*, Journal of Materials Science, 1998, 33(9), p.2421-2429.

[106] Y.-M. Liu, W.-D. Zhang and H.-W. Zhou, *Mechanical properties of epoxy resin/hydroxyl-terminated polyester blends: effect of two-phase structure*, Polymer International, 2005, 54(10), p.1408-1415.

[107] M. Tanoglu, S. Robert, D. Heider, S. H. McKnight, V. Brachos and G. J. J.W., *Effects of thermoplastic preforming binder on the properties of S2 glass fabric reinforced epoxy composites*, International Journal of Adhesion and Adhesives, 2001, 21, p.187-195.

[108] L. Boogh, B. Pettersson and J.-A. E. Manson, *Dendritic hyperbranched polymers as toughenersfor epoxy resins*, Polymer, 1999, 40(9), p.2249-2261.

[109] R. Mezzenga, L. Boogh and J.-A. E. Manson, *A review of dendritic hyperbranched polymer as modifiers in epoxy composites*, Composite Science and Technology, 2001, 61, p.787-795.

[110] J. Verrey, Y. Winkler, V. Michaud and J.-A. E. Manson, *Interlaminar fracture toughness improvement in composites with hyperbranched polymer modified resin*, Composites Science and Technology, 2005, 65(10), p.1527-1536.

[111] M. DeCarli, K. Kozielski, W. Tian and R. J. Varley, *Toughening of a carbon fibre reinforced epoxy anhydride composite using an epoxy terminated hyperbranched modifier*, Composites Science and Technology, 2005, 65(14), p.2156-2166.

[112] C. B. Bucknall and A. H. Gilbert, *Toughening tetrafunctional epoxy resins using polyetherimide*, Polymer, 1989, 30.

[113] D. J. Hourston, J. M. Lane and H. X. Zhang, *Toughening of epoxy resins with thermoplastics: 3. An investigation into the effects of composition on the properties of epoxy resin blends*, Polymer International, 1997, 42, p.349-355.

[114] C. Su and E. M. Woo, *Cure kinetics and morphology of amine-cured tetraglycidyl-4,4-diaminodiphenylmethane epoxy blends with poly(ether imide)*, Polymer, 1995, 36, p.2883-2894.

[115] M. I. Giannotti, C. R. Bernal, P. A. Oyanguren and M. J. Galante, *Morphology and fracture properties relationshop of epoxy-diamine systems simutanelously modified with polysulfone and poly(ether imide)*, Polymer Engineering & Science, 2005.

[116] M. Naffakh, M. Dumon and J. F. Gerard, *Study of a reactive epoxy-amine resin enabling in situ dissolution of thermoplastic films during resin transfer moulding for toughening composites*, Composites Science and Technology, 2006, 66, p.1376-1384.

[117] M.-S. Lu, J.-L. Chen, Y.-S. Li, F.-C. Chang, M.-S. Li and C.-C. Ma, *The kinetics, thermal and mechanical properties of epoxy-polycarbonate blends cured with aromatic amine*, Journal of Polymer Research, 1998, 5(2), p.115-124.

[118] C.-H. Y. J. P. B. Trong-Ming Don, *Structures and properties of polycarbonate-modified epoxies from two different blending processes*, Journal of Applied Polymer Science, 1999, 74(10), p.2510-2521.

[119] V. Rajulu, G. Babu Rao, L. Ganga Devi, P. J. Balaji, J. He and J. Zhang, *Interlaminar shear strength of polycarbonate toughened epoxy compsoites reinforced with glass rovings*, Advances in Polymer Technology, 2003, 22(4), p.373-377.

[120] R. A. Pearson and A. F. Yee, *Toughening mechanisms in thermoplastics-modified epoxies: 1. Modification using poly(phenylene oxide)*, Polymer, 1993, 34(17), p.3658-3670.

[121] Q. Guo, J. Huang, L. Ge and Z. Feng, *Phase separation in anhydride-cured epoxy resin containing phenolphthalein poly(ether ether ketone)*, European Polymer Journal, 1992, 28, p.405-409.

[122] F. Bejoy, L. V. Rao, J. Seno, C. K. Bina, Y. Ramaswamy, J. Jesmy and T. Sabu, *Poly(ether ether ketone) with pendent methyl groups as a toughening agent for amine cured DGEBA epoxy resin*, Journal of Materials Science, 2006, 41(17), p.5467-5479.

[123] T. Iijima, T. Tochimoto and M. Tomoi, *Modification of epoxy resins with poly(aryl ether ketone)s*, Journal of Applied Polymer Science, 1991, 43, p.1685-1692.

[124] R. S. Raghava, *Role of matrix-particle interface adheshion on fracture toughness of dual phase epoxy-polyethersulfone blend*, Journal of Polymer Science: Part B, 1987, 25, p.1017-1031.

[125] C. B. Bucknall and I. K. Partridge, *Phase separation in epoxy resins containing polyethersulphone*, Polymer, 1983, 24, p.639-644.

[126] R. S. Raghava, *Development and characterization of thermosetting-thermoplastic polymer blends for applications in damage-tolerant composites*, Journal of Polymer Science Part B: Polymer Physics, 1988, 26(1), p.65-81.

[127] Z. Fu and Y. Sun, *Epoxy resin toughened by thermoplastics*, Polymer Preparation 1988, 29(2).

[128] I. Blanco, G. Cicala, Lo Faro and C. Antonio Recca, *Development of a toughened DGEBA/DDS system toward improved thermal and mechanical properties by the addition of a tetrafunctional epoxy resin and a novel thermoplastic*, Journal of Applied Polymer Science, 2003, 89(1), p.268-273.

[129] S. Elliniadis, J. S. Higgins, N. Clarke, T. C. B. McLeish, R. A. Choudhery and S. D. Jenkins, *Phase diagram prediction for thermoset/thermoplastic polymer blends*, Polymer, 1997, 38(19), p.4855-4862.

[130] B. S. Kim, T. Chiba and T. Inoue, *Phase separation and apparent phase dissolution during cure process of thermoset/thermoplastic blend*, Polymer, 1995, 36(1), p.67-71.

[131] A. McKinnon, S. D. Jenkins, P. T. McGrail and R. A. Pethrick, *A dielectric, mechanical, rheological and electron microscopy study of cure and properties of a thermoplastic-modified epoxy resin*, Macromolecules, 1992, 25(13), p.3492-3499.

[132] G. Cicala, A. Recca and C. Restuccia, *Influence of hydroxyl functionalized hyperbranched polymers on the thermomechanical and morphological properties of epoxy resins*, Polymer Engineering & Science, 2005, 45(2), p.225-237.

[133] I. Martinez, M. D. Martin, A. Eceiza, P. Oyanguren and I. Mondragon, *Phase separation in polysulfone-modified epoxy mixtures. Relationships between curing conditions, morphology and ultimate behavior*, Polymer, 2000, 41(3), p.1027-1035.

[134] R. J. Varley, J. H. Hodgkin, D. G. Hawthorne, G. P. Simon and D. McCulloch, *Toughening of a trifunctional epoxy system Part III. Kinetic and morphological study of the thermoplastic modified cure process*, Polymer, 2000, 41, p.3425-3436.

[135] L. Matejka, K. Dusek, J. Plestil, J. Kriz and F. Lednicky, *Formation and structure of the epoxy-silica hybrids*, Polymer, 1999, 40(1), p.171-181.

[136] C. K. Riew, A. R. Siebert, R. W. Smith, M. Fernando and A. J. Kinloch, *Toughened epoxy resin: Preformed particles as toughener*, Polymeric

Materials Science and Engineering, Proceedings of the ACS Division of Polymeric Materials Science and Engineering,(1993) p. 5.

[137] Y. Nakamura, M. Yamaguchi and A. Kitayama, *Effect of particles size on fracture toughness of epoxy resin filled with angular-shaped silica*, Polymer, 1991, 32(12), p.2221-2032.

[138] E. Urbaczewski-Espuche, J. F. Gerard, J. P. Pascault, G. Reiffo and J. Sautereau, *Toughness improvement of an epoxy/anhydride matrix. Influence on processing and fatigue properties of unidirectional glass-fiber composites*, Journal of Applied Polymer Science, 1994, 47, p.991-1002.

[139] J. Lee and A. F. Yee, *Role of inherent matrix toughness on fracture of glass bead filled epoxies*, Polymer, 2000, 41(23), p.8375-8385.

[140] Y. Nakamura, M. Yamaguchi, M. Okubo and T. Matsumoto, *Effects of particle size on mechnical and impact properties of epoxy resin filled with spherical silica*, Journal of Applied Polymer Science, 1992, 45, p.1281-1289.

[141] N. Amdouni, H. Sautereau and J. F. Gerard, *Epoxy composites based on glass beads. II. Mechanical properties*, Journal of Applied Polymer Science, 1992, 46, p.1723-1735.

[142] J. Spanoudakis and R. J. Young, *Crack propagation in a glass particle-filled epoxy resins*, Journal of Materials Science, 1984, 19, p.473-486.

[143] J. Lee and A. F. Yee, *Inorganic particle toughening II: toughening mechanisms of glass bead filled epoxies*, Polymer, 2001, 42, p.589-597.

[144] G. C. Eastmond and G. Mucciarello, *Polymer filler interaction in composites with grated filler particles*, Polymer, 1982, 23, p.164.

[145] Y. G. Lin, J. P. Pascault, H. Sautereau and W. de Gruyter, Polymer, 1986, 23, p.373.

[146] N. Amdouni, J. Sautereau, J. F. Gerard, F. Fernagut, G. Coulon and J. M. Lefebvre, *Coated glass beads epoxy composites: influence of the interlayer thickness on pre-yielding and fracture properties*, Journal of Materials Science, 1990, 25(2), p.1435-1443.

[147] D. Maxwell, R. J. Young and A. J. Kinloch, *Hybrid particulate-filled epoxy polymers*, Journal of Materials Science Letters, 1984, 3(1), p.9-12.

[148] A. J. Kinloch, D. Maxwell and R. J. Young, *Fracture of hybrid-particulate composites*, Journal of Materials Science Letters, 1985, 20, p.4169-4184.

[149] N. Schroder, L. Koncolm, W. Doll and R. Mulhaupt., *Mechanical properties of epoxy-based hybrid composites containing glass beads and alpha,omega-oligo(butylmethacrylate)diol*, Journal of Applied Polymer Science, 2003, 88, p.1040-1048.

[150] J. Sandler, M. S. P. Shaffer, T. Prasse, W. Bauhofer, K. Schulte and A. H. Windle, *Development of a dispersion process for carbon nanotubes in an epoxy matrix and the resulting electrical properties*, Polymer, 1999, 40(21), p.5967-5971.

[151] A. Allaoui, S. Bai, H. M. Cheng and J. B. Bai, *Mechanical and electrical properties of a MWNT/epoxy composite*, Composites Science and Technology, 2002, 62(15), p.1993-1998.

[152] F. H. Gojny and K. Schulte, *Functionalisation effect on the thermal-mechanical behaviour of multi-wall carbon nanotube/epoxy composites*, Composites Science and Technology, 2004, 64(15), p.2303-2308.

[153] D. Puglia, L. Valentini, I. Armentano and J. M. Kenny, *Effects of single-walled carbon nanotube incorporation on the cure reaction of epoxy resin and its detection by raman spectroscopy*, Diamond and Related Materials, 2003, 12, p.827-832.

[154] L. Valentini, I. Armentano, D. Puglia and J. M. Kenny, *Dynamics of amine functionalised nanotubes/epoxy composites by dielectrix relaxation spectroscopy*, Carbon, 2004, 42(2).

[155] J. Zhu, J. D. Kim, H. Peng, J. L. Margrave, V. N. Khabashesku and E. V. Barrera, *Improving the dispersion and integration of single-walled carbon nanotubes in epoxy composites through functionalization*, Nano Letters, 2003, 3, p.1107-1113.

[156] T. Yokozeki, Y. Iwahori, M. Ishibashi, T. Yanagisawa, K. Imai, M. Arai, T. Takahashi and K. Enomoto, *Fracture toughness improvement of CFRP laminates by dispersion of cup-stacked carbon nanotubes*, Composites Science and Technology, 2009, 69(14), p.2268-2273.

[157] S. Spindler-Ranta and C. E. C.E. Bakis, *Carbon nanotube reinforcement of a filament winding resin*, Proceedings of 47th international SAMPE Symposium and Exhibition,(Long Beach, California, 2002) p. 1775-1787.

[158] V. P. Veedu, A. Cao, X. Li, K. Ma, C. Soldano, S. Kar, P. M. Ajayan and M. N. Ghasemi-Nejhad, *Multifunctional composites using reinforced laminae with carbon-nanotube forests*, Nature Materials, 2006, 5(6), p.457-462.

[159] M. H. G. Wichmann, J. Sumfleth, F. H. Gojny, M. Quaresimin, B. Fiedler and K. Schulte, *Glass-fibre reinforced composites with enhanced mechanical and electrical properties – benefits and limitations of a nanoparticle modified matrix* Engineering Fracture Mechanics, 2006, 73, p.2346-2359.

[160] M.-S. Kim, S.-E. Lee, W.-J. Lee and C.-G. Kim, *Mechanical properties of MWNT-loaded plain-weave glass/epoxy composites*, Advanced Composite Materials, 2009, 18(3), p.209-219.

[161] V. C. S. Chandrasekaran, M. H. Santare and S. G. Advani, *Pseudo reinforcement effect of multi-walled carbon nanotubes in epoxy/glass fibre hybrid composites*, Proceedings of the 9th international conference on Textile Composites,(Newark, 2008) p. 34-41.

[162] A. Godara, L. Mezzo, F. Luizi, A. Warrier, S. V. Lomov and A. W. van Vuure, *Influence of carbon nanotube reinforcement on the processing and the mechanical behaviour of carbon fiber/epoxy composites*, Carbon, 2009, 47, p.2914-2923.

[163] Y. Zhou, F. Pervin, S. Jeelani and P. K. Mallick, *Improvement in mechanical properties of carbon fabric-epoxy composite using carbon nanofibers*, Journal of Materials Processing Technology, 2008, 198(1-3), p.445-453.

[164] N. A. Siddiqui, R. S. C. Woo, J.-K. Kim, C. C. K. Leung and A. Munir, *Mode I interlaminar fracture behavior and mechanical properties of CFRPs with nanoclay-filled epoxy matrix*, Composites Part A: Applied Science and Manufacturing, 2007, 38(2), p.449-460.

[165] S. J. Ahmadi, Y. D. Huang and W. Li, *Synthetic routes, properties and future applications of polymer-layered silicate nanocomposites*, Journal of Materials Science, 2004, 39(6), p.1919-1925.

[166] S.-J. Park, B.-J. Kim, D.-I. Seo, K.-Y. Rhee and Y.-Y. Lyu, *Effects of a silane treatment on the mechanical interfacial properties of montmorillonite/epoxy*

nanocomposites, Materials Science and Engineering: A, 2009, 526(1-2), p.74-78.

[167] C. Kaynak, G. I. Nakas and N. A. Isitman, *Mechanical properties, flammability and char morphology of epoxy resin/montmorillonite nanocomposites*, Applied Clay Science, 2009, 46(3), p.319-324.

[168] J. E. Masters, *Improved impact and delamination resistance through interleafing*, Engineering Materials, 1989, 37, p.317-348.

[169] J. E. Masters, *Correlation of impact and delamination resistance in interleaved laminates*, Proceedings of 6th ICCM/2nd ECCM (Elsevier Applied Science, London, 1989) p. 3.96-93.107.

[170] A. Duarte, I. Herszberg and R. Paton, *Impact resistance and tolerance of interleaved tape laminates*, Composite Structures, 1999, 47, p.753-758.

[171] O. Ishai, H. Rosenthal, N. Sela and E. Drukker, *Effect of selective adhesive interleaving on interlaminar fracture toughness of graphite/epoxy composite laminates*, Composites, 1988, 19(1), p.49-54.

[172] F. Ozdil and L. F. Carlsson, *Mode I interlaminar fracture of interleaved graphite/epoxy*, Journal of Composite Materials, 1992, 26(3), p.432-459.

[173] N. Sela, O. Ishai and L. Banks-Sills, *The effect of adhesive thickness on interlaminar fracture toughness of interleaved CRRP specimens*, Composites, 1989, 20(3), p.257-264.

[174] E. Altus and O. Ishai, *The effect of soft interleaved layers on the combined transverse cracking/delamination mechanisms in composite laminates*, Composites Science and Technology, 1990, 39, p.13-27.

[175] S. Rechak and C. T. Sun, *Optimal use of adhesive layers in reducing impact damahe in composite laminates*, Journal of Reinforced Plastics and Composites, 1990, 9, p.569-582.

[176] S. Matsuda, M. Hojo, S. Ochiai, A. Murakami, H. Akimoto and M. Ando, *Effect of ionomer thickness on mode I interlaminar fracture toughness for ionomer toughened CFRP*, Composites: Part A, 1999, 30, p.1311-1319.

[177] M. R. Groleau, Y. B. Shi, A. F. Yee, J. L. Bertram, H. J. Sue and P. C. Yang, *Mode II fracture of composites interlayered with nylon particles*, Composites Science and Technology, 1996, 56(11), p.1223-1240.

[178] F. Gao, G. Jiao and Z. Lu, *Mode II delamination and damage resistance of carbon/epoxy composite laminates interleaved with thermoplastic particles*, Journal of Composite Materials, 2007, 41(1), p.111-123.

[179] B. J. Derkowski and H. J. Sue, *Morphology and compression-after-impact strength relationship in interleaved toughened composites*, Polymer Composites, 2003, 24(1), p.158-170.

[180] L. Walker, M.-S. Sohn and X.-Z. Hu, *Improving impact resistance of carbon fibre composites through interlaminar reinforcement*, Composites Part A, 2002, 33, p.893-902.

[181] M.-S. Sohn and X.-Z. Hu, *Mode II delaminatiopn toughness of carbon fibre/epoxy composites with chopped Kevlar fibre reinforcement*, Composites Science and Technology, 1994, 52, p.439-448.

[182] J. Kim, M. Shioya, H. Kobayashi, J. Kaneko and M. Kido, *Mechanical properties of woven laminates and felt composites using carbon fibers. Part 2: interlaminar properties*, Composites Science and Technology, 2004, 64, p.2231-2238.

[183] N. Alif, L. A. Carlsson and L. Boogh, *The effect of weave pattern and crack propagation direction on mode I delamination resistance of woven glass and carbon composites*, Composites: Part B, 1998, 29.

[184] A. P. Mouritz, C. Baini and I. Herszberg, *Mode I interlaminar fracture toughness properties of advanced textile fibreglass composites*, Composites: Part A, 1999, 30.

[185] T. Osada, A. Nakai and H. Hamada, *Initial fracture behaviour of satin woven fabric composites*, Composite Structures, 2003, 61, p.333-339.

[186] P. T. Curtis and S. M. Bishop, *An assessment of the potential of woven carbon fiber-reinforced plastics for high performance applications*, Composites, 1984, 15(4), p.259-265.

[187] B. Schrauwen and T. Peijs, *Influence of matrix ductility and fibre architecture on the repeated impact response of glass fibre reinforced laminated composites*, Applied Composite Materials, 2002, 9, p.331-352.

[188] M. A. Portanova, *Impact damage tolerance of textile composites*, Proceedings of the 28th International SAMPE Technical Conference,(SAMPE, 1996) p. 351-362.

[189] W. C. Jackson and M. A. Portanova, *Impact damage resistance of textile composites*, Proceedings of the 28th SAMPE Technical Conference,(SAMPE, 1996) p. 339-350.

[190] V. A. Guenon, T. W. Chou and J. W. Gillespie, *Toughness properties of a 3-dimensional carbon epoxy composite*, Journal of Materials Science, 1989, 24(11), p.4168-4175.

[191] F. K. Ko, in "*Composite Materials Series; Textile Structural Composites*", edited by T. W. Chou, Ko, F.K. (Elsevier Science Publishers, 1989) p. 129-171.

[192] L. C. Dickinson, G. L. Farley and M. K. Hinders, *Translaminar reinforced composites: a review*, Journal of Composite Technology and Research 1999, 21(1), p.3-15.

[193] K. A. Dransfield, C. Baillie and Y. W. Mai, *On the effects of stitching in CFRPs - I. Mode I delamination toughness*, Composites Science and Technology, 1994, 58(6), p.815-827.

[194] L. K. Jain, K. A. Dransfield and Y. W. Mai, *On the effects of stitching in CFRPs - II: Mode II delamination toughness*, Composites Science and Technology, 1998, 58(6), p.829-837.

[195] I. K. Partridge, D. D. R. Cartie and T. Bonnington, in "*Advanced Polymer Materials: Structure Property Relationship*", edited by G. O. Shonaike and S. G. Advani (CRC Press, 2003).

[196] R. C. L. Dutra, B. G. Soares, E. A. Campos and J. L. G. Silva, *Hybrid composites based on polypropylene and carbon fiber and epoxy matrix*, Polymer, 2000, 41, p.3841-3849.

[197] C. J. Wang, B. Z. Jang, J. Panus and B. T. Valaire, *Impact behavior of hybrid-fiber and hybrid-matrix composites* Journal of Reinforced Plastics and Composites, 1991, 10(4), p.356-378.

[198] B. Z. Jang, L. C. Chen, C. Z. Wang, H. T. Lin and R. H. Zee, *Impact resistance and energy absorption mechanisms in hybrid composites*, Composites Science and Technology, 1989, 34(4), p.305-335.

[199] A. A. J. M. Peijs, R. W. Venderbosch and P. J. Lemstra, *Hybrid composites based on polyethylene and carbon fibres Part 3: Impact resistant structural composites through damage management*, Composites, 1990, 21(6), p.522-530.

[200] A. A. J. M. Peijs, P. Catsman, L. E. Govaert and P. J. Lemstra, *Hybrid composites based on polyethylene and carbon fibres Part 2: influence of composition and adhesion level of polyethylene fibres on mechanical properties*, Composites, 1990, 21(8), p.513-521.

[201] A. Andonova, G. Bogoeva-Gaceva and B. Mangovska, *Hybrid C/PET/epoxy composites*, Journal of Materials Science, 1995, 30, p.1545-1550.

[202] D. J. Hourston, J. M. Lane and N. A. MacBeath, *Toughening of epoxy resins with thermoplastics. Ii. Tetrafunctional epoxy resin-polyetherimide blends*, Polymer International, 1991, 26(1), p.17-21.

[203] J. H. Hodgkin, G. P. Simon and R. J. Varley, *Thermoplastic Toughening of Epoxy Resins: a Critical Review*, Polymers for Advanced Technologies, 1998, 9, p.3-10.

[204] D. J. Hourston and J. M. Lane, *The toughening of epoxy resins with thermoplastics: 1. Trifunctional epoxy resin-polyetherimide blends*, Polymer, 1992, 33(7), p.1379-1383.

[205] B. G. Min, Z. H. Stachurski and J. H. Hodgkin, *Cure kinetics of elementary reactions of a diglycidyl ether of bisphenol A/diaminodiphenylsulfone epoxy resin: 2. Conversion versus time*, Polymer, 1993, 34(21), p.4488-4495.

[206] J. L. Hedrick, I. Yilgor, G. L. Wilkes and J. E. McGrath, *Chemical modification of matrix Resin networks with engineering thermoplastics* Polymer Bulletin, 1985, 13(3), p.201-208.

[207] ASTM D638-03 Standard Test Method for Tensile Properties of Plastics, (ASTM International).

[208] ASTM D5045-99 Standard test methods for plane-strain fracture toughness and strain energy release rate of plastic materials, (ASTM International).

[209] H. K. Hseih, C. C. Su and E. M. Woo, *Cure kinetics and inter-domain etherification in an amine-cured phenoxy/epoxy system* Polymer, 1998, 39(11), p.2175-2183.

[210] http://www.cytec.com/engineered-materials/Priform.htm.

[211] J. T. Carter, C. Lo Faro, R. K. Maskell and P. T. McGrail, *Flexible polymer element as toughening agent in prepregs,* Cytec Technology Corp. Wilmington, DE, US, US patent number 7192634

[212] http://www.emsgriltech.com/.

[213] U. Beier, F. Wolff-Fabris, F. Fisher, J. K. W. Sandler, V. Altstadt, G. Hulder, E. Schmachtenberg, H. Spanner, C. Weimer, T. Roser and W. Buchs, *Mechanical performance of carbon fibre-reinforced composites based on preforms stitched with innovative low-melting temperature and matrix soluble thermoplastic yarns*, Composites Part A, 2008, 39, p.1572-1581.

[214] ASTM D3039-00 Standard Test Method for Tensile Properties of Polymer Matrix Composite Materials, (ASTM International).

[215] ASTM D5528-01 Standard test method for mode I interlaminar fracture toughness of unidirectional fibre-reinforced polymer matrix composites, (ASTM International).

[216] T. K. O'Brien and R. H. Martin, *Round robin testing for Mode I interlaminar fracture toughness of composite materials*, ASTM Journal of Composites Technology and Research, 1993, 15(4), p.2690281.

[217] ASTM D2344-00 Standard Test Method for Short-Beam Strength of Polymer Matrix Composite Materials and Their Laminates, (ASTM International).

[218] P. J. Hogg and G. A. Bibo, in "*Mechanical testing of advance fibre composites*", edited by J. M. Hodgkinson (CRC Press, 2000) p. 211-244.

[219] P. J. Hogg, J. C. Pritchard and D. L. Stone, in "*Composites Testing and Standardisation: ECCM-CTS : European Conference on Composites Testing*

and Standardisation" (European Association for Composite Materials, Amsterdam, 1992) p. 357-377.

[220] M. Kuwata, *Mechanisms of interlaminar fracture toughness using non-woven veils as interleaf materials*, 2010, Queen Mary, University of London; PhD thesis

[221] G. S. Springer, *Environmental Effects on Composite Materials* (Technomic, Westport, USA, 1981).

[222] BS EN 60068-2-45 Basic environmental testing procedures: immersion in cleaning solvents, (British Standard).

[223] ASTM C581 Determining chemical resistance of thermosetting resins used in glass-fibre reinforced structures intended for liquid service, (ASTM International).

[224] ASTM D543 Resistance of plastics to chemical reagents, (ASTM International).

[225] ISO 1776 Glass: resistance to attack by hydrochloric acid at 100°C, (International Organization for Standardization).

[226] F. R. Jones, in "*Reinforced plastics durability*", edited by G. Pritchard (CRC Press, 2000) p. 70-110.

[227] J. A. Hough and F. R. Jones, *Effect of thermoplastic additives and carbon fibres on the thermally enhanced moisture absorption by epoxy resins*, Eleventh International Conference on Composite Materials (ICCMIII) edited by M. L. Scott,(Composites Structures Society, Cambridge, UK, 1997) p. 421-431.

[228] J. A. Hough, F. R. Jones and Z. D. Xiang, *Thermally enhanced moisture absorption and related degradation mechanisms in composite materials*, Proceedings 4th International Conference Deformation and Fracture of Composites,(Institute of Materials, London, 1997) p. 181-190.

[229] G. Pritchard, in "*Mechanical testing of advanced fibre composites*", edited by J. M. Hodgkinson (CRC Press, 2000) p. 269-291.

[230] P. Ciselli, Z. Wang and T. Peijs, *Reinforcing potential of carbon nanotubes in oriented polymer fibres*, Materials Technology, 2007, 22(1), p.10-21.

[231] Z. Wang, P. Ciselli and T. Peijs, *The extraordinary ordinary reinfocing efficiency of single-walled carbon nanotubes in oriented poly(vinyl alcohol) tapes*, Nanotechnology 2007, 18(45), p.455709.

[232] F. H. Gojny, M. H. G. Wichmann, B. Fiedler and K. Schulte, *Influence of different carbon nanotubes on the mechanical properties of epoxy matrix composites*, Composites Science and Technology, 2005, 65(15-16), p.2300-2313.

[233] B. Fiedler, F. H. Gojny, M. H. G. Wichmann, M. C. M. Nolte and K. Schulte, *Fundamental aspects of nano-reinforced composites*, Composite Science and Technology, 2006, 66(16), p.3115-3125.

[234] J. H. Du, J. Bai and H. M. Cheng, *The present status and key problems of carbon nanotube based polymer composites*, Express Polymer Letters, 2007, 2(1), p.40-48.

[235] Y. X. Zhou, P. X. Wu, Z. Y. Cheng, J. Ingram and S. Jeelani, *Improvement in electrical, thermal and mechanical properties of epoxy by filling carbon nanotube*, Express Polymer Letters, 2008, 2(1), p.40-48.

[236] J. Sandler, M. S. P. Shaffer, T. Prasse, W. Bauhofer, K. Schulte and A. H. Windle, *Ultra-low electrical percolation threshold in carbon-nanotube-epoxy composites*, Polymer, 2003, 44(19), p.5893-5899.

[237] R. Zhang, A. Dowden, H. Deng, M. Baxendale and T. Peijs, *Conductive nerwork formation in the melt of carbon nanotube/thermoplastic polyurethane composite*, Composites Science and Technology, 2009, 69(10), p.1499-1504.

[238] R. Zhang, A. Dowden, H. Deng, M. Baxendale and T. Peijs, *Universal resistivity-strain dependence of carbon nanotube/polymer composites*, Physical Review B, 2007, 76(19), p.195433.

[239] F. Inam and T. Peijs, *Re-aggregation of carbon nanotubes in two-component epoxy system*, Journal of Nanostructured Polymers and Nanocomposites, 2006, 2(3), p.87-95.

[240] J. D. Currey, *Encyclopedia of Materials: Science and Technology* (Elsevier Science Ltd., 2001).

[241] B. Schrauwen, P. Bertens and T. Peijs, *Influence of hybridisation and test geometry on the impact response of glass fibre reinforced laminated composites*, Polymer and Polymer Composites, 2002, 10(4), p.259-272.

[242] P. Karapappas, A. Vavouliotis, A. P. Tsotra, V. Kostopoulos and A. Paipetis, *Enhanced fracture properties of carbon reinforced composites by the addition of multi-wall carbon nanotubes*, Journal of Composite Materials, 2009, 43(9), p.977-985.

[243] J. Njuguna, K. Pielichowski and J. R. Alcock, *Epoxy based fibre reinforced nanocomposites*, Advanced Engineering Materials, 2007, 9(10), p.835-847.

[244] T. Mahrholz, J. Mosch, D. Rostermundt, U. Riedel, L. Herbeck and M. Sinapius, *Fibre reinforced nanocomposites for spacecraft structures: Manufacturing characterization and application.*, European Conference on Spacecraft Structures, Materials and Mechanical Testing,(Noordwijk, The Netherlands, 2005) p. 1445-1454.

[245] G. Romhany and G. Szebenyi, *Interlaminar crack propagation on MWCNT/fibre reinforced hybrid composites*, Express Polymer Letters, 2009, 3(3), p.145-151.

[246] C. Chen and D. Curliss, *Resin matrix composites: Organoclay-aerospace epoxy nanocomposites , Part II*, SAMPE Journal, 2001, 37(5), p.11-18.

[247] B. P. Rice, C. Chen, L. Cloos and D. Curliss, *Carbon fibre composites: Organoclay aerospace epoxy nanocomposites, Part I*, SAMPE Journal, 2001, 37(5), p.7-9.

[248] S. Tsantzalis, P. Karapappas, A. Vavouliotis, A. P. Tsotra, A. Paipetis, V. Kostopoulos and K. Friedrich, *Enhancement of the mechanical performance of an epoxy resin and fibre reinforced epoxy resin composites by the introduction of CNF and PZT particles at the microscale*, Composites Part A: Applied Science and Manufacturing, 2007, 38(4), p.1076-1081.

[249] S. Tsantzalis, P. Karapappas, A. Vavouliotis, A. P. Tsotra, V. Kostopoulos, T. Tanimoto and K. Friedrich, *On the improvement of toughness of CFRPs with resin doped with CNF and PZT particles*, Composites Part A: Applied Science and Manufacturing, 2007, 38(4), p.1159-1162.

[250] F. H. Chowdhury, M. V. Hosur and S. Jeelani, *Studies on the flexural and thermomechanical properties of woven carbon/nanoclay-epoxy laminates*, Materials Science and Engineering A, 2006, 421(1-2), p.298-306.

[251] F. Hussain, D. Dean, A. Haque and M. Shamsuzzoha, *S2 glass/vinylester polymer nanocomposites: Manufacturing, structures, thermal and mechanical properties*, Journal of Composite Materials, 2005, 37(1), p.16-27.

[252] A. Haque, M. Shamsuzzoha, F. Hussain and D. Dean, *S2 glass/epoxy polymer nanocomposites: Manufacturing, structures, thermal, and mechanical properties*, Journal of Composite Materials, 2003, 37(20), p.1821-1873.

[253] J. J. Qiu, C. Zhang, B. Wang and R. Liang, *Carbon nanotube integrated multifunctional multiscale composites*, Nanotechnology, 2007, 18(27), p.275708.

[254] E. T. Thostenson, W. Z. Li, Z. Wang, Z. F. Ren and T. W. Chou, *Carbon nanotube/carbon fibre hybrid multiscale composites*, Journal of Applied Physics, 2002, 91(9), p.6034-6037.

[255] K. L. Kepple, G. P. Sanborn, P. A. Lacasse, K. M. Gruenberg and W. J. Ready, *Improved fracture toughness of carbon fibre composite functionalized with multiwalled carbon nanotubes*, Carbon, 2008, 46(15), p.2026-2033.

[256] J. Gou, W. Hollinghead, A. Whitaker, B. Sheffer, J. Foster and D. Hui, Processing of fibre reinforced composites with carbon nanofibre-modified matrix using resin transfer molding, in "Proceedings of the 11th International Conference on Composites/Nano Engineering (ICCE-11)" (SC, USA, 2004).

[257] D. P. N. Vlasveld, H. E. N. Bersee and S. J. Picken, *Creep and physical aging behaviour of PA6 nanocomposites*, Polymer, 2005, 46(26), p.12539-12545.

[258] D. P. N. Vlasveld, W. Daud, H. E. N. Bersee and S. J. Picken, *Continuous fibre composites with a nanocomposite matrix: Improvement of flexural and compressive strength at elevated temperatures*, Composites Part A: Applied Science and Manufacturing, 2007, 38(3), p.730-738.

[259] M. A. van Es, *Polymer-clay nanocomposites: the importance of particle dimensions*, 2001, Delft University of Technology; Dissertation

[260] E. P. Giannelis, *Polymer layered silicate nanocomposites*, Advanced Materials, 1996, 8(1), p.29-35.

[261] Y. Kojima, A. Usuki, M. Kawasumi, A. Okada, T. Kurauchi and O. Kamigaito, *Sorption of water in nylon 6-clay hybrid*, Journal of Applied Polymer Science, 1993, 49(7), p.1259-1264.

[262] H. L. Qin, Q. S. Su, S. M. Zhang, B. Zhao and M. S. Yang, *Thermal stability and flammability of polyamide 66/montmorillonite nanocomposites*, Polymer, 2003, 44(24), p.7533-7538.

[263] T. Kashiwagi, R. H. Harris, X. Zhang, R. M. Briber, B. H. Cipriano, S. R. Raghavan, W. H. Awad and J. R. Shields, *Flame retardant mechanism of polyamide 6-clay nanocomposites*, Polymer, 2004, 45(3), p.881-891.

[264] L. Qu, Y. Zhao and L. Dai, *Carbon microfibres sheathed with aligned carbon nanotubes: towards multidimensional, multicomponent and multifunctional Nanomaterials*, Small, 2006, 2(8-9), p.1052-1059.

[265] S. J. V. Frankland, J. C. Riddick and T. S. Gates, *Multi-ccale modeling of carbon nanotube/carbon fibre/epoxy lamina*, Materials Research Society Symposium Proceedings, 2006, 887, p.61-70.

[266] Cycom 823 Technical Data Sheet, (Cytec Engineered Materials, 2004).

[267] M. Cadek, J. N. Coleman, K. P. Ryan, V. Nicolosi, B. G., A. Fonseca, J. B. Nagy, K. Szostak, F. Beguin and W. J. Blau, *Reinforcement of polymers with carbon nanotubes: the role of nanotube surface area*, Nano Letters, 2004, 4(2), p.353-356.

[268] F. Inam and T. Peijs, *Transmission light microscopy of carbon nanotubes-epoxy nanocomposites involving different dispersion methods*, Advanced Composite Letters, 2006, 15(1), p.7-13.

[269] A. Internationals, *ASTM D790-03 Standard test methods for flexural properties of unreinforced and reinforced plastics and electrical insulating materials.*

[270] E. T. Thostenson and T. W. Chou, *Aligned multi-walled carbon nanotube-reinforced composites: processing and mechanical characterization*, Journal of Physics D: Applied Physics, 2002, 35(16), p.77-80.

[271] E. T. Thostenson, C. Li and T. W. Chou, *Nanocomposites in context*, Composites Science and Technology, 2005, 65(3-4), p.491-516.

[272] D. Dean, A. M. Obore, S. Richmond and E. Nyairo, *Multiscale fibre-reinforced nanocomposites: synthesis, processing and properties*, Composites Science and Technology, 2006, 66(13), p.2135-2142.

[273] A. Guz and Y. Y. Rushchitskii, *Comparison of mechanical properties and effects in micro- and nanocomposites with carbon fillers (carbon microfibres, graphite microwhiskers, and carbon nanotubes*, Mechanics of Composite Materials, 2004, 40(3), p.179-190.

[274] M. B. Bryning, M. F. Islam, J. M. Kikkawa and A. G. Yodh, *Very low conductivity threshold in bulk isotropic single-walled carbon nanotube-epoxy composites*, Advanced Materials, 2005, 17(9), p.1186-1191.

[275] A. A. Mamedov, N. A. Kotov, M. Prato, D. M. Guldi, J. P. Wicksted and A. Hirsch, *Molecular design of strong single-wall carbon nanotube/polyelectrolyte multilayer composites*, Nature of Materials, 2002, 1(3), p.190-194.

[276] R. W. Venderbosch, T. Peijs, H. E. H. Meijer and P. J. Lemstra, *Fibre-reinforced composites with tailored interphases using PPE/epoxy blends as a matrix system*, Composites Part A: Applied Science and Manufacturing, 1996, 27(9), p.895-905.

[277] H. Kishi, K. Uesawa, S. Matsuda and A. Murakami, *Adhesive strength and mechanisms of epoxy resins toughened with pre-formed thermoplastic polymer particles*, Journal of Adhesion Science and Technology, 2005, 19(15), p.1277-1290.

[278] K. C. Lee, H. H. Yu, S. J. Hwang, Y. S. Li, M. H. Cheng and C. C. Lin, *Preparation and characterization of the modified carbon nanotubes enhanced epoxy resin composites*, Materials Science Forum, 2006, 505-507, p.1075-1080.

[279] S. M. Yuen, C. C. M. Ma, H. H. Wu, H. C. Kuan, W. J. Chen, S. H. Liao, C. W. Hsu and H. L. Wu, *Preparation and thermal, electrical, and morphological properties of multiwalled carbon nanotube and epoxy composites*, Journal of Applied Polymer Science, 2007, 103(2), p.1272-1278.

[280] L. R. Xu, V. Bhamidipati, W. H. Zhong, J. Li, C. M. Lukehart, E. L. Curzio, C. Liu and M. J. Lance, *Mechanical property characterization of a polymeric nanocomposite reinforced by graphitic nanofibres with reactive linkers*, Journal of Composite Materials, 2004, 38(18), p.1563-1582.

[281] G. S. Zhuang, G. X. Sui, Z. Sun and R. Yang, *Pseudo reinforcement effect of multiwalled carbon nanotubes in epoxy matrix composites*, Journal of Applied Polymer Science, 2006, 102(4), p.3665-3672.

[282] M. H. G. Wichmann, K. Schulte and H. D. Wagner, *On nanocomposite toughness*, Composites Science and Technology, 2008, 68(1), p.329-331.

[283] H. Deng, R. Zhang, C. T. Reynolds, E. Bilotti and T. Peijs, *A novel concept for highly oriented carbon nanotubes composite tapes or fibres with high strength and electrical conductivity*, Macromolecular Materials and Engineering, 2009, 294(11), p.749-755.

[284] E. Bilotti, R. Zhang, H. Deng, M. Baxendale and T. Peijs, *Fabrication and Property Prediction of Conductive and Strain Sensing TPU/CNT Nanocomposite Fibres*, Journal of Materials Chemistry, 2010, DOI: 10.1039/c0jm01827a.

[285] C. Li, E. T. Thostenson and T.-W. Chou, *Sensors and actuators based on carbon nanotubes and their composites: A review*, Composites Science and Technology, 2008, 68(6), p.1227-1249.